Prosthetic Joint Replacements in Hips and Knees: Pilot study for the development of a single imaging test in patients with painful prosthetic joint replacements. ^{18}F-Fluoride PET-CT and Conventional Radionuclide Bone Scans

Oludolapo Olasunkanmi Adesanya

MBBS, PG Dip (Nuclear Medicine), MRCP, FRCR

[redacted]

Thesis submitted to the University of Warwick

for the degree of Doctor of Philosophy

February 2021

Table of Contents

Acknowledgments

I am thankful to my supervisors Professor Charles Hutchinson and Dr Nigel Williams for their constant encouragement, patience and guidance. I have learnt a great deal from working with them both.

I am thankful to all the participants in the research, as without them there would have been no study. I am grateful to Siemens PETNET Solutions, NIHR Clinical Research Network as well as the superb team of clinical scientists in the Nuclear Medicine department, UHCW headed by Dr James Cullis.

I dedicate this work to my wife, Flo
To my children, Ayo and Lola
To my mother, Grace and my late father, Isaac
Thank you for your love, endless support and encouragement.

Declaration

I, Oludolapo Adesanya declare that any material contained in this thesis is my own work except where it contains work based on collaborative research,

The collaborative work involved data generation and data analysis with:

Ms Kimberley Saint & Dr Nigel Williams – physics experiments

Mr Matthew Galloway – physics experiments

Dr James Cullis & Mr Samuel Colclough – physics experiments

Parts of this thesis have been published by the author:

1. Adesanya O, Sprowson A, Masters J, Hutchinson C. Review of the role of dynamic 18F-NaF PET in diagnosing and distinguishing between septic and aseptic loosening in hip prosthesis. J Orthop Surg Res. 2015;10(1):5.
2. Adesanya O, Hutchinson C. Designing a New Molecular Probe: The Potential Role for Tilmanocept (Lymphoseek®) in the Assessment of Patients with Painful Hip and Knee Joint Prostheses. The open orthopaedics journal. 2017;11:212.
3. Adesanya O, Foguet P, Hutchinson C. The Promising Role of Dynamic 18F-NaF PET-CT in Diagnosing Symptomatic Joint Prosthesis. Integrative Biomedical Sciences. 2015;1(2).
4. Poster presentations: The British Nuclear Medicine Society Autumn Meeting, London, 2nd September 2015. Nuclear Medicine Communications. 2015;36(11):1157-8. Also publised at wrap.warwick.ac.uk
5. Poster presentations (P024): Saint K, Adesanya O, Williams N, editors. The Impact of Small Dental Implants on the PET-CT Derived SUVs of Localised Lesions. EUROPEAN JOURNAL OF NUCLEAR MEDICINE AND MOLECULAR IMAGING; 2011: SPRINGER 233 SPRING ST, NEW YORK, NY 10013 USA.

I am aware of University regulations governing plagiarism and I declare that this document is all my own work except where I have stated otherwise. I consider myself ready for PhD.

. . . . . .

Oludolapo Adesanya 15th February 2021

Summary

An increasing number of annual joint replacement operations are performed. Prosthetic infection and aseptic loosening is very important and distinguishing between them allows prompt and accurate treatment but there is no consensus on how best to image these patients.

I also reviewed the role of CT in prosthetic joint imaging with a spectrum of usual pathologic conditions and CT patterns. This showed that CT plays a significant role in detecting and demonstrating complications of joint prosthesis surgery but it may not be sufficient in itself. CT can be combined, in hybrid imaging, such as SPECT-CT and PET-CT.

I assessed the magnitude of the problem with a retrospective study of painful prosthetic joints in UHCW from symptom onset to diagnosis. This demonstrated significant delays in diagnosis and the need for streamlined and reduced imaging tests with some patients undertaking multiple non-imaging and imaging tests.

I performed a systematic review of the role of ^{18}F-NaF showed that sodium fluoride positron emission tomography (^{18}F-NaF-PET) is a promising tool with high sensitivity and specificity in the assessment of joint replacements after the ninth post-surgical month. A further study confirmed the practicality of performing dynamic ^{18}F NaF PET-CT in detecting aseptic loosening of lower limb prostheses but future research trials with larger patient populations are required.

Beam hardening artefacts occur in CT and hybrid imaging of metallic prosthetic joints. A series of physics experiments to evaluate and correct beam hardening artefacts was performed to alleviate the problem. Beam hardening artefacts from prostheses reduce image quality on ^{18}F PET-CT. The experiments included pre-filtering with Aluminium; dual-energy CT and mathematical algorithms with MATLAB® filtered back projection. The results showed no significant difference in artefact reduction between the different methods. The artefact-reduction techniques introduce other secondary artefacts with subsequent image quality reduction.

Analysis of data from the prospective dynamic ^{18}F-NaF PET-CT trial showed inconsistent results due to data corruption and dynamic ^{18}F-NaF data loss but quantitative methods with Time-Activity Curves and trend line assessment of ^{99m}Tc-MDP 3-phase bone scans was more accurate. The trial problems were identified and suggestions were made for a larger study with opt-in methods for patient recruitment and more involved use of allied healthcare staff for patient recruitment.

I designed and obtained funding for a study to use a novel radiopharmaceutical agent - ^{99m}Tc-Tilmanocept (Lymphoseek®) to assess periprosthetic membranes in vivo. Lymphoseek® binds to the mannose receptor on the cell surface of macrophages and multinucleated giant cells which are likely to reflect wear particle aseptic loosening. Further in vitro periprosthetic membranes tests will also be performed using immunochemistry. This study has not yet been performed but it is hoped that a negative Tilmanocept scan would reassuringly make a diagnosis of wear particle induced aseptic loosening unlikely.

List of Illustrations

List of Tables

List of abbreviations

2D Two dimensional

3D Three dimensional

ADME drug absorption, distribution, metabolism, elimination and efficacy

ARSAC Administration of Radioactive Substances Advisory Committee

BHC Beam Hardening Correction

CD Cluster of Differentiation

CLRN Comprehensive Local Research Network

CLUT Colour Look Up Table

CQC Care Quality Commission

CRP C-reactive protein

CT Computed Tomography or Computed Axial Tomography

DNA Deoxyribonucleic acid

DNPG Dynamic PET-CT group

DTPA Diethylene Triamine Pentaacetic Acid

EANM European Association of Nuclear Medicine

EMI Electric and Musical Industries

EPR Environmental Permitting Regulations

ESR Erythrocyte Sedimentation Rate

Fab′ Fanolesomab

FDG ^{18}F-fluoro-2-deoxyglucose

FOV Field of View

^{68}Ga ^{68}Gallium

General Electric GE™

GFR Glomerular Filtration Rate

GSI Gemstone Spectral Imaging

HAMA Human anti-mouse antibody

HDP Hydroxymethylene diphosphonate

HEDP Hydroxy Ethylidene Diphosphonic Acid

HMPAO HexaMethylPropyleneAmine Oxime

HRQoL Health-Related Quality of Life

Ig Immunoglobulin

IND investigational new drug

^{111}In ^{111}Indium

IRD Infrared dye

IRMER Ionising Radiation (Medical Exposure) Regulations

IRR Ionising Radiation Regulations

kDa KiloDalton

KeV Kiloelectronvolt

kV Kilovoltage

KVp peak kilovoltage

mA MilliAmpere

MAR Metal Artefact Reduction

MBq MegaBecquerel

MDP Methylene Diphosphonate

MHRA Medicines and Healthcare products Regulatory Agency

mSv MilliSievert

MRI Magnetic Resonance Imaging

NaF Sodium Fluoride

NCA Nonspecific cross-reacting antigen

NPV Negative Predictive Value

O-MAR Orthopaedic metal artefact reduction

PACS Picture Archiving and Communication System

PCR Polymerase Chain Reaction

PET Positron Emission Tomography

PET-CT Positron Emission Tomography Computed Tomography

PJI Prosthetic Joint Infection

PMMA Polymethylmethacrylate

PPV Positive Predictive Value

PROMs Patient Reported Outcome Measures

QALYs Quality-Adjusted Life Years

rDNA Recombinant DNA

RNA Ribonucleic acid

rRNA Ribosomal ribonucleic acid

RSA93 Radioactive Substances Act 1993

SPECT Single Photon Emission Computed Tomography

SPECT-CT Single Photon Emission Computed Tomography Computed Tomography

SUVmax Standardised Uptake Value (maximum)

TAC Time Activity Curve

^{99m}Tc ^{99m}Technetium

THR Total Hip Replacement

TKR Total Knee Replacement

UKR Unicompartmental Knee Replacement

UHCW University Hospital Coventry & Warwickshire

UHMWPE Ultra-high-molecular-weight polyethylene

ViP Volume Imaging Protocol

VMS Virtual Monochromatic Spectral

WCC White Cell Count

Chapter 1 Background and History of Joint Prostheses with Theoretical Framework and Context Information

1.1.1 Abstract

Background: There is a steady increase in the use of prosthetic joint replacement medical devices to treat arthropathy with about 40,000 joint replacements of the knee and hip now occurring in the United Kingdom annually. Diagnosing the complications of joint prostheses often require imaging and an understanding of historic evolution of the different prosthetic types. This provides a historical vignette of pros and cons of the original and then subsequently developed joint prostheses as well as methods employed to investigate complications of treatment. Tomography was first suggested just over 100 years ago and Computed Axial Tomography (CT) was first developed almost 50 years ago. CT scans play an important imaging role before and after joint implant surgery as well as in hybrid imaging modalities such as SPECT-CT and PET-CT.

Method: A review of English language publications that significantly impact on the knowledge of joint implant developers and the history joint prostheses. This was performed by accessing information on the history of joint prostheses and pathology carried out through PubMed, EMBASE, Cochrane and Google Scholar online databases at the same time also focusing on prosthetic materials and prosthesis patent holders. It chronicled the use of imaging techniques used in the assessment of joint prostheses as well as the advent of ^{18}F-Fluoride PET and related PET-CT artefacts. In addition, a comprehensive review of literature to summarise the role of CT in imaging complications of prosthetic joint surgery as well as the role of CT before and after joint implant surgery; the development of metal artefact reduction techniques in CT for prosthetic joint imaging; the added value of CT in hybrid imaging modalities such as SPECT-CT and PET-CT and lastly, a collated CT reporting checklist for CT prosthetic joint assessment was garnered.

Results: Joint preservation surgery has been in use for almost 200 years. This chapter provides historical background of the use of joint prostheses and the use of imaging techniques in the assessment of joint prostheses infection and loosening, which are significant complications of joint replacement surgery. There is a wide variety of imaging techniques including ^{18}F-Fluoride PET and PET-CT, which can produce varying types of confounding imaging artefacts. Further information is required on the potential role for and the rational use of ^{18}F-NaF and PET-CT. CT has a role to play in diagnosing and distinguishing between septic and aseptic prosthetic joint loosening but metal artefact reduction techniques are often required. A table of useful reporting points and radiographic CT features for the radiologist to assess along with the significance of the radiographic features was issued.

Conclusion: The more frequent use of prosthetic joint replacement medical devices to treat arthropathy and an aging population mean that there is likely to be a requirement for more resources to diagnose the complications of joint prostheses. There is a potential role for dynamic sequential multiphase ^{18}F-NaF PET-CT but this requires further research to identify whether it can cost-effectively and accurately detect periprosthetic infection and periprosthetic loosening. The combined use of very sensitive moderately specific dynamic ^{18}F-NaF PET-CT and a radionuclide predictive biomarker of macrophages in periprosthetic tissue are likely to increase the efficiency and accuracy of diagnosis. Furthermore, CT scans and the use of CT in hybrid imaging play an important role in imaging joint prostheses. The use of a reporting checklist can be helpful to the radiologist in the assessment of painful prosthetic joints.

1.1.2 INTRODUCTION

About 40,000 annual joint replacements of the knee and hip occur in the United Kingdom, using a wide variety of implants (1, 2). Prosthetic infection and loosening are significant complications of joint replacement surgery (3). Approximately 0.4 to 4% of these are complicated by deep infection but the true figure is probably less than 1% (2). Further complications of joint prostheses include aseptic loosening with an incidence of 2-18% and 2-3% respectively in the knees and hips (4) but infection has much more devastating consequences (5). The diagnosis of prosthetic infection and loosening is very important both to patient wellbeing and mobility as well as the health economy. Treatment of an infected prosthesis is well in excess of £30,000 (5) and prosthetic infection rates following surgical revision are considerably higher, with an occurrence rate of about 40% of patients (5).

The incidence of infection after 2 years is relatively low but not out of the question, with a rate of less than 0.2% (2). Deep infection is usually preceded by (superficial) wound infection in up to a third of cases (2, 6). The presence of pain, fever, restricted joint movement, sinus formation and discharge are significant indicators of prosthetic joint infection; backed up with radiological evidence, haematological features and positive microbiological cultures from the prosthesis (2). Patients invariably have elevated serum inflammatory markers such as erythrocyte sedimentation rate (ESR) and/or C-reactive protein (CRP). In fact, the presence of a normal CRP and ESR make deep infection unlikely. Leucocytosis, on the other hand, is more variable and tends to be raised when acutely infected (2, 7). The measurement of serum interleukin-6 (IL-6) is more accurate than CRP, ESR and the white cell count (7). Microbiologically, coagulase-negative Staphylococcus and Staphylococcus aureus are the commonest causes; two-thirds of cases tend to be single organism related and the other third are multi-organism related.

In modern medicine, the use of prostheses in joint replacement now forms an important part of the management of patients with arthropathy to alleviate pain and to improve mobility, whilst maintaining stability and preserving joints (8).

Early surgical attempts to treat joint disease involved joint excisions and amputations, which were sometimes performed liberally (9, 10). One of the earliest recorded surgical attempts at treating severe joint disease whilst preserving the joint was made by Anthony White in Westminster Hospital, London. Although he was credited with the first excision arthroplasty in 1821, White did not publish or report this new surgical procedure. Excision arthroplasty improved patient pain and maintained mobility, but it also resulted in poor stability (9). Thereafter in 1826, the first osteotomy on a hip was performed in Philadelphia by John Rhea Barton (9). Some of the other early attempts at joint surgery also involved total hip arthroplasty techniques to relieve patient suffering due to joint pain and immobility. Similarly, there were further surgical attempts to remove arthritis spur calcium deposits and irregular cartilage in order to make the joint surfaces more smooth (11).

One of the most common indications for early joint replacements was in the management of tuberculous arthritis (12). There are reports of John Murray Carnochan, a New York surgeon making the first attempts to use artificial material to replace joint surfaces by using wood to replace the hip joint in 1840 (11, 13). This was followed by the use of ivory about half a century later by Professor Themistocles Gluck (12). He pioneered joint replacements and performed the first human total joint replacement despite suffering severe criticism from both his peers and superiors he replaced a knee joint in Berlin using a hinged ivory prosthesis in 1890. Thereafter, Gluck developed models for replacements of the shoulder, elbow, and wrist (12). In March 1892, Dr Jules-Emiles Pean in Paris closely followed this by performing a prosthetic shoulder joint replacement using platinum and rubber which was cemented with plaster and pumice (14), but the joint replacement only lasted 2 years due to infection (15). Gluck is known to have contributed significantly to Pean's work and Gluck also designed prostheses for several other joints making use of elephant ivory (14, 16). In 1914, F. Koenig made a subsequent attempt at shoulder prosthesis implantation, also using ivory (15). Then the use of glass moulds was reported soon afterwards by Marius Smith-Petersen operating in Massachusetts General Hospital, Boston, but operating with glass had to be abandoned because some of the glass moulds broke (17). In New York, further progress was made using

modern era monoblock designs for prostheses which were successfully applied to shoulder replacements by Charles Neer (15, 16).

The first modern era shoulder replacement using anatomically-shaped prostheses was performed by Krueger in 1950 employing the use of resin and Vitallium® (15, 18). Vitallium® had been developed in 1932 by Albert W. Merrick for the Austenal Laboratories® (19) and the Austenal Laboratories® later patented it on May 15 1934. Vitallium® was initially used as a cast for metal dentures and consists of an inert alloy with more than 50 per cent cobalt, 10 – 40 per cent of chromium, and was later developed for gas turbine blades in 1941 (20-22). This new alloy was quite revolutionary due to its inert, light, strong, biocompatible and corrosion-resistant properties; and is still being used today (19). While the newly patented Vitallium® proved to be a great success, the hip resurfacing technique was not adequate as a consequence of poor implant design, inadequate instrumentation, crude surgical techniques and the use of inappropriate materials, rather than inherent difficulty with the surgical procedure itself (23). Acrylic material was used in Paris in 1947 in the first attempt at prosthetic knee replacement with a hinged knee endoprosthesis by French brothers, Jean and Robert Judet (24-26). Thereafter, the first successful knee replacement was performed by Moore, using metal in 1950 (25).

One of the pioneers of modern-day total hip replacement was Professor Sir John Charnley, a British orthopaedic surgeon from Lancashire, England (27). Charnley developed the low-frictional torque arthroplasty which used dentist's methacrylate cement for a Moore femoral prosthesis. He developed it at Wrightington Hospital in Lancashire from 1958 to the early 1960s (27-31). Later on, due to the failure of approximately 1 out of every 10 prosthesis in a 10 year period (32), the first hip joint resurfacing was embarked upon in 1951 by Sir John using Teflon/Teflon bearings, but the Teflon was not robust enough and succumbed to early damage of the prosthetic material (33). Hip resurfacing entails surgical excision of diseased femoral head and acetabular surfaces and then shaping the surfaces as well as replacing the joint surfaces with materials such as metal or acrylic (33).

The rising number of hip and knee prostheses implanted yearly in most western countries, including the United Kingdom (1, 2) is due to a combination of population growth, worsening obesity (34), a growing number of knee injuries as well as expanding indications for joint replacements (35). Most contemporary hip and knee replacements occur due to advanced osteoarthritis (36), with an increasing number occurring following femoral fractures (36) due to newer surgical approaches. On the other hand, improved medical therapy of inflammatory arthropathy means that number of knee and hip joint replacements due to rheumatoid arthritis are on the wane (36).

Prosthetic infection and loosening are well recognised and significant complications of joint replacement surgery (3). It is believed that 1 out of every 10 prostheses will fail within 10 years of surgery and that 2 out of every 10 prostheses which necessitates re-revision will fail in 5 years (32). Thus, the diagnosis of prosthetic infection and loosening is very important both to patient well-being and mobility as well as the health economy. Generally speaking, the cure rate of infection is quite similar in both hip and knee prostheses and the mean time from surgery to diagnosis is just under 14 months but majority of patients present after 3 months (2). The management of these cases could be conservative or surgical. Antibiotics, joint lavage and debridement may be applied acutely whilst one or two-stage revisions for prosthetic infections are more helpful in chronic cases; amputation is a last resort (2).

Deep prosthetic infections can be classified according to the Coventry classification which was later modified by Fitzgerald into acute cases which occur within 2 weeks of surgery; delayed phase (occurring 12 weeks to 2 years following joint surgery) and presumed haematogenous cases which are usually those cases which occur after 2 years (2, 37). Prosthetic infections could arise from contamination during the surgical operation or afterwards by the spread of blood borne pathogens (2).

Due to the anticipated increase in numbers of both hip and knee arthroplasty surgery (38), there is likely to be an increased need for assessing complicated joint prostheses more efficiently. Therefore, research into this area is required and further advancements in the use of imaging to diagnose and distinguish

loosening from infected joint prostheses will contribute to knowledge in this field. Furthermore, I have chosen to investigate patients presenting with painful joint prostheses because pain is one of the first clinical indications of complications (39).

1.1.3 Imaging Techniques

There is no consensus on imaging algorithms for the diagnosis of loosening and infection (32). The usual current imaging investigations used in prosthetic joints include serial radiographs, ultrasound, Magnetic Resonance Imaging (MRI), Computed Tomography (CT), contrast arthrography and conventional Nuclear Medicine studies (40, 41). In the majority of cases, plain films are adequate for the assessment of prostheses. The sensitivity, specificity and accuracy for the plain radiographs are approximately 43%, 86% and 64%, respectively (42, 43). The use of plain radiographs for diagnosing loosening in un-cemented arthroplasties also has the disadvantage of poorer sensitivity due to the lack of a cement-bone interface between which loosening lucencies may been visualized (44). Indications for ultrasound include assessment of soft-tissue collections, guiding joint aspiration and capsular biopsy (41). Ultrasound can be particularly useful in the hips and may guide drainage but has no role to play in diagnosing loosening with accuracy (45).

Radioisotope investigations yield functional detail and are generally highly sensitive but they relatively less specific for diagnosing infection and loosening (40, 41) whilst lacking a great deal of anatomical detail (46). Metal-related artefacts in computed tomography and magnetic resonance imaging scans can significantly degrade image quality and diagnostic yield (41, 46). Despite CT and MRI metal-related artefacts, they do have a role in diagnosing periprosthetic collections, although the significant artefacts in the region of the prosthesis can render them uninterpretable. The use of artefact-reduction in CT and MRI could potentially result in an increased usage of CT and MRI in the imaging of prosthetic joints.

Newer techniques using PET-CT (Positron Emission Tomography-Computed Tomography) have been investigated. Although the use of ^{18}F-FDG (^{18}F-fluoro-2-deoxyglucose) PET-CT in prosthetic imaging was initially hailed as promising (3, 39), ^{18}F-FDG uptake in prosthetic joint infection has yielded limited results (47). The sensitivity, specificity, and accuracy of the combined use of radiolabelled leukocyte with bone marrow imaging outperforms ^{18}F-FDG in diagnosing infected hips and knee prostheses (48) as illustrated in a recent meta-analysis of the use of ^{18}F-FDG-PET in detecting prosthetic hip or knee joint infection in which 11 studies involving 635 prostheses yielded a pooled sensitivity and specificity of FDG-PET for the detection of prosthetic hip or knee joint infection ranging from 68.0-90.8% and 79.7-91.4%, respectively (49). However, PET-CT research into joint prosthetic imaging using ^{18}F-NaF (Sodium Fluoride) has also shown promising results (41).

Contrast arthrography is a more invasive test and requires test operators to be more practically skilled than in other routinely used imaging techniques as a result this is not a routinely used examination for prosthetic joint assessment.

A meta-analysis of more than 30 wide ranging English-language medical papers published over almost 30 years between 1975 and 2004 (50) compared the use of several radiological techniques in the diagnosis of aseptic loosening of hip prostheses using plain radiography, subtraction arthrography, nuclear arthrography and bone scintigraphy. Although the study demonstrated no statistical difference in the diagnostic accuracy amongst the different radiological techniques, plain radiographs and bone scans were proven to be beneficial for femoral components due to their ease of use, low cost, noninvasiveness, as well as relative low radiation dose to the patient (32).

Nuclear arthrography is performed using intra-articular injection of a radionuclide such as non-soluble ^{111}Indium labelled sulphur colloid, in combination with radiographic contrast. Some authors advocate 20mls of low-osmolar contrast media with 300 strength combined with 1ml of 10MBq ^{111}In labelled sulphur colloid (51). This may be performed in combination with a technetium labelled MDP (Methylene Diphosphonate) bone scan for correlation. Some of the problems with this technique are that it is an invasive and skilled

procedure requiring intra-articular injection. In addition, despite being non-soluble, some of the indium could get absorbed systemically and the presence of ^{111}indium in the urinary bladder is an important indicator of systemic absorption (52).

Differentiating prosthetic joint infection from aseptic mechanical loosening can be difficult even with a thorough clinical assessment and a battery of imaging and non-imaging diagnostic tests (46, 53). Some authors advocate the use of radionuclide imaging as the mainstay and modality of choice in the investigation of suspected prosthetic joint infection (46). The use of a combination of radiolabelled leukocyte and bone marrow scans can improve the accuracy of bone scans with a combined accuracy of about 90% in diagnosing prosthetic joint infection (46, 54). There are several important limitations in the use of in vitro labelled leucocytes (46). The in-vitro labelling process is quite demanding in terms of staff man-hours and radiopharmacy space and is therefore not always available. Furthermore, it involves the lengthy handling of human blood and blood products with its inherent risks (55).

The combination of labelled white cell scans with complementary radionuclide imaging using bone marrow or bone scans is often required in bone infection. This not only makes interpretation difficult but also adds to healthcare cost as well as patient inconvenience (55). Recently discontinued radionuclide infection agents include murine monoclonal anti-granulocyte antibodies, such as Fanolesomab (NeutroSpec®) (56) and radionuclide labelled antibiotics have been investigated for a potential role in prosthetic joint imaging (46). Other radionuclide infection imaging agents in current use include radiolabelled antibiotics and ^{18}F-FDG PET (55). In a meta-analysis of monoclonal antibody fragment imaging in 13 studies involving 522 joint prostheses; there was an estimated sensitivity and specificity of 83% and 80%, respectively (49). Analyses uncovered no significant statistical differences between the various subgroups of monoclonal antibody fragments. For weighted analysis, there was a sensitivity of 90% for a specificity of 80% (57). ^{99m}Tc-sulesomab scan (LeukoScan®) is one of the more common murine monoclonal antibody fragments of the IgG1 class (58). LeukoScan® is a 50 kDa fragment antigen binding (Fab′) that binds to the NCA-90 antigen on the surface of human white

cells (58). There are varying clinical reports as to whether human anti-mouse antibody (HAMA) is a contraindication to LeukoScan® usage since the antibody fragment is a xenobiotic (58, 59). A sole ^{99m}Tc-sulesomab scan (LeukoScan®) has 100% sensitivity and negative predictive value but a poor specificity of only 20%. To improve test accuracy and positive predictive value would require combining the ^{99m}Tc-sulesomab scan with a ^{99m}Tc- bone scan or a ^{99m}Tc-nanocolloid bone marrow scan (54) but murine monoclonal anti-granulocyte antibodies have been discontinued (56).

A large number of aseptically loosened prostheses result from inflammatory/immune reactions (60) which involve histiocytes, giant cells, lymphocytes and plasma cells (61). The cells secrete pro-inflammatory cytokines and proteolytic enzymes with resultant osteolysis and loosening (61). Loose joint prostheses have a periprosthetic pseudomembrane (61) which is composed of histiocytes (95% of samples), giant cells (80% of samples), lymphocytes, plasma cells (25% of samples) and neutrophils (less than 10% of samples). The presence of a significant number of neutrophils in samples is what distinguishes periprosthetic infection from aseptic loosening (58, 61). White cells in general are present in both inflammation and infection, and because white cells take up ^{18}F-FDG,^{18}F-FDG-PET is incapable of differentiating aseptic loosening from the infected joint prosthesis (55).

1.1.4 The Advent of ^{18}F Fluoride PET

Fluorine is the ninth element in the periodic table; it is a monovalent halide that often exists in nature as an inorganic anion bound to other cations. There are 17 isotopes of Fluorine (from ^{15}F to ^{31}F) with ^{19}F alone, being the solitary stable isotope (62, 63). ^{18}F is an artificial radionuclide which was first produced in 1936 (62, 63).

^{18}F may be produced within nuclear reactors by using fast neutron bombardment of lithium-6 enriched solid lithium carbonate targets (62). This method is inefficient and produces impure fluorine. The use of cyclotrons in the production of ^{18}F is a more convenient and commercially viable method of

producing pure ^{18}F. The promising role of Fluoride in nuclear medicine was first discovered by Anbar et al in 1959; they explored the role of monofluorosulphonates, difluorophosphates and fluoroborates as competitors for iodine uptake in the thyroid gland in a similar fashion to perchlorate ions (64). In addition, Anbar suggested a role for ^{18}F in brain imaging. The value of fluoride in bone imaging was first recognised by Monte Blau and team in 1962 (65, 66). ^{18}F decays to ^{18}O (oxygen-18) with a half-life of 109.7 minutes for 97% by the emission of positrons which leads to the production of 0.51MeV annihilation photons (62, 63). The remaining 3% of ^{18}F decay is by electron capture (62, 63). ^{18}F is usually administered in its salt form as ^{18}F-NaF and may be taken either orally or intravenously. Oral intake is less reliable due to the possible reaction with gastric contents which may result in the formation of insoluble compounds, but oral intake is more conducive when microbiological purity is less than acceptable. Consuming as much water as possible and emptying the urinary bladder reduces the radiation dose as well as decrease urine–related artefact.

The uptake of ^{18}F cations in bone occurs via the mechanism of ion exchange with the hydroxyl anions on the surface of hydroxyapatite crystals (67); these crystals are small-sized and thus present large surface areas for ion exchange in bone molecules which are in equilibrium with plasma (66). The rate limiting steps in the ion exchange process is blood flow and most ^{18}F-NaF is retained in bone after a single pass due to its high first pass extraction. $^{18}F^-$NaF blood concentration levels rapidly fall to 20% of peak levels within 30 minutes; 10% of peak levels within 60 minutes and approximately 1% by 5 hours (66, 68). Fluoride is excreted via the kidneys; it is filtered through glomerular capillaries, but approximately one quarter of the filtered fluoride is reabsorbed through the nephron tubules (68, 69) and there is a reasonably direct correlation between glomerular filtration rate (GFR) and ^{18}F clearance as well as chloride clearance (another halide) (69). Because $^{18}F^-$NaF is rapidly cleared from the body with rapid achievement of high bone: soft tissue ratios (66), the most favourable scan times are between 2 and 4 hours after oral intake (66)

1.1.5 ^{18}F-FDG PET versus Other Nuclear Medicine Techniques

The 2 PET tracers that are generally used to assess bone disease are ^{18}F-Sodium Fluoride and ^{18}F-FDG (70). Although the use of ^{18}F-FDG PET-CT in prosthetic imaging was initially hailed as promising (3, 39), ^{18}F-FDG usage in joint prosthesis infection has yielded limited results (47) and the sensitivity, specificity, and accuracy of the combined use of radiolabelled leukocyte/marrow imaging outperforms ^{18}F-FDG in detecting joint prosthetic infection in both hips and knees (48). In a blinded study of 35 patients, ^{18}F-FDG PET did not perform any better than three-phase bone scintigraphy in patients with prosthetic joint replacement infections, and conventional radiography was more sensitive but less specific than ^{18}F-FDG PET (71). ^{18}F-NaF PET-CT is slightly more specific than ^{18}F-FDG PET-CT in the assessment of hip prostheses (72). PET scanners have become obsolete equipment and since 2000 PET-CT scanners have replaced dedicated PET scanners (73).

1.1.6 PET-CT Artefacts

The high density related to metallic components of prostheses result in artefacts in both PET and PET-CT images (74). These occur when attenuation artefacts in PET are corrected with the use of transmission scans, which are generated with CT or germanium-68 (^{68}Ge). These attenuation corrected artefacts mimic periprosthetic increased metabolic activity, which are said to be more evident when there is patient motion between the emission and transmission scans. The employment of attenuation-weighted iterative reconstruction may reduce these artefacts (74). It is well recognised that these artefacts may result in false positive interpretation in patients with suspected infection. Marked increased activity in the attenuation-corrected images requires confirmation with the non-attenuation-corrected images and the follow up of this artefactual increased uptake for over a year usually confirms no change in the periprosthetic intensity on the attenuation corrected images (75).

1.1.7 The Future

PET-CT combines 2 sensitive data sets yielding both anatomical and functional information. The rapid accumulation of ^{18}F-Fluoride ion within the skeleton makes it the ideal isotope for the demonstration of prosthetic infection and sequential imaging of prostheses with ^{18}F-NaF shows great promise (76). Further advantages of this technique include a shorter scanning time and resultant increased patient throughput which may further offset the relatively higher unit cost of ^{18}F-NaF versus ^{99m}Tc-HDP (hydroxydiphosphonate) dynamic bone scans (77). ^{18}F-NaF Dynamic (sequential multiphase) images with Time-Activity-Curves may yield more diagnostic information (78) and therefore more accurately diagnose loosening of joint prostheses; diagnose infection of joint prostheses; and distinguish loosening from infection of joint prostheses. We will investigate whether sequential multiphase ^{18}F-NaF PET-CT, as a single imaging investigation, is a more cost-effective and accurate method of detecting of periprosthetic infection/loosening.

In the near future ^{99m}Tc-Technetium Tilmanocept (Lymphoseek®) may reliably demonstrate the accumulation of macrophages around joint prostheses and therefore identify the presence of periprosthetic loosening versus infection of joint prostheses using both quantitative and visual analysis.

1.1.8 The Need for More Research

Prosthetic joint replacements are becoming increasingly more common (79) and there are several outstanding wide-ranging reviews of prosthetic joint complications (80). There are several reviews of arguments for and against different imaging investigations for symptomatic joint prostheses, each of which to some extent reflects the authors' personal clinical and research bias as well as expertise (43, 46, 81, 82). There are unresolved conflicts and gaps in research of failed prosthesis imaging that still require exploration. In addition, there are new developments that are required due to improvements in the state of knowledge in metal artefact reduction, positron imaging, ^{18}F-NaF supply and

radionuclide imaging of mannose receptors (CD206) located on the surface of macrophages. Due to the speed of basic science and clinical research in this field, a strictly comprehensive review is perhaps impossible, but this thesis will attempt to present a brief review of the attributes of different imaging tests available for investigating the complications of joint prostheses.

This review would cover historical and current state of imaging modalities in prosthetic joint imaging; the history and role of ^{18}F-NaF PET as well as CT and multimodality imaging while reviewing methods for overcoming artefacts from metallic prostheses. The motivation for this research is the lengthy time and non-standardized test algorithms for investigating patients with painful joint prostheses. The specific principles covered include physics of PET and CT as well as artefacts, PET scanning techniques including immunology and microbiology.

1.1.9 Conclusion

There is an increasing use of prosthetic joint replacement medical devices to treat arthropathy as well as a continuing increase in aging population which means that there is likely to be a requirement for more resources to diagnose the complications of joint prostheses. The combined use of very sensitive moderately specific dynamic ^{18}F-NaF PET-CT and a radionuclide predictive biomarker of macrophages in periprosthetic tissue are likely to increase the efficiency and accuracy of diagnosis.

1.2 Role of CT in Prosthetic Joint Imaging; Pathologic Spectrum and CT Patterns

1.2.1 Introduction

The history of tomography dates back to 1914 when it was first suggested by polish radiologist Karol Mayer. Various authors subsequently developed the initial idea further and individually built their own equipment as well as published additional work in the area (83). Alongside further developments in electronics, the Computed Axial Tomography (CT) scanner was first developed and commercialized in 1972 by Sir Godfrey Hounsfield, an engineer at Electric and Musical Industries (EMI), the same company that sold The Beatles' records (83, 84). Hounsfield and Dr Jamie Ambrose, a consultant radiologist in Atkinson Morley's Hospital, Middlesex presented a paper ''Computerised Axial Tomography (A new means of demonstrating some of the soft tissue structures of the brain without the use of contrast media)'' in April 1972 at the 32nd Congress of the British Institute of Radiology (85) and the following month Hounsfield and Dr James Bull presented the first clinical images at a neurology postgraduate course at the Albert Einstein College of Medicine, New York (85). Since then, successive generations of CT scanners have been developed with significantly improved image quality and reduced scanning times.

With the relative recent growth of hybrid imaging, the role of computer tomography technique (CT) is being reassessed for the provision of anatomic information, due to poor structural detail in conventional radionuclide images performed for possible prosthetic joint instability, component loosening and mal-positioning (43).

CT has advantages over Magnetic Resonance Imaging (MRI) due to quicker scan times, superior views of the acetabular roof, better images of heterotopic bone, cement and metallosis (86). CT is superior to ultrasound because it is

less operator-dependent and has superior bony detail. CT and ultrasound may guide percutaneous joint infections, biopsies and aspirations (87).

CT scans have an important role before and after joint implant surgery (88). Computed Tomography data is used in computer-aided custom-made prostheses for prototyping to produce precise pelvic models used to design and manufacture joint prostheses (88, 89).

1.2.2 CT in Preoperative Planning and Intra-Operative Planning

Preoperative surgical planning is not routinely performed but some authors suggest that CT scans of the pelvis may have an important role to play in the assessment of ideal acetabular implant positioning in order to ensure total hip arthroplasty implant stability, i.e., to gauge whether more than 70% of the bone-implant interface would be covered and also that the acetabular implant is placed as close to the anatomical rotation centre as possible (90).

Prior to revision, computed tomography-based or imageless navigation systems can improve the accuracy of component positioning (91, 92). The final orthogonal alignment results from CT are much closer within acceptable number of degrees of the predicted surgical plans, but problems may arise in the talus in ankle replacements due to the differing preference regarding the extent of gutter debridement amongst surgeons (93). CT scans are used as the basis for commercially available robotic surgical systems which can be adapted to assist preoperative planning and intraoperative placement of knee prostheses (94), resulting in improved prosthetic component alignment and improved bone-implant fit, reduced implant loosening particularly in non-cemented prostheses (94). However, disadvantages include the requirement for fiducial markers, increased operating times and higher treatment costs (94).

The role of Magnetic Resonance Imaging (MRI) in patient specific cutting guides is small and although MRI can lead to reduced operating times and also

improve the consistency of prosthetic joint alignment it does lead to significantly increased overall medical costs (95).

1.2.3 Postoperative Planning

CT-based systems can be used in accuracy assessments of post-operative patient-specific instrumentation systems for joint replacements (96, 97). There are several types of orthopaedic devices that can be implanted in several joints – most commonly in order of occurrence knee, hip, ankle, shoulder and elbow followed by wrist and then carpal and tarsal joints (98). However, current trends and industry projections suggest that it is more likely that an increase in the number of upper extremity arthroplasty will exceed the steady increasing requirements for hip and knee arthroplasties (99). This section of the chapter concentrates on the role of CT in the 2 most common joint replacements that currently occur.

1.2.4 CT in Post-Operative Imaging of the Hip

The indicators of hip replacement infection on CT are a volume of periprosthetic fluid of more than 1 ml and prosthetic acetabular malpositioning (100). Component malpositioning also can result from aseptic loosening, instability, polyethylene wear as well as joint instability and dislocation (101). Further confirmatory evidence of prosthetic sepsis can be provided by positive bacterial culture from joint fluid aspirate obtained under CT guidance all resulting in 70% sensitivity, 100% specificity and 100% positive predictive value (100).

The American academy of orthopaedic surgeons advocates that there is no compelling evidence for the use of CT as a diagnostic test for periprosthetic joint infection, stating that there is an unclear balance between benefits and potential

harm (102). The American academy of orthopaedic surgeons also advocate a central role for blood tests (ESR and CRP), as well as joint aspiration (including frozen section aspiration) (102), and also state that nuclear imaging has a limited role in the diagnosis of periprosthetic joint infection (102), despite the fact that it is well recognised that nuclear medicine studies have high negative predictive values (103) and also that combined nuclear medicine studies have high positive predictive values (103).

Loosening at the bone/cement interface or prosthesis/bone interface is demonstrated on radiographs as a progressive increase in radiolucency on serial radiographs (104), often of up to 2 mm at the interface or a change in position on serial imaging. Loosening may also occur at the prosthesis/cement interface (105). CT is able to demonstrate more subtle bony change including erosion and periosteal reaction (106). Postoperative findings must always be interpreted in conjunction with clinical symptoms and previous imaging (105), because CT artefacts are known to occur more commonly around the acetabulum. In addition, artefactual radiolucency at the metal-cement interface may also occur secondary to the Mach effect (107) and radiolucencies around revised prostheses are generally wider (105). Other radiographic signs of loosening include the development of bony sclerosis in the region of the distal tip of the prosthesis, cement fracture, prosthesis fracture, prosthesis movement as well as prosthetic rotation (105). Prosthetic micro-abrasive wear of polyethylene or polymethylmethacrylate (PMMA) cement can result in particle deposition in periprosthetic tissues, which incites a multinucleate giant cell granulomatous inflammatory response, resulting in periprosthetic osteolysis and a form of endosteal scalloping on plain radiographs and CT, known as particle inclusion disease (105, 108-110). Metal wear results in periarticular metallic fragments (105).

Particle inclusion disease, also known as histiocytic response results in focal osteolysis and was first recognised by John Charnley. It was initially thought to be secondary to cement (105), but is now known to be induced by deposited foreign bodies (metallic, PMMA cement, as well as polyethylene fragments) following implant wear 1 to 5 years post-surgery (105). Polyethylene inclusion disease is now most common because of reduced use of cemented implants

(105). On radiographs, inclusion disease may be distinguished from loosening by focal endosteal scalloping as opposed to linear radiolucency which occurs in loosening and infection (105). Periarticular soft tissue density and fluid may also occur in particle inclusion disease (105). Inclusions and fractures are elegantly demonstrated on cross-sectional imaging. The bony defects produced by particle inclusion disease result in an increased fracture risk and therefore requires close follow up with radiographs or CT (105).

Low-grade infection can be difficult to distinguish from aseptic loosening on imaging alone. High-grade infection results in joint effusion, osteolysis and sclerosis (105) as well as other signs of infection on the plain radiograph consistent with osteomyelitis (105). On plain radiographs, infection may also be difficult to distinguish from the endosteal scalloping of particle inclusion disease (105). CT defines bony changes in better detail as well as assesses adjacent soft tissue change much more clearly when compared with radiographs.

1.2.5 CT in Post-Operative Imaging of the Knee

The hip and knee are the most replaced joints in the human body (111, 112). Age-related degenerative change commonly affects the knee (111), whilst rheumatoid arthritis and osteoarthritis are the 2 commonest indications for knee arthroplasty (111). Depending on disease severity, the type of joint replacement undertaken may be total or limited to a single compartment (111). Commonly employed knee prostheses consist of cobalt-chromium alloys for both the condylar and tibial components with an ultrahigh molecular weight polyethylene (UHMWPE) layer on the tibial component (111, 112). Other employed metals have involved the use of binary titanium and zirconium alloys (111, 112) with improved biocompatibility and reduced reaction (113). Total knee prostheses are either of the unconstrained or semi-constrained category and their implantation requires sacrifice of the anterior (together with or without the posterior) cruciate ligaments (111). The patella may also be resurfaced to

reduce post-surgical anterior knee pain and the requirement for revision (114). Total knee replacement is one of the most successful joint replacement procedures in orthopaedic surgery (101, 115). Total knee replacements last longer than unicompartmental replacements; with survival rates of greater than 90% after 15 years (101) and total knee replacements generally last from 10 to 15 year with all being well, or 20 years at the most (111).

Adequate total knee replacements require fitted condylar and tibial components, employing 5 to 8 degrees of valgus alignment with normal tension maintained between the surrounding soft tissue structures (111). The failure of prostheses often result from a combination of factors including infection, aseptic loosening, implant wear, unsuitable mechanical load, fatigue failure at implant: bone interfaces due to repeated remodelling in response to altered mechanical loads, excessive implant motion resulting in resorption, and possibly hydrodynamic pressure (116). Albeit rare, some of the most common symptoms experienced after knee surgery include pain, instability and reduced range of movement (111). Imaging is required to exclude post-surgical complications and other unrelated conditions (111). For this to happen, an understanding of surgical techniques and surgical dates is important (111). Immediate post-surgical radiographs are required to assess the alignment of implant components. Haemorrhage and infection tend to occur more commonly in the subacute stage. Radiographs are also able to demonstrate effusions and intra-articular haemorrhage (111), but CT also has a role to play (111).

Technical artefacts arising from metal prostheses may be overcome to a degree by using pre-scanning techniques to perform the CT scan in a specific manner (117). The degree of artefact produced depends on the amount and type of metal present in the prosthesis, with titanium producing less artefact than cobalt (82). Titanium is the one of the most ideal alloy components for prostheses due to its suitable biocompatible composition which limits unfavourable tissue reactions, corrosion resistance and resistance to chemical breakdown in vivo (113). Titanium also possesses high levels of strength, low elasticity levels and produces relatively less debris (113).

CT scans provide detailed structural information which can also enhance the surgical planning stage (117). CT scans provide a means to measure the relationship between direct post-operative stem anteversion and rotational stability, because gradually worsening retroversion of a cemented stem on CT is a good indicator of prosthetic loosening and impending failure (118). Thus, an anteversion angle of less than 10° is detrimental to the future prospects of cemented hip prosthetic stems (118).

Prosthetic joint loosening is a clinical-radiologic diagnosis, but endosteal resorption of cortical bone in the mid-femur on CT is an indicator of primary prosthetic failure and could also contribute to further aseptic prosthetic loosening (119).

1.2.6 CT in Diagnosing and Distinguishing Between Septic and Aseptic Loosening in Hip Prostheses

The diagnosis of post-surgical hip complications may require multiple imaging tests (105), but plain film radiography remains the basis of post-surgical musculoskeletal radiology and it generally forms the initial evaluation of symptomatic post-surgical joint prostheses (82). In addition to plain radiographs, multi-slice CT may be used for additional assessment of joint prostheses in the detection of infected prostheses (106, 120). Oedema and haematoma in the immediate post-surgical period can mimic soft tissue infection (120), but CT is able to illustrate soft tissue infective changes such as abscesses following the administration of intravenous contrast and CT can guide percutaneous abscess drainage and other intervention procedures such as arthrography and synovial biopsy (120). Additionally, CT can detect bony changes of infection such as cortical and trabecular erosion; periosteal reaction, sequestration, fistulae, cortical tracts, sinus tracts and soft tissue defects (120). CT can also detect aseptic complications such as periprosthetic fractures, aseptic loosening, osteolysis, heterotopic bone formation, trochanteric bursitis as well as osteolysis

from foreign body granulomatosis (82). Care should be taken because osteolysis may confused with pre-existing cysts or geodes as well as spot-welds with stress-shielding (121). In an epidemiological study of the 60,355 total knee arthroplasty revision procedures performed in the United States during a 15 month period between October 2005 and December 2006 (122), the most common identified causes of failed prostheses were infection in 25.2% and aseptic mechanical implant loosening in 16.1% of the failed prostheses. Other causes of prosthetic failure included dislocation, implant fracture, periprosthetic fracture, periprosthetic osteolysis, bearing surface wear; and other mechanical complications of prosthetic joint implants (122). The presence of post-operative surgical site infection, synchronous malignancy, prior revision arthroplasty, nosocomial infection as well as operating room time of greater than 3 hours are some of the most significant prognostic factors which can predict prosthetic joint infection (103). The success of total knee replacements also depends on the preoperative condition of the patient, the design and materials of the components and the surgical technique used (101).

Artefacts from metallic prostheses can result in unreadable CT images. More artefacts are visualized in larger metallic implants as well as cobalt chrome prostheses (as opposed to titanium) (82, 123). Several methods can be employed to reduce the detrimental effect of beam hardening artefact and to also improve image resolution. These include pre-image acquisition techniques such as optimal patient positioning; increasing the peak kilo-voltage (KVp) and tube current; and the use of overlapping slices, increasing slice thickness (82, 123, 124). Post-processing image reconstruction techniques including the use of multi-planar reformats; including the use of soft tissue windows for bulky metallic implants and bone window viewing for small metallic hardware (82, 124).

2.7 Proposed CT Reporting Checklist

A systematic approach to radiographic evaluation of prosthetic joints using a checklist of important reporting points would help direct the radiologist to specific significant features when assessing prosthetic joints (90). In order to emphasise the role of CT in the diagnosing periprosthetic complications, this proposed CT reporting checklist (Table 1) provides an important tool for the radiologist in the assessment of painful prosthetic joints using CT (125).

Table 1. *CT reporting checklist in the assessment of prosthetic joints*

Reporting points	Radiographic features to assess for and significance
Prior radiographic and CT findings	Is the implant positioned properly and intact? Is the prosthesis position stable with good component fixation? Is the host bone abnormal and is there any adverse soft tissue feature such as muscle atrophy? Comparison with baseline radiographs helps detect complications.
Periprosthetic bone	Assess for periprosthetic fractures, as well as the presence, character and quantity of periprosthetic osteolysis. Also estimate the total amount of the prosthetic component such as acetabular cup that is fixed to bone. This also helps for accurate surgical planning.
Precise component position	Assess component positioning/alignment, for polyethylene wear and component fractures. Examine for excessive version which can lead to subluxation and dislocation.
Periprosthetic fluid collections	Look for periprosthetic bursae, periarticular and deep collections with sinus tracks to the skin. CT arthrography may also demonstrate communication with the joint.
Ossified masses	Identify and localize ossified masses. Define the extent of the ossified mass and assess whether the mass bridges the joint.
Periprosthetic soft tissue	Assess for soft tissue support, heterotopic ossification, metal-on-metal granulomatosis/pseudotumour
Pre-op Component selection	Ischial tuberosity line, ilioischial line,

1.2.8 Hybrid Imaging

CT scans and radionuclide imaging can form part of a multi-modality algorithm (126). Hence, integrated functional and anatomical imaging with SPECT-CT and PET-CT scans may be employed to diagnose prosthetic joint septic and aseptic loosening. SPECT-CT images can be performed following the injection of ^{99m}Tc-labeled bone isotopes (127) and PET-CT images may be obtained using ^{18}F labelled radiopharmaceuticals such as ^{18}F-fluorine labelled Sodium (^{18}F-NaF) and ^{18}F-fluorine labelled Fluorodeoxyglucose (^{18}F-FDG) (128), but ^{18}F-NaF is more accurate than ^{18}F-FDG in the assessment of joint prostheses (129).

Bone SPECT-CT with ^{99m}Tc-labelled phosphonates demonstrate increased periarticular bone turnover in the subchondral region, which corresponds with osteophytes, meniscal injury and osteochondral lesions on CT and bone SPECT-CT is able to accurately assess early osteoarthropathy (130). SPECT-CT animal experimental studies with radioactive ligands of a folic acid analogue has demonstrated synovial activated macrophages accumulation in cartilage damage in osteoarthropathy (130) and furthermore there may be a role for ^{99m}Tc labelled Tilmanocept® SPECT-CT imaging (128). In addition, Tilmanocept® imaging with PET-CT has been proposed using ^{68}Gallium (^{68}Ga) labelled Tilmanocept® to demonstrate CD206 receptor on activated macrophages and multinucleated giant cells due to wear particles in aseptic loosening and periprosthetic pseudotumours (128).

1.2.9 Reducing Metallic Artefact

The high proton density (Z) composition of embedded metallic prostheses result in artefacts that create a contradiction between the true attenuation coefficients in the reconstructed image of the metallic object and the measured CT Hounsfield Units (131). These metal streak artefacts result from a varying combination of beam hardening, scatter, photon starvation, partial volume

averaging and aliasing (131). The degree of artefact produced is dependent on the type and quantity of metal.

Metallic artefacts can be reduced before the image acquisition using pre-scan methods. Further artefact reduction can be accomplished using concurrent as well as post-scan techniques.

Pre-scan and concurrent techniques include patient positioning, increasing peak voltage KVp and tube current (mAs), overlapping slices which results in increasing the effective mAs. The most ideal position for imaging would be one with the least diameter of metal for the x-ray beams to traverse (105).

Metal artefact reduction (MAR) algorithms have employed interpolation methods, iterative projection modification and filtered back projection methods (131). Commercial post-processing software packages such as the orthopaedic metal artefact reduction (O-MAR) algorithm from Philips® (131), monochromatic gemstone spectral imaging (GSI) from GE® which employs dual-energy CT, and gemstone spectral imaging (GSI) monochromatic imaging metal artefact reduction (MAR) algorithm also from GE® (132). MARs should be used with caution, because it underestimates metal implant length and unintentionally introduces more artefacts (132). Both the metal artefact reduction algorithms induced other secondary artefacts and also result in an increased radiation dose (125, 132). With the MARs technique, a filtered back-projection image is created when the initial CT image is reconstructed and back-projected to generate CT images (125). If the uncorrected and raw images are dissimilar, other reconstructions are produced and fewer artefacts are produced with a higher number of reconstructions (125). Dual-energy techniques involve scanning the same body part at two different energy levels (125). Dual-energy CT scanners produce virtual monochromatic spectral (VMS) images which display what the prosthesis would have looked like if the image had been produced by a single photon energy x-ray beam (133).

Several methods have been combined with some success; image-based weighted superposition of images obtained from different metal artefact reduction methods such as linear interpolation of re-projected metal traces and multi-dimensional adaptive filtering of the raw data result in reduced corrupted

CT values and fewer secondary artefacts (134) and the quality of images produced is usually better than that produced from one single MAR method (134).

The use of multi-planar reformats can improve visualisation of periprosthetic pathology (105). Furthermore, improved visualisation of bony/metal interfaces can be achieved by reviewing images with soft tissue algorithms and alternatively applying bony algorithms for periprosthetic soft tissue (105).

1.2.10 Summary of the Role of Computed Axial Tomography (CT) in Prosthetic Joint Imaging

In this latter section of the chapter, the literature relating to the role of Computed Axial Tomography (CT) in prosthetic joint imaging and the detection of complications of prosthetic joint surgery was reviewed. CT has an important role to play before and after surgery as well as in the production of prototypes to be used in the design and manufacture of joint prostheses. CT is often combined, in hybrid imaging, with other modalities such as SPECT-CT and PET-CT. Although beam hardening artefact has the potential to reduce the diagnostic yield from CT there are several pre-scan, scan and post-scan artefact reduction methods. Further commercial and in-house artefact reduction methods can also be used to produce diagnostic quality CT images.

1.2.11 Summary

- There is a steady increase in use of prosthetic joint replacement to treat arthropathy.
- The demand for resources to diagnose complications of joint prostheses is likely to rise.
- Efficiency and accuracy of diagnosis may be achieved by combining dynamic ^{18}F-NaF PET-CT and a radionuclide biomarker of macrophages.
- CT and SPECT-CT have an important role in periprosthetic imaging

Chapter 2 Painful Joint Prostheses; a Retrospective Study of the Use of Dynamic Bone Scans (and Other Imaging Modalities) – From Symptom Onset to Diagnosis

2.1 Abstract

Background: A significant number of patients with joint prostheses may go on to experience pain at the site of arthroplasty at some point after surgery. It is useful to understand the profile of patients and symptoms with painful joint prostheses; including the use of imaging investigations and the time interval from symptom onset to diagnosis. It is not entirely clear whether an increased number of imaging investigations can prolong the length of time from symptom onset to diagnosis.

Method: This was a retrospective study of 27 adults who had bone scans for painful knee and hip prostheses over a 3 month period at the University Hospital Coventry & Warwickshire nuclear medicine department between January and March 2007. The study was performed retrospectively using data collected from the hospital's radiology information system records of all bone scans that were performed over the specified period and the final diagnosis was confirmed using microbiology, clinical follow up, surgical findings or other radiological data.

Results: Nineteen female and eight male patients were identified with an age range from 28 to 86 years and an average age of 64 years. The time range of symptom onset to diagnosis was 2 months to 121 months. All but one patient had plain radiographs and only one patient had an MRI scan of the painful joint. Almost twice as many knees were investigated over the time period and the most common symptom in these set of patients was pain. Dynamic bone scans were performed from 2 to 120 months post-joint replacement. The overall average length of time from symptom onset to diagnosis in this group was 42.9 months.

Conclusion: The length of time from symptom onset to diagnosis for patients with painful joint prostheses dynamic isotope bone scans ranged from 2 months to 121 months with an average of 42.9 months delay in diagnosing painful joint prostheses. Factors including the use of multiple non-imaging tests including the use of anatomical imaging modalities as well as functional imaging modalities may have contributed to the delays in reaching a diagnosis. A streamlined reduced number of imaging tests and fused functional anatomical imaging may improve the speed of diagnosing painful joint prostheses.

2.2 Introduction

The diagnosis of post-surgical hip and knee joint replacement complications often require various imaging tests (135). False positives bone scans commonly persist for several months after joint replacement surgery. The aim of our retrospective study was to identify and demonstrate the delay in diagnosing the cause of painful joint prostheses. Joint prosthetic failure occurs in less than 1 in 10 patients during the lifetime of the joint prostheses, mostly due to aseptic loosening and less commonly due to infection (5). Prosthetic joint infections result in higher morbidity, prolonged hospitalisation and significantly higher treatment costs (5) due to additional surgery and antibiotic therapy with possible recurrent infirmity (5). Infection rates following surgical revision are significantly higher than after primary replacement. Furthermore, infection rates following primary joint replacement are more common in the elbow and knee than in hip and shoulders (5). Coagulase-negative staphylococci is the responsible microbe in a third of cases (5). Aseptic loosening is usually due to metallic and non-metallic particulate deposition leading to macrophage phagocytosis and osteolysis (5). Current research into new imaging modalities or isotopes for painful prosthetic joint imaging is limited. There is a debate over what the optimal imaging or imaging pathway for prosthetic joint replacements and a lack of consistency of what imaging modality is utilised in the United Kingdom. It is also important for the advancement of treatment of painful joint prostheses to diagnose complications in a quicker and more streamlined manner (136).

2.3 Research Question

In patients with painful joint prostheses that are investigated with dynamic isotope bone scans what is the length of time from symptom onset to diagnosis?

2.4 Aim

The objectives of this retrospective review were 1: To measure the proportion of patients undergoing nuclear medicine bone scan investigations who have a final diagnosis of infected prostheses and 2: To describe the time interval between onset of symptoms, imaging tests and final diagnosis.

2.5 Materials and Methods

A 3 month study of all dynamic bone scans performed for painful joint prostheses over a 3 month period at University Hospital Coventry & Warwickshire nuclear medicine department between January and March 2007. The choice of 3 months was based on the estimated number of scans performed each week and also because the aim was to provide a retrospective snapshot of clinical practice as opposed to a lengthy retrospective study.

All patients with painful joint prostheses referred to the university hospital nuclear medicine department over a 3-month period between January 2007 and March 2007 were included (n = 27). The study was performed retrospectively using data collected from the hospital's radiology information system records of all bone scans that were performed over the specified period. Twenty seven patients met the criteria and the final diagnosis was confirmed microbiologically. Where there was no confirmatory microbiological result, results from clinical follow up as well as surgical and radiological data were used.

The final diagnosis of the painful joint was confirmed with surgery, or microbiologically or, in the absence of these, clinical follow up as well as surgical findings were used. Where available, other radiological investigations were used. We also assessed patient demographics, reported symptoms, the type and number of imaging tests as well as the time it took to make a diagnosis.

The microbiological definition of prosthetic joint infection include the preoperative aspiration as well as the intraoperative isolation of similar microorganisms which are indistinguishable from three or more independent specimens, taken as part of a standard set of 5 or 6 periprosthetic intraoperative tissue samples or the explanted prostheses (137, 138). Clinical features of a sinus tract that communicates with the prosthesis or persistent wound drainage over a joint is also considered evidence of prosthetic joint infection (138).

Radiological evidence of prosthetic joint infection includes positive findings from plain radiographs, bone scans, white cell scans, magnetic resonance imaging (MRI), computed tomography (CT), and ultrasound scans (138, 139).

Surgically, the presence of acute inflammation as seen on histopathologic examination of the periprosthetic tissue at the time of surgical debridement or the presence of purulence is acceptable evidence of prosthetic joint infection (138).

2.6 Results

The retrospective study identified 27 adults who had bone scans for painful knee and hip prostheses over a 3 month period. Nineteen female and eight male patients were identified. Their ages ranged from 28 to 86 years, with an average age of 64 years (Figures 1 and 2). The time range of symptom onset to diagnosis was 2 months to 121 months (Figure 3). All but one patient had plain radiographs and only one patient had an MRI scan of the painful joint (Table 2) and almost twice as many knees were investigated over the time period (Table 3). All the patients had their inflammatory blood markers measured. The

diagnosis and treatment of painful joint prostheses can be challenging and time consuming, resulting in multiple unhelpful investigations and therefore delayed treatment. The most common symptom in these set of patients was pain (table 4). Dynamic bone scans were performed from 2 to 120 months post-joint replacement (Figure 4). Twenty-six out of twenty-seven patients had a final diagnosis. The mean time from scan to diagnosis was 9.5 months. The overall average length of time from symptom onset to diagnosis in this group was 42.9 months (Table 5) and only 7% of these patients had infected prostheses; this contrasts with the much shorter duration of about 1 month to 6 months of symptoms and time to diagnosis in cases with virulent coagulase-negative staphylococcus prosthetic joint infections (140, 141).

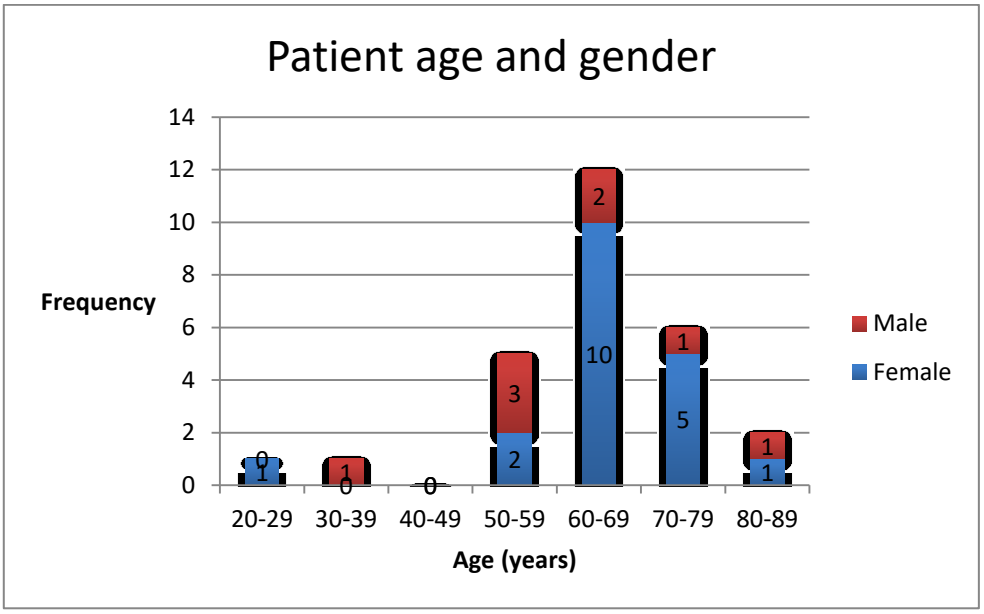

Figure 1. *Frequency histogram of patient gender ratio according to age*

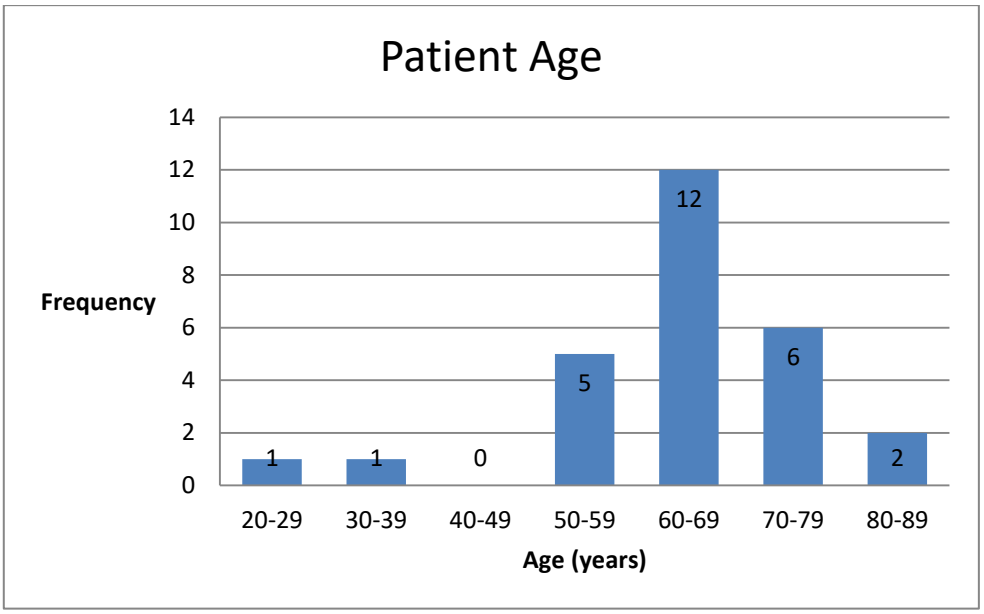

Figure 2. *Frequency histogram of patient age (years)*

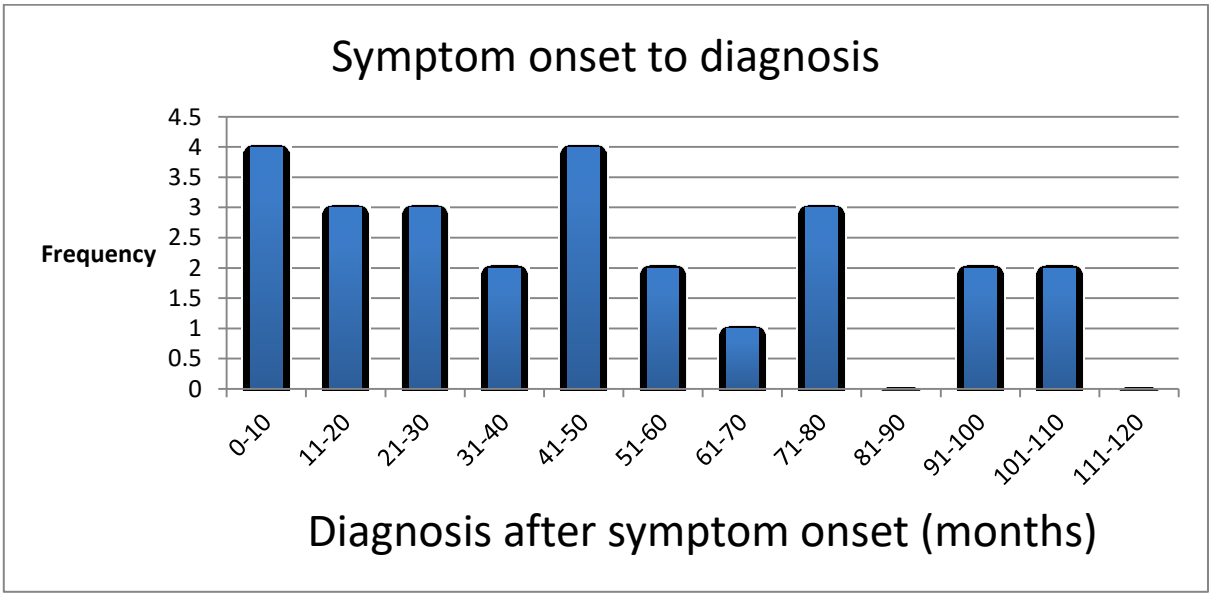

Figure 3. *Frequency histogram of symptom onset to diagnosis*

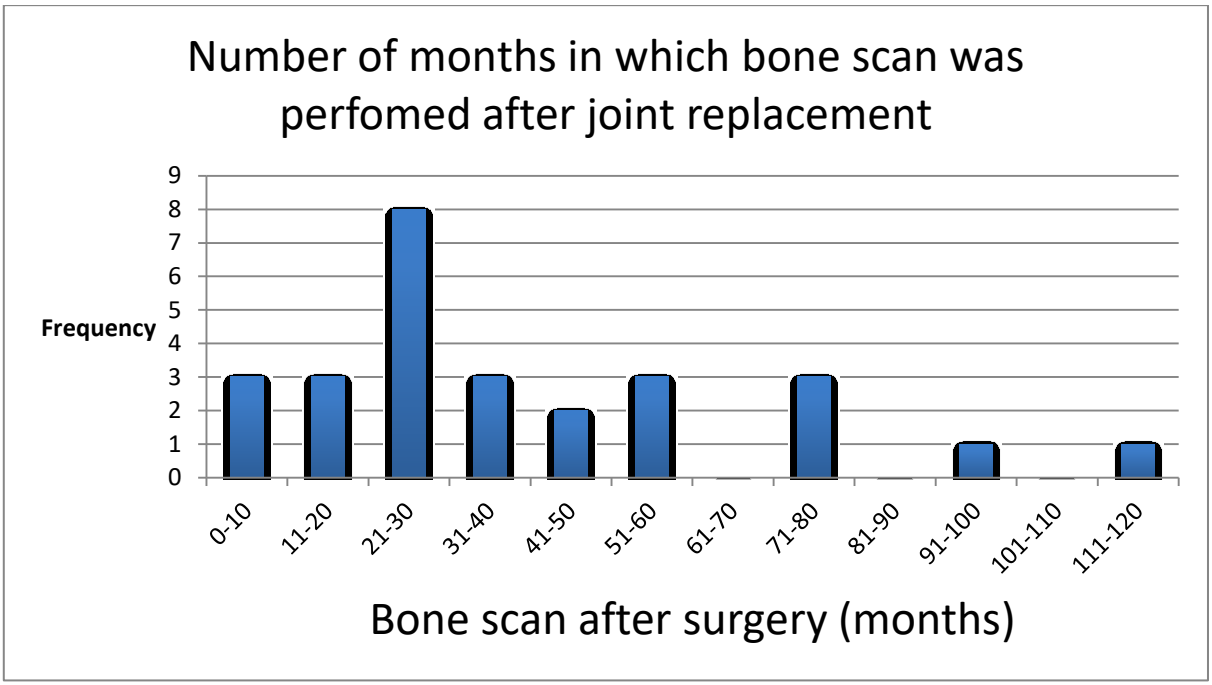

Figure 4. *Frequency histogram of time of bone scans post-joint replacement*

Table 2. *Other imaging modalities*

Other imaging	Number of tests
Radiographs	27
MRI	1
CT	0
Ultrasound	0

Table 3. *Type of joint replaced*

Replaced joint	Number of joints
Knee	17
Hip	10

Table 4. *Presenting symptoms of patients*

Presenting symptoms	Numbers
Pain	27
Swelling	9
Progressive deformity	1
Instability	2
Clicking	1
Weakness	1
Stiffness	2

2.7 Discussion

Delayed diagnosis of painful joint prostheses can be defined as the time of symptom onset to the time of diagnosis or more than 25 days in hip arthroplasty and more than 42 days after knee arthroplasty (142). The group studied included both men and women across a wide age range (28-86 years). Pain and swelling were the most common presenting complaints and these corresponded with symptoms most frequently quoted in the literature (103, 143).

The median number of months from initial prosthetic surgery to the onset of symptoms was 15.5 months (interquartile range of 2 to 39 months). The median number of months from symptom onset to the bone was 11 months (interquartile range of 2 to 22 months).

The median number of months from the time of the bone scan to the final diagnosis was 7.5 months (interquartile range of 4 to 14 months). Diagnostic delays occurred in the majority of patients (Table 5) in this retrospective study. Studies have shown that patients having to wait for multiple out-patient investigations (144) as well as the duplication of investigations (144) especially when significant non-standardised variations occur in the diagnostic work-up can lead to diagnostic delays (145). There is an excess of females which may partly be explained by the higher propensity of rheumatoid arthritis in females as well a reflection of the longer survival of females (146). Additionally, there is a strong association in general between old age and obesity as independent factors with diagnostic delays (147) and this combined with the fact that post-surgical function is worse in older female patients who undergo hip and knee joint replacements (148) may contribute to a high number of diagnostic delays in those presenting with symptomatic joint prostheses.

Table 5. *Diagnostic timeline and criteria used in the diagnosis of painful prosthetic joints*

Patient no.	Replaced Joint	Onset of symptoms from date of surgery (months)	Scan date from symptom onset (months)	Date of diagnosis from time of scan (months)	Criteria used and Diagnosis (months)
1	Left UKR	12	11	14	(C,R) Loose
2	Left THR	120	35	0	(C,R) Unstable, torn muscle, broken wires
3	Right TKR	0	18	11	(C,R,S) Neuroma
4	Right hip hemi-arthroplasty	44	6	9	(C,R,S) Trochanteric bursitis, iliotibial tract failure
5	Right TKR	8	13	16	(C,R) Patellar arthropathy
6	Left TKR	2	12	4	(C,R,S,M) Unstable, loose
7	Left TKR	2	1	10	(C,R) Lumbar referred pain

Patient no.	Replaced Joint	Onset of symptoms from date of surgery (months)	Scan date from symptom onset (months)	Date of diagnosis from time of scan (months)	Criteria used and Diagnosis (months)
9	Left TKR	65	5	12	(C,R,S,M) No diagnosis
10	Right TKR	24	22	6	(C,R,M) Infection
11	Left TKR	0	36	10	(C,R,S,M) Loose
12	Right TKR	4	2	5	(C,R) Neuroma
13	Right TKR	21	5	23	(C,R,S,M) Referred pain
14	Right TKR	23	11	6	(C,R,S,M) Loose
15	Right TKR	96	2	1	(C,R) No diagnosis. Improved after steroids
16	Bilateral THR	30	1	11	(C,R,S,M) Bilateral iliopsoas tendinitis
17	Right TKR	42	3	0	(C,R) Unstable

Patient no.	Replaced Joint	Onset of symptoms from date of surgery (months)	Scan date from symptom onset (months)	Date of diagnosis from time of scan (months)	Criteria used and Diagnosis (months)
19	Right UKR	6	22	5	(C,R,S,M) Loosening
20	Right hip resurfacing	0	30	6	(C,R,S,M) Pseudotumour
21	Left THR	0	25	N/A	(C,R) No diagnosis
22	Right hip resurfacing	15	1	3	(C,R) Aseptic loosening
23	Left TKR	0	37	26	(C,R,S,M) ?Aseptic loosening
24	Left TKR	N/A	N/A	20	(C,R,S,M) ?aseptic loosening
25	Right THR	39	1	30	(C,R) Trochanteric bursitis
26	Left THR	24	50	4	(C,R) Loose acetabular cup
27	Right UKR	16	13	16	(C,R) Aseptic loosening

Note. Key: C = Clinical, S = Surgical, R = Radiological, M = microbiological, RA = Rheumatoid Arthritis, THR = total hip replacement, TKR = total knee replacement, UKR = unicompartmental knee replacement

The early diagnosis of septic periprosthetic loosening is vital for successful therapy (149) as less invasive treatment may only be feasible in patients with a less than a 3 week duration of infection (149). Furthermore, a delayed diagnosis can result in reduced joint function, worsening morbidity and the requirement for more complicated or repeated surgery (150, 151), but selected patients may benefit from less aggressive surgery (151).

Although causality for the lengthy diagnostic period for painful joint prostheses has not been identified in this study, possible contributory factors include multiple imaging and non-imaging tests, often at different hospital sites and interspersed with multiple clinic appointments under different doctors. Furthermore, disagreements in image interpretation even between expert readers can lead to additional diagnostic difficulty (152). Surprisingly, there is no data regarding medicolegal cases for delayed diagnosis of painful joint prostheses. However, recent reviews confirm that leg-length discrepancy is the commonest reason given for patient discontent and medicolegal action in hip arthroplasty (153) and that the use of patient-specific instrumentation increases the exposure to malpractice suits (154).

No single diagnostic test for painful joint prostheses achieves all the ideal qualities of high levels of accuracy, safety, ready availability, cost-effectiveness as well as widespread acceptance (152). Imaging investigations therefore often rely on algorithms or a combination of tests. Multiple investigations may result in additional healthcare costs and consequently delayed diagnoses (155). Patients that initially present with vague medical symptoms may result in misdiagnoses, delayed diagnoses and repeated hospital visits may occur (156). A positive test does not necessarily satisfy criteria of a gold standard test as false-positive and false negative results are possible. However, many clinicians still assume that positive tests with positive clinical features of infection constitute a positive gold standard, and also that patients with no clinical evidence of infection and

negative test results constitute the negative gold standard (157). It is well understood that when single tests or investigations yield non-specific results which are singly insufficient to confirm a diagnosis, clinicians frequently to resort to the use of a panel of investigations, often combining several clinical, radiological and pathology investigations to reach a final diagnosis (158). The combination of positive test results from either of more than one diagnostic study caries more clinical weight than a single test by improving test sensitivity but this may also result in a modest reduction in test specificity (159). In addition, the combination of data from anatomical and functional data sources can yield significantly higher sensitivity and specificity than scanning performed with either technique (160). However, there are disadvantages to the routine use of multiple investigations which can result in increased cost of patient care as well as increasing patient's radiation exposure. For example, radiation doses from a CT scan of the pelvis and knee with give a dose of 6 mSv and 1 mSv respectively, while the dose from a knee radiograph is 0.001 mSv (161). Our retrospective study has shown a significant time lag between symptom onset and diagnosis of up to three and a half years.

Developing a single imaging test that combines high end functional and anatomical data, such as in ^{18}F-NaF PET-CT may provide accurate diagnostic information. Challenges with the use of ^{18}F-NaF PET include the scarce availability of PET-CT scanners and PET-CT experts; relative high cost and scarcity of ^{18}F-NaF isotope; short half-life of ^{18}F; artefacts from prostheses on CT and PET. Some of these challenges will be addressed and solutions proposed over the coming chapters. In complicated joint prostheses, there is a direct relationship between delayed diagnosis and patient morbidity. Delayed diagnosis often results in a reduction in the preservation of joint function, worse outcomes and also leads to increased healthcare costs (162) because there is a limited time for successful implant treatment with retention following prosthetic joint infections (163).

Critical analysis of this retrospective study indicates that although researchers generally prefer prospective studies over retrospective studies, the follow-up period with retrospective studies which goes forward in time can make retrospective studies epidemiologically similar to prospective studies (164).

Notwithstanding that the diagnosis of the cause of the painful prosthetic joint was clearly defined as the research end point, further flaws originated from the retrospective design and the absence of a control group. The lack of a control group made it difficult to identify potential confounding factors resulting in bias. In addition, the short study period of 3 months resulted in a small and limited sample size which could potentially undermine the value of the results, decrease statistical power and potentially lead to Type II error skewing. However, the findings from this spot check demonstrated what has always been suspected and to prolong the study would not have demonstrated any further benefit in spite of wasting time and resources. Further limitations of the study include selection bias because only symptomatic joint prostheses referred for isotope bone scans were included in the study. Lastly, reduced statistical power of the study was caused by the limited number of gold standard microbiological tests. Positively, the retrospective data collection in this study and reliance on clinical notes, laboratory reports as well as radiology reports was an inexpensive and a quick method of testing the hypothesis with already existing data. The study did not introduce observer variability and no technical difficulty was encountered. Newly identified knowledge suggests a possible association between referrals for dynamic isotope bone scans and diagnostic delays of up to 121 months in patients with painful joint prostheses. This is important with the current rising trend in usage of multimodality imaging in nuclear medicine and there is a role for further research in this field.

2.8 Conclusion

In patients with painful joint prostheses that are investigated with dynamic isotope bone scans the length of time from symptom onset to diagnosis ranges from 2 months to 121 months with an average of 42.9 months. This small series demonstrates that delays do exist in diagnosing painful joint prostheses. Factors including the use of multiple non-imaging tests including the use of anatomical imaging modalities as well as functional imaging modalities contributed to the delays in reaching a diagnosis, further adding to diagnostic delay. The

retrospective study indicated that a streamlined reduced number of imaging tests may contribute to an improvement in the speed of diagnosing painful joint prostheses. Fused functional anatomical imaging may also solve or reduce the need for repeated hospital visits for multiple imaging tests in the investigation of painful joint prostheses. The diagnostic delays do not imply causation as a result of the number of investigations ordered.

2.9 Summary

- There are diagnostic delays in diagnosing painful joint prostheses.
- Multiple non-imaging tests are usually combined with anatomical imaging modalities as well as functional imaging modalities to reach a diagnosis
- Fused functional anatomical imaging may form part of the solution to the diagnostic delay in the investigation of painful joint prostheses.

Chapter 3 The Role of ^{18}F-NaF PET in Diagnosing and Distinguishing Between Aseptic Loosening and Septic and Aseptic Loosening in Hip and Knee Prostheses; a Systematic Review of the Evidence (41)

3.1 Abstract

Background: Joint replacement surgery is an important and commonly used intervention for severe arthritis. Implant failure is a cause of morbidity for patients who have undergone joint arthroplasty. Determining the cause for failure is fundamental to the further management of such patients. Amongst the most important causes for failure include infection and aseptic loosening. Differentiating between these two conditions is problematic using clinical and biochemical tests. Novel radiological techniques such as SPECT-CT and PET-CT have been increasingly used to differentiate between these two problems.

Method: A systematic review of MEDLINE, EMBASE (University of Warwick Encore) and Cochrane library database was undertaken to identify diagnostic studies of sodium fluoride (^{18}F-NaF) Positron Emission Tomography (PET) in joint prostheses to diagnose loosening and/or infection.

Results: The review identified 3 prospective studies (Figure 5) that met the inclusion criteria. The selected studies consist of a total number of 94 patients (these included 110 joints). There were 96 hips and 14 knees, of which 35 were asymptomatic and 65 joints were symptomatic. Only one study differentiated aseptic loosening from infection. A weighted average of sensitivity and specificity of the different studies was determined. The sensitivity of ^{18}F-NaF PET in identifying prosthetic infections was found to be 97.04%; The weighted specificity, positive predictive value (PPV), negative predictive value (NPV) and accuracy were 88.11%, 84.68%, 98.82% and 87.33% respectively.

Conclusion: Sodium fluoride positron emission tomography ^{18}F-NaF PET is a promising tool with high sensitivity and specificity in the assessment of joint replacements, but it possibly will be of limited use before the ninth post-surgical month. However, this can be overcome by routinely imaging 'at risk' prostheses at three month intervals for the detection of abnormal rates of decline in periprosthetic ^{18}F-NaF uptake. The CT component in ^{18}F-NaF PET-CT may add further diagnostic value.

3.2 Background

There is an increasing trend to apply hybrid imaging in the investigation of painful joint prostheses, often employing SPECT-CT, which combines the high resolution of CT and the functional sensitivity of Single Photon Emission Tomography (SPECT) (165). Attempts have been made to employ PET-CT to identify aseptic loosening and infection with ^{18}F-Fluorodeoxyglucose (FDG) and Sodium Fluoride ^{18}F-NaF (71, 166). Sodium fluoride metabolism uptake in bone is reliant on the rate of blood flow, which is the rate-limiting step and most of the sodium fluoride delivered is retained by bone after a single pass of blood (68). The 1st pass rate varies among different bone components (68), i.e., the degree ^{18}F-NaF uptake in bone marrow is negligible when compared with the bony cortex levels (68). The second factor that affects ^{18}F-NaF tracer bony uptake is the rate of bone turnover (167). ^{18}F-NaF bone uptake is dependent on the exchange of fluoride ions with hydroxyl ions in hydroxyapatite crystal to form fluorapatite (167). ^{18}F-NaF is freely diffusible across membranes and one hour after injection, only 10% of ^{18}F-NaF remains in plasma.^{18}F-NaF is rapidly cleared from plasma and excreted by the renal system following glomerular filtration and tubular secretion (68, 168).

The aim of this study is to perform a systematic review of the literature to evaluate the capacity of sodium fluoride (^{18}F-NaF) positron emission tomography (PET) in distinguishing between septic and aseptic failure in hip and knee replacements. This is intended as a scoping exercise and literature review of the role of PET-CT in joint prostheses imaging and should also

demonstrate the evidence for PET-CT in distinguishing between these two causes of failure.

3.3 Methodology

3.3.1 Study Design

A systematic review of the literature was undertaken according to the methods described in the Cochrane Handbook for Systematic Review of Interventions. The PRISMA (Preferred Reporting Items for Systematic Reviews and Meta-Analyses) guidelines were adopted for all literature to date at the time of reporting (2015) but a small number of studies returned.

3.3.2 Research Question

What is the evidence for use of sodium fluoride PET in differentiating between septic and aseptic failure of hip and knee replacements.

3.3.3 Inclusion Criteria

Prospective studies in humans that reported data on sodium fluoride in joint prosthesis imaging to diagnose loosening and/or infection.

3.3.4 Exclusion Criteria

Studies were excluded where other isotopes other than sodium fluoride were used. Studies were limited to English language and filters for human studies and clinical trials were applied.

3.3.5 Search Strategy

Studies were identified using MeSH terms and keywords in MEDLINE, EMBASE, Cochrane and Dynamed. 133 studies were excluded at title and abstract, 1 was excluded at full paper review. No paper was added after review of the references.

PubMed MESH search terms -(((((((((infection) OR sepsis) OR loosening) OR aseptic loosening) OR osteolysis)) AND ((((prosthesis) OR joint replacement) OR knee replacement) OR hip replacement)) AND ((((((sodium fluoride) OR

fluoride) OR fluorine) OR NaF) NOT FDG) NOT fluorodeoxyglucose))) NOT dental. See table 3 for full search builder.

Two independent authors checked all data used in the analysis. When disagreements arose, these were resolved by consensus. Initially, the title and abstracts were reviewed. Potentially relevant papers were then reviewed in their entirety. The references cited by each potentially relevant paper were scrutinized in order to locate additional potentially relevant papers.

3.3.6 Statistics

The summative weighted sensitivities and specificities were calculated from the data extracted.

3.4 Results

Following the extraction of data (Figure 5), 3 studies were selected which satisfied the required characteristics. Data was extracted from each study and is summarised in Table 6. The review identified 3 prospective studies (169-171) that met our search criteria. A flow diagram of systematic review methodology resulted in a final 3 prospective studies (Figure 5) which satisfied the required characteristics and which were selected. The selected studies consist of a total number of 94 patients with 110 joint replacements (Table 6). There were 96 hips and 14 knees, of which 35 were asymptomatic and 65 joints were symptomatic. Only one study differentiated aseptic loosening from infection (169). Minimum time from surgery varied from 3 months to just over 12 months. Twenty two patients were followed up surgically while the remaining patients were followed up clinically for periods varying from 6 months to 12 months. A weighted average of sensitivity and specificity of the different studies was determined (Table 7). The sensitivity of ^{18}F-NaF-PET in identifying prosthetic joint infections was found to be 97.04%; this was calculated from the weighted average sensitivity from the 3 different studies. The weighted specificity, PPV, NPV and accuracy were 88.11%, 84.68%, 98.82% and 87.33% respectively. Of the 3 studies, Sterner et al (23) reported the lowest specificity.

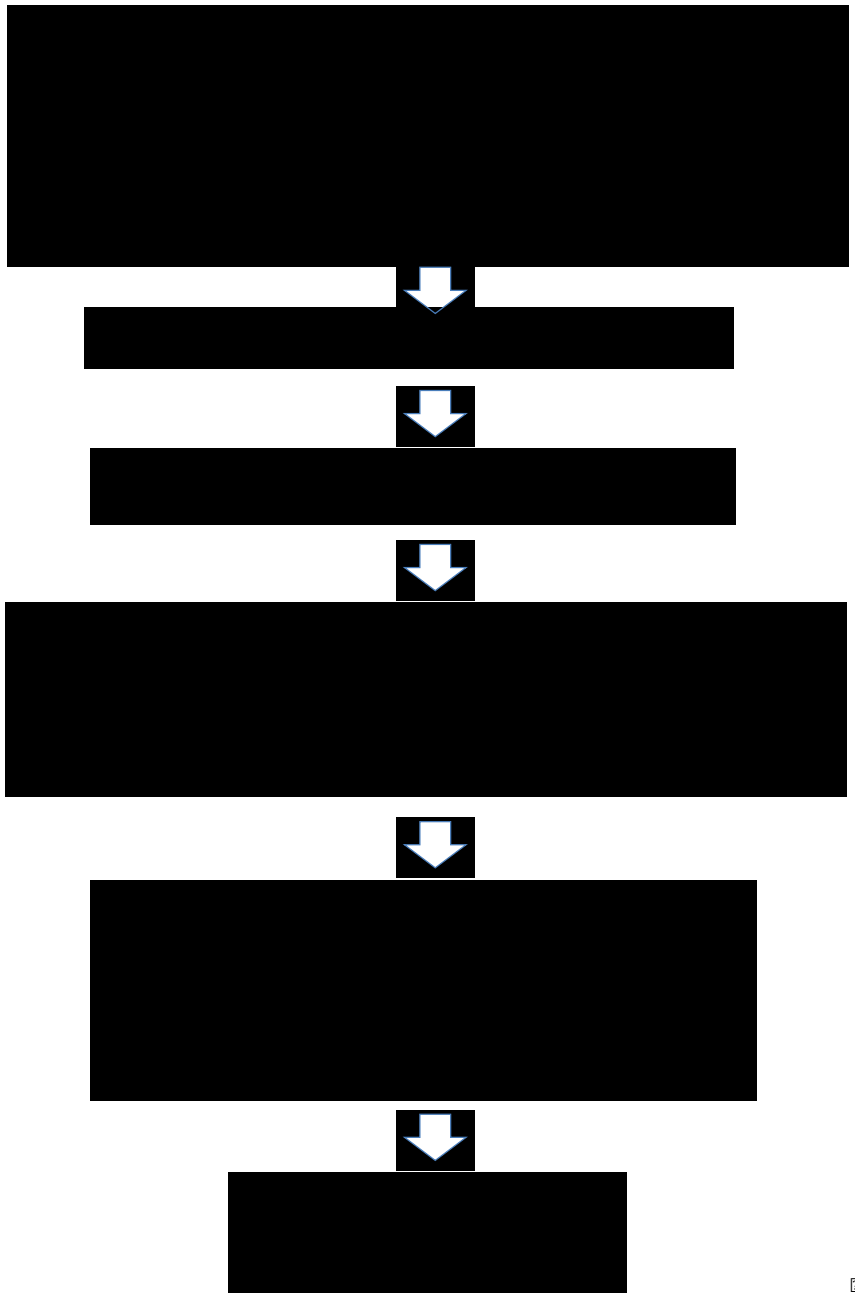

Figure 5. *Flow diagram of systematic review methodology examining evidence for use of Sodium Fluoride PET in differentiating between septic and aseptic failure of hip and knee replacements*

Table 6. *Summary of included studies of Sodium Fluoride PET in differentiating between septic and aseptic failure of hip and knee replacements*

Authors	Kobayashi N et al	Sterner et al	Creutzig H
Year	2011	2007	1976
Patients	49	14	31
Gender (M/F)	N/A	9/6	N/A
Hip joints	65	0	31
Knee joints	0	14	0
Symptomatic joints	38	14	13
Control group	Yes	No	Yes
Asymptomatic	27	0	18
Minimal time from surgery	12 months	13 months	3 to 9 months
Minimal clinical follow-up	12 months	6 months	12 months
Surgical follow-up	11	6	5
Differentiate aseptic loosening	Yes	No	No

Table 7. *Results from the included studies examining evidence for use of Sodium Fluoride PET in differentiating between septic and aseptic failure of hip and knee replacements*

Authors	Kobayashi N et al	Sterner et al	Creutzig H
Patient (joints)	49 (65)	14 (14)	31 (31)
TP	36	5	13
TN	23	5	14
FP	6	4	4
FN	2	0	0
Sensitivity, %	95	100	100
Specificity, %	88	56	78
PPV, %	95	56	76
NPV, %	98	100	100
Accuracy, %	91	71	87

3.5 Discussion

The value of fluoride in bone imaging was first recognised by Monte Blau and team in 1962 (65, 66). Hans Creutzig in Hannover, then in West Germany, was the first to demonstrate the importance of ^{18}F-NaF PET in joint prosthetic infection in 1976 with 31 THR (171). He also mapped the comparable normal periprosthetic pattern of both ^{99m}Tc-HEDP and ^{18}F-NaF uptake in the post-surgical period from 3 to 12 months using uptake ratio in both symptomatic and asymptomatic prostheses. NaF uptake levels are said to be similar to levels of HEDP (170). The ratios were found to decline rapidly (Figures 6 & 7) and reach a nadir at 6-9 months following surgery with more rapid decline demonstrated in the femoral component (171). Interestingly, departures from this normal pattern of decline preceded the development of symptoms in patients with bone and soft tissue infections (171). In this study, the distinction between aseptic loosening and infection was unclear (171). Images were acquired 3 hours after the injection of 148 MBq of ^{18}F-sodium fluoride. Relatively poor quality images from using coincidence imaging and a 5"-rectilinear scanner may have accounted for inability to distinguish soft tissue infection from bone infection (171). The 3 hour uptake period would also have been detrimental, because early high target-to-background ratios in result in peak bone uptake levels around 45–60 minutes after radioisotope injection (68). At 60 minutes after radioisotope injection, only 10% of ^{18}F-Fluoride remains in plasma due to negligible plasma protein binding, rapid blood and renal clearance, and high bone uptake (68).

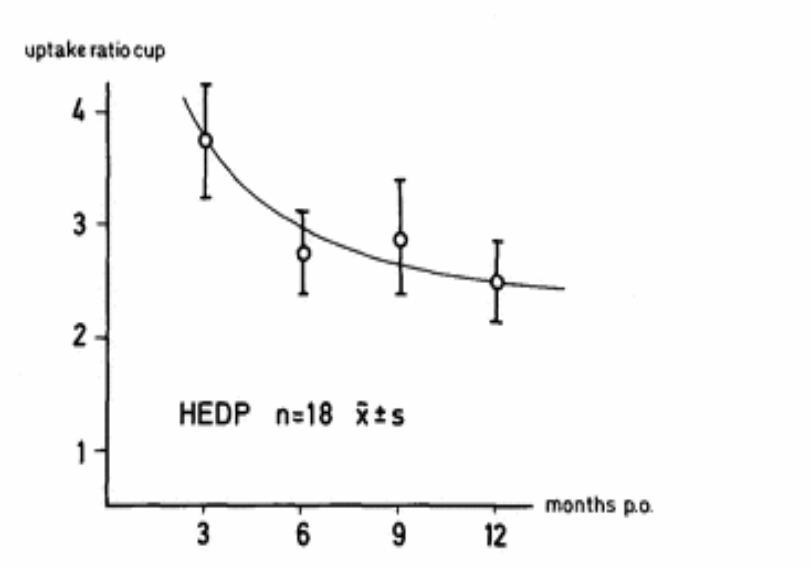

Figure 6. *Graphical representation of HEDP bone scan uptake ratio over the cup plotted against the number of months after joint replacement surgery in patients without complications.*

Note: This has been adapted from Creutzig H. Bone imaging after total replacement arthroplasty of the hip joint. A follow-up with different radiopharmaceuticals from Eur J Nucl Med. 1976 Aug 12;1 (3):178 with kind permission from Springer Science + Business Media B.V.

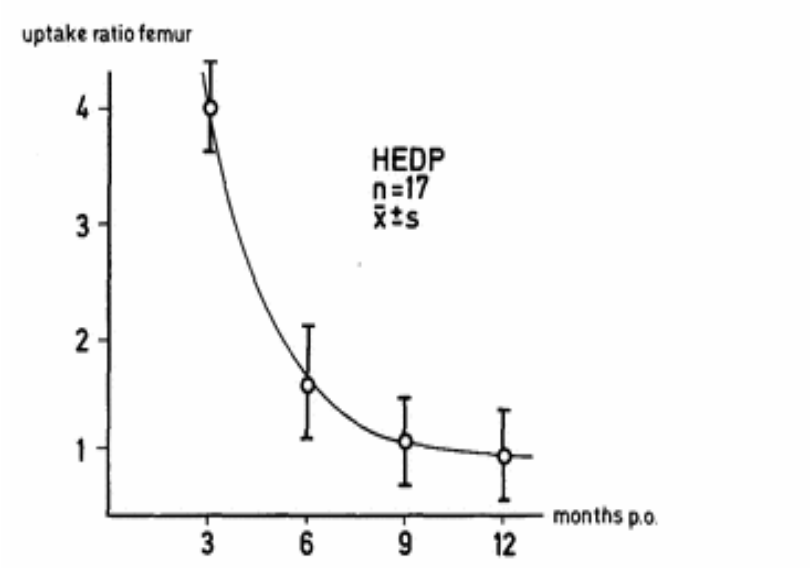

Figure 7. *Graphical representation of HEDP bone scan uptake ratio over the thigh plotted against the number of months after joint replacement surgery in patients without complications.*

Note: This has been adapted from Creutzig H. Bone imaging after total replacement arthroplasty of the hip joint. A follow-up with different radiopharmaceuticals from Eur J Nucl Med. 1976 Aug 12;1 (3):178 with kind permission from Springer Science + Business Media B.V.

Thomas Sterner performed the only prospective study with the use of ^{18}F-NaF in imaging knee prostheses, but no attempt was made to differentiate aseptic loosening from infection (170). 14 symptomatic knee prostheses were examined and no control group was employed. Of these 14 patients, 6 underwent surgery for confirmation of the imaging findings and the other 8 were followed up clinically for 6 months. The relatively low specificity in this study may have arisen from several factors including the fact that this the study included only knees, the sample size was relatively small and finally that even intermediate levels of periprosthetic uptake were regarded as positive for aseptic loosening or infection (170). Sterner et al also regarded the scan as abnormal if (a) there was relatively more uptake in the prosthesis/bone interface than in normal/bone/soft tissue or contralateral asymptomatic prostheses, (b) the increased uptake included half the bone/metal interface in the femoral component; or (c) if the tibial stem in the tibial component was involved.

Furthermore, they discovered that the use of semi-quantitative analysis with standardized uptake values (SUVs) yielded no added value (170). Image quality in this study was bound to be better because the authors employed an ECAT-Exact HR+ (Siemens Medical Systems) PET scanner 1 minute and 60 minutes after the injection of 350MBq of ^{18}F-Fluoride (170).

In 2011, Naomi Kobayashi et al published a prospective study of ^{18}F-NaF PET in 65 hip prostheses; to date, this has been the only prospective trial which differentiated aseptic loosening from sepsis (169). Images were acquired 40 minutes after injection of 185 MBq of ^{18}F-Fluoride using a SET 2400W device (Shimadzu, Kyoto, Japan). She was able to distinguish between normal, aseptic loosening and infected prostheses. The first method involved measuring the degree of ^{18}F-Fluoride uptake in periprosthetic tissues (SUVmax). Average values for the normal, aseptic and septic loosening prostheses were estimated to be 4.9 $\pm$ 2.5, 8.1 $\pm$ 2.9, and 10.5 $\pm$ 3.4, respectively (169). When a threshold SUVmax of 6.9 is applied for diagnosis of infection, the test had a sensitivity and specificity of 81% and 80% respectively (169). Furthermore, when a threshold SUVmax of 4.9 is applied for aseptic loosening, the test yields a sensitivity and specificity of 95% and 82% respectively (169). PET images were also analysed for the pattern and distribution of ^{18}F-Fluoride PET uptake and categorised into 3 types. Type 1 uptake showed no significant ^{18}F-Fluoride uptake; Type 2 uptake shows mild localized uptake on the cup side or stem. Type 3 pattern of uptake demonstrates significant uptake which extends through more than half of the bone-implant interface (169). 96% of Type 1 uptake cases were normal, 80% of Type 2 pattern were due to aseptic loosening and 95% of Type 3 pattern cases were due to infection (169). The final diagnosis of infection was obtained by a combination of microbiologic culture, histopathology and polymerase chain reaction (PCR) analysis of bacterial DNA with 2 different primer and probe sets, one specific for the detection of methicillin-resistant staphylococcus and another for broad-range detection by universal PCR that targets a part of 16S rDNA gene, with increased sensitivity (169, 172). Many polymerase chain reactions that detect the universal 16S rRNA bacterial gene have problems with false-positive results due to necrotic bacteria detected by polymerase chain reactions (173). The clinical importance of positive results in the absence of other clinico-

pathologic and radiological features of infection is of uncertain significance, but specificity can be improved by combining a universal polymerase chain reaction with subsequent bacterial sequencing (173).

Critical analysis of this systematic review which collated, assessed and synthesised evidence from 3 previous experiments in order to demonstrate the role of ^{18}F-NaF PET in diagnosing and distinguishing between septic and aseptic loosening in hip and knee prostheses shows that the study did not combine numerical data from the 3 separate studies. Furthermore, the studies did not meet the criteria for randomized controlled trials which have higher levels of evidence. Therefore, the study does not meet the criteria for a meta-analysis. The main limitations of this study include the heterogeneity of the systematic review which included studies from 2 continents over a period lasting more than 35 years. The study is also limited by the small number of 3 papers which reduces the statistical significance of its findings. The small number of studies which resulted from using the PRISMA guidelines may inadvertently increase the likelihood of reporting bias and evidence selection bias. The study was also susceptible to biases arising in all the included primary studies. The first and second papers had 2 blinded observers hence reducing intra-observer variability. However, the third paper made was not read by dual blinded observers hence introducing intra-observer variability. Newly identified knowledge suggests that sodium fluoride positron emission tomography (^{18}F-NaF-PET) is a promising tool in diagnosing and distinguishing between septic and aseptic loosening in joint prostheses; with a high sensitivity and specificity after the ninth post-surgical month. In addition, routine ^{18}F-NaF-PET imaging of high risk prostheses at three month intervals may be beneficial.

3.6 Conclusion

Our small series demonstrates that Sodium fluoride positron emission tomography (^{18}F-NaF-PET) is a promising tool in diagnosing and distinguishing between septic and aseptic loosening in joint prostheses. It demonstrates high sensitivity and specificity in the assessment of joint replacements after the ninth post-surgical month. Routine imaging of 'at risk' prostheses at 3 month intervals for the detection of abnormal rates of decline in periprosthetic ^{18}F-NaF uptake may overcome this problem. The CT component in ^{18}F-NaF PET-CT also adds diagnostic value.

3.8 Summary

- Sodium fluoride positron emission tomography ^{18}F-NaF PET has a promising role in the assessment of joint replacements after the ninth post-surgical month.
- The sensitivity and specificity of ^{18}F-NaF PET in the assessment of joint replacements is low in immediate post-surgical period.
- The CT component of ^{18}F-NaF PET-CT may add further diagnostic value.

Chapter 4 The Promising Role of Dynamic ^{18}F-NaF PET-CT in Diagnosing Symptomatic Joint Prostheses (78)

4.1 Abstract

Background: There is an increasing number of lower limb arthroplasties and multiple imaging modalities are often used in the investigation of painful joint prostheses. Research into decreasing the time and cost of investigations is required and the purpose of this study was to test the feasibility of dynamic ^{18}F-NaF PET-CT in order to establish proof of principle as a case study for the use of in the assessment of knee and hip prostheses.

Method: Approval was granted by the research ethics committee and informed consent was obtained. A patient with bilateral knee prostheses (1 symptomatic/painful and 1 asymptomatic) was scanned with dynamic ^{18}F-NaF PET-CT. In addition, knee aspirate was obtained from the asymptomatic knee and serum C-reactive protein and erythrocyte sediment rate levels as well as a peripheral white cell count were obtained and then a 12 month clinical follow up. The images were interpreted as normal, aseptic loosening or sepsis as defined by the hypothetical graphical pattern of tracer uptake produced at the bone–prosthesis interface. A final diagnosis was made by a combination of joint aspiration microbiology and clinical follow-up for 1 year in addition to C-reactive protein and erythrocyte sediment rate levels as well as peripheral white cell count. ^{18}F-NaF PET results also were compared with 3-phase dynamic bone scan results and plain radiographs.

Results: The dynamic ^{18}F-NaF PET-CT scan revealed no significant uptake in the asymptomatic right knee and increased uptake in the symptomatic left knee with an aseptic loosening pattern. The degree of uptake in the symptomatic joint exceeded background levels and also exceeded levels of uptake in the asymptomatic knee. The pattern of uptake and curve slope in both the

asymptomatic and symptomatic joints matched the pattern of uptake in our hypothesis based on the understood pattern of uptake in dynamic bone scans. The imaging aseptic pattern corresponded with the absence of infection in blood tests as well as microbiological cultures and the histopathological examination of the periprosthetic membrane.

Conclusion: Diagnostic quality dynamic ^{18}F-NaF PET-CT images with graphical data from symptomatic joint prostheses can be acquired and archived successfully. ^{18}F-NaF PET-CT can detect aseptic loosening of lower limb prostheses and dynamic ^{18}F-NaF PET-CT may be more useful than 3 phase bone scans in the assessment of painful hip and knee prostheses but more research is required.

4.2 Introduction

The feasibility of dynamic ^{18}F-NaF PET-CT was assessed as an imaging tool for investigating symptomatic joint prostheses in a single case study. This is an important area of research in order to reduce time and cost of investigations by reducing the number of imaging tests (128). In addition, the importance of this is highlighted by the fact that there is an increasing number of lower limb arthroplasties (174).

4.3 Aim

The aim was to test the hypothesis that dynamic ^{18}F-NaF PET-CT is feasible and that dynamic ^{18}F-NaF PET-CT may be used to diagnose symptomatic joint prostheses by employing the graphical uptake pattern of ^{18}F-NaF in the periprosthetic region (Figure 8). This is intended as a scoping exercise and literature review of the role of ^{18}F-NaF PET in joint prosthesis imaging.

4.4 Research Question

Is dynamic ^{18}F-NaF PET-CT a feasible test and can diagnostic quality dynamic ^{18}F-NaF PET-CT images with graphical data be acquired and archived successfully from symptomatic joint prostheses?

4.5 Materials and Methods

Our patient was a 72 year old female with a painful left knee total knee replacement studied with dynamic ^{18}F-NaF PET-CT. She had undergone routine clinical and laboratory studies for the evaluation of painful prostheses, in addition to the dynamic ^{18}F-NaF PET-CT scan. The ^{18}F-NaF PET-CT scan was obtained more than 12 months after joint replacement surgery. The interval between arthroplasty and PET-CT was 8 years. The patient gave written informed consent for the study.

Dynamic ^{18}F-NaF PET-CT images were acquired using a GE Discovery ST with 16 slice CT (GE Healthcare®) volume imaging protocol (ViP) (175). The patient fasted for at least 6 hours before receiving the injection. CT images of the joints were acquired, followed by dynamic PET image acquisition in list mode from the time of injection till 30 to 40 minutes after bolus intravenous administration of 250 MBq ^{18}F-NaF (175). The images were reconstructed using ordered-subset expectation maximization, and images were corrected for attenuation.

Image Interpretation – two experienced radiologists read the studies independently, and in the case of discrepancies, a consensus was reached following discussion. When an area of increased uptake was detected in the bone–prosthesis interface for either hip or knee arthroplasty compared with adjacent bone and soft tissue, the region of interest was assessed using time-activity curves with simple standardized uptake value (SUV) analysis and background subtraction (176).

Graphical interpretation was performed using our hypothesis to decide if there is a diagnosis of infection, aseptic loosening or neither (figure 8). The CT images

were analysed visually for malalignment by ruling out gross malpositioning of the prosthetic components and also assessing for periprosthetic fluid collections and ossified masses (106).

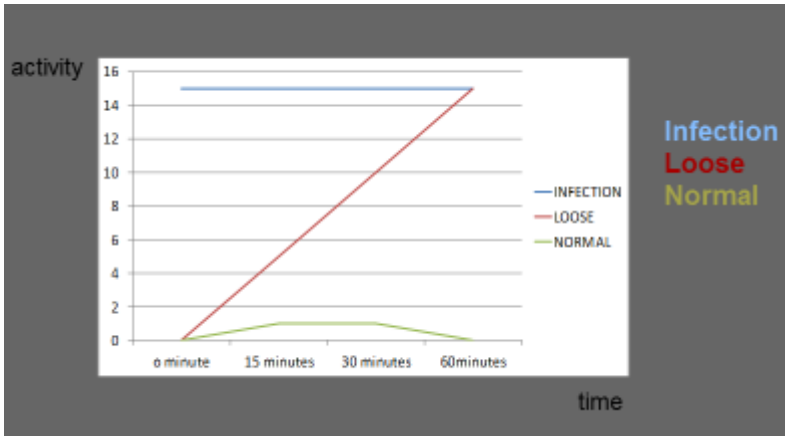

Figure 8. *Time-Activity-Curve of sequential multiphase ^{18}F-NaF PET-CT scan of joint prostheses*

Note: Sequential multiphase ^{18}F-NaF PET-CT Time-Activity-Curve in the dynamic Imaging of joint prostheses with expected appearances in dynamic ^{18}F-NaF PET-CT for infection (blue), loosening (red) and normal (yellow) Prostheses. The hypothetical graphical pattern images are based on the pharmacokinetics ^{18}F-NaF uptake in the body and at the bone–prosthesis interface (figure 8) (66, 67).

Follow-up - The final diagnosis was made by joint aspiration and clinical follow-up for 1 year. The arthroplasty would have been considered infected if aspiration cultures grew organisms, if infection was clinically obvious, if microbiological samples demonstrated infection with sensitivity of 72% (177), or elevated synovial neutrophils with sensitivities between 84 and 95% (177). Arthroplasties would be considered aseptic if the preceding investigations were negative and this was backed by normal C-reactive protein and erythrocyte sediment rate levels as well as a normal peripheral white cell count. Lastly, if an

arthroplasty does not require surgical exploration during the follow-up period it is considered to be uninfected.

4.6 Results

The dynamic ^{18}F-NaF PET-CT scan revealed no significant uptake in the asymptomatic right knee and increased uptake in the symptomatic left knee with aseptic loosening pattern (Figure 8). The degree of uptake in the symptomatic joint exceeded background levels and also levels of uptake in the asymptomatic knee. The pattern of uptake and curve slope in both the asymptomatic and symptomatic joints matched the pattern of uptake in our hypothesis based on the understood pattern of uptake in dynamic bone scans (Figure 8) (178). However, the difference in the size and also the dissimilar type of prosthesis is a confounding factor, i.e., larger symptomatic left total knee prosthesis and a smaller right asymptomatic unicompartmental prosthesis (Figures 9 and 10). The corresponding 3-phase bone scan (Figures 11 and 12) revealed delayed phase marked uptake in left femoral and tibial components in the symptomatic left knee only favouring aseptic loosening. The NaF PET-CT graphs showed a steeper slope and higher plateau of uptake in the symptomatic loose knee prosthesis, when compared with asymptomatic knee prostheses (Figure 13) as well as in the symptomatic loose knee prosthesis, when compared with left knee soft tissue background (Figure 14). The CT component revealed no gross malpositioning or abscess. The peripheral blood erythrocyte sedimentation rate (ESR) was 26 mm/hour (reference range 0-35); C-reactive protein (CRP) was 5 mg/L (reference range <11); total peripheral white blood cell count was 8.26 x 10^9 g/L (reference range 4-11); peripheral neutrophilic count was 4.85 x 10^9 g/L (reference range 2-7). The left knee aspirate and periprosthetic membrane were negative for pathogenic organisms on both microbiological cultures and the histopathological examination.

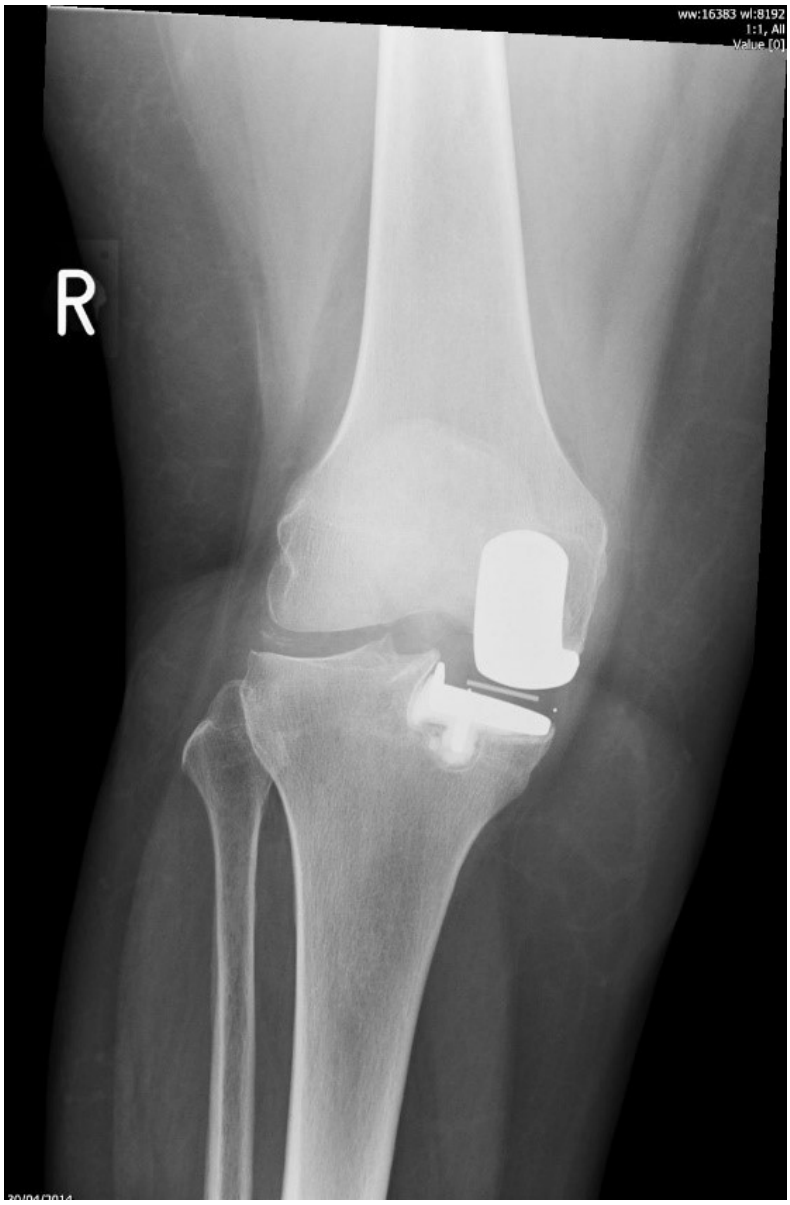

Figure 9. *Asymptomatic right knee radiograph with unicompartmental replacement*

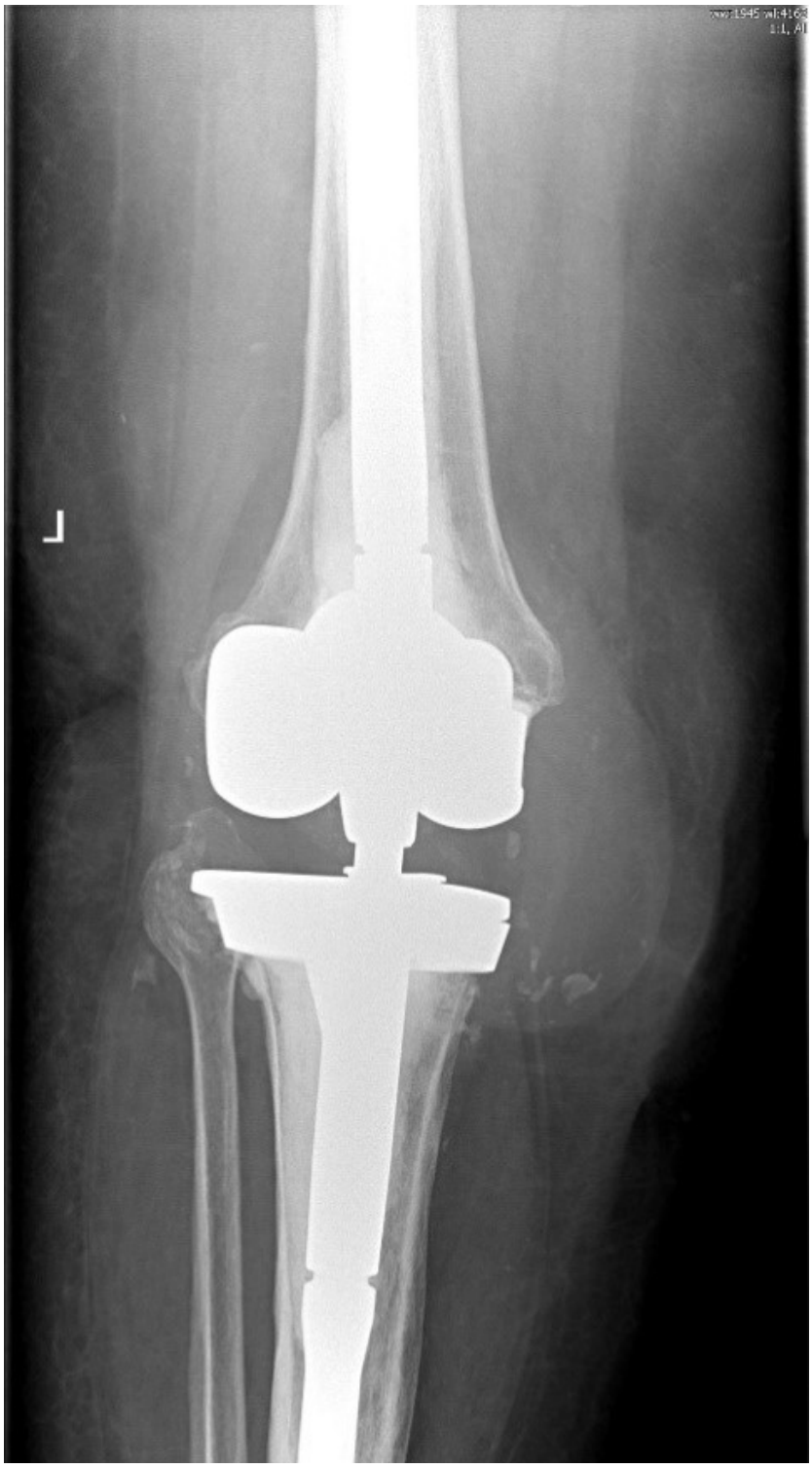

Figure 10. *Symptomatic left knee radiograph of total knee prosthesis* (the difference in size and types of prostheses is a confounding factor)

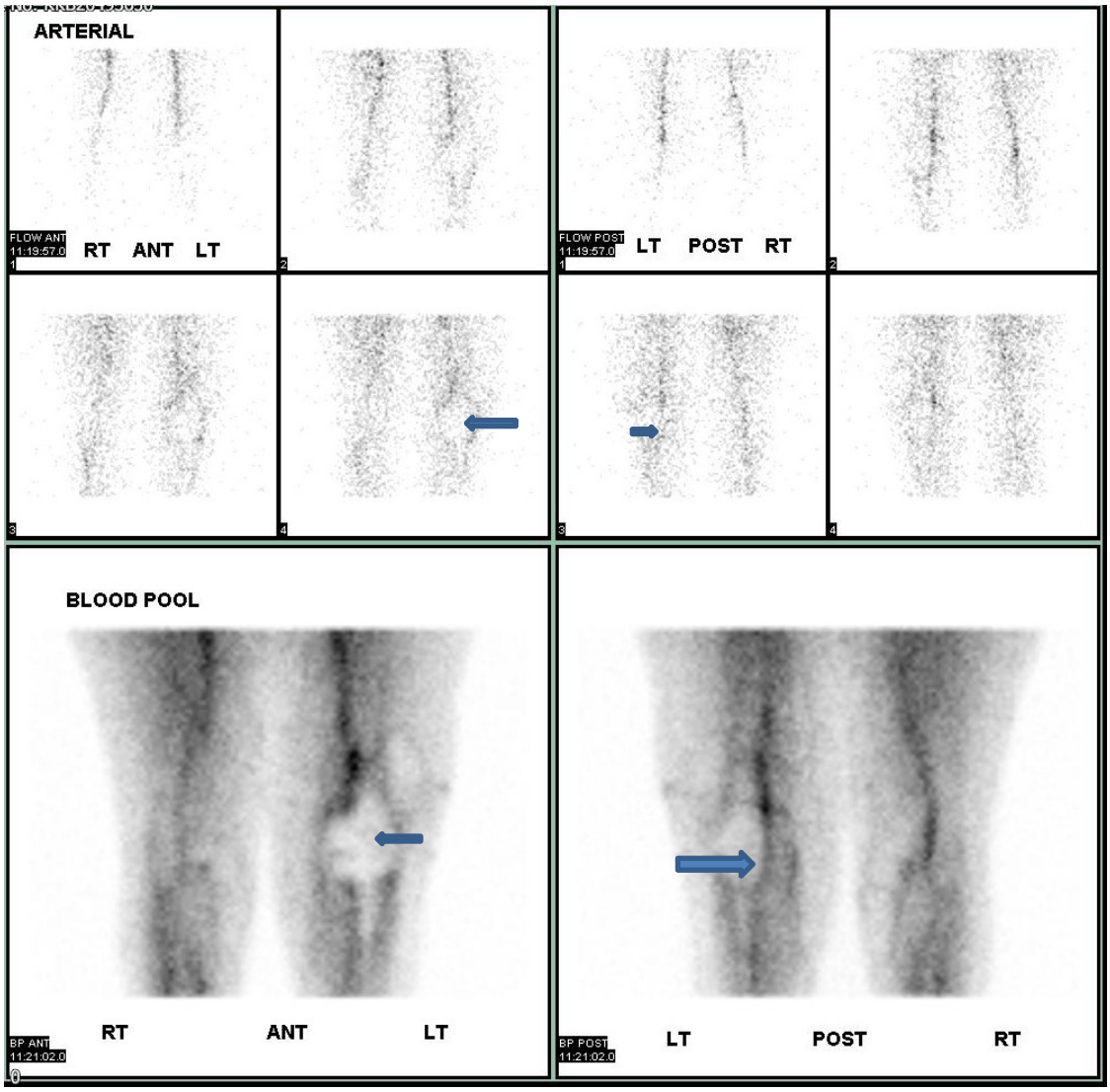

Figure 11. *Left total knee replacement on arterial and venous phase bone scan images*

Note: The blue arrows in the images shows minimally increased uptake in the symptomatic left knee prosthesis

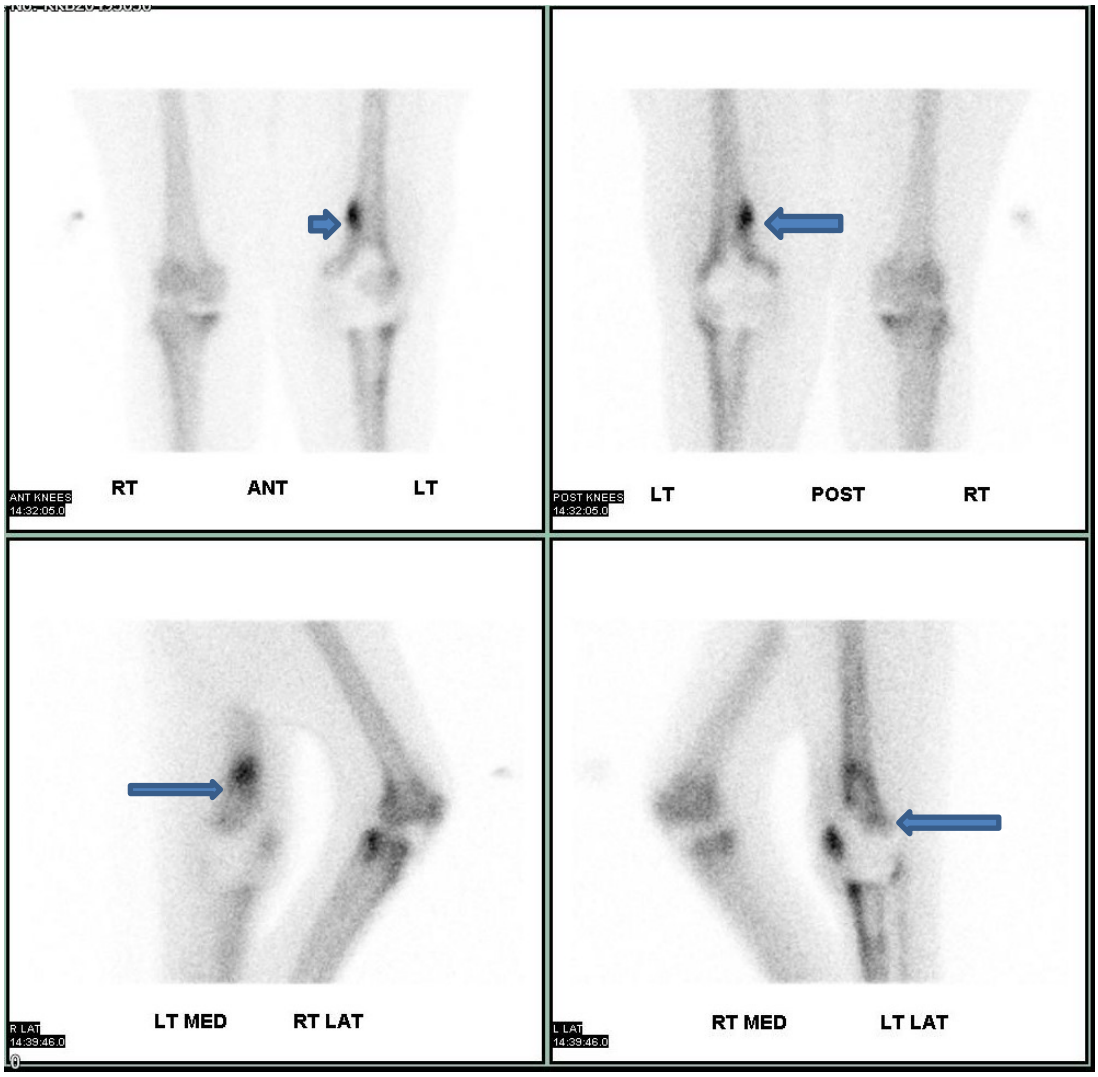

Figure 12. *Left total knee replacement on delayed phase bone scan images*

Note: The blue arrows in the delayed phase bone scan images shows marked uptake in left femoral and tibial components in the symptomatic left knee

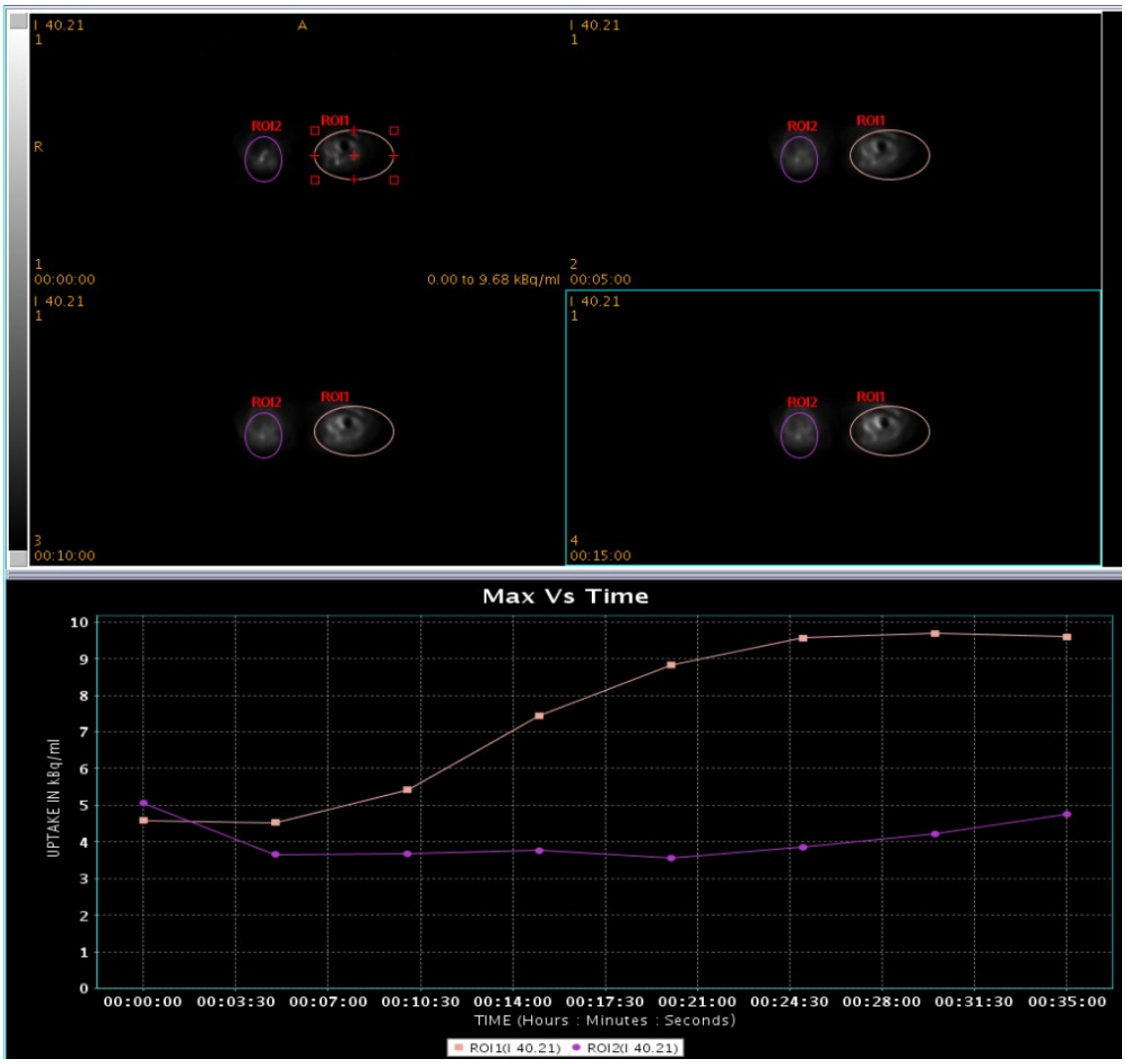

Figure 13. *Time-Activity-Curves NaF PET-CT scan (SUVmax vs Minutes)*

Note: This graph shows a gradual increase in the SUVmax levels in the symptomatic left knee (pink curve) which plateaus at 25 minutes versus no significant change in SUVmax levels of the right knee (purple curve).

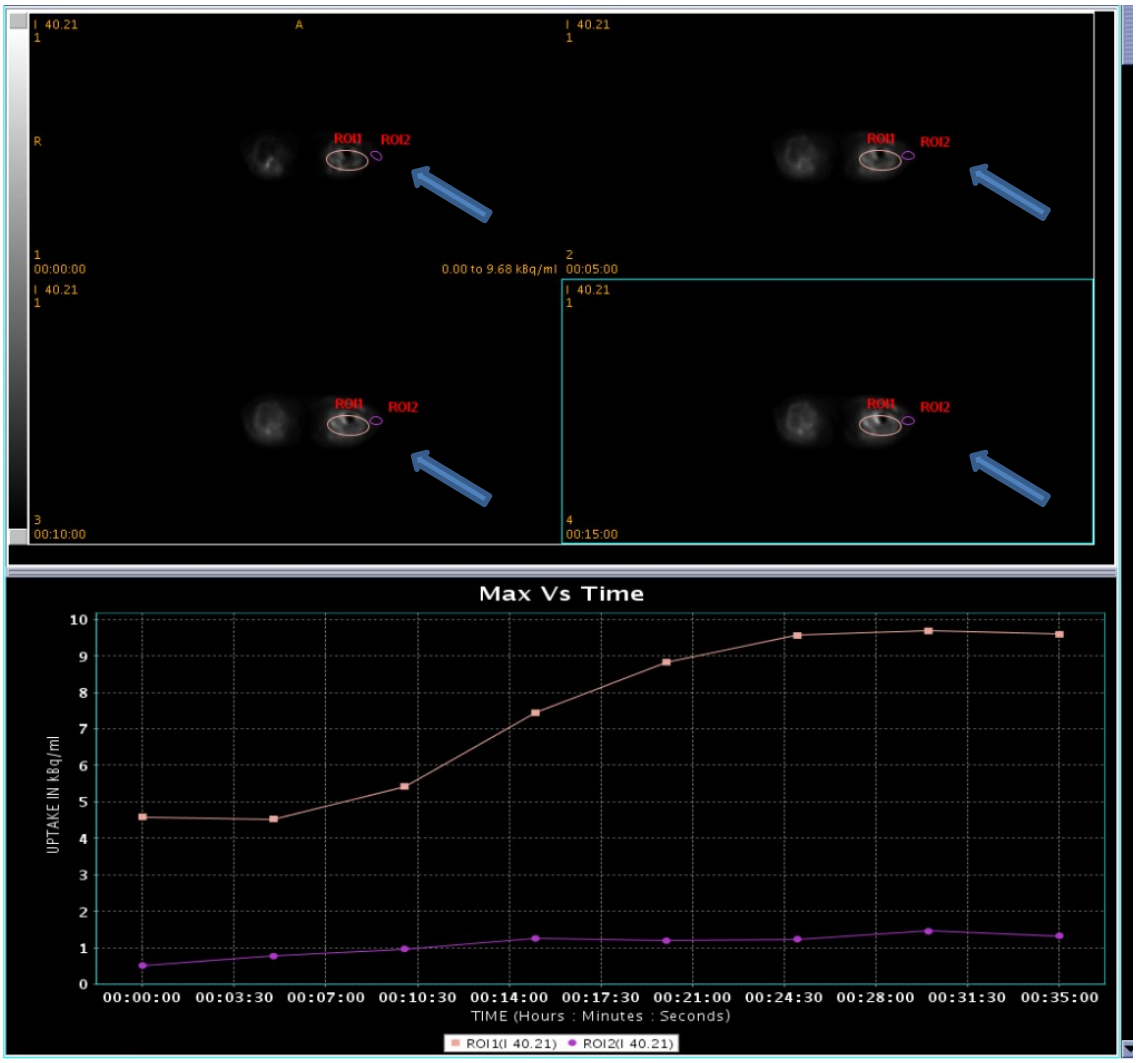

Figure 14. *Time-Activity -Curves NaF PET-CT scan (SUVmax vs Minutes)*

Note: This graph in a patient with confirmed aseptic loosening shows a gradual increase in the SUVmax levels in the symptomatic left knee (pink curve) which plateaus at 25 minutes versus soft tissue background (blue arrows) in the left calf muscle with no significant increase in SUVmax levels (purple curve)

The results from this patient who had a symptomatic left TKR and an asymptomatic right UKR demonstrate normal CRP, ESR, WCC as well as the knee aspirate and periprosthetic microbiology. The final diagnosis of the symptomatic left TKR was aseptic loosening and this was determined by imaging and long-term clinical follow up. The interval between surgery and ^{18}F-NaF PET-CT was more than 1 year. Further research is required to confirm this proof of concept for uptake of ^{18}F-NaF in painful prosthesis as well as clearly define the appearance of infection using this promising technique. One of the major advantages of ^{18}F-NaF PET-CT over conventional nuclear medicine techniques is the simplicity of the approach and the timely availability of results within an hour (174).

4.7 Discussion

^{18}F-NaF PET-CT has been used extensively for the detection of bone metastases. However, ^{18}F-NaF uptake is not specific for bone malignancy and increased bone uptake may occur with any other condition resulting in increased blood flow and increased bone turnover (41, 68), hence lowering ^{18}F-NaF specificity. ^{18}F-NaF accumulation has been reported in fractures and a variety of metabolic bone disease such as renal osteodystrophy, Paget's disease and fibrous dysplasia (179) as well as infection or inflammation (180). This study demonstrates that the use of dynamic ^{18}F-NaF for diagnosing the presence or absence of prosthetic loosening is feasible and that there is a relatively higher degree of ^{18}F-NaF uptake in symptomatic joints when compared with asymptomatic joints. Studies also show that there is a relatively higher degree of ^{18}F-NaF uptake in infection when compared with aseptic loosening (169). Larger trials are required, especially to prove the role of this novel technique for the detection of periprosthetic infection because pre-surgical accurate diagnosis or elimination of periprosthetic infection significantly allows clinical teams to accurately plan management (174). Current assessment methods often require the combination of clinical signs, laboratory findings and often several sequential imaging studies (181) to differentiate aseptic loosening

from post-operative change and infection with an acceptable sensitivity and specificity (182). Although the plain radiograph gives important information regarding joint stability, malrotation and malalignment as well as the type of prosthesis (183); the role of plain radiographs in the diagnosis of infection associated with prostheses is limited because of nonspecific findings common to both septic and aseptic loosening (174).

Joint aspiration or biopsy is a valuable preoperative diagnostic tool for the detection of sepsis, with a sensitivity and specificity ranging from 50% to 93% and from 82% to 97%, respectively (174), but this degree of accuracy remains too low to exclude sepsis with certainty (174) and prior antibiotic administration may further reduce sensitivity (174). Nuclear medicine imaging has a valuable role to play in assessing joint prostheses for infection. The 3-phase radionuclide bone scan is the most common nuclear medicine investigation for the assessment of prosthetic joint sepsis (55). However, the presence of orthopaedic hardware reduces the sensitivity of bone scans (182). Two other limitations are the lengthy examination time and the cost of the examinations (174). Sequential radionuclide bone and gallium scans were the first combined studies used to diagnose osseous infection (182) and have been applied to painful lower limb prostheses since the 1970s (174), but are less favoured due to reported low sensitivity of 38% at the lower end of the spectrum in literature (174) or overall accuracy of 65 to 80% at the more optimistic end (182). ^{111}In-labeled white blood cell scanning combined with ^{99m}Tc-sulphur colloid bone marrow imaging has a sensitivity, specificity, and accuracy of 86%– 100%, 89%–94%, and 89%–96%, respectively (174). Disadvantages of Indium-labelled leukocyte imaging include the demanding man-hours required for in vitro labelling with resultant increasing opportunities for iatrogenic errors (174) and also the requirement for delayed imaging at 24 hours post-injection (174). Occasionally, there is a requirement for additional bone marrow imaging, resulting in relatively higher radiation exposure. Attempts have been made with limited success to replace ^{111}Indium-labelled white cell imaging with ^{99m}Technetium-labelled murine monoclonal anti-granulocyte antibody fragments. ^{99m} Tc-–labelled murine monoclonal antibody of the immunoglobulin bind with high affinity to CD-15 receptors present on the surface membrane of

human polymorphonuclear leukocytes (53, 184) and do not require in vitro labelling process. Antibody fragment imaging has a high negative predictive value (185), but murine antibodies have a reduced plasma half-life of few hours when compared with human IgG half-life of 3 weeks (186). In addition, the murine IgG invokes a HAMA response that results in faster removal of the mouse IgG, and may rarely, also result in anaphylactic hypersensitivity response (186). The decreased circulating half-life requires increasing administered doses (which can then lead to increasing risk of HAMA, or a reduced effectiveness of the study (186). Since the completion of this study monoclonal antibodies have been permanently discontinued by Immunomedics™ GmbH and the European Union (187).

Early attempts to justify the use of ^{18}F-FDG PET as a single, cost-effective method of diagnosing periprosthetic infection (71, 174) have since been proven to be incorrect due to false positive nonspecific periprosthetic uptake (188). The cost of ^{18}F-NaF PET-CT is substantially lower than the combined costs of sequential studies comprising 2 to 3 commonly performed radionuclide scans (mainly ^{111}In-labeled white blood cell scans, bone scans and bone marrow scans) (166, 174). Furthermore, tomographic images with PET provide better spatial resolution than planar conventional nuclear medicine modalities (174), significantly improving test accuracy (166, 174). Dynamic ^{18}F-NaF PET-CT can be completed within an hour, compared with 4 hours to 2 days for other nuclear medicine methods (174).

Critical analysis of the feasibility study which was designed to establish proof of principle for the use of dynamic ^{18}F-NaF PET-CT in the assessment of knee prostheses revealed limitations. Generally, the results from small first-stage sample feasibility studies are limited and usually highly variable. Feasibility study results can if relied upon can diminish the quality of subsequent clinical trial design (189). Furthermore, the very limited data and small size meant that very little statistical information could be deduced from the results of this study and no meaningful clinical end point was presented. However, the feasibility study helped guide the subsequent trial protocol design and implementation by identifying more practicable and economic methodology. Considering the small size, there is further concern that selection bias or volunteer bias may have

played a role in the feasibility study outcome. Lastly, the images were not reviewed by non-blinded observers and hence potentially introducing possible error from intra-observer variability.

4.8 Conclusion

^{18}F-NaF PET-CT of knee prostheses is feasible and diagnostic quality dynamic ^{18}F-NaF PET-CT images with graphical data from symptomatic knee prostheses can be acquired and archived successfully. This preliminary data demonstrates early proof of the principle that dynamic ^{18}F-NaF PET-CT can detect aseptic loosening of lower limb prostheses. The CT component provides anatomical correlation. Dynamic ^{18}F-NaF PET-CT may be more useful than 3 phase bone scans in the assessment of painful hip and knee prostheses. Routine clinical use should not be initiated until the accuracy of dynamic ^{18}F-NaF PET-CT is fully validated. Future research trials with larger patient populations are required to establish a role for dynamic ^{18}F-NaF PET-CT for detecting aseptic loosening and septic loosening. New knowledge identified that dynamic ^{18}F-NaF PET-CT can detect aseptic loosening of lower limb prostheses and that future research trials with larger patient populations are indicated to establish a specific role for dynamic ^{18}F-NaF PET-CT.

4.9 Summary

- Dynamic ^{18}F-NaF PET-CT can detect aseptic loosening of lower limb prostheses.
- CT component provides anatomical correlation.
- Dynamic ^{18}F-NaF PET-CT may be more useful than 3 phase bone scans in the assessment of painful hip and knee prostheses.
- Future research trials with larger patient populations are required to establish a role for dynamic ^{18}F-NaF PET-CT for detecting aseptic loosening and septic loosening.

Chapter 5 Evaluating and Correcting Beam Hardening Artefact from Prostheses on Dynamic ^{18}F-NaF PET-CT – Using Pre-Filtering with Aluminium; Dual-Energy CT and Mathematical Algorithm with MATLAB® Filtered Back Projection

5.1.1 Abstract

Background: Metallic joint prostheses result in beam hardening artefacts which add undesired background activity to the images, degrade image quality and reduce the diagnostic yield in periprosthetic region. Beam hardening artefact also has the undesired effect of introducing increased activity levels on the emission images. There are different proprietary methods of correcting artefacts in periprosthetic tissues. Artefact reduction techniques often introduce secondary artefacts and reduce image quality around the prosthetic-bone interface.

Methods: All scans have been carried out on the same GE Healthcare® Discovery 710 PET-CT system PET-CT scanner under controlled conditions to evaluate and compare different methods of correcting which result from metallic joint prostheses in ^{18}F-NaF PET-CT. Three techniques of correcting beam hardening artefacts were assessed - pre-filtering with Aluminium using an ^{18}F-PET-CT phantom; dual-energy CT using an ^{18}F- PET-CT phantom and post-scan image manipulation employing MATLAB® mathematical algorithm and filtered back projection on images that were acquired from 6 patients. The phantom based experiment was performed 4 times using pre-filtering with Aluminium and dual-energy CT simultaneously. The hip prosthesis phantom consisted of a cylindrical Perspex® phantom containing a metallic femoral component surrounded by low levels of ^{18}F activity which was scanned with or without an additional Aluminium dome filtering at either 120 KVp or 140 KVp peak Kilovoltage energies. 15 CT density maps of CT periprosthetic lucency using the French colour look-up table (CLUT) were assessed to distinguish between symptomatic and asymptomatic joint prostheses.

Results: No significant difference was identified between the use of 120 KVp, 140 KVp with or without aluminium. The post-scan image manipulation with MATLAB® reduced beam hardening artefacts in some of the images but the manipulated images introduced secondary artefacts and resulted in reduction in image quality and some loss of anatomic detail around the prosthetic-bone interface. The CT density maps of CT periprosthetic lucency did not distinguish accurately between symptomatic and asymptomatic joint prostheses, nor was it able to distinguish aseptic loosening from septic loosening.

Conclusion: Beam hardening artefacts from prostheses contribute to poor image quality on ^{18}F PET-CT. Pre-filtering with Aluminium; dual-energy CT and mathematical algorithms with MATLAB® filtered back projection reduce beam hardening artefact but with no significant difference. There is also no significant difference in beam hardening artefact reduction between pre-filtering with Aluminium; dual-energy CT and mathematical algorithms with MATLAB® filtered back projection. Artefact-reduction techniques should be used with caution because they introduce other secondary artefacts with subsequent image quality reduction.

5.1.2 Problem Statement

Beam hardening artefacts from prostheses interfere with CT and ^{18}F PET image quality.

Would the use of pre-filtering with Aluminium improve image quality?

Would the use dual-energy CT improve image quality?

Would the use of mathematical algorithms with MATLAB® filtered back projection improve image quality?

5.1.3 Hypothesis

Pre-filtering with Aluminium, dual-energy CT and MATLAB® filtered back projection can improve image quality.

5.1.4 Aim

To measure image quality of a metallic prosthesis phantom without any additional processing/material; (a) pre-filtering with Aluminium (b) with the use dual-energy CT and (c) with the use of MATLAB® filtered back projection.

5.1.5 Apparatus and Materials

Titanium alloy femoral component of hip prosthesis (Figure 15), Cylindrical Perspex® phantom (Figures 15 and 16), Aluminium dome (Figure 16), 5 litre solution of a low concentration of 0.05 MBq/ml ^{18}F-Fluorodeoxyglucose (^{18}F-FDG), GE Healthcare® Discovery 710 PET-CT system PET-CT scanner, GE Healthcare Xeleris® version 4 workstation and MATLAB® software (The Mathworks, Natick, Massachusetts).

Figure 15. *Perspex® phantom containing femoral prosthesis*

Note: This photograph shows the 15 cm long and 20 cm diameter cylindrical Perspex® phantom which contains a fixed central femoral component of hip prosthesis composed of metallic alloys of titanium. The Perspex was filled with a 5 litre solution of a low concentration of 0.05 MBq/ml ^{18}F-Fluorodeoxyglucose (^{18}F-FDG) which surrounded the central prosthesis.

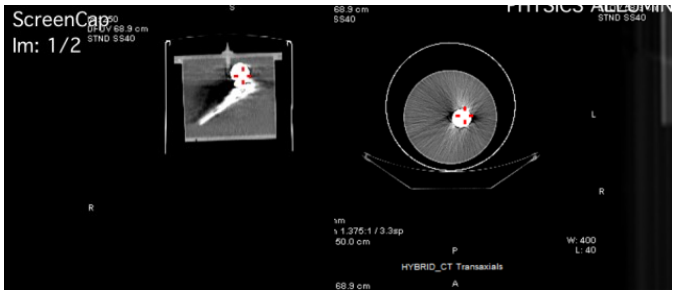

Figure 16. *Sagittal and axial CT images of Perspex® phantom containing femoral prosthesis*

Note: These are sagittal and axial CT images of the cylindrical Perspex® phantom containing a fixed central femoral component of hip prosthesis and surrounded by ^{18}F-FDG. The cylindrical Perspex® phantom is encased by a domed Aluminium shield.

5.1.6 Method

The experiments were performed under controlled conditions to evaluate and compare different methods of correcting which result from metallic joint prostheses in ^{18}F-NaF PET-CT.

Beam hardening artefacts from a hip prosthesis phantom surrounded by low levels of ^{18}F activity were compared with and without an additional pre-scan pre-filtering with Aluminium dome to assess for improvements in the beam hardening artefact. Further beam hardening artefacts from the hip prosthesis phantom were compared at different energies to assess for improvements in the beam hardening artefact. Lastly, the post-scan technique of periprosthetic beam hardening artefact improvement or worsening was assessed using images from 6 patients that had undergone ^{18}F-NaF PET-CT scans of joint prostheses. Post-scan image manipulation was performed using open source in-house mathematical algorithm employing MATLAB® for filtered back projection in order to assess for change.

5.1.7 Variables

- Independent variables – presence or absence of Aluminium filter; dual-energy 120 KVp and 140 KVp; use or non-use of MATLAB® filtered back projection
- Dependent variables - beam hardening artefact on PET-CT
- Confounding variables-^{18}F-FDG dose (MBq), room temperature (degrees Celsius)
- Controlled variable – hip prosthesis, scan time (minutes)

5.1.8 Expected Results

Pre-filtering with Aluminium, use of mathematical algorithms and dual-energy CT would improve image quality but may introduce secondary artefacts. Image quality would be most improved using the dual energy CT method.

5.1.9 Treatment of Results (Linking of Expected Results to Hypothesis)

If pre-filtering with Aluminium, MATLAB® and dual-energy CT improve image quality, and then the hypothesis is correct. If image quality is most improved using the dual energy CT method, then the second part of the expected results is correct.

5.1.10 Physics Principles (Connect Methodology to Problem Statement)

Metallic prostheses have high proton densities (Zahl), thus resulting in beam hardening artefact and false positive PET uptake. Correction with pre-acquisition, scanning as well as post-processing methods can alleviate some of these issues.

5.1.11 Sources of Error/Assumptions/Limitations

There are other inherent factors including the atomic number which affect image quality. The location of radioactivity at different points in relation to the prosthesis may be more open to interpretation. Further limitations of this study include the small number of case as well as the fact that the phantom experiments were only performed once for each category. Furthermore, only six post-scan software manipulations were performed. The study was also susceptible to biases arising two non-blinded observers. Additional limitations in the application of these techniques occurred due to secondary artefacts as well as the heterogeneous diagnoses and different type and composition of the prostheses.

5.2.1 Methodology; Pre-Filtering with Aluminium and Dual-Energy CT

Pre-filtering with Aluminium has visible effect on beam hardening artefact on CT and PET using ^{18}F as well as improves the quality and diagnostic quality of PET-CT images with prostheses.

All scans have been carried out on the same GE Healthcare® Discovery 710 PET-CT system PET-CT scanner and with the help of Mr Samuel Colclough, clinical scientist Dr James Cullis, consultant Clinical scientist, both from University Hospital Coventry & Warwickshire.

A cylindrical Perspex® phantom, 18 cm long and 20 cm in diameter containing a fixed central femoral component of hip prosthesis composed of metallic alloys of titanium (figures 15 and 16). The central prosthesis is surrounded by a 5 litre solution of low concentration of about 0.05 MBq/ml ^{18}F-Fluorodeoxyglucose (^{18}F- FDG). The cylindrical Perspex® phantom was filled with the solution and then sealed.

The phantom was placed at the centre of the imaging field of view and its axis was perpendicular to the long axis of the patient couch. Imaging was performed with a GE Healthcare® Discovery 710 PET-CT system PET-CT scanner (GE Healthcare, Waukesha WI) with a gantry bore diameter of 70 cm and a spatial resolution of approximately 4.5 mm (190). Computed Tomographic images of the phantom were obtained and positron emission tomographic reconstructions were obtained with the same stipulated number of minutes for each bed position. Tomographic reconstructions were performed with a 3D ordered subset expectation maximization (OSEM) method (VUE Point) and attenuation correction was performed with the low dose CT images. Further decay corrections were made for injected radioactivity by the PET scanner.

The PET-CT scans were performed four times using 2 different peak Kilovoltage energies (both with and without aluminium), i.e., 120 KVp with aluminium, 140 KVp with aluminium, 120 KVp without aluminium and 140 KVp without aluminium (Tables 8 and 9). Regions of interest (ROIs) in each of the four sets of images were selected once by a radiologist and physicist working together.

5.2.2 Results

Table 8. *Pre-filtering with Aluminium and dual-energy CT*

Scan type	Periprosthetic SUVmax	Background SUVmax	P/B SUVmax ratio	P/B SUVmax difference
120 KVp with aluminium	8.88	7.98	1.11	0.9
140 KVp with aluminium	9.07	8.16	1.11	0.91
120 KVp without aluminium	8.58	7.5	1.14	1.08
140 KVp without aluminium	10.04	8.16	1.23	1.88

Table 9. *Pre-filtering with Aluminium and dual-energy CT*

Scan type	Chi square test value	P value	Significance
120 KVp with aluminium	0.99	0.80	Not significant at p<0.5
140 KVp with aluminium	0.83	0.84	Not significant at p<0.5
120 KVp without aluminium	0.99	0.80	Not significant at p<0.5
140 KVp without aluminium	0.84	0.84	Not significant at p<0.5

Note: Because the p-value is greater than 0.05; the null hypothesis is not rejected and it *cannot* be concluded that a significant difference exists between the use of 120 KVp, 140 KVp with or without aluminium.

5.3.1 Post-Imaging Manipulation

Post-imaging manipulation with in-house mathematical beam hardening correction (BHC) algorithms with MATLAB® has visible effect on beam hardening artefact on CT and PET using ^{18}F and can improve the quality and diagnostic quality of PET-CT images with prostheses.

5.3.2 Introduction

Interpretation of CT into hybrid imaging using SPECT-CT and PET-CT images in the assessment of post-surgical complications of joint replacement surgery is impeded by the presence of beam hardening artefacts caused by metal implants.

5.3.3 Aim

The purpose of this project was to design a simple post-imaging process that would reduce beam hardening artefact on the CT component to allow for more accurate quantitative evaluation of periprosthetic osteolysis.

5.3.4 Background

Metal-related artefact result from several mechanisms including beam hardening, scatter, Poisson noise, motion and edge effects (191).

The statistical error of low photon counts in CT images from low dose (mA) results in Poisson noise and appears as randomly distributed hypodense and hyperdense lines on the CT image, usually in the direction of most attenuation (191). There are several commercially available metal artefact reduction

algorithms which may be applied following image acquisition. One of the newer methods uses Metal Deletion Technique (MDT) (US 8233586B1) which is a patented iterative technique which reduces artefacts from all these mechanisms (192), but it is not FDA approved and currently only intended for research use.

5.3.5 Method

Six patients with ten prostheses in total were imaged using a GE Healthcare® Discovery 710 PET-CT system PET-CT scanner (GE Healthcare, Waukesha WI) with a gantry bore diameter of 70 cm and a spatial resolution of approximately 4.5 mm (190). All the imaged prostheses were located in one or both knee joints of the patients that were imaged. ^{18}F-NaF PET-CT - Dynamic images were acquired using a GE Discovery ST with 16 slice CT (GE Healthcare®) volume imaging protocol (ViP) (78, 175). The patients fasted for at least 6 hours before receiving the injection. CT images of the joints were acquired, followed by dynamic PET image acquisition in list mode from the time of injection till 30 to 40 minutes after bolus intravenous administration of 250 MBq ^{18}F-NaF (175). The images were reconstructed using ordered-subset expectation maximization, and images were corrected for attenuation (78). All analyses of the CT images were performed with the help of Mr Matthew Galloway, clinical scientist from University Hospital Coventry & Warwickshire.

MATLAB® (The Mathworks, Natick, Massachusetts) with parallel-beam algorithm was used to open the DICOM image stacks from the local hard disk. One of the first steps would be to use Hounsfield units of 3,000 and above to identify metal objects in each image.

Then identify projections affected by metal and then forward project the 2D distribution of metal images from multi-angular projections to obtain a metal sinogram and also forward project the whole image to obtain a whole image sinogram (193). Sinograms are plots of the projected data – the horizontal axis

represents the tube angle and the vertical axis represents the detector number (191).

Identify the metal sinogram on the whole image sinogram and then correct the image by replacing it with a realistic Hounsfield unit by calculating the mean Hounsfield unit on either side of the metallic prosthesis.

Then delete the metal pixels by using forward back projection to iteratively replace metal images (2) with dedicated built-in plugins. These images which do not have any metal in them are reconstructed with forward back projection using MATLAB® "iradon.m" routine (193, 194) thus creating images without the metal included. The metal from the original image is the re-inserted back into the back projected images to recreate the mathematically reprocessed image. The MATLAB® iradon function performs filtered back projection by "smearing back" pixel grid images of each acquired image projection using a low pass filter. This process is reiterated for each projection and then the contribution from each projection is added up (195).

The CT images from 15 patients with hip or knee prostheses that had been scanned as part of a separate experiment were assessed for periprosthetic lucency by the sole radiologist in this study using OsiriX® Pixmeo SARL Switzerland which used to be an open source software (OSS) with practical features for the analysis, interpretation and post-processing of radiological images (196) as a fast, simple and intuitive DICOM viewer program that runs on an Apple Macintosh operating system (macOS) version 10.11.6 (197). Images were presented with the French colour look-up table (CLUT) due to its superior contrast: background ratio and the degree of periprosthetic lucency in the images were assessed visually. Inter-observer variability and reliability cannot be tested due to there being a sole observer in this study. In order to ensuring reliability the method was assessed using normal bone cortex: air, normal bone cortex: marrow and normal bone cortex: soft tissue interface. The CT images are subject to beam hardening artefact from the prostheses and images were assessed once.

5.3.6 Results

Although the post-scan image manipulation with MATLAB® resulted in reduced beam hardening artefact in some of the images the manipulated images introduced secondary artefacts and resulted in reduction in image quality and some loss of anatomic detail around the prosthetic-bone interface (Figures 17 and 18).

The 15 CT density maps of CT periprosthetic lucency using the French CLUT did not distinguish accurately between symptomatic and asymptomatic joint prostheses, nor was it able to distinguish aseptic loosening from septic loosening (Table 10) and (Figures 17 to 22).

Table 10. *Periprosthetic lucency or reduced density using CT density maps and CLUT scores*

Patient	Right CLUT Score	Left CLUT Score	Symptomatic Side	Diagnosis
1	5	10	Left	Bilateral TKR with aseptic loosening in left TKR
2	10	N/A	Right	Unilateral right TKR with aseptic loosening
3	10	10	Left	Bilateral TKR with unstable left TKR
4	5	4	Right	Right TKR/ Left UKR with synovitis
5	5	10	Left	Bilateral TKR with left aseptic loosening

Patient	Right CLUT Score	Left CLUT Score	Symptomatic Side	Diagnosis
6	6	10	Right	Bilateral TKR with right synovitis
7	1	4	Left	Left TKR/ Right UKR with loose left TKR
8	9	10	Right	Bilateral TKR with infected right TKR
9	9	5	Right	Bilateral THR with loose right
10	7	N/A	Right	Unilateral Right TKR with loosening
11	N/A	6	Left	Unilateral left TKR with loosening
12	9	6	Right	Bilateral THR with loose right

Patient	CLUT Score Right	CLUT Score Left	Symptomatic Side	Diagnosis
13	6	N/A	Right	Unilateral Right THR with loosening
14	5	4	Right	Bilateral THR with right loosening
15	5	3	Right	Bilateral THR with right fracture

Note: CLUT = Colour Look-Up Table; CLUT 1-10 with 1 being the least radiolucent and 10 the most radiolucent (1= white, 2, pink, 3=purple, 4=blue, 5=turquoise, 6= olive green, 7= light green, 8 = light brown, 9 = dark brown, 10 = black); N/A = Not Applicable; TKR = Total knee replacement.

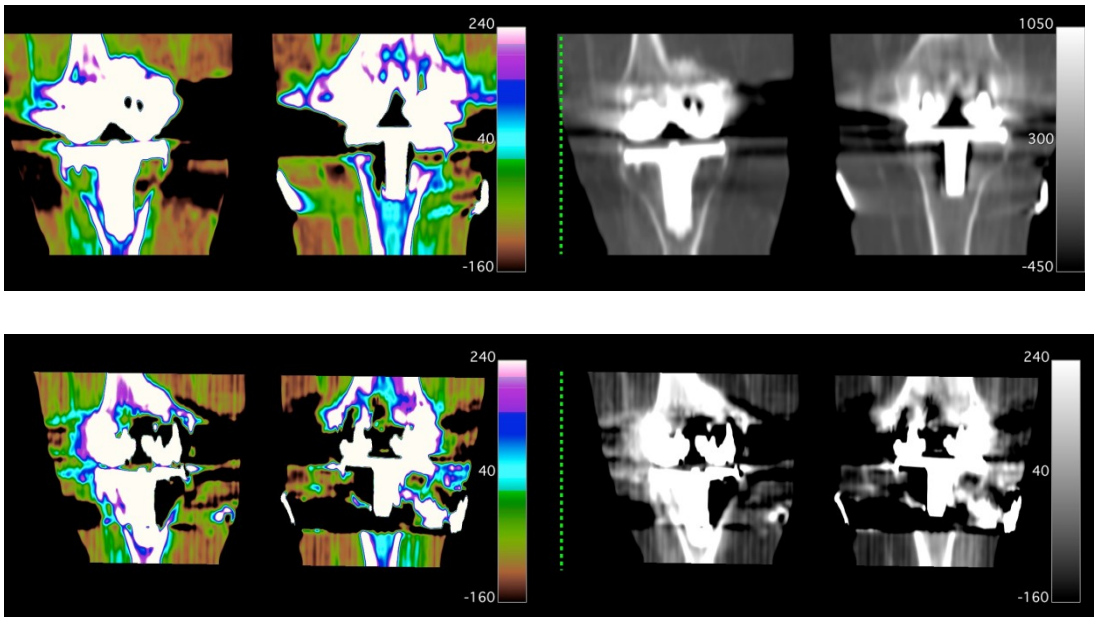

Figure 17. *Post-scan image manipulation with MATLAB® resulting in image deterioration*

Note: Symptomatic left total knee replacement in patient with bilateral knee replacements and symptomatic left total knee replacement diagnosed with Instability (not loose and not septic). The OsiriX® density map images (left) and CT images (right) show beam hardening artefact but the post-scan image manipulation with MATLAB® show a reduction in image quality and loss of anatomic detail around the prosthetic-bone interface (lower set of images)

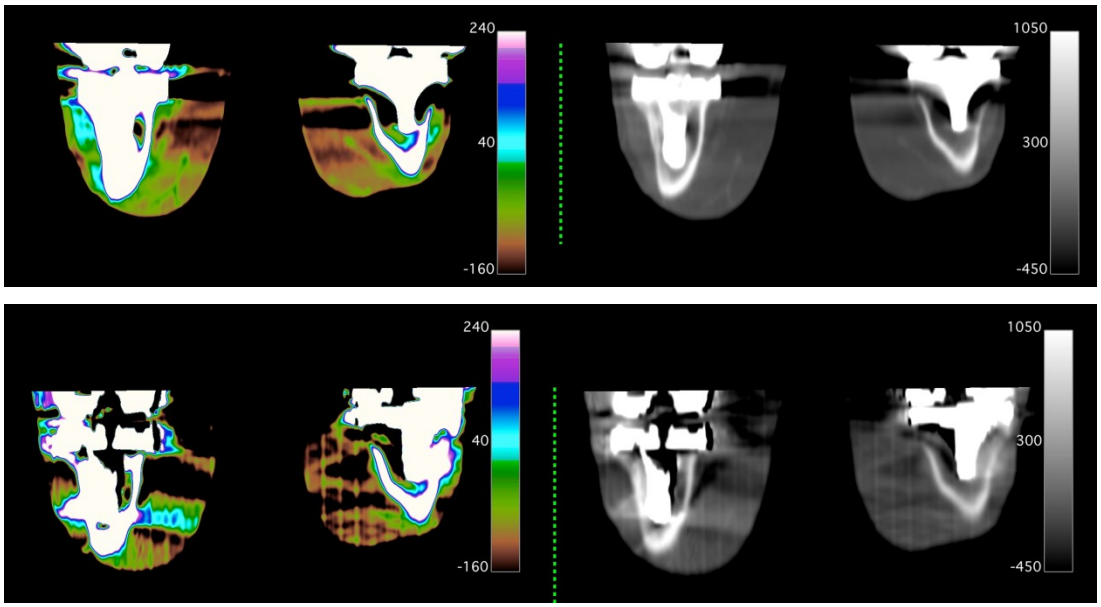

Figure 18. *Post-scan image manipulation with MATLAB® resulting in image deterioration*

Note. OsiriX® density map images (left) and CT images (right) in patient with synovitis in symptomatic right total knee replacement and asymptomatic left knee replacement. The OsiriX® density map images (left) and CT images (right) show beam hardening artefact but the post-scan image manipulation with MATLAB® show a reduction in image quality and loss of anatomic detail around the prosthetic-bone interface (lower set of images)

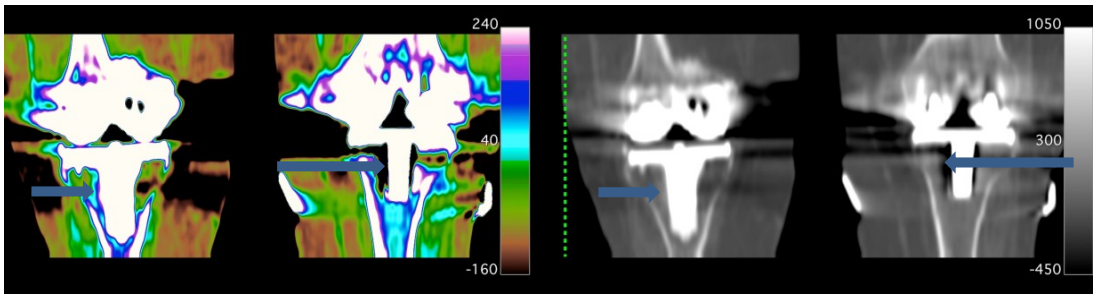

Figure 19. *Patient 3 with symptomatic left total knee replacement*

Note: This patient has bilateral knee replacements and a symptomatic left total knee replacement. OsiriX® density map images (left) and CT images (right). Patient with symptomatic left total knee replacement diagnosed with Instability (not loose and not septic) as well as asymptomatic right knee replacement. There is relative increased lucency or reduced density in the symptomatic left over asymptomatic right prosthesis (blue arrows).

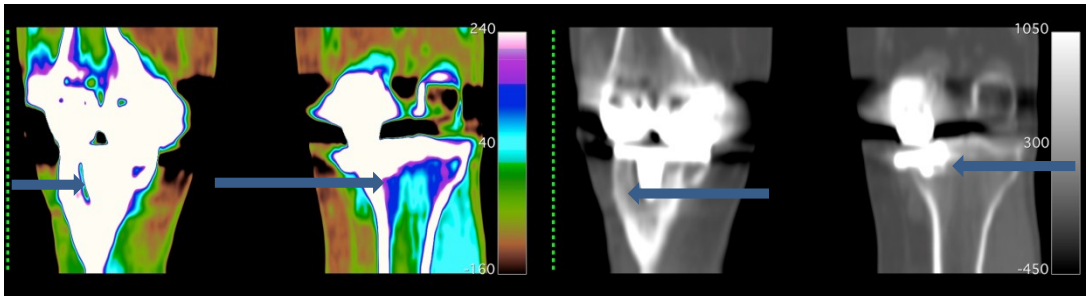

Figure 20. *Patient 4 with symptomatic right total knee replacement*

Note: OsiriX® density map images (left) and CT images (right) in a patient with synovitis in a symptomatic right total knee replacement and an asymptomatic left knee replacement. There is relative increased lucency or reduced density in the symptomatic right over asymptomatic left prosthesis (blue arrows). However, the larger symptomatic right knee prosthesis is a confounding factor.

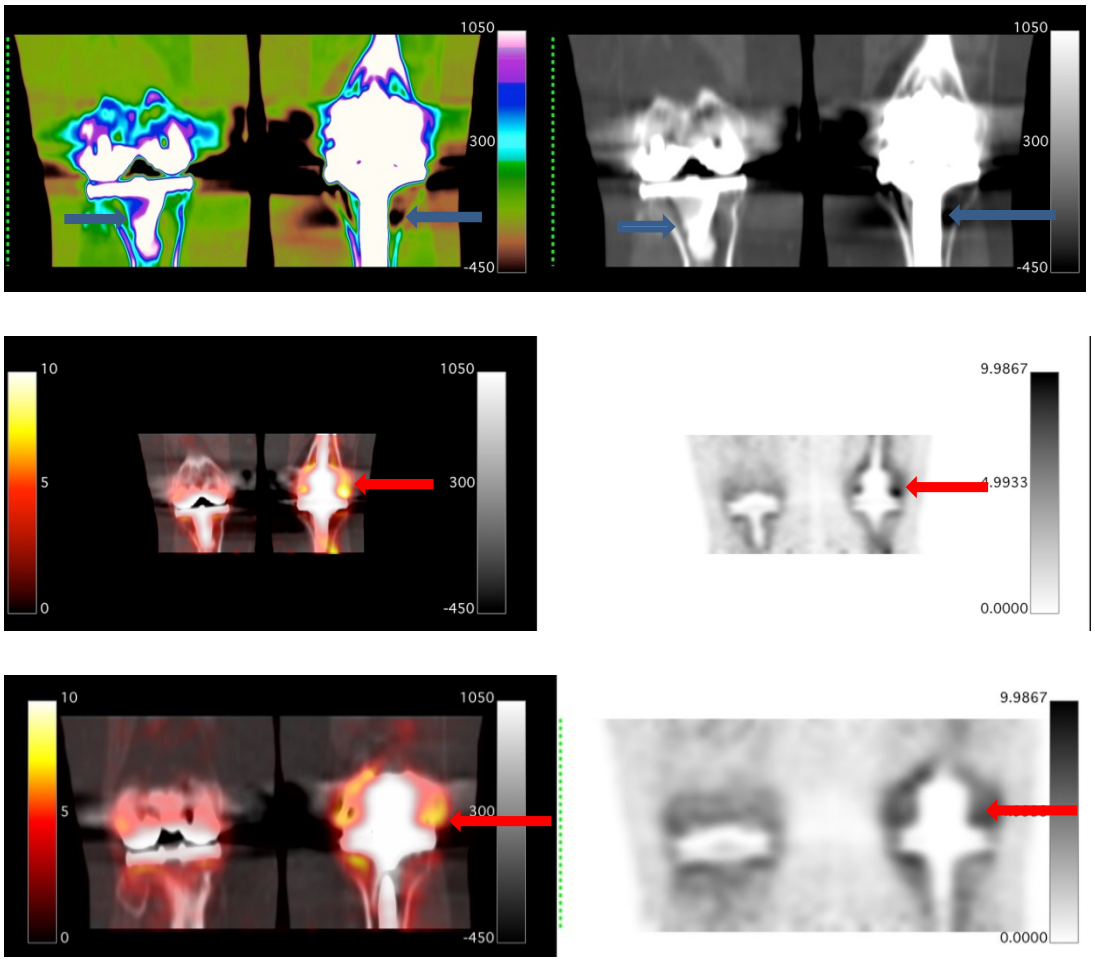

Figure 21. *Patient 5 with symptomatic aseptic loosening left total knee replacement*

Note: Osirix® density map images (left) and CT images (right) in a patient with aseptic loosening in symptomatic left total knee replacement and asymptomatic right knee replacement. No relative increased lucency or reduced density in the symptomatic left knee over asymptomatic right knee (blue arrows). The symptomatic left total knee with aseptic loosening replacement shows increased periprosthetic uptake on NaF PET-CT (left) and late phase isotope bone scan (left) in patient with bilateral knee replacements (red arrows).

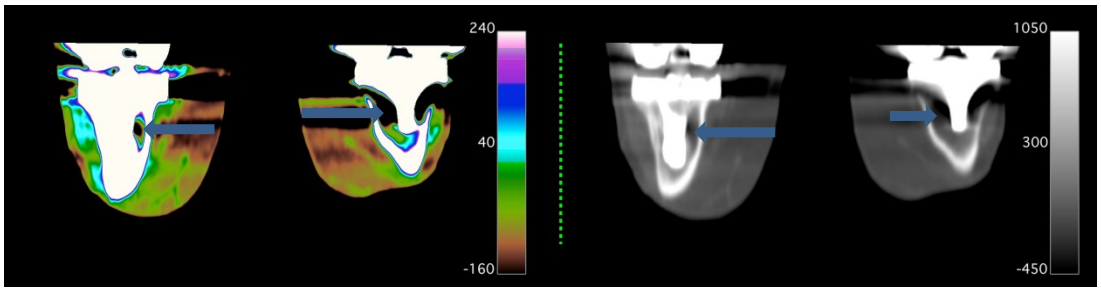

Figure 22. *Patient 6 with synovitis in symptomatic right total knee replacement.*

Note: Osirix® density map images (left) and CT images (right) in a patient with synovitis in a symptomatic right total knee replacement and an asymptomatic left knee replacement. There was no relative increased lucency or reduced density in the symptomatic over asymptomatic prostheses (blue arrows)

5.3.7 Discussion

The type of mathematical algorithm applied for image post-processing can have profound results on image noise, image contrast and image signal-to-noise ratio (SNR), leading to a resultant enhanced or diminished ability to detect any differences in density (198). Evaluation of all 10 prostheses revealed image and periprosthetic uptake distortion on the reconstructed images due to aliasing artefacts, edge enhancement and Poisson artefacts (Figures 23 and 24). The use of mathematical algorithms improve image resulted in image distortion and reduced accuracy with no improvement in the quality and diagnostic quality of CT images with joint prostheses.

The use of this technique resulted in drawbacks including ray aliasing artefacts which appeared on the images as cross-hatched distortion lines on the reconstructed tomographic images emanating from the centre and produced after applying the filtered-back projection algorithm (199). Aliasing distortions in this case resulted from either using an undersampling of projection data, because an inadequate number projections were recorded or both (199) and aliasing artefacts can be mitigated by forward projecting as many images as possible (199).

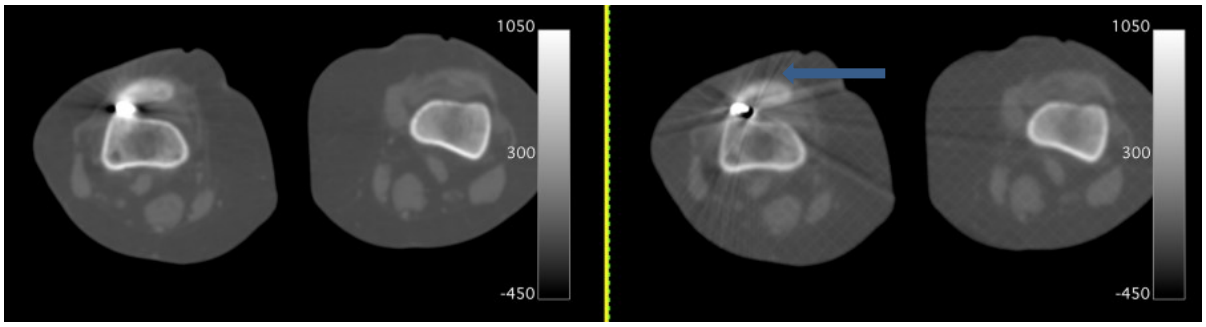

Figure 23. *Poisson artefact appearing secondarily on the filtered-back projection images*

NOTE: This image demonstrates Poisson secondary artefact on similar images (blue arrow) through the knees in the reconstructed tomographic images on the right after applying the filtered-back projection algorithm to the axial image on the left.

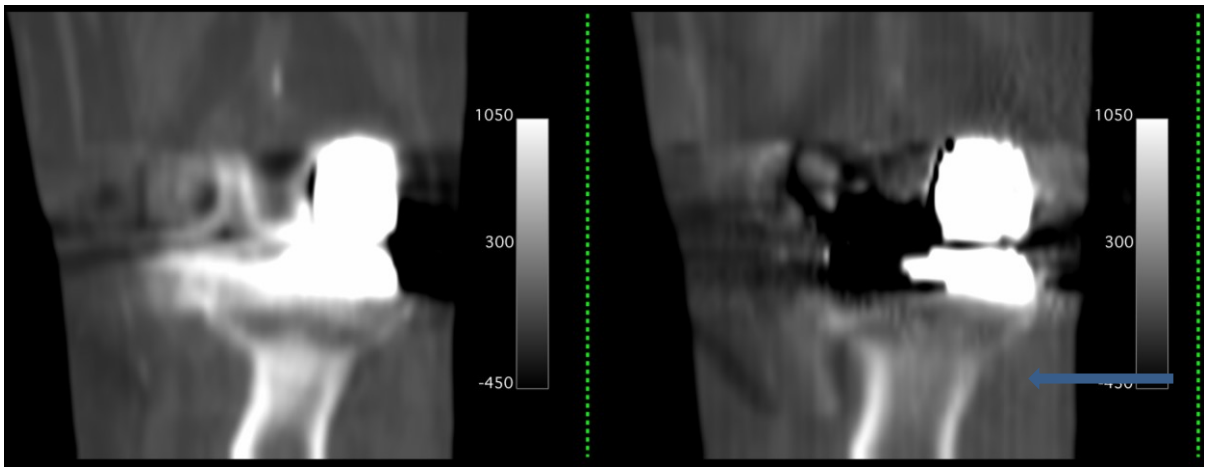

Figure 24. *Ray aliasing artefact appearing secondarily on the filtered-back projection images*

Note: image demonstrating ray aliasing artefacts on similar images through the knees in the reconstructed tomographic images on the right (blue arrow) after applying the filtered-back projection algorithm to the coronal image on the left.

Edge enhancement results from the suboptimal implementation of filtered back projection at the borders of a limited field of view resulting in a sinogram outside the field of view set to zero (191) producing a sharp bright rim at the image edge, which is intensified by filtered back projection (191).

Poisson artefacts results from photon counting errors (192) due to low photon counts and resemble dark and bright lines that are projected in the direction of greatest attenuation or highest number of Hounsfield units (191). Poisson artefacts are not improved by filtered back projection (192).

5.4 Conclusion

Beam hardening artefacts from prostheses contribute to poor image quality on ^{18}F PET-CT. Pre-filtering with Aluminium; dual-energy CT and mathematical algorithms with MATLAB® filtered back projection reduce beam hardening artefact but with no significant difference. The artefact-reduction techniques should be used with caution because they introduce other secondary artefacts with subsequent image quality reduction. Positively, this demonstrated and documented some secondary artefacts. In addition, this makes a case for potential radiation dose reduction to the patient because imaging with 140 KVp did not produce any significant difference over imaging with 120 KVp. New knowledge identified that there is no significant difference in beam hardening artefact reduction between pre-filtering with Aluminium; dual-energy CT and mathematical algorithms with MATLAB® filtered back projection. Further research in to metal artefact reduction is ongoing in both commercial and academic settings due to image degradation from metal. Research into prosthetic joint beam hardening artefact in dynamic PET-CT requires further research.

5.5 Summary

- Beam hardening artefacts from prostheses reduce image quality on ^{18}F PET-CT.
- Beam hardening artefact can be reduced with Pre-filtering with Aluminium; dual-energy CT and mathematical algorithms with MATLAB® filtered back projection.
- There is no significant difference in artefact reduction between the different methods.
- The artefact-reduction techniques introduce other secondary artefacts with subsequent image quality reduction.
- Beam-hardening artefact evaluation and reduction in dynamic ^{18}F PET-CT requires further research.

Chapter 6 Dynamic ^{18}F-NaF PET-CT and 3-Phase Bone Scan Prosthetic Joint Clinical Study

6.1 Abstract

Background: Imaging investigations for painful joint prostheses frequently involve serial radiographs or multiple cross-sectional studies. Hybrid imaging using PET and CT may obviate the requirement for multiple imaging tests. This study aimed to prospectively evaluate the usefulness of ^{18}F- NaF PET-CT using a sequential multiphase technique in comparison to bone scan in the diagnosis of periprosthetic joint loosening and infection.

Methods: This pilot prospective study included 15 patients with 25 prostheses with symptoms of painful joint prostheses. Sequential ^{18}F-NaF PET-CT and conventional 3-phase bone scans with planar images was performed in all patients. The final diagnosis was made by microbiological, biochemical and surgical findings as well as clinical follow up. The PET-CT and bone scan images were also assessed with GE ADW 4.6 and Xeleris® version 4 workstations as well as using MATLAB® open source software. The R^2 bone scan trendline pattern was calculated from 3-phase bone scans with a final diagnosis of aseptic or septic prosthesis and lastly CT periprosthetic lucency was assessed with the use of French colour look-up table (CLUT) density maps on OsiriX® version 10.0.2 running on an Apple Macintosh operating system (macOS) version 10.11.6.

Results: Out of the 15 patients and 25 prostheses that were scanned, 15 were symptomatic and 10 were asymptomatic. Of the 15 symptomatic prostheses – 1 patient died, 2 patients had results from clinical follow up and 12 patients had results from surgical follow up. Out of the 12 patients that underwent surgery 3 were infected and 9 were loose or other. 3-phase bone scans were 100 % sensitive for sepsis and inflammation but had a 42% false positive rate for sepsis/inflammation. In addition, the 3-phase bone scans were 58 % sensitive for aseptic loosening. Some dynamic PET images were unavailable for review

due to data corruption and image data storage difficulties. In addition, there were inconsistent results from the dynamic ^{18}F-NaF PET-CT and ^{18}F-NaF SUVmax levels. Results revealed poor correlation between the ^{18}F-NaF uptake patterns, dynamic NaF pattern and the bone scan uptake pattern with the final diagnoses. However, there was statistical correlation between the final diagnosis and the R^2 bone scan trendline pattern with an optimal cut-off point of 0.2 above which the likelihood of a septic joint was higher. CT periprosthetic lucency and CT density maps did not distinguish aseptic loosening from septic loosening.

Conclusion: Dynamic ^{18}F-NaF PET-CT is feasible but has not been proven to be an accurate or ideal test to investigate periprosthetic infection or loosening. R^2 values from ^{99m}Tc-MDP dynamic bone scans greater than 0.2 favour periprosthetic septic loosening or inflammation. Combining dynamic bone scan R^2 values with CT periprosthetic lucency from SPECT-CT may improve test accuracy even further.

6.2 Aims

1. To validate a new imaging method of diagnosing loosening of joint prosthesis.

2. To validate a new imaging method of diagnosing infection of joint prosthesis.

3. To validate a new imaging method of distinguishing loosening from infection of joint prosthesis.

4. To see whether ^{18}F-NaF PET- CT is more cost-effective and accurate in the detection of infection/loosening.

Hypothesis: Sequential multiphase ^{18}F-Fluoride PET-CT as a single imaging investigation can identify the presence of loosening and infection of joint prostheses, with the use of quantitative and visual analysis of joint prostheses.

Research Questions: Is sequential multiphase ^{18}F-Fluoride PET-CT as a single imaging tool able to reliably diagnose loosening of joint prostheses?

Is sequential multiphase ^{18}F-Fluoride PET-CT as a single imaging tool able to reliably diagnose periprosthetic infection in joint prostheses?

Is sequential multiphase ^{18}F-Fluoride PET-CT more accurate and cost-effective in the detection of infection/loosening?

6.3 Materials and Methods

This was a pilot study using a prospective uncontrolled case series (longitudinal observational study) of patients with symptomatic knee and hip joint prostheses awaiting surgical revision.

The patients were selected based on clinical presentations of painful knee or hip arthroplasties and were recruited from the implant revision waiting list over a 2 year period. The initial goal had been to scan 50 prostheses as proof of concept in order to ensure adequate numbers of hips and knees with both septic and aseptic loosening as well as other possible diagnosis. Ultimately, 15 patients with 25 prostheses were scanned.

All patients had conventional isotope bone scans and multiphasic ^{18}F-NaF PET-CT scans; and serum inflammatory markers. All patients were followed up clinically and some had post-surgical microbiological and histological evaluation of the joint prostheses. The trial algorithm that was followed is schematically represented as a flow diagram of the progress through the phases of prospective uncontrolled longitudinal observational study (Figure 25).

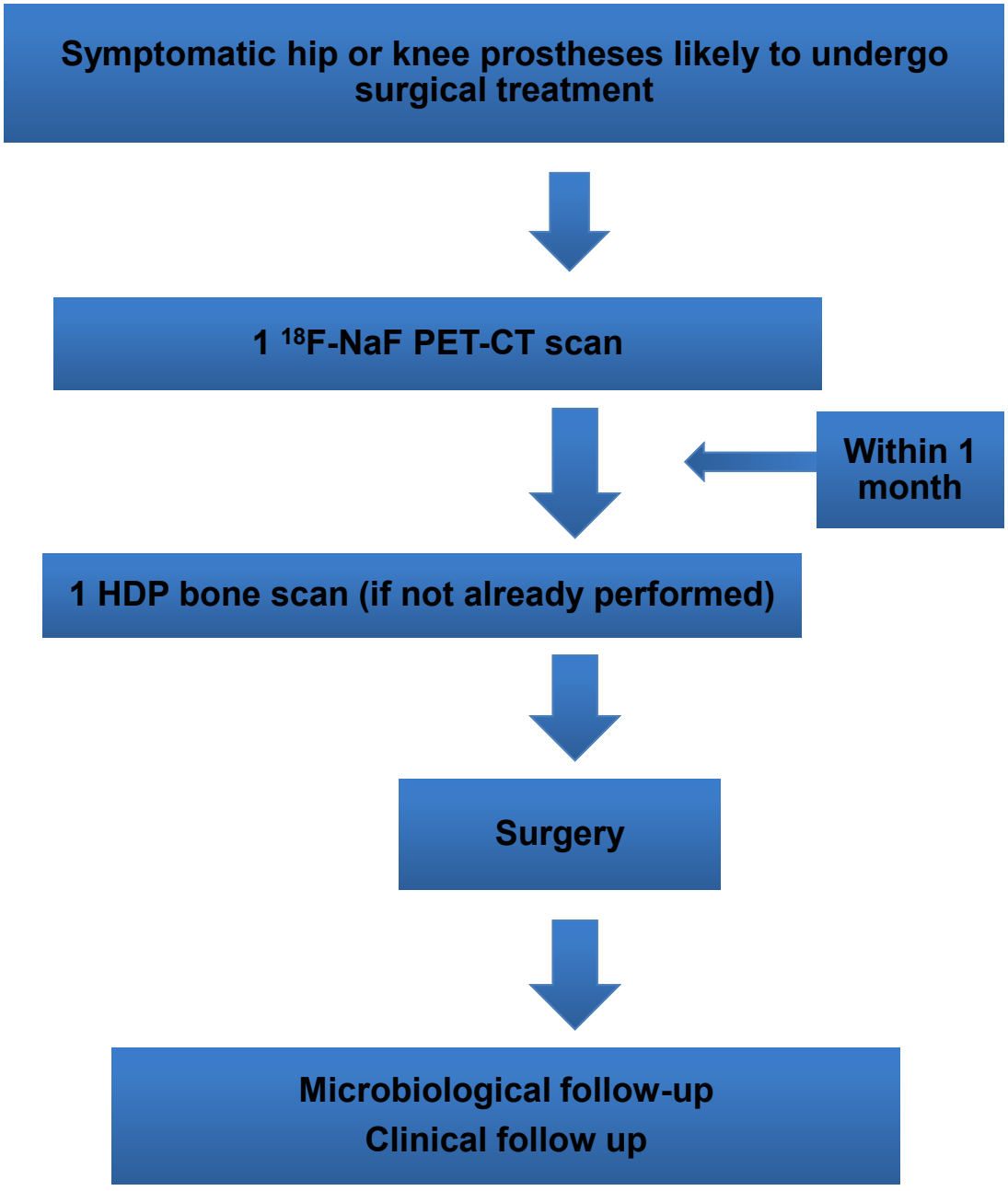

Figure 25. *Trial algorithm*

Analysis of PET-CT data: Visual scoring was performed as described by Kobayashi et al (169), with 3 types of PET-CT image findings defined according to the ^{18}F-NaF pattern of uptake with sub-groupings, based on the localization of the ^{18}F-NaF pattern of uptake, was divided as follows: (Type 1) no localized uptake; (Type 2) minor localized uptake; and (Type 3) more extensive diffuse periprosthetic uptake that extends over one half of the bone-implant interface (169).

Automated computerised analysis was performed using the Advantage Workstations (versions ADW 4.6 and ADW 4.3) software as well as Xeleris® version 4 both developed by the GE Healthcare. Bone scan images were analysed with Xeleris® version 4 and Insignia® InSight PACS version 8.2. CT density maps were obtained using OsiriX® software version 10.0.2. Two versions of the ADW 4.6 and ADW 4.3 were used due to a change in hospital equipment and also different functionalities on the newer version ADW 4.6.

Images were also assessed with Xeleris® version 4 and MATLAB® open source software programmes developed by the Nuclear Medicine department University hospital Coventry & Warwickshire and statistics information was provided by the Statistics department, University of Warwick.

Statistical analysis: Statistical analyses of the relationship between the uptake type classification, intensity of activity and the final diagnosis was performed using the extended Fisher exact test. The differences between the maximum standardized uptake values (SUVmax) for each diagnosis was analysed by 1-way analysis of variance followed by a Fisher protected least significant difference (PLSD) test. Graphical curves of the SUVmax values were plotted for the diagnosis of infection and loosening generated using GE Healthcare Advantage Workstation 4.6 software. P values of less than 0.05 were considered statistically significant.

Inclusion Criteria:

1. Symptomatic hip or knee prostheses awaiting surgical revision.

2. No previous major surgical procedure on the joint in 12 months

3. All patients of childbearing potential had to be screened for pregnancy.

4. Written informed consent.

Exclusion Criteria:

1. Other concurrent uncontrolled medical conditions

2. Pregnant or lactating (due to potential harmful radiation dose to the foetus)

3. General status that does not allow the investigations.

4. Any condition that compromised the patient's ability to give informed consent such as severe medical and psychiatric illnesses.

5. Prosthetic Joint replacement performed within the last 12 months.

Patients recruited from University Hospital Coventry and Warwickshire joint revision waiting list with help of Mrs Sue Price (secretary to Mr Pedro Foguet – orthopaedic surgeon).

6.4.1 Results

In total, 15 patients and 25 prostheses were scanned. These consistent of 9 hips ad 16 knees (Table 11).

Table 11. *Imaged prostheses*

Trial No.	TYPE OF PROSTHESIS	BONESCAN (number of joints)
1	Left KR	1
2	Right KR	1
3	Left KR	2
4	Right KR	2
5	Left KR	2
6	Right KR	2
7	Left KR	2
8	Right KR	2
9	Right HR	2
10	Right KR	1
11	Left KR	1
12	Right HR	2
13	Right HR	1
14	Right HR	2
15	Right HR	2

Note :KR = knee replacement, HR = hip replacement

Due to data corruption and storage difficulties, 5 static ^{18}F-NaF PET images and 10 dynamic graphs from ^{18}F-NaF PET imaging were unavailable for analysis (Table 12). All the successfully archived bone scans, CT images, dynamic NaF graphs and static NaF uptake images are detailed in (Tables 12 and 13).

Table 12. *Successfully archived images*

3-phase bone scan	CT scan	Dynamic NaF graph	Static NaF uptake
25 joints (15 symptomatic joints)	25 joints (15 symptomatic joints)	9 joints (5 patients, 5 symptomatic joints)	18 joints (10 patients, 10 symptomatic joints)

Note: Some patients had unilateral whilst others had bilateral joint replacements

Table 13. *List of patients and their successfully archived images*

Patient no.	Prosthesis	Bone scan	CT	Dynamic NaF graph	Static NaF uptake
1	1	+	+	+	+
2	1	+	+	-	+
3	2	+	+	-	+
4	2	+	+	+	+
5	2	+	+	-	+
6	2	+	+	-	+
7	2	+	+	+	+
8	2	+	+	-	+
9	2	+	+	+	+
10	1	+	+	-	-
11	1	+	+	-	-
12	2	+	+	+	+
13	1	+	+	-	-
14	2	+	+	-	-
15	2	+	+	-	-

Note :(+) successfully archived, (-) unsuccessfully archived

Of the 25 prostheses scanned, 15 joints were symptomatic and 10 joints were asymptomatic. Of the 15 patients that were scanned – 1 patient was lost to follow up due to death; 1 patient was diagnosed with results from clinical follow up and the remaining 13 patients were diagnosed following surgical revision. The commonest organisms cultured were Proteus Vulgaris, Pseudomonas Aeruginosa, and Staphylococcus Aureus by enrichment from cross-contamination (Table 14). All other relevant laboratory results are shown in Table 14. Out of the 13 patients that underwent surgery, 3 patients were inflamed or infected and 10 patents were loose or other (Table 14). The 3-phase bone scans were correlated with clinical and surgical findings as well as the type of successfully archived dynamic ^{18}F-NaF image (Table 15). 5 static ^{18}F-NaF PET-CT images and 6 ^{18}F-NaF graphs were successfully archived but there were 4 incomplete sets of ^{18}F-NaF PET-CT images (Table 15).

Table 14. *Laboratory Results*

TRIAL NO	ESR	CRP	WCC	NEUTROPHILS	PATHOLOGY ASPIRATE	MICRO-BIOLOGY/ HISTO-	CLINICAL	SURGERY
1	17	10	7.82	4.55	Neg.	Neg.	Not septic	No infection
2	13	<3	7.8	5.24	NS	NS	Not septic	No surgery
3	28	7	7.1	4.3	Neg.	Neg.	Not septic	Instability, Not loose, No infection
4	22	3	7.06	4.57	Neg.	Neg.	Negative	Loose, Synovitis
5	24	9	9.97	6.13	Neg.	Neg.	Loose	Loose
6	38	7	11.6	8.4	Neg.	Neg.	Loose	Synovitis, No infection
7	26	9	6.42	3.29	Neg.	Neg.	Loose	Failed mechanism Not infected
8	57	26	7.24	5.15	Neg.	PV, PA	Infected	Infected
9	46	10	6.2	4.03	Neg.	Neg.	Loose	Loose

TRIAL NO	ESR	CRP	WCC	NEUTROPHILS	PATHOLOGY ASPIRATE	MICRO-BIOLOGY/ HISTO-	CLINICAL	SURGERY
10	7	3	7.09	4.64	SA (e)	Neg.	Loose	Loose
11	7	6	7.3	4.1	Neg.	Deceased	Loose	Deceased
12	8	<3	5.29	3.48	Neg.	Neg.	Loose	Loose
13	95	8	7.12	4.41	Neg.	Neg.	loose	Loose
14	58	53	2.55	1.29	Neg.	Neg.	Not infected	Not infected
15	7	<3	5.84	4.13	Neg.	Neg.	Loose Peri-prosthetic fracture	Broken femoral stem

Note: Neg. = Negative, NS = No sample, PV = Proteus Vulgaris, PA = Pseudomonas Aeruginosa, SA (e) = Staphylococcus Aureus by enrichment - from cross-contamination

Table 15. *Bone scan findings*

TRIAL NO	CLINICAL	SURGERY	DYNAMIC NaF	3-PHASE BONE SCAN	P/B % BONE SCAN
1	Not septic	No infection	Graph	3-phase positive	30
2	Not septic	No surgery	Static	Late-phase positive	-100
3	Not septic	Instability Not loose No infection	Static	3-phase positive left	47.8
4	Negative	Loose, Synovitis	Graph	3-phase positive	41.6
5	Loose	Loose	Static	Late-phase positive	35
6	Loose	Synovitis No infection	Static	3-phase positive	57.8
7	Loose	Failed mechanism Not infected	Graph	3-phase positive	54
8	Infected	Infected	Static	3-phase positive	51.8
9	Loose	Loose	Graph	Late-phase positive	49
10	Loose	Loose	Incomplete	3-phase positive	54
11	Loose	Deceased	Incomplete	Late-phase positive	46

TRIAL NO	CLINICAL	SURGERY	DYNAMIC NaF	3-PHASE BONE SCAN	P/B % BONE SCAN
12	Loose	Loose	Graph	Late-phase positive	46
13	Loose	Loose	Graph	Late-phase positive	50
14	Not infected	Not infected	Incomplete	3-phase positive	30.2
15	Loose	Broken femoral stem	Incomplete	Right hip normal	-17.5

Note: P/B = Periprosthetic: Bone ratio.

Only 1 patient of the 3 patients with inflamed or infected joints was infected with Proteus Vulgaris and Pseudomonas Aeruginosa (Table14). The other 2 patients demonstrated non-infected inflammatory arthropathies. There was a single case of Staphylococcus Aureus contaminant in an aseptic joint that was grown by enrichment only. 3-phase bone scans were 100 % sensitive for sepsis and inflammation but had a 42% false positive rate for sepsis/inflammation (Tables 15 and 16). The 3-phase bone scan uptake patterns were correlated with final diagnosis of aseptic loosening or septic prostheses (Table 16) to reveal 58 % sensitivity for aseptic loosening (Tables 15 and 16). All 3 patients with synovitis or septic loosening exhibited higher periprosthetic/background percentage ratios above 40 but there were 6 false positive cases of high periprosthetic/background percentage ratios in aseptic loosening (Table 15).

6.4.4 Analysis of Bone Scan Periprosthetic Uptake Pattern

The bone scan periprosthetic uptake images were correctly interpreted as positive for aseptic loosening in 7 of 12 patients (Table 16) and correctly interpreted as positive for infection/inflammation in 3 of 3 patients and 5 patients were incorrectly identified as septic (Table 16). The bone scan uptake pattern was assessed by applying the final prosthetic joint diagnosis using two-tailed Fisher's exact test, p = 0.2 (Table 16), indicating that null hypothesis can be accepted and the results show no significant effect of the final prosthetic joint diagnosis on the bone scan pattern, i.e., independence between final prosthetic joint diagnosis and the bone scan pattern (Table 16).

Table 16. *Bone scan uptake pattern with final diagnosis*

Dynamic bone scan pattern	Aseptic	Septic/inflamed
3-phase positive	5*	3*
Late-phase positive	7*	0*

Note: *p>.05

6.4.5 Analysis of Bone Scan R^2 Trend Line

The R^2 trend line was calculated using a linear equation (Equation 1) which was plotted on a 25 cm chart representing the relationship between periprosthetic uptake (y) versus time (x) from a dynamic bone scan of a symptomatic joint. The regression line is used to visually depict the relationship between the independent (x) and dependent (y) variables of time and uptake respectively in the graph and is graphically represented as:

Equation 1. *Bone scan trend line equation*

$$y = mx + b$$

or

y = slope(x) + (y-intercept)

m is the slope and

b is the y-intercept where the curve crosses the y-axis.

The coefficient of correlation "R" is the degree of relationship between the 2 variables - x and y whilst the coefficient of determination is the square of coefficient of correlation R^2. To create the bone scan trendline, use a 25 cm chart of dynamic bone scan periprosthetic uptake plotted against time. Calculate y which is the intercept. Then calculate the slope m. Thereafter, calculate R and R^2 from the graph. The graph also demonstrates a linear regression line or trendline From the trendline, calculate to see if m is greater than 0.5 or if $R^2 > 0.2$ as the higher values are more likely to be infected or inflamed as seen on boxplot chart (Figure 26). The diagnosis of prosthetic joint loosening or infection was confirmed in 15 of 15 joints using the R^2 bone scan trendline cut off of 0.2. The R^2 trendline therefore had 100% sensitivity for sepsis and inflammation as well as 100% sensitivity for aseptic loosening. There was strong concordance obtained between the final prosthetic joint

diagnosis and the R^2 bone scan trend line pattern as shown in Table 17 and Figure 26.

Table 17*Bone scan R^2 trend line pattern in aseptic and septic/inflamed joints*

R^2 Bone scan Trendline	Aseptic	Septic/inflamed
>0.2	0*	3*
<0.2	12*	0*

Note: *p<.05

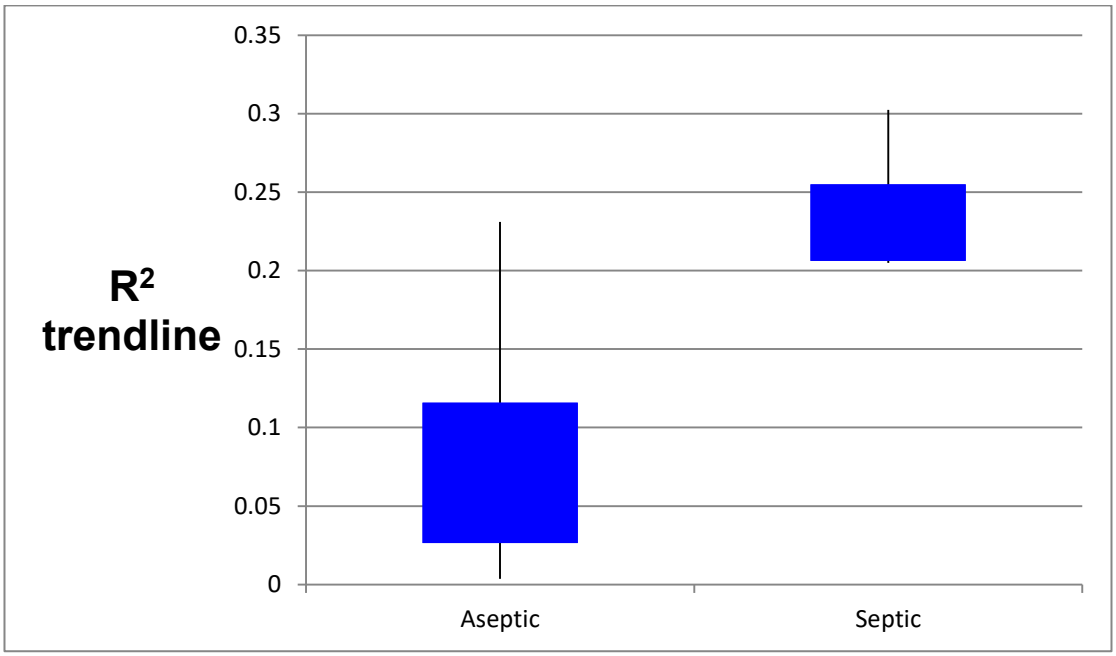

Figure 26. *Box and whisker plot of 3-phase bone scan R^2 trend line pattern*

Note: The box and whisker plot of 3-phase bone scan R^2 trend line pattern with the final diagnoses of aseptic or septic prosthesis.

The R^2 bone scan trendline pattern was calculated in 3-phase bone scans with a final diagnosis of aseptic or septic prosthesis. It was determined that an R^2 bone scan trendline of 0.2 was the optimal cut-off point above which the likelihood of a septic joint was higher using the two-tailed Fisher's exact test *p* value = .0022 (Table 17). The null hypothesis can therefore be rejected and the results that the final prosthetic joint diagnosis has a significant effect of on the R^2 bone scan trendline pattern, i.e., dependence between final prosthetic joint diagnosis and the R^2 bone scan trendline pattern which is considered to be very statistically significant (Table 17). The optimal cut-off point of 0.2 is also shown on the box and whisker plot of the 3-phase bone scan R^2 trend line pattern (Figure 26). The R^2 trendline pattern was correctly interpreted as positive for aseptic loosening in 12 of 12 patients (Table 17) and correctly interpreted as positive for infection/inflammation in 3 of 3 patients. There was no false positive or false negative case in both the aseptic loosening and infection/inflammation group (Table 17). The patient with an infected prosthesis was indistinguishable from inflammatory synovitis on the bone scan trendline images (Table 18). Figures 27 to 41 demonstrate the relevant 3-phase bone scan R^2 trend line images in all 15 patients.

Table 18. *Final diagnoses with CT, NaF PET and bone scan trend line results*

TRIAL NO	CLINICAL	SURGERY	BONE SCAN TREND-LINE RIGHT	BONE SCAN TREND-LINE LEFT	DYNAMIC NaF	NaF UPTAKE	CT LUCENCY
1	Not septic	No infection	0.06095	0.03212	Loose pattern	Type 2	Positive
2	Not septic	No surgery	0.03932	0.00319	Nil	Type 2	Positive
3	Not septic	Instability Not loose No infection	0.00485	0.12549	Nil	Type 2	Positive
4	Negative	Loose, Synovitis	0.30232	0.32277	Loose pattern	Type 3	Positive
5	Loose	Loose	0.00604	0.23101	Nil	Type 2	Positive
6	Loose	Synovitis No infection	0.20751	0.11472	Nil	Type 3	Positive
7	Loose	Failed mechanism Not infected	0.07755	0.13825	Infected pattern	Type 2	Positive

TRIAL NO	CLINICAL	SURGERY	BONE SCAN TREND-LINE RIGHT	BONE SCAN TREND-LINE LEFT	DYNAMIC NaF	NaF UPTAKE	CT LUCENCY
8	Infected	Infected	0.20486	0.0218	Nil	Type 3	Positive
9	Loose	Loose	0.10591	0.00151	Loose pattern	Type 3	Positive
10	Loose	Loose	0.10029	0.00084	Nil	Nil	Positive
11	Loose	Deceased	0.00079	0.02198	Nil	Nil	Positive
12	Loose	Loose	0.02378	0.03831	Loose pattern	Type 3	Positive
13	loose	Loose	0.00358	0.04999	Nil	Nil	Positive
14	Not infected	Not infected	0.02895	0.11915	Nil	Nil	Positive
15	Loose	Broken femoral stem	0.03233	0.0381	Nil	Nil	Positive

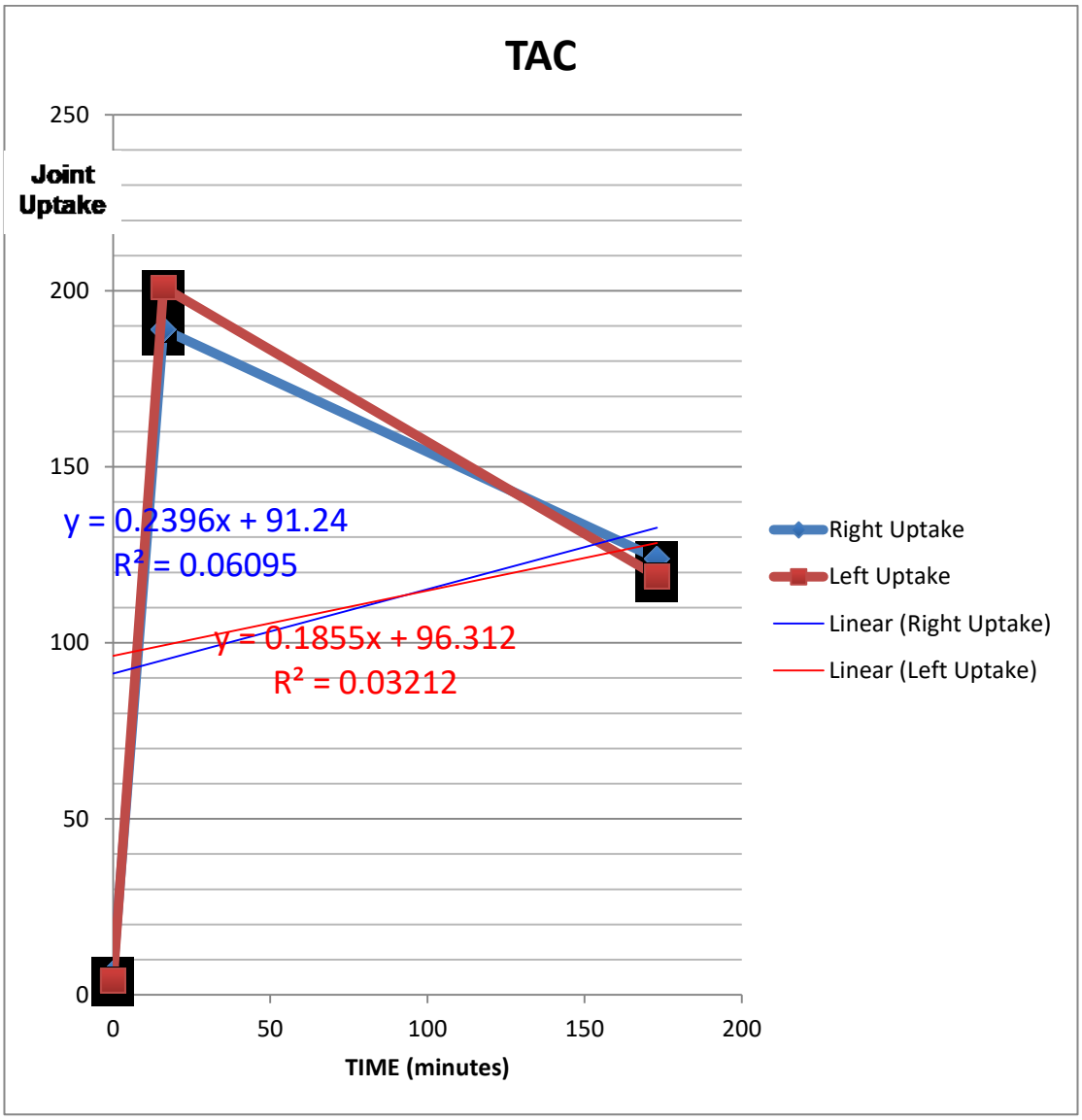

Figure 27. *Bone Scan TAC & trend line*

Note: Patient 1 with symptomatic unilateral left TKR (red) showing bone scan TAC & trend lines for both the symptomatic left knee (red) and the asymptomatic normal knee (blue).

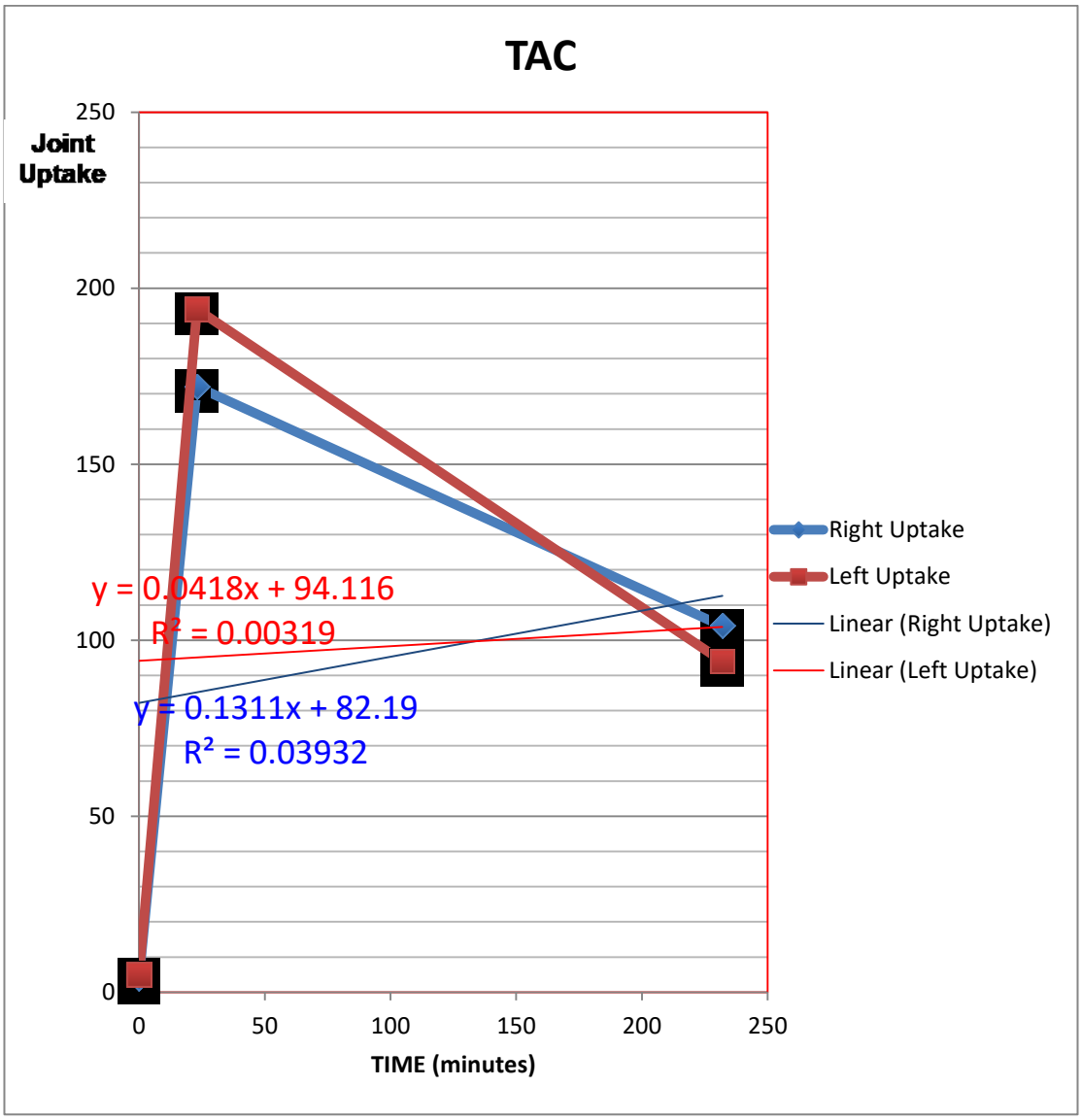

Figure 28. *Bone scan TAC & trend line*

Note: Patient 2 with symptomatic unilateral right TKR (blue) showing bone scan TAC & trend lines for both the symptomatic right knee (blue) and the asymptomatic normal knee (red).

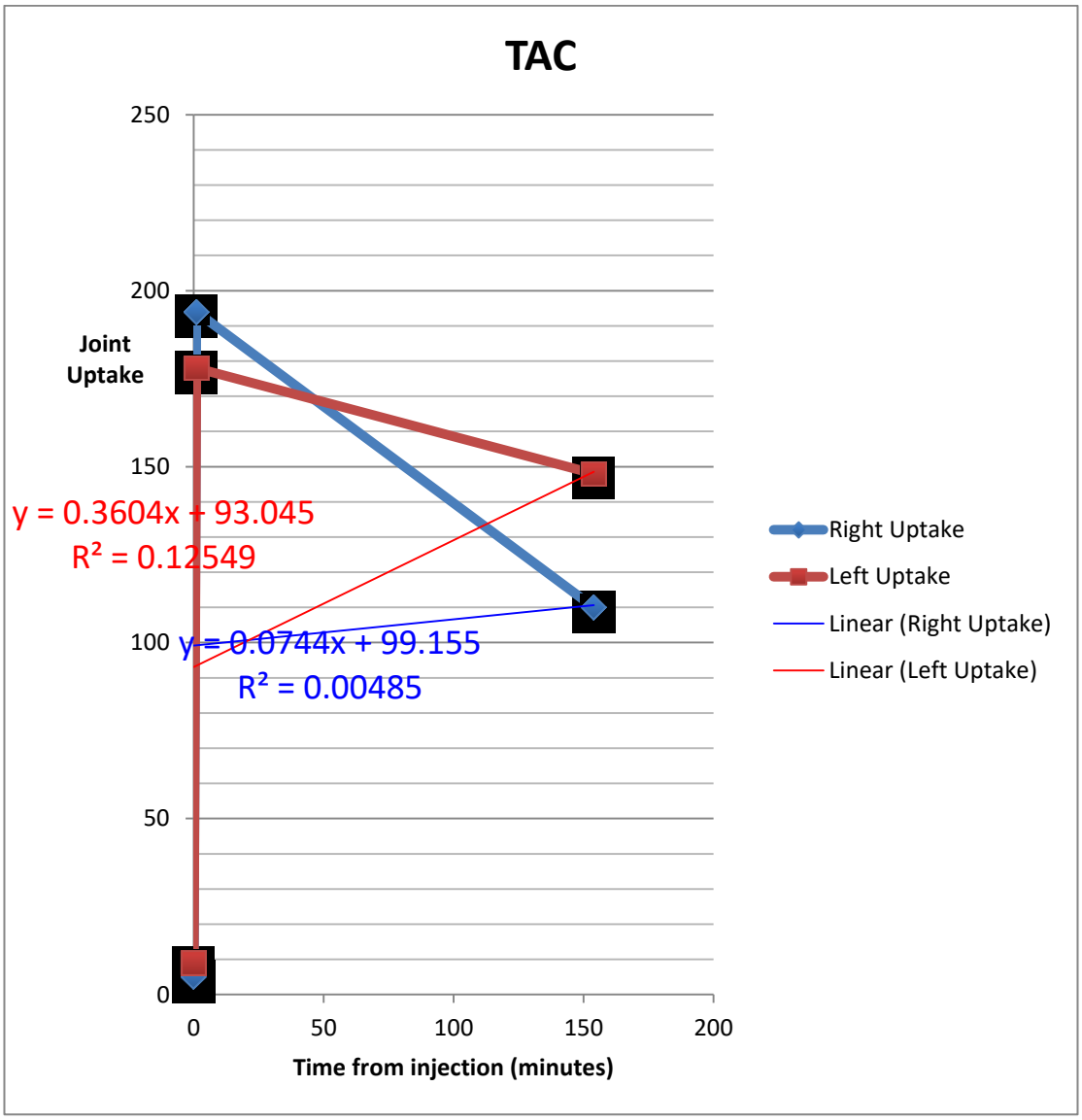

Figure 29. *Bone scan TAC & trend line*

Note: Patient 3 with bilateral TKR. This shows symptomatic left TKR (red) and the asymptomatic right TKR (blue) bone scan TAC & trend lines.

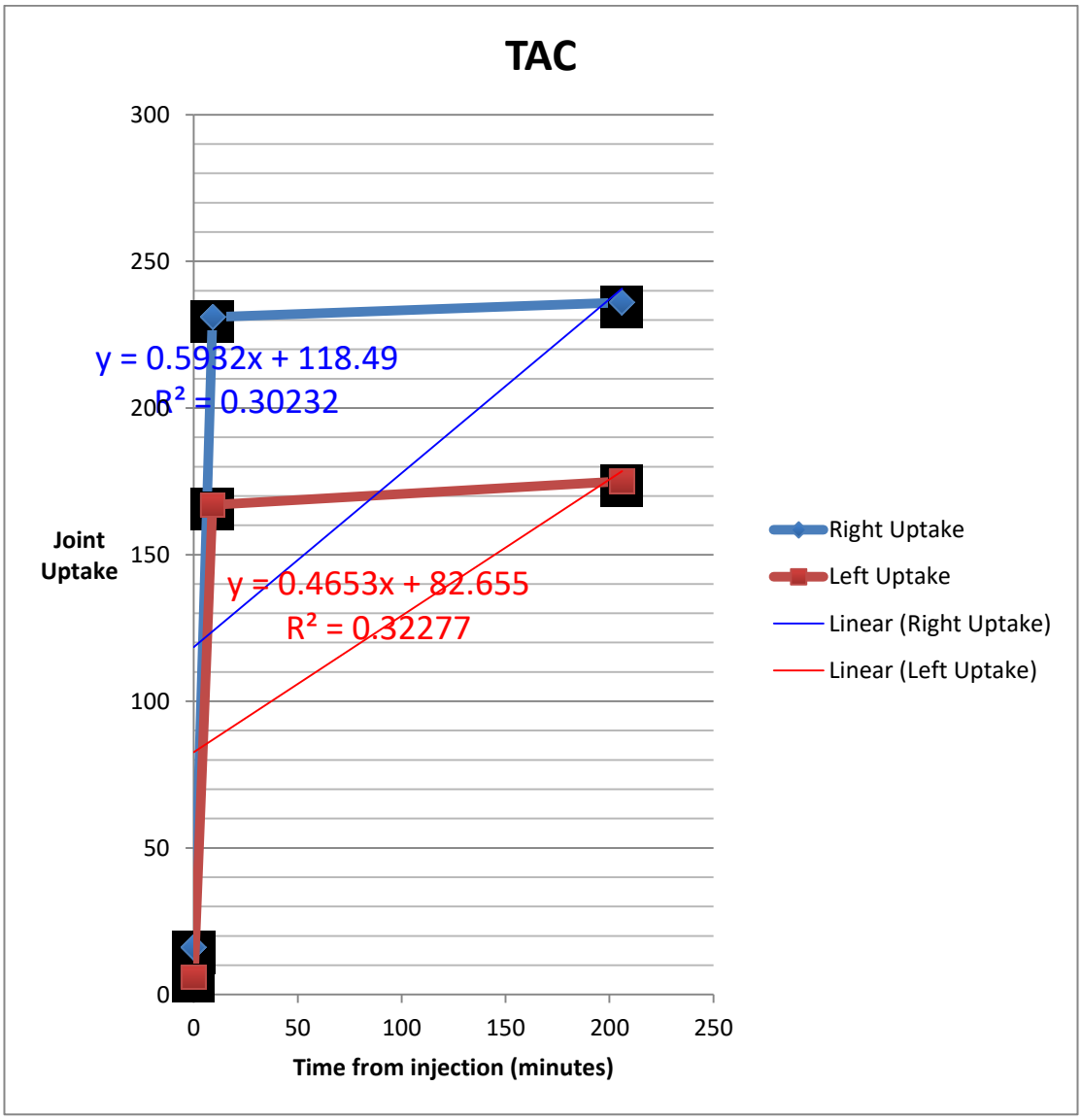

Figure 30. *Bone scan TAC & trend line*

Note: Patient 4 with bilateral TKR. This shows symptomatic right TKR (blue) and the asymptomatic left TKR (red) bone scan TAC & trend lines.

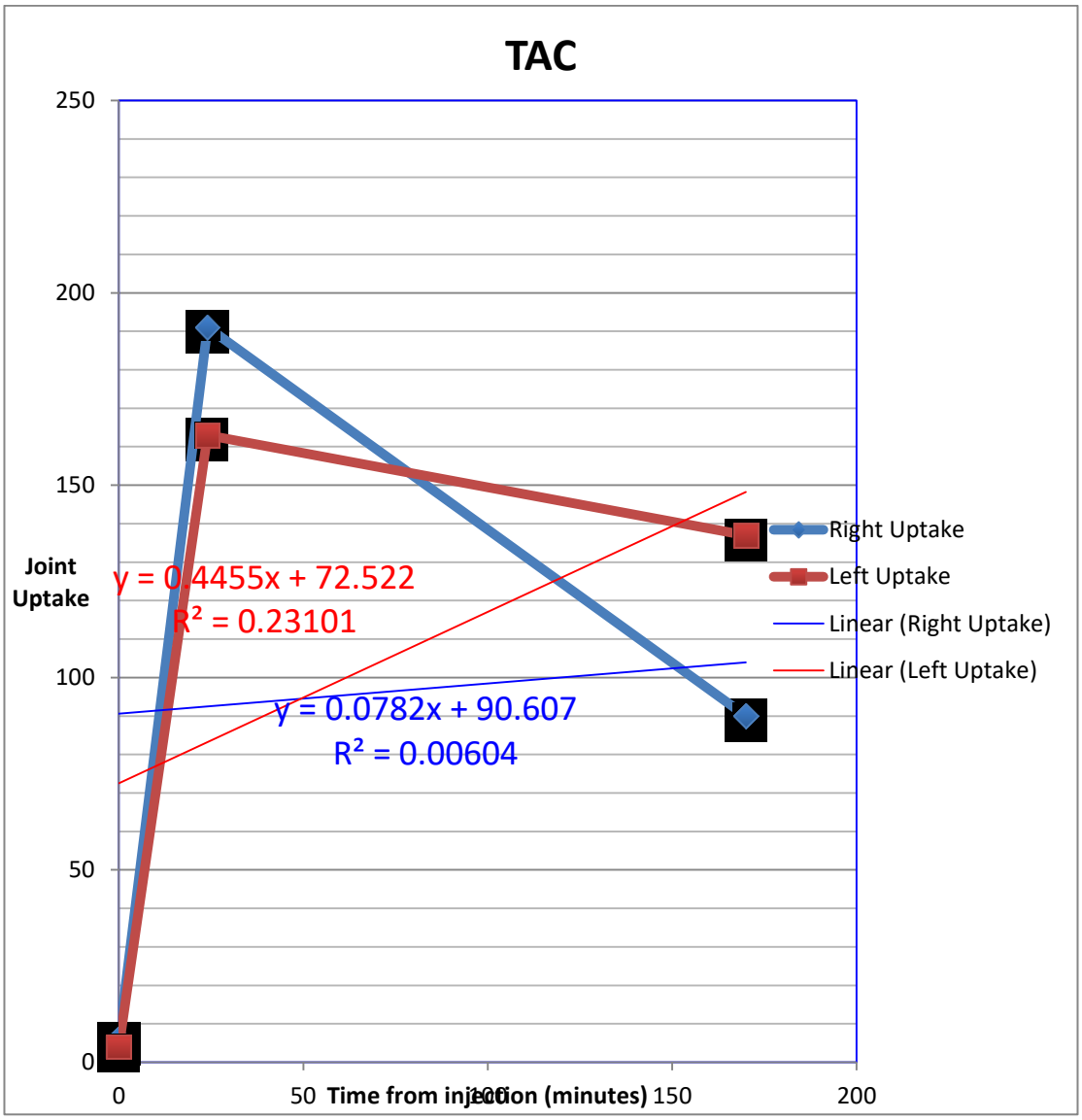

Figure 31. *Bone scan TAC & trend line*

Note: Patient 5 with bilateral TKR. This shows symptomatic left TKR (red) and the asymptomatic left TKR (blue) bone scan TAC & trend lines.

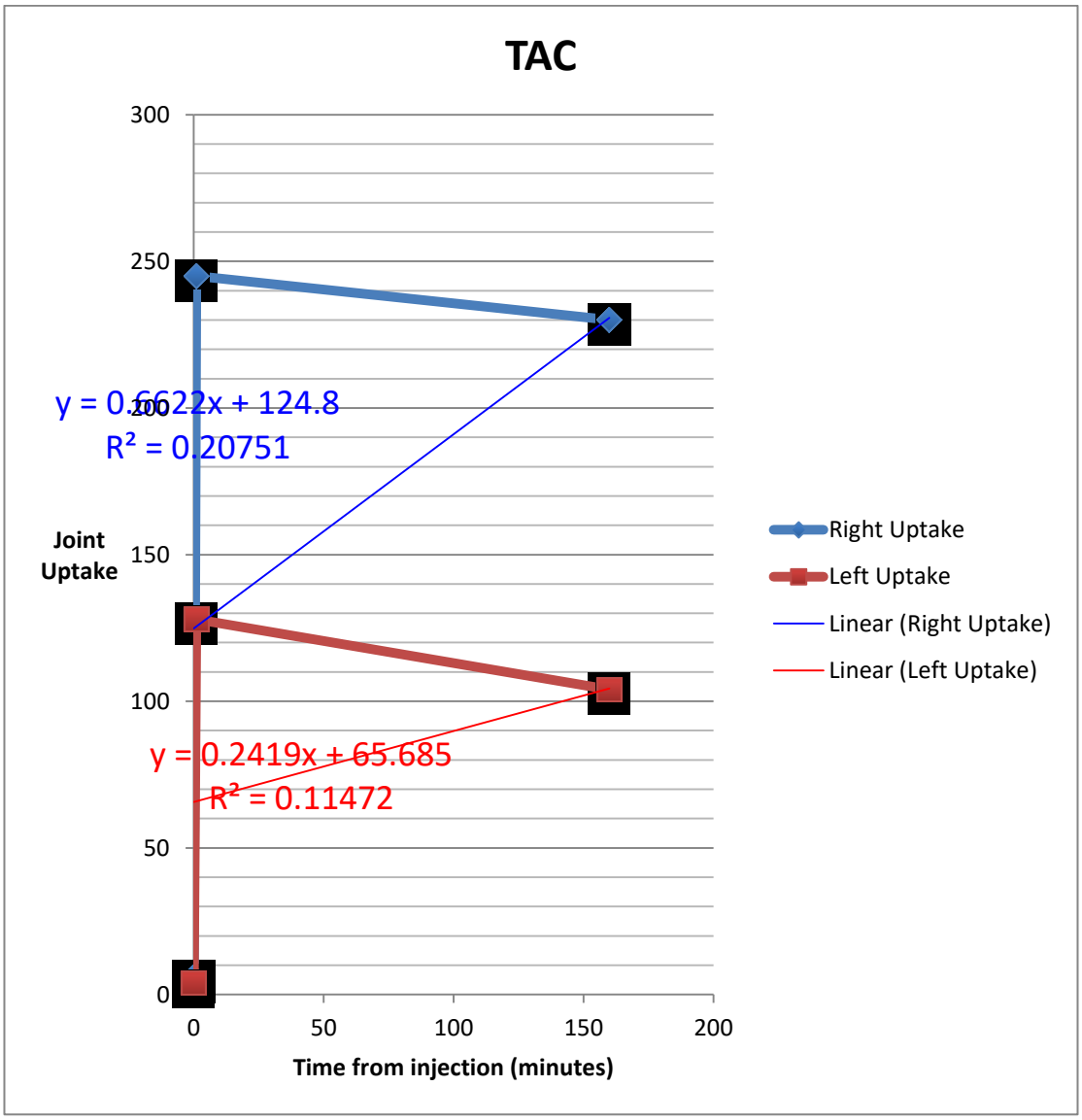

Figure 32. *Bone scan TAC & trend line*

Note: Patient 6 with bilateral TKR. This shows symptomatic right TKR (blue) and the asymptomatic left TKR (red) bone scan TAC & trend lines.

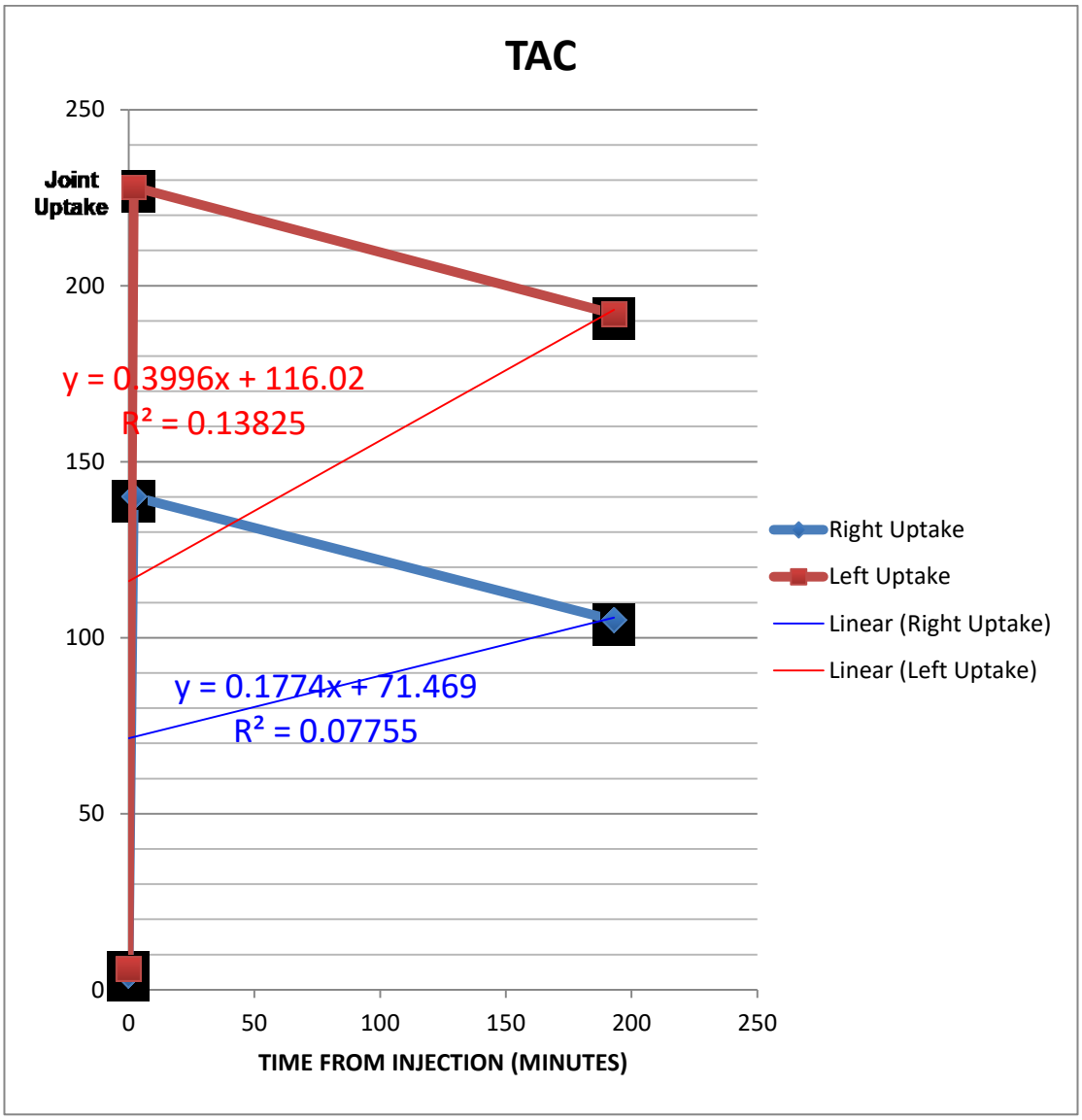

Figure 33. *Bone scan TAC & trend line*

Note: Patient 7 with bilateral TKR. This shows symptomatic left TKR (red) and the asymptomatic left TKR (blue) bone scan TAC & trend lines.

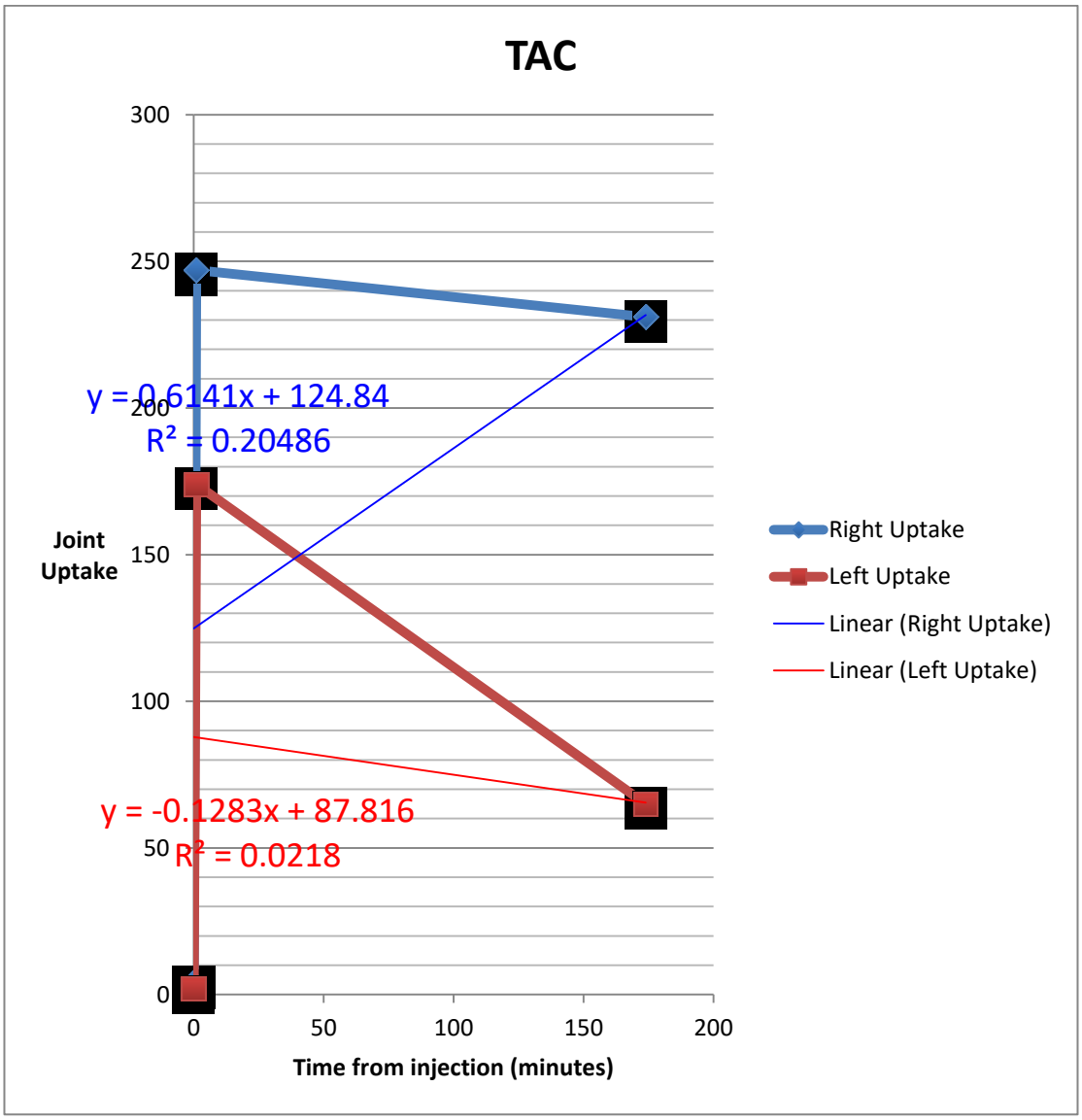

Figure 34. *Bone scan TAC & trend line*

Note: Patient 8 with bilateral TKR. This shows symptomatic right TKR (blue) and the asymptomatic left TKR (red) bone scan TAC & trend lines.

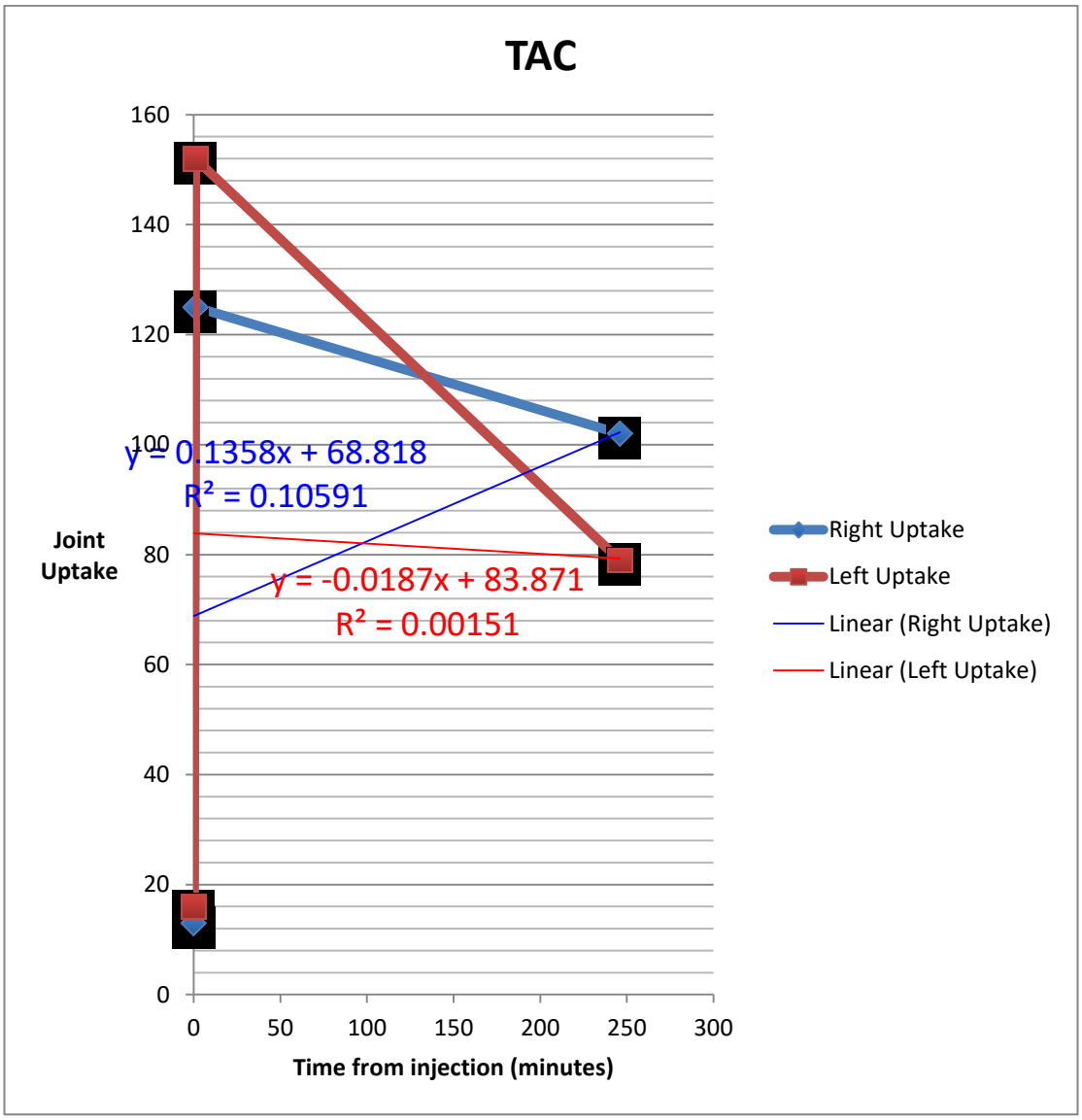

Figure 35. *Bone scan TAC & trend line*

Note: Patient 9 with bilateral THR. This shows symptomatic right THR (blue) and the asymptomatic left THR (red) bone scan TAC & trend lines.

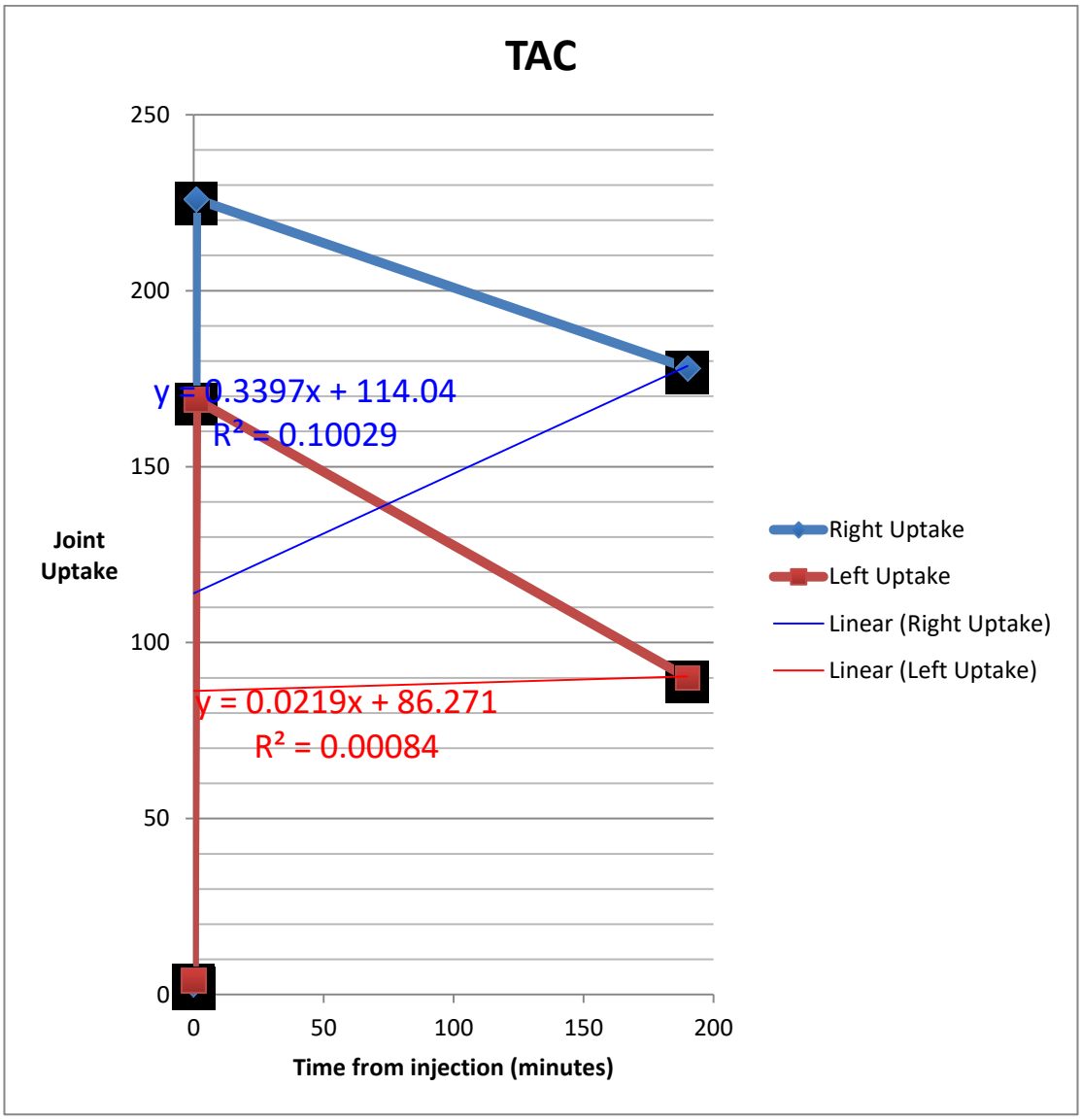

Figure 36. *Bone scan TAC & trend line*

Note: Patient 10 with symptomatic unilateral right TKR. This shows symptomatic right TKR (blue) and the asymptomatic normal left knee (red) bone scan TAC & trend lines.

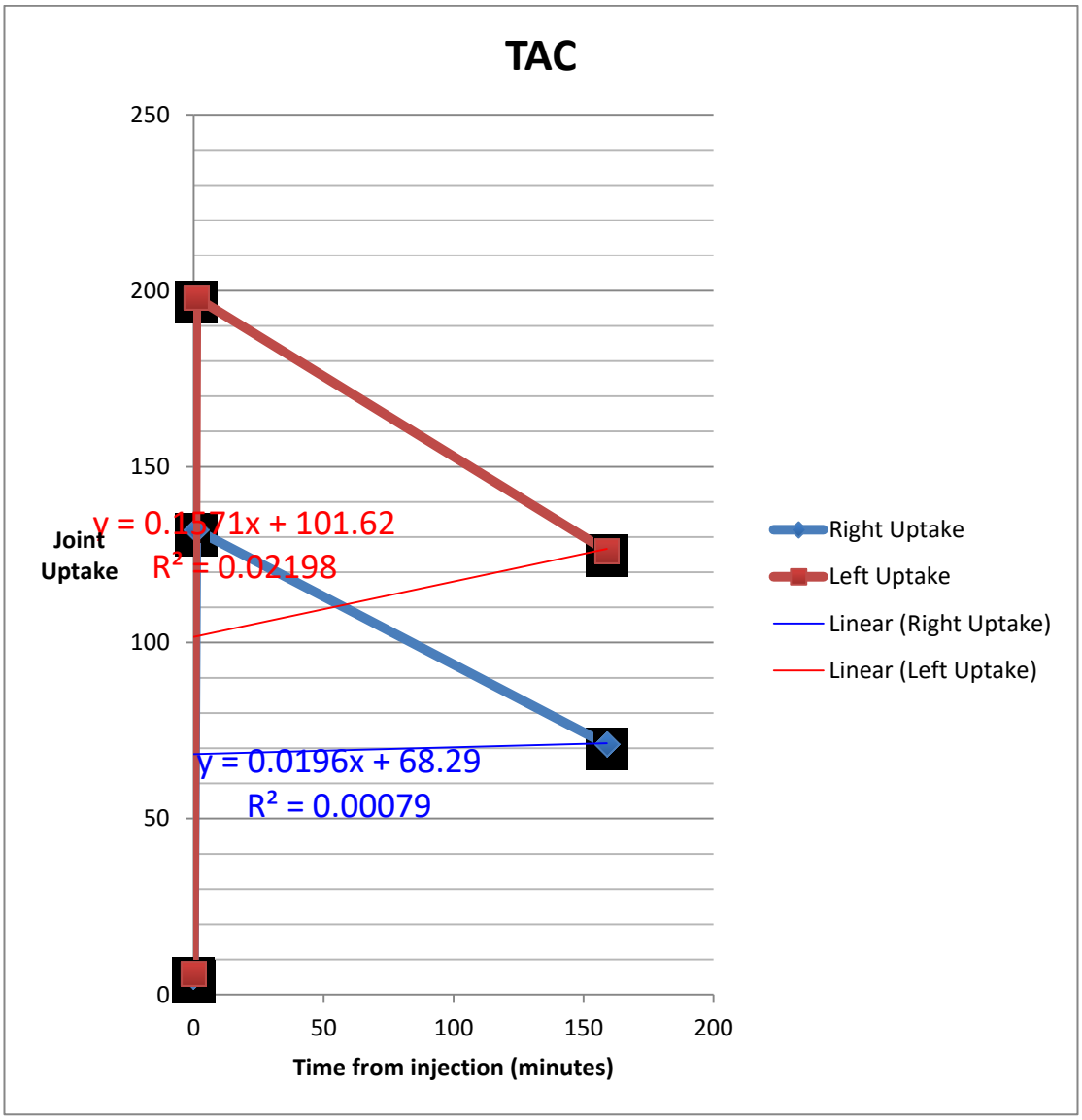

Figure 37. *Bone scan TAC & trend line*

Note: Patient 11 with symptomatic unilateral left TKR. This shows symptomatic left TKR (red) and the asymptomatic normal right knee (blue) bone scan TAC & trend lines.

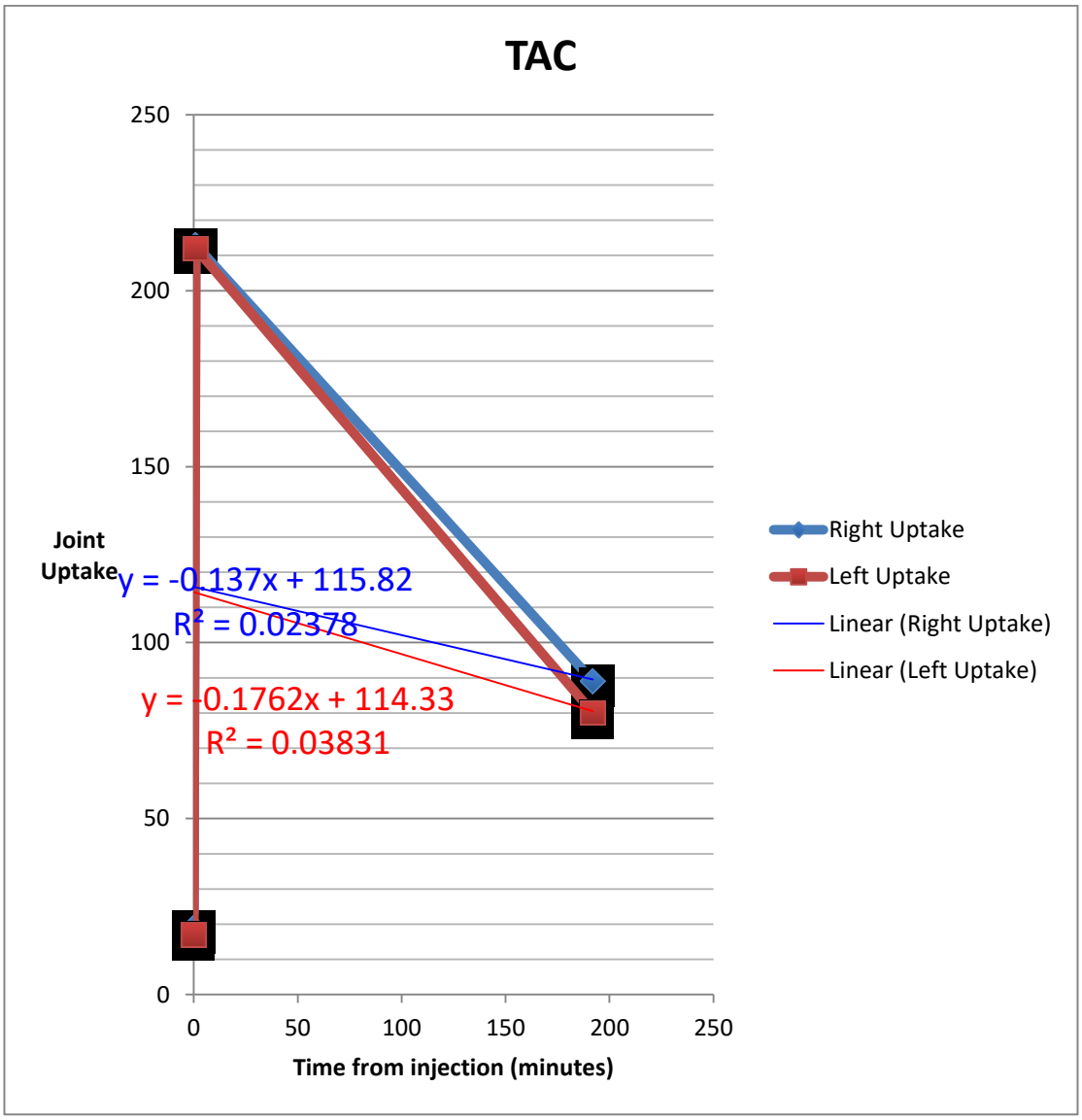

Figure 38. *Bone scan TAC & trend line*

Note: Patient 12 with bilateral THR. This shows symptomatic right THR (blue) and the asymptomatic left THR (red) bone scan TAC & trend lines.

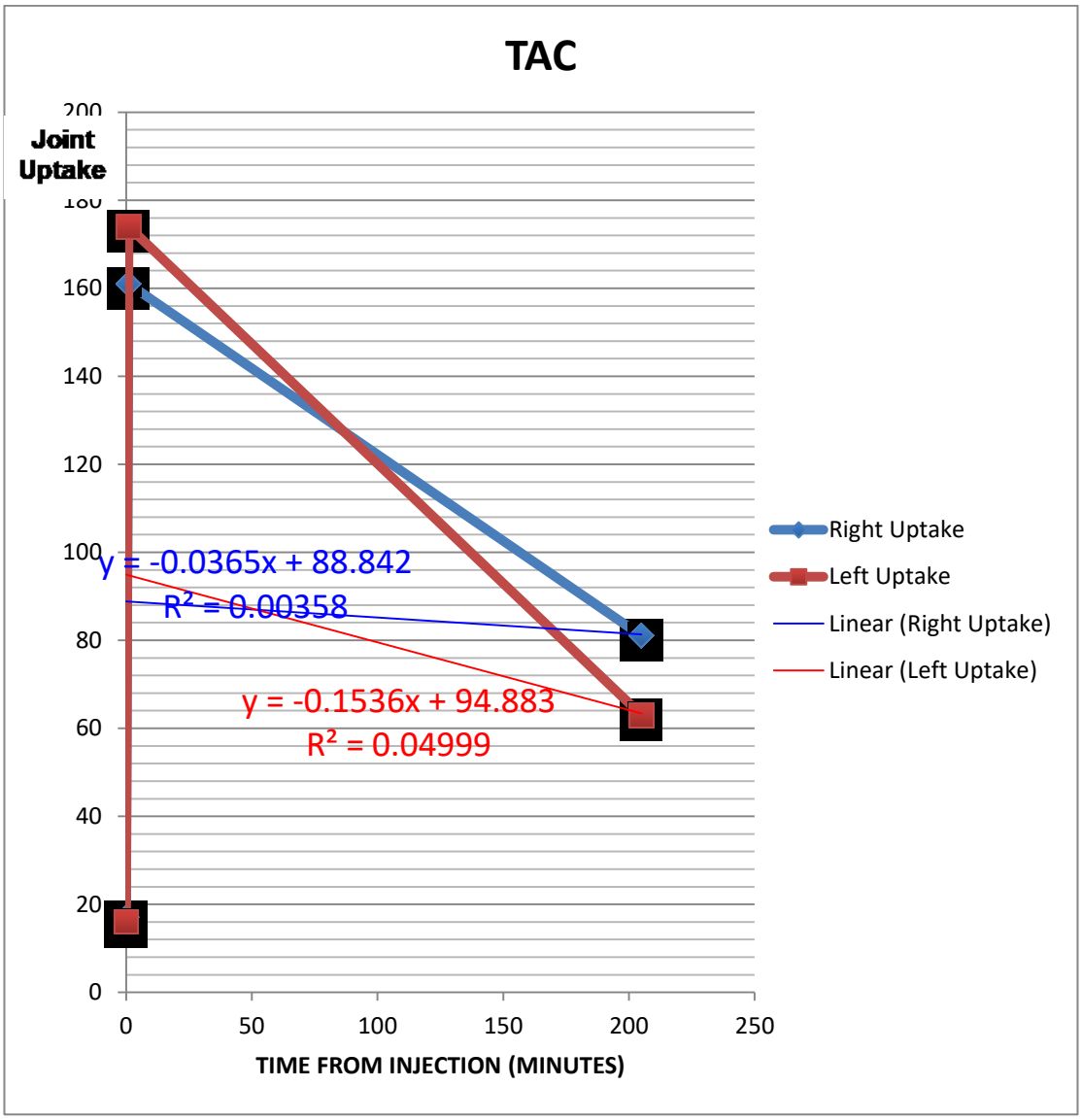

Figure 39. *Bone scan TAC & trend line*

Note: Patient 13 with bilateral THR. This shows symptomatic right THR (blue) and the asymptomatic left THR (red) bone scan TAC & trend lines.

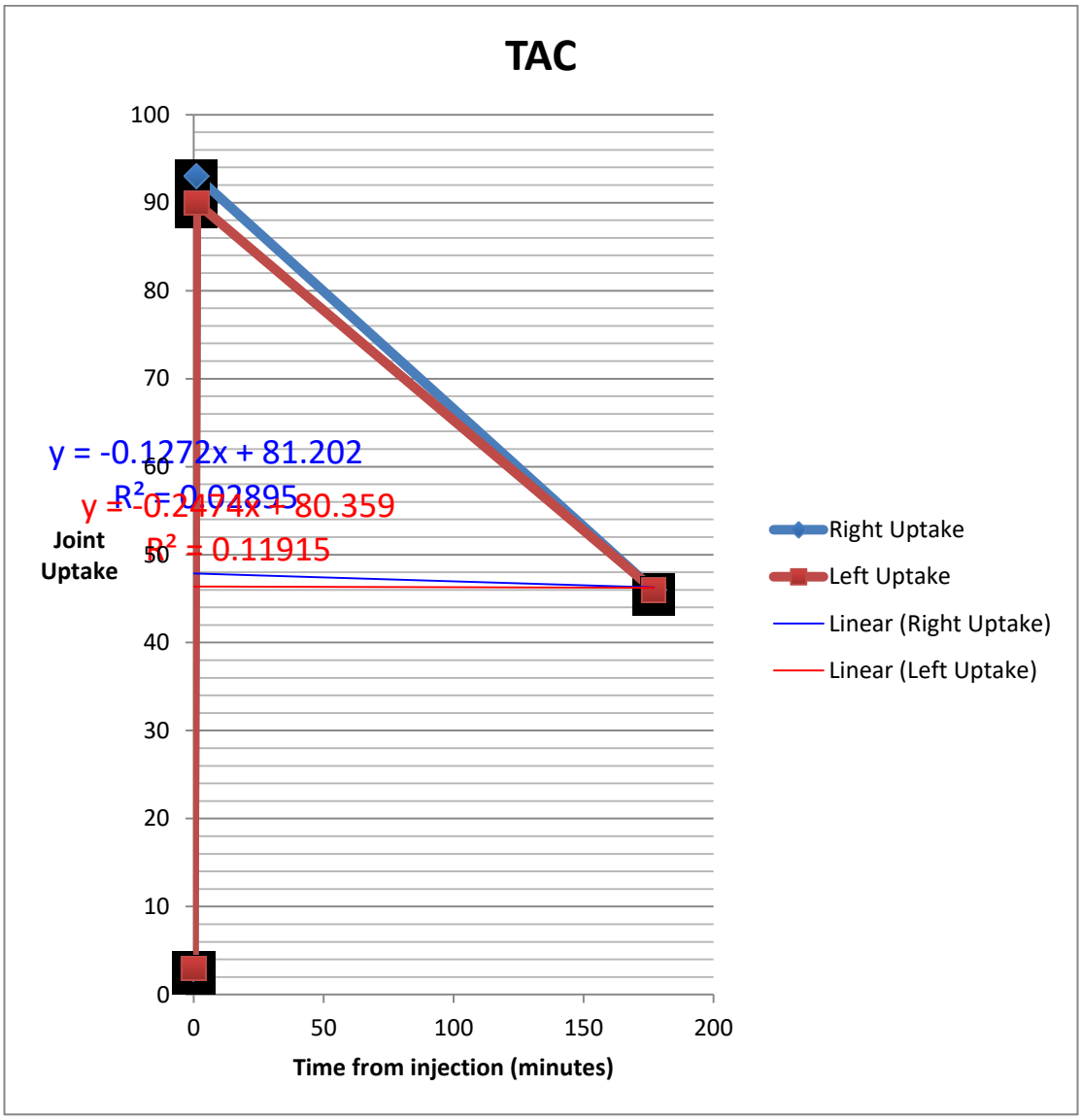

Figure 40. *Bone scan TAC & trend line*

Note: Patient 14 with bilateral THR. This shows symptomatic right THR (blue) and the asymptomatic left THR (red) bone scan TAC & trend lines.

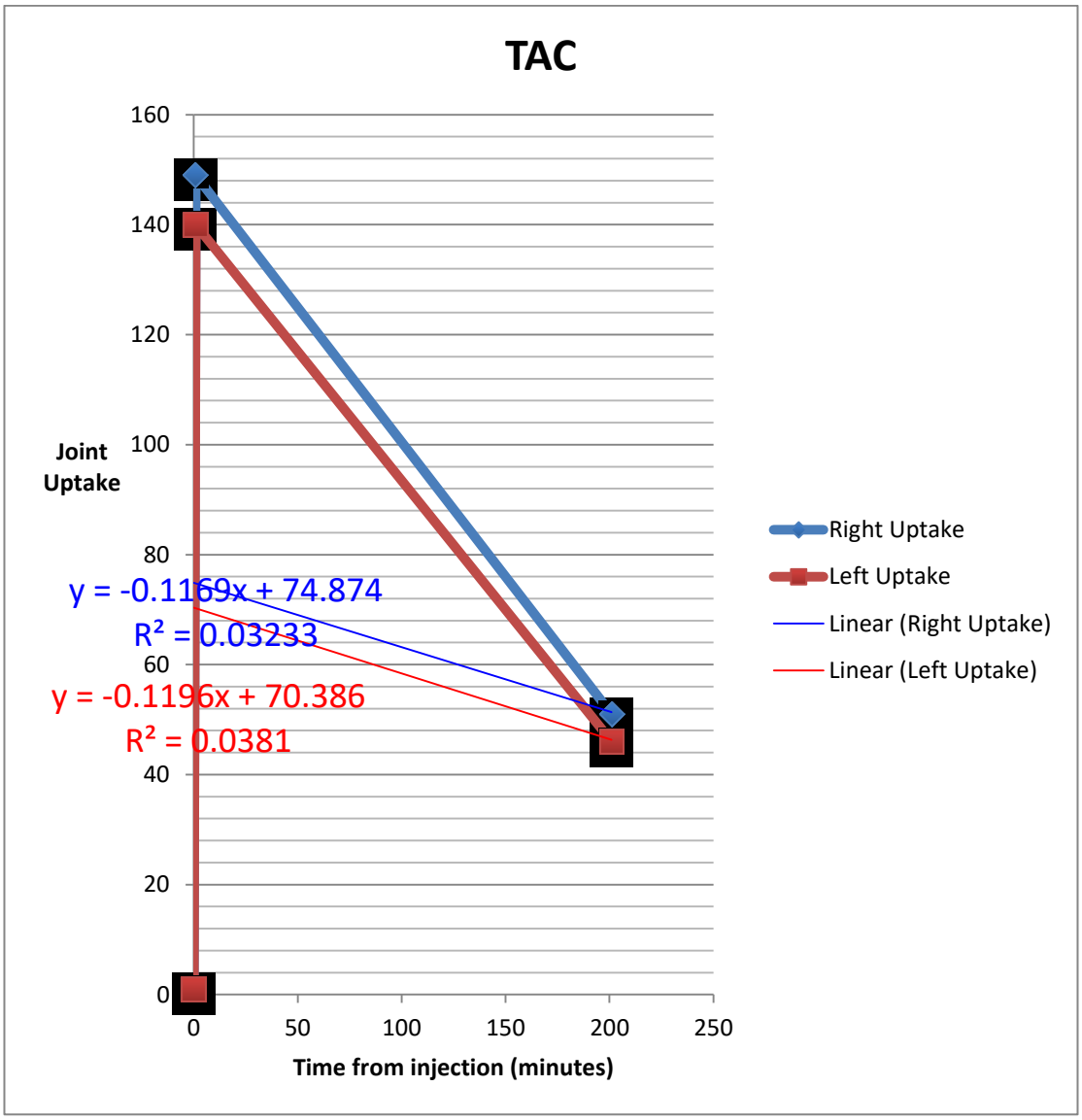

Figure 41. *Bone scan TAC & trend line*

Note: Patient 15 with bilateral THR. This shows symptomatic right THR (blue) and the asymptomatic left THR (red) bone scan TAC & trend lines.

6.4.2 Analysis of NaF Periprosthetic Uptake Pattern

The NaF periprosthetic uptake images were correctly interpreted as positive for aseptic in 5 of 5 patients (Table 19) and correctly interpreted as positive for infection/inflammation in 3 of 3 patients. 2 patients were incorrectly identified as septic (Table 19).

The NaF uptake pattern was assessed by applying the final prosthetic joint diagnosis using two-tailed Fisher's exact test, $p = .1667$ (Table 19), indicating that null hypothesis can be accepted and the results show no significant effect of the final prosthetic joint diagnosis on the NaF uptake pattern, i.e., independence between final prosthetic joint diagnosis and the NaF uptake pattern (Table 19).

The NaF PET-CT static images were correctly interpreted as positive for aseptic loosening in 5 of 5 patients (Table 19) and incorrectly interpreted as positive for infection in 2 of 5 patients (Figure 42).

Table 19. *NaF uptake pattern with final diagnosis in aseptic and septic/inflamed joints*

NaF uptake pattern	Aseptic	Septic/inflamed
Type 1	0*	0*
Type 2	5*	0*
Type 3	2*	3*

Note: *$p>.05$

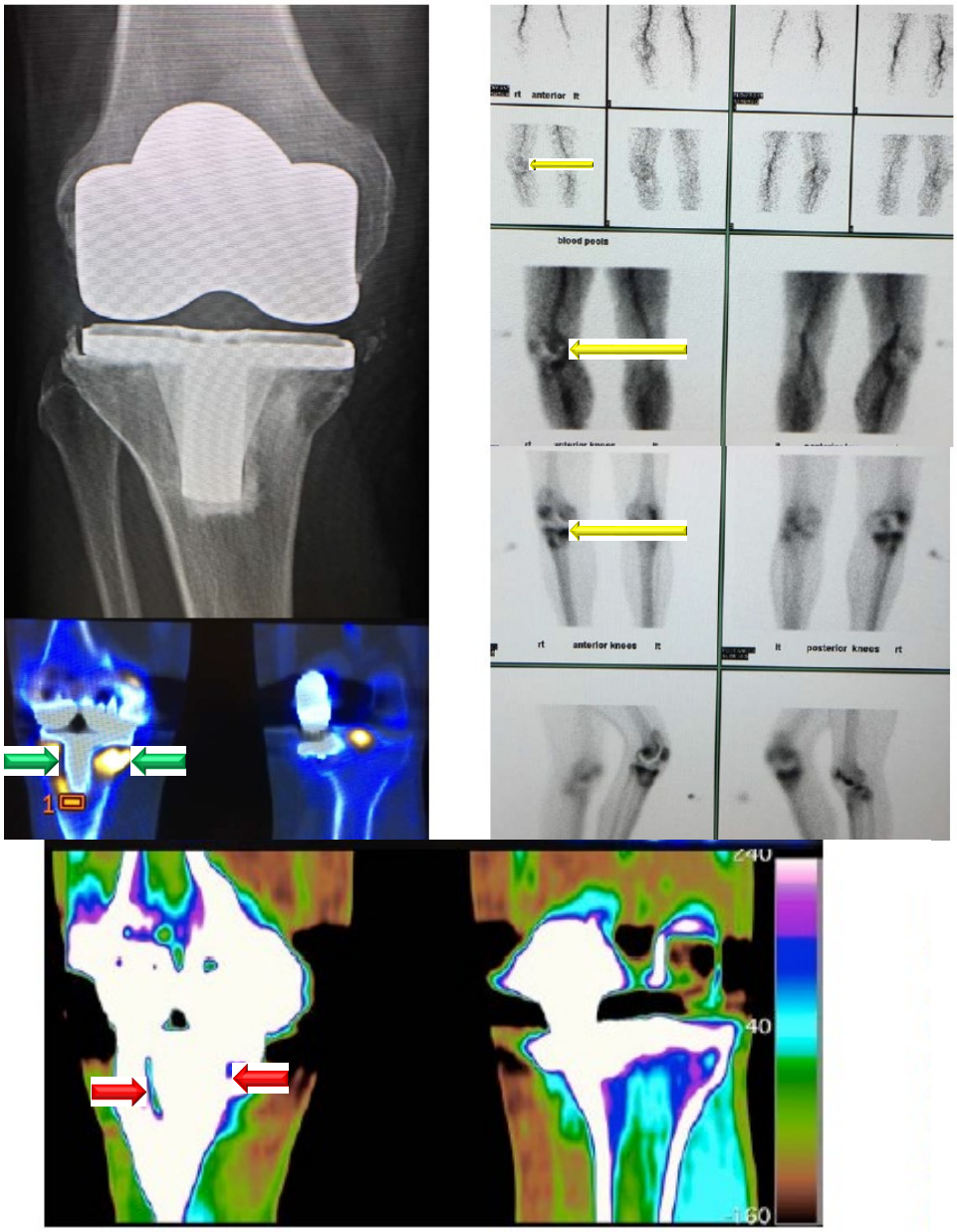

Figure 42. *Plain radiograph, NaF PET-CT, CT density map and bone scan*

Note: Patient 4's plain radiograph of the right knee with TKR shows periprosthetic radiolucency. The NaF PET-CT of the knees shows periprosthetic activity (green arrows). The CT density map of the right TKR shows periprosthetic radiolucency (red arrows). The arterial phase bone scan, blood pool phase and delayed phase bone scan show 3-phase increased uptake (yellow arrows).

6.4.3 Analysis of NaF Dynamic Time-Activity Curve

The dynamic NaF periprosthetic uptake images (Figures 43 and 44) were correctly interpreted as positive for aseptic loosening in 3 of 4 patients (Table 20) and the only infection/inflammation was incorrectly interpreted as negative for infection/inflammation in 1 of 1 patient. 1 patient was incorrectly identified as septic (Table 20). The dynamic NaF uptake pattern was assessed by applying the final prosthetic joint diagnosis using two-tailed Fisher's exact test, p = 1 (Table 20), indicating that null hypothesis can be accepted and the results show no significant effect of the final prosthetic joint diagnosis on the dynamic NaF uptake, i.e., independence between final prosthetic joint diagnosis and the dynamic NaF uptake pattern (Table 20).

Table 18. *Dynamic NaF pattern with final diagnosis in aseptic and septic/inflamed joints*

Dynamic NaF uptake pattern	Aseptic	Septic/inflamed
Normal pattern	0*	0*
Loose pattern	3*	1*
Infected pattern	1*	0*

Note: *p>.05

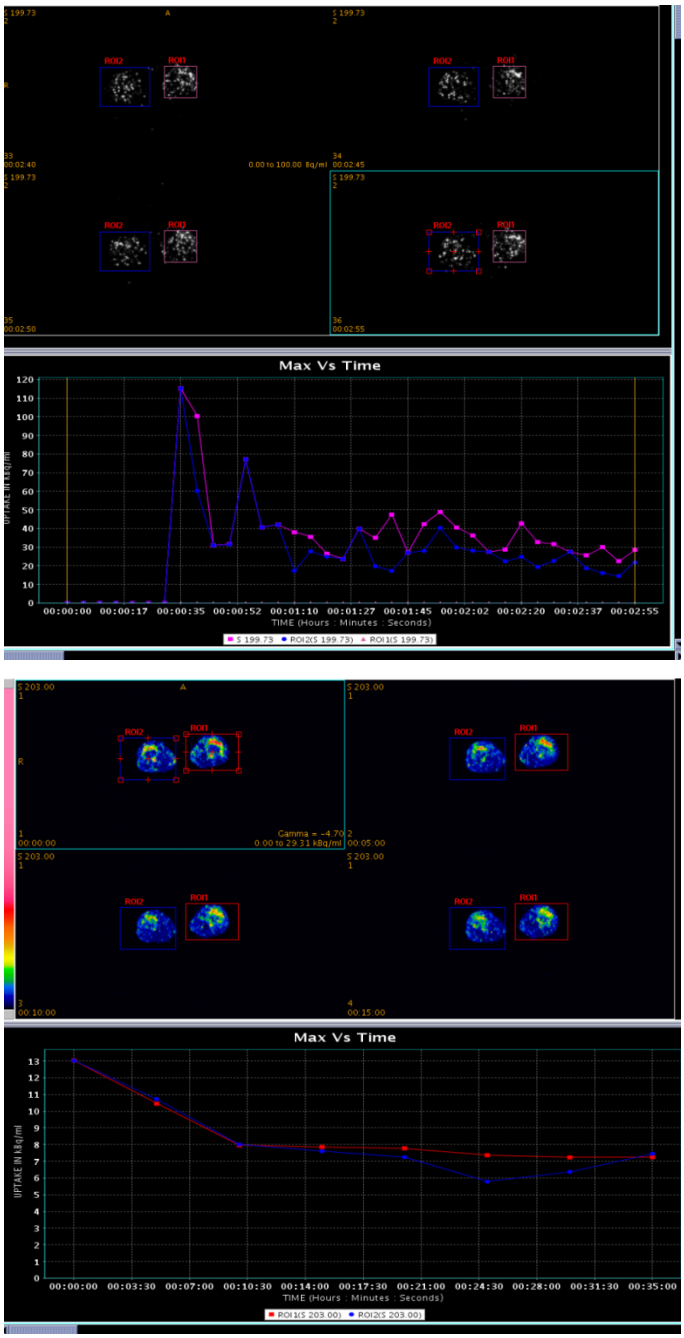

Figure 43. *Dynamic NaF graphs*

Patient 1 with a symptomatic left knee replacement (purple and red) which shows only relatively mildly increased uptake on the left when compared with the normal right knee (blue). The uptake curve demonstrates a gradual fall post-peak which matches with that of a non-septic or aseptically loose prosthesis which was confirmed with surgical findings.

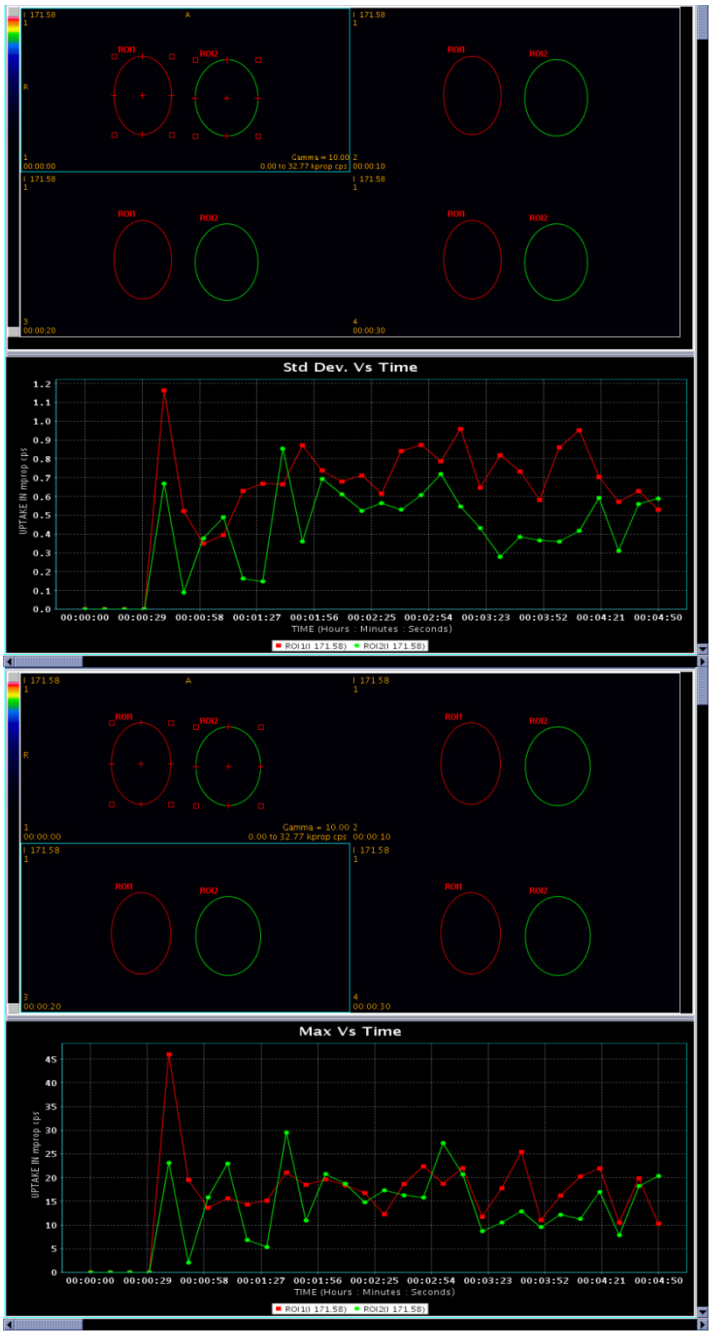

Figure 44. *Dynamic NaF graphs*

Patient 12 with symptomatic right hip showing confirmed aseptic loosening (red) and asymptomatic left hip (green). Symptomatic right hip with relative mildly increased uptake when compared with the normal left hip. The uptake curve is gradually rising and therefore suggestive of aseptic loosening which corresponded with surgical findings of aseptic loosening.

6.4.6 CT Periprosthetic Lucency Analysis

Periprosthetic lucency as seen on the CT density map images (Figure 45) were positive in 12 of 12 patients with aseptic loosening (Table 21) and positive in 3 of 3 patients with infection/inflammation. CT periprosthetic lucency and CT density maps did not distinguish aseptic loosening from septic loosening (Tables 18 and 21). Hence, CT periprosthetic lucency is a poor discriminator between aseptic loosening and infection/inflammation (Table 21). The CT lucency was assessed by applying the final prosthetic joint diagnosis using two-tailed Fisher's exact test, $p = 1$ (Table 21), indicating that null hypothesis can be accepted and the results show no significant effect of the final prosthetic joint diagnosis on the CT lucency, i.e., independence between final prosthetic joint diagnosis and the CT lucency (Table 21). Fisher's exact test was used to determine the statistical significance of differences between variables. The CT density map demonstrated periprosthetic radiolucency in all patients regardless of the final diagnosis (Table 21) and (Figure 42).

Table 19. *Periprosthetic lucency on CT*

CT Lucency	Aseptic	Septic/inflamed
Positive	12*	3*
Negative	0*	0*

Note: *p>.05

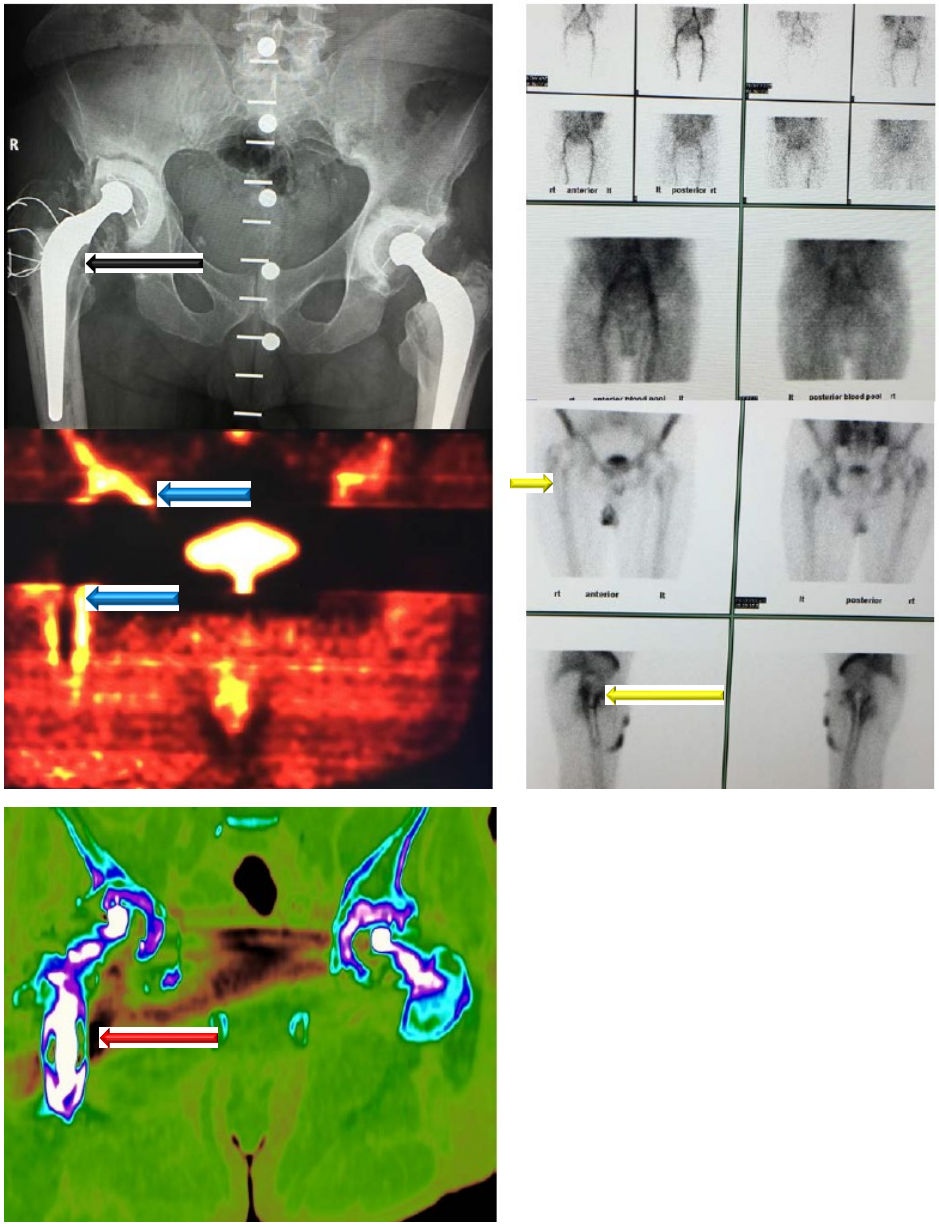

Figure 45. *Plain radiograph, NaF PET-CT, CT density map and bone scan*

Patient 9's plain radiograph of right THR shows periprosthetic radiolucency (black arrows). The NaF PET-CT of the hip demonstrates increased periprosthetic activity (blue arrows). The CT density map of the right THR shows periprosthetic radiolucency (red arrows). The arterial phase bone scan and blood pool phase bone scan without increased uptake. The delayed phase bone scan shows periprosthetic increased uptake (yellow arrows)

In summary, the results were affected by the reduced number of scans due to data corruption and storage difficulties with some of the ^{18}F-NaF PET images which were unavailable for analysis (Table 13) which ultimately contributed to the inconsistent results from the dynamic ^{18}F-NaF PET-CT (Table 18) and (Figures 43 and 44). Similarly, reduced numbers contributed to inconsistent static ^{18}F-NaF results (Tables 19 and 20). Thus results revealed no significant correlation between the ^{18}F-NaF uptake patterns; dynamic NaF pattern; bone scan uptake pattern and periprosthetic lucency with the final diagnoses (Tables 19, 20, 16 and 21 respectively). However, there was significant correlation between the R^2 trend line and the final diagnoses (Table 17).

6.5.1 Discussion

The diagnosis of periprosthetic aseptic loosening or septic periprosthetic loosening can be challenging, and any new imaging technique to diagnose or exclude periprosthetic complications should attract attention. Distinguishing between periprosthetic joint infection and aseptic loosening by conventional radiology and nuclear medicine techniques can be difficult and prolonged (105). An accurate diagnosis of periprosthetic aseptic loosening or septic periprosthetic loosening can be made from a combination of clinical features, laboratory investigations including standard joint radiographs and joint aspirates. However, in some patients the diagnosis remains unclear prior to revision joint surgery (200). Plain radiographs and conventional nuclear medicine often cannot distinguish between septic and aseptic periprosthetic loosening. Radionuclide imaging is currently not reliably specific enough for infection and is unable to distinguish infection from inflammation (201). Consequently, in the final diagnosis, patients with synovitis had similar results to septic loosening. One of the main limitations of this issue is that radionuclide imaging techniques would be unable to detect infection when prosthetic joint replacements are used in the management of rheumatoid arthritis. In addition, although CT and MRI artefacts can result in non-diagnostic images (202),

metal related artefacts can be reduced to an extent by using metal artefact reduction techniques (202).

The goal of this trial was to compare dynamic ^{18}F-Sodium fluoride (^{18}F-NaF) PET-CT with 3-phase bone scans in diagnosing prosthetic loosening and in distinguishing between aseptic or septic loosening. NaF PET-CT static periprosthetic uptake images were correctly interpreted as positive for aseptic loosening in 5 of the 5 patients. On the other hand, 3 out of the 3 patients with infection/inflammation were correctly identified but there were 2 false positive cases of infection/inflammation. One explanation for false positives in the 2 patients diagnosed with sepsis could be the long femoral stems, heterotopic ossification as well as the presence of multiple periprosthetic wires and screws. In the limited number of successfully archived dynamic NaF pattern images; there was 1 false positive case of dynamic NaF pattern which was possibly related to the unusually long femoral and tibial stem components in the total knee replacement. Hence, neither the static NaF PET-CT nor the dynamic NaF PET-CT scans have shown improved accuracy over conventional bone scans.

Analysis of periprosthetic uptake in 3-phase bone scan images showed 7 true positive aseptic loosening cases and 3 true positive cases of septic loosening. However, there were 5 false positive of aseptic loosening which were incorrectly identified as septic loosening cases. In the analysis of bone scan R^2 trend lines, we found 12 cases of true positive aseptic loosening and 3 cases of true positive septic loosening. This R^2 trend line method shows promise as there was no false positive or false negative case.

CT periprosthetic lucency analysis was positive in all 12 cases of aseptic loosening as well as all 3 cases of infection/inflammation. Hence, CT periprosthetic lucency was not able to distinguish between aseptic loosening and infection/inflammation.

The evidence purports that bone scan R^2 trend line analysis can be useful in the evaluation of suspected periprosthetic sepsis and aseptic loosening. The addition of CT data from SPECT-CT could provide additional information that may influence disease management. CT has been proven useful especially

when periprosthetic fractures, pseudotumours and collections are suspected (106).

Therefore, the accuracy of highly sensitive but poorly specific NaF PET-CT and conventional bone scans can be improved when bone scan data is combined with R^2 trend line data to assist in the differentiation of infection from aseptic loosening. Additional information from CT images could reveal complications which are not related to aseptic or septic loosening (106). Results from the trial demonstrate inconsistent results from both dynamic ^{18}F-Sodium fluoride (^{18}F-NaF) PET-CT and ^{18}F-Sodium fluoride (^{18}F-NaF) SUVmax levels. The small numbers in the infected category as well as the loss of NaF data in both dynamic ^{18}F-NaF PET-CT and ^{18}F-NaF most likely contributed to the inconsistent findings.

In conclusion, both static and dynamic NaF PET-CT have not yet been proven to be useful as a single imaging technique in the evaluation of suspected of periprosthetic joint infection and aseptic loosening. Furthermore, dynamic NaF PET-CT is burdensome due to high data and long transfer times. Conventional bone scans show better results when combined with R^2 Trendline results from additional information that may influence the management of the disease. Lastly, CT periprosthetic lucency was found to be nonspecific and is thought to be a poor discriminator of aseptic loosening and septic loosening.

6.5.2 Discussion of Trial Problems Encountered and Critical Analysis

General problems encountered in the study include the identification of eligible trial patients; patient recruitment and retention; prolonged period between scan dates and surgery dates and patient frailty.

Patient recruitment was a significant obstacle in performing the trial and we managed to recruit and scan 15 patients from a potential pool of 190 patients (Figure 46). Difficulty in patient recruitment would need to be considered when planning future larger trials. Clinical trial recruitment is often slower and more difficult than anticipated, resulting in several trials failing to reach their target

sample size within the allocated timescale (203). Our trial recruitment process was radiology led and the processes were inefficient as we had no prior relationship with the patients. This was unexpectedly more time-consuming than usual and there was not enough face-to-face contact with trial participants. The recruitment would have been better led by orthopaedic surgeons, nurses or physiotherapists. The longwinded process involved the initial identification of patients via hospital waiting lists for joint revision surgery. The surgical waiting list was based on a first-come-first served basis as opposed to severity of symptoms. Thereafter, there was a time lag between patient recruitment, prosthetic joint imaging and revision surgery or joint aspiration.

There was a risk of selection bias in this recruitment process because only patients that were contactable by telephone during working hours were enrolled. Further selection bias resulted from nonresponse bias (204) due to the fact that only patients on the waiting list for revision surgery were recruited and patients considered well enough for non-surgical treatment would have been excluded.

The targeting and enlistment of participants from the waiting list was performed by a radiologist and not a clinician or nurse. However, patient recruitment is well known to be improved through favourable long-standing patient-physician relationships (205) and nurse-led patient recruitment is just as effective as and more cost-effective than doctor-led recruitment (206). Nurses and physiotherapists that are directly involved in orthopaedic patient care are more likely than radiologists to develop rapport with patients making them more likely to be successful at recruiting patients on to clinical trials than radiologists who have not had prior dealings with the patient. In addition, allied clinical personnel such as nurses and physiotherapists that are familiar with the clinical trial can establish how well patients understand and are satisfied with being recruited on a one-to-one basis (207, 208). Furthermore, the referral of patients for imaging tests is not normally under the control of radiologists and therefore the process of patient identification and enrolment for imaging-centred clinical trials is therefore more likely to occur optimally when performed by the caring clinical team (209).

Other requirements for successful patient recruitment include a supportive departmental leadership, dedicated experienced administrative trial personnel and available trial infrastructure (209). Furthermore, opt-out methodology in medical trial recruitment can be more efficient and more successful than opt-in methods (210, 211), but opt-out methods of recruitment are more appropriate to survey-type studies only (212). Opt-in methods are essential for satisfactory informed consent and medical ethical standards (211).

Following the identification of eligible patients, the prolonged pre-surgery waiting list occasionally resulted in a time lag between imaging and surgery dates which resulted in reduced patients' enthusiasm with the clinical trial recruitment process. Some other factors which resulted in reduced patients' willingness to enrol in the clinical trial included the lack of opportunities to improve their chances of a cure, no actual alteration in their received treatment or specialist care, but this perceived lack of additional care was offset by the altruistic chance to contribute towards medical research (205). Expedient factors that were used in our study included the altruistic motives, the promise to cover travel costs as well as the potential of undergoing a better test. Although we adequately explained the study over the telephone and in the multipage letter, we found that the later involvement of family members led to patient withdrawal (2). Other helpful factors that can lead to improved recruitment rates include the use of optimistic language in patient letters and leaflets as well as the provision of practical or psychological assistance (205).

Other important steps in the successful recruitment process include enrolling a sufficient representative selection of the population and receiving informed consent by direct recruitment from outpatient clinics and initial face to face trial discussions by orthopaedic nurses, surgeons and physiotherapists (213) followed up by trial literature. This method is likely to avoid any ethical issues including telephone cold calling whilst limiting trial costs and improving patient retention.

Figure 46. *Patient recruitment*

Note: The patients were recruited to the trial from the prosthetic joint revision surgical waiting list. Those retained following recruitment were scanned according to the trial protocol.

Analyses of randomised controlled trials in elderly patients demonstrate approximately 50% median rates for recruitment and 15% attrition rate (214) which matches our high dropout rate of 50%. These group of patients are generally are elderly with reduced mobility and despite the ongoing complaints of joint pain and relatively lengthy scan times we did not have any patient terminate the scan procedure. The use of blankets, pillows and knee rests improved patient comfort.

One specific problem encountered was a false positive case resulting from rheumatoid arthritis. Therefore any patient with inflammatory arthropathy may need to be screened out and excluded from any future potential clinical study. The incidence of claustrophobia in Positron Emission Tomography is significantly lower than in Magnetic Resonance Imaging (215). The non-completion rate was 0%, because no test was discontinued due to anxiety, discomfort, fear or claustrophobia. There was no requirement for the use of anxiolytic and sedative medication, noise-reduction techniques, special psychological support, anxiety reduction protocols, or cognitive behavioural

therapy (216). Patients were scanned supine and no complication was observed in any of the patients. Patients should be kept comfortable due to relatively longer scan acquisition timing over one bed position which occurs during the dynamic PET technique immediately following the inline CT (217, 218) to avoid spatial misregistration artefact (219).

^{18}F-Sodium fluoride (^{18}F-NaF) supply schedule was less reliable than ^{18}F-Fluorodeoxyglucose (^{18}F-FDG) supply in many parts of England. Therefore, ^{18}F-Sodium fluoride (^{18}F-NaF) scan times would need to match the production timetables and delivery timetable of the preferred NaF supplier (220), but with technological improvements in radiosynthesis, the worldwide supply of ^{18}F-Sodium fluoride (^{18}F-NaF) is on the increase (221). Commonly used cyclotron-produced radiotracers are commercially available in the United Kingdom from Erigal Limited (Erigal), Siemens PET-CT, IBA Molecular UK Limited (IBA Molecular UK) and General Electric (GE®) Healthcare. ^{18}F-Sodium fluoride (^{18}F-NaF) production sites in the United Kingdom as at February 2018 are Erigal Limited with production sites at Keele, Preston and Sutton. Siemens PETNET has sites at Mount Vernon hospital as well as in Nottingham. General Electric (GE®) Healthcare does not directly manufacture and deliver radiotracers around the country but instead provides synthesizer cassettes to PET centres using the FASTlab™ system. IBA Molecular UK has sites at Dinnington and Guildford for the production of FDG, but IBA do not produce ^{18}F-Sodium fluoride (^{18}F-NaF) (222). FASTlab™ is a high performance chemistry system which features a single-use cassette system that contains pre-measured quantities of all chemicals required for the synthesis of specific radiopharmaceuticals. This is thought to be flexible, economical and results in its high yield and high reproducibility (223). PET-CT requires a co-registered CT scan to correct attenuation defects and the effective radiation dose of a single large synovial joint from ^{18}F-Sodium fluoride (^{18}F-NaF) is close to 5 times more than the dose from planar bone scintigraphy (128). ^{18}F-Sodium fluoride (^{18}F-NaF) PET-CT study costs almost 4 times more than for planar bone scintigraphy (128). The

^{18}F-Sodium fluoride (^{18}F-NaF) PET-CT scan is usually completed in 30 minutes whilst it takes 3 to 4 hours to acquire the planar dynamic bone scan images. Despite, the relatively low PET-CT usage in England when compared with other parts of Europe, there is limited capacity on the available PET-CT scanners in many parts of the United Kingdom as PET-CT demand has grown by 14% per annum over the last decade (224).

The PET-CT machine was changed from a GE Discovery ST with 16 slice CT (GE Healthcare®) to a GE Discovery 710 with 64 slice CT (GE Healthcare®) in 2015 and some patients were scanned in my absence both resulting in partial data loss and data corruption of dynamic NaF images that had been stored in the hard drive of the GE Discovery ST. The large data set results in system overload once the bandwidth of the system is exceeded leading to image failure and losses. This was a major limitation of the study for which the following learning points will be emphasised. Four major causes of PACS image loss include (225)

- Vendor Incompatibility – the lack of conformance between machinery and computer systems from different sellers.
- Unsupported Options - when two DICOM devices do not match each other on advanced transfer options, system failure may arise and the computer systems stop communicating
- System overload – occurs when the limits of the bandwidth are exceeded resulting in image failure and losses become inevitable
- Collateral image loss – image loss occurs due to other unrelated problems such as blackouts and server failures

To prevent these unpredicted events from happening, daily audits of PACS images need to be performed in a manner similar to daily quality assurance tests on machinery should be performed to ensure that there is no case of partial series loss or complete series missing (225). In order to ensure test uniformity between the multicentre trial participants, the set-up process will need to create standard operating procedures that would ensure consistent high-quality imaging data based on quality assurance, fixed imaging protocols and system characterisation (226). Optimal protocols should include

standardised patient preparation instructions, matched scan statistics and standard activity prescription as well as standardised scanning protocols including bed position timing, bed overlap, the use of 2D or 3D, resolution as well as reconstruction protocols for each centre (227). The framework for image transfer and storage can be achieved via compact discs, or better still with the use of internet-based and cloud-based technologies (228). Phantoms should be used to harmonize both data acquisition and processing as well as analysis parameters (229). The criteria for radiology reporting should be sufficiently robust to allow for blinded radiology reporting (230).

The important statistical issues that need to be considered in setting up a NaF trial include assessing numbers needed to allocate to the clinical trial size; the new imaging test that needs to be compared with a control group of patients receiving a standard imaging investigation; randomization of patients to different comparative groups to avoid bias; Stratification the randomization process will need to be stratified or restricted to make sure that different investigations are comparable (231). Although small pilot trials can be beneficial and may help in the planning of trial protocols and schedules to avoid unacceptable levels of patient harm before rolling it out to a larger patient group (232), but even pilot trials can be controlled by randomization (233) to avoid uncontrolled pilot studies can be as misleading due to their small sizes and also due to random differences between different groups (232). Most randomised clinical trials in the United Kingdom do not achieve their original recruitment target and about half the trials have their recruitment period extended (203, 213). Some of the strategies that were employed to improve recruitment included regular visits to the orthopaedic department, making amendments to trial inclusion criteria by increasing the patient age range and also removing restrictive exclusion criteria, as well as presentation to consultant orthopaedic groups, research team meetings and national nuclear medicine meetings (203).

6.5.3. Single versus Multicentre Trial

Single-centre trials are the preferred trial method because they are less expensive, easier to run and also because logical multi-centre trial planning may lead to an unequal distribution of patients across centres (234).

Multicentre trials are often spread unevenly between sites. Some authors argue that this reflects inefficiency, poor planning and or poor control in execution (234). Patient recruitment often mirror attendance rates in clinics or other recruitment venues (234). Therefore, recruitment and coordination of multi-centre trials must allow for disparity in the number of recruited patients per centre (234). In order to achieve statistical relevance by increasing sample size and complete recruitment within acceptable time period trials in a timely manner, multi-centre trials are able to provide a major advantage by recruiting patients simultaneously from a number of centres. The multicentre trial also produces more representative trial conclusions regarding the whole population.

Multiple independent trials may also provide a summary of trial data from different sources and are beneficial for evaluating adverse events, but multiple independent trials have less statistical strength than single and multi-centre trials (235). Organisational and extra-organisational practises, structures and processes contribute towards the progress or obstruction of the patient recruitment process (236). Specifically, competition for research participants between different organisations, conflict between clinical and clinical research work, a perceived staff increased workload burden due to the trial patients as well as perceived vulnerability of older patients to excessive research exposure are considered detrimental (236, 237). Rigid ethical regulations as well as the structure and relationships within clinical research teams are also influential (236).

6.5.4 Change in Practice and Future Research

Dynamic positron emission tomography computed tomography (PET-CT) with ^{18}F-Sodium fluoride (^{18}F-NaF) was thought to be more accurate than conventional imaging techniques for diagnosis of complicated joint prostheses. Up to now however, there has been no evidence to show that dynamic ^{18}F-Sodium fluoride (^{18}F-NaF) PET-CT leads to improved management of patients in routine clinical practice.

This pilot study provides prior feasibility work before setting up to a single centre or multicentre randomized controlled trial. It demonstrates ideal recruitment methods and rates, obstacles to patient participation in clinical trials, as well as suggests the acceptability of dynamic ^{18}F-Sodium fluoride (^{18}F-NaF) PET-CT. The information from this feasibility study will be of value to researchers and funders in the design and commissioning of future research in to prosthetic joint infection imaging (238). The ideal trial would be a multicentre trial to improve trial recruitment numbers and patients could be entered in the two arms of dynamic sodium fluoride ^{18}F-Sodium fluoride (^{18}F-NaF) PET-CT versus isotope bone scans.

Before treatment or revision, patients from multiple centres will be randomly assigned to either the conventional imaging group (CIG) or the dynamic ^{18}F-Sodium fluoride (^{18}F-NaF) PET-CT group (DNPG). Patients will be followed up with surgery, microbiology, biochemistry and clinically for 2 years. The primary outcome measure will be speed and accuracy of true positive and true negative diagnoses. A balance between patient safety, access to innovative technologies and improved patient care should be maintained when introducing new uses for radiopharmaceuticals or new radiopharmaceuticals for clinical use (239). International standards of quality assurance, good manufacturing practice and risk assessment studies should be adhered to and it is important to collaborate with both clinical and nonclinical professionals as well as industry and academia (239).

Dynamic sodium fluoride ^{18}F-Sodium fluoride (^{18}F-NaF) PET-CT will also undergo economic evaluation to calculate its cost-effectiveness and possible

cost-savings when used to investigate painful joint prostheses. The role of SPECT-CT bone (^{99m}Tc-HDP) scans will be assessed at the same time. The potential cost saving would be obtained chiefly from the reduced clinic visits, reduced imaging and non-imaging investigations (240), reduced use of pharmaceuticals as well as avoidance of unnecessary surgery such as examination under anaesthesia. The economic benefits can be obtained by examining Patient Reported Outcome Measures (PROMs) to calculate the quality-adjusted life years (QALYs) (241) and the improvement in health-related quality of life (HRQoL) (241). The analysis will provide a cost–utility ratio using dynamic sodium fluoride ^{18}F-Sodium fluoride (^{18}F-NaF) PET-CT and SPECT-CT bone (^{99m}Tc--HDP) scans, yielding a cost per QALY gained (241).

Quantification and graphical presentation of test results are potential ways of solving some of the difficulties in assessing nuclear medicine images. The importance and relative ease of interpretation as well as improved accuracy of graphical presentation of cardiac imaging tests results has been demonstrated in radionuclide imaging (242) with significant superior results when compared with visual interpretation (242). Furthermore, quantitative radionuclide angiographic data from dynamic brain imaging using ^{99m}Tc-HMPAO can be presented graphically resulting in an effortless non-invasive way of demonstrating cerebral perfusion without any blood sampling (243). Graphical time activity curves can also be applied to the in vitro studies such as in the measurements of radionuclide concentration in the marine environment where there are non-detect values (244).

6.5.5 Lessons Learnt and How to Address Trial Problems

The planned study should ideally be a multicentre trial to improve patient recruitment numbers via the orthopaedic department's nurses, physiotherapists or surgeons. Data from ^{99m}Tc-HDP bone scans and dynamic sodium fluoride ^{18}F-Sodium fluoride (^{18}F-NaF) PET-CT will be analysed and presented with graphs. Dynamic sodium fluoride ^{18}F-Sodium fluoride (^{18}F-NaF) PET-CT images

are data-heavy and both image transfer and storage process will require close supervision to avoid data corruption and loss of data. The relative limited availability of ^{18}F-Sodium fluoride (^{18}F-NaF) PET-CT and its higher cost of ^{18}F-Sodium fluoride (^{18}F-NaF) PET-CT may be reduced by batching patients and scanning in bulk. In addressing some of the queries that we received from the research ethics committee, although there is a higher patient radiation dose which mainly comes from the CT component (245), this should be partially offset by the reduced requirement for repeated imaging. The life cycle of the scanner should be taken into consideration before the start of the trial to avoid scanner replacements during trial period. There should be a more robust trial plan for data transfer and storage to minimise data loss or corruption.

6.6 Conclusion

Dynamic ^{18}F-NaF PET-CT is feasible but it produces large data files which can be corrupted resulting in data loss. Dynamic ^{18}F-NaF PET-CT as a single imaging investigation is not a reliable method of diagnosing infection or loosening of joint prostheses. Dynamic ^{18}F-NaF PET-CT has not been proven to be a reliable method of differentiating loosening from infection of joint prostheses. Dynamic ^{18}F- NaF PET-CT on its own has not been proven to be more cost-effective and accurate in the detection of infection/loosening of joint prostheses.

Although significant problems were encountered with the ^{18}F-Sodium fluoride (^{18}F-NaF) PET-CT imaging and data storage, this trial has demonstrated that image acquisition is possible and may provide additional data. This trial has conclusively demonstrated that it is possible to extract new graphical mathematical data such as m and R^2 (Equation 1) from the commonly used ^{99m}Tc-MDP dynamic bone scan. Further research is required to replicate this level of accuracy in using R^2 values greater than 0.2 in larger studies whether to distinguish septic loosening or inflammation from aseptic loosening. Combining this method with CT periprosthetic lucency from SPECT-CT may improve the

accuracy even further. In addition, ^{99m}Tc-MDP dynamic bone scans are cheaper and more widely available than ^{18}F-Sodium fluoride (^{18}F-NaF) PET-CT.

More evidence from further research with larger numbers of ^{18}F-Sodium fluoride (^{18}F-NaF) PET-CT scans is required before firm conclusions can be drawn from the usefulness of dynamic^{18}F-Sodium fluoride (^{18}F-NaF) PET-CT to distinguish septic loosening or inflammation from aseptic loosening.

6.7 Summary

- Useful graphical mathematical data can be extracted from the commonly used ^{99m}Tc-MDP dynamic bone scan which may distinguish septic loosening or inflammation from aseptic loosening.
- This is important because ^{99m}Tc-MDP dynamic bone scans are cheaper and more widely available than ^{18}F-Sodium fluoride (^{18}F-NaF) PET-CT.
- R^2 values greater than 0.2 may indicate septic loosening or inflammation
- CT periprosthetic lucency from SPECT-CT may improve the accuracy even further.
- Further research with larger numbers is required with improved patient recruitment strategies.

Chapter 7 Research Proposal. Labelling Study - A Potential Role for Lymphoseek® In the Assessment of Patients with Painful Hip and Knee Joint Prostheses – Background & Proposal.

7.1 Abstract

Background: This experiment was designed and planned but was not carried out. The study was designed to analyse how Lymphoseek®, a new radiopharmaceutical that binds to the mannose receptor on the cell surface of macrophages can assist in the radiological assessment of patients with painful hip and knee joint prostheses from wear particle induced loosening. This imaging test is based on the innovative demonstration of the accumulation of activated macrophages in aseptically loose periprosthetic membranes. It is expected that our outcomes will show the need for more medical imaging research in this area and that the imaging of periprosthetic membranes in the future should involve a combination of anatomical and functional imaging.

Methods: Two groups of experiments will be performed – in vivo intravenously injections in pre-surgery joint revision patients and ex vivo examination of surgically extracted periprosthetic membranes in patients with painful joint prostheses using ^{99m}Tc-Tilmanocept. Lastly, ex vivo confirmatory immunohistochemistry experiments will be performed on the fresh periprosthetic membranes from these same 10 patients after joint revision surgery on the painful failed knee and hip arthroplasties by using CD68 or CD206. The ex vivo fixed tissue specimens will also be labelled using haematoxylin-eosin for the histological examination The purpose of the histological examination is to rule-out infection based on the degree polymorphonuclear leukocytic infiltration and/or confirm the presence of foreign body particles; macrophages and multinucleated giant cells in aseptic loosening (246).

Results: This experiment was designed but not performed and no result is available. However, it is hoped that the results will demonstrate that Lymphoseek® binds to the mannose receptor on the cell surface of macrophages in aseptic wear particle induced loosening in prosthetic joints.

Conclusion: This experiment was designed but not performed. It is expected that it will assist in the radiological assessment of patients with painful hip and knee joint prostheses using the novel technique of a macrophage mannose receptor imaging in humans to demonstrate periprosthetic membrane aseptic loosening. It is also hoped that radionuclide scintigraphy with ^{99m}Tc-Tilmanocept SPECT-CT scan will be a useful imaging investigation in the assessment of the painful knee arthroplasty and that a negative ^{99m}Tc-Tilmanocept scan would reassuring make a diagnosis of aseptic loosening unlikely.

7.2 Background and Introduction

Due to the disabling nature of arthritis, surgical attempts have been made for well over a century to treat diseased joints (9). At least 40,000 hip and knee replacements are carried out every year in the UK (2). Approximately 0.4 to 4% of these are complicated by deep infection but the true figure is probably less than 1% (2). Complications of joint prostheses include aseptic loosening with an incidence of 2-18% and 23% respectively in the knees and hips (4), but infection has much more devastating consequences (5). The mean time from surgery to diagnosis is just under 14 months with the majority of patients presenting after 3 months (2). The diagnosis of prosthetic aseptic loosening and infection is very important both to patient well-being and mobility as well as the health economy. Management of these cases could be conservative or surgical.

The clinical features of aseptic loosening consist mainly of joint pain in the absence of clinical features of infection (247) such as sinus formation or discharge and also an absence of leucocytosis, elevated erythrocyte sedimentation rate (ESR) and/or C-reactive protein (CRP) (2, 7, 247). Current imaging investigations used in prosthetic joints include serial radiographs,

contrast arthrography, ultrasound, MRI, CT and conventional Nuclear Medicine studies. The sensitivity, specificity and accuracy for the plain radiographs are approximately 43%, 86% and 64%, respectively (170). Although serial radiographs are insensitive, non-specific and generally unhelpful (248), they often are sufficient and are also able to detect periprosthetic factures (45). CT and MRI are particularly useful for periprosthetic collections, but they produce significant artefact in the region of the prostheses which can render them uninterpretable. Ultrasound has no role to play in diagnosing loosening with accuracy (45) and contrast arthrography is invasive and requires skilled staff. Nuclear medicine techniques are generally very sensitive for aseptic loosening and prosthetic infection but due to low specificity there is often a requirement to combine with different imaging tests (249, 250). Conventional nuclear medicine studies employed in the investigation of painful joint prostheses include dynamic 3-phase radionuclide bone scans as well as radionuclide infection/inflammatory scans which include labelled white cell scans and ^{67}Gallium imaging. Until recently, labelled monoclonal immunoglobulin fragments such as sulesomab (LeukoScan©) were used to distinguish aseptic loosening from periprosthetic infection (128) with an accuracy of over 80% (249) but immunoglobulins were beset with problems such as human anti-mouse antibody (HAMA) response due to the production of endogenous antibodies (128) as well as anaphylactic and other hypersensitivity reactions (128). The use of monoclonal antibodies was permanently discontinued in 2018 by Immunomedics™ GmbH and the European Union for commercial reasons (187). ^{99m}Tc-HDP (hydroxydiphosphonate) /MDP (methylene diphosphonate) planar bone scans have a sensitivity of 66.7%, specificity of 94.5% and accuracy of 87.5% for detecting infection and aseptic loosening (72) but differentiating one from the other can be difficult. With bone scans, infection usually demonstrates diffusely increased uptake on both the blood pool and delayed phases, whilst aseptic loosening bone scans tend to feature focal uptake at the prosthetic tip usually on the delayed phase only. Hence, combination imaging remains the gold standard in radionuclide diagnosis of prosthetic infections (47). Consequently, a combination of indium-labelled white cell Imaging using SPECT-CT with bone or bone marrow imaging with ^{99m}Tc-HDP or ^{99m}Tc sulphur colloid respectively is currently thought to be one of the most accurate ways of distinguishing aseptic

loosening from prosthetic joint infections. Other combinations which have been tried with varying results include ^{67}Gallium imaging and labelled Immunoglobulin imaging (178) but monsoonal antibodies have since been discontinued (187). The accuracy of imaging techniques is improved when combined with ESR and CRP measurements (251). Positron Emission Tomography (PET) in conjunction with CT (PET-CT) is a relative new Nuclear Medicine imaging technique. It is well established as a powerful diagnostic tool in oncology but has rapidly broadening applications as new radiopharmaceuticals and methodologies become available. The radionuclides used in PET imaging typically decay by positron emission with short half-lives (less than 120 minutes) and PET scanners benefit from improved sensitivity and spatial resolution compared to conventional gamma cameras due to the coincidence detection of the two annihilation photons, arising from a positron/electron interaction which permits an imaging modality that is not burdened with a collimator (252). PET imaging is intrinsically tomographic and tomographic imaging, as opposed to planar imaging offers clear advantages in terms of localisation of pathology and image contrast allowing differentiation between bony cortex and marrow as well as the acquisition of images in a considerably shorter periods of time than with single photon emission computerised tomography (SPECT). PET-CT scanners incorporate high quality CT devices and, although the primary purpose of this transmission device is to assist with attenuation correction of the PET emission data, diagnostic quality CT images are available for localising functional information and the radiological assessment of any structural changes (252). Two readily available PET radiopharmaceuticals which have been investigated in the differentiation of aseptic loosening from prosthetic joint infection are ^{18}F-Fluorodeoxyglucose (FDG) and ^{18}F-NaF (253) with widely variable accuracy (49, 254) but negative results are more informative than positive ones (255). In general, than Leukocyte imaging has a greater role to play than FDG PET-CT in distinguishing aseptic loosening from prosthetic joint infection (256). In essence, there is currently no effective single imaging test capable of both diagnosing and distinguishing between aseptic loosening and infection of joint prostheses. Plain radiographs and dynamic planar bone imaging are accepted first line techniques to evaluate symptomatic hip and knee prostheses. Technical limitations and poor specificity result in these frequently being accompanied by

additional nuclear medicine investigations such as radiolabelled white cell scans or in the recent past - LeukoScan© investigations. These additional investigations are costly and time consuming for both patients and staff and may still not offer a definitive diagnosis. ^{18}F-NaF PET-CT is very sensitive to change in bone metabolism but lacks specificity in distinguishing between simple loosening or loosening with underlying infection (41, 78).

Histopathological studies of the periprosthetic membranes performed demonstrate 4 types of periprosthetic membranes (246) and surgical sampling of the prosthetic interface membrane yields better specimens for more accurate histopathological diagnosis of prosthetic joint infections than from pseudocapsule specimens (257). The 4 types are:

1. Type I - Wear particle induced type (detection of foreign body particles; macrophages and multinucleated giant cells occupy at least 20% of the area (246).

2. Type II - Infectious type (granulation tissue with neutrophilic granulocytes, plasma cells and few, if any, wear particles (246).

3. Type III - Combined type (aspects of type I and type II occur simultaneously (246).

4. Type IV - Indeterminate type (neither criteria for type I nor type II are fulfilled (246).

The incidence of histopathological membrane types was: type I (54.3%), type II (19.7%), type III (5.4%) and type IV (15.4%) with 5.1% of cases not being assessable (246). The results showed a high correlation between histopathological and microbiological results (246).

Activated macrophages heavily infiltrate periprosthetic membranes with aseptic loosening and express CD206 (cluster of differentiation) receptors. This technique for the in vitro detection of periprosthetic membrane tissues infiltrated

with CD206 positive cells was developed based on ^{99m}Tc-Tilmanocept (Lymphoseek®) scintigraphy which is marketed by Norgine B.V for sentinel lymph node mapping by binding to activated macrophages in lymph nodes (258). This study aims to investigate whether Technetium, ^{99m}Tc-Tilmanocept (Lymphoseek®), accumulates in the periprosthetic membrane to different degrees in the 4 histological types based on the classification by Morawietz (246) and to evaluate the specificity of ^{99m}Tc -Tilmanocept (Lymphoseek®) binding to activated CD206 positive cells in periprosthetic membranes. ^{99m}Tc-Tilmanocept (Lymphoseek®) is a radiopharmaceutical macromolecule with a molecular weight of 28-kilodalton, a diameter of 0.007 μm and a surface area of 7.1nm^2 (259, 260). It is comprised of a dextran backbone (10-kilodalton) to which multiple units of mannose and DTPA (diethylenetriaminepentaacetic acid) are attached (259). It is the mannose backbone that binds to the CD206 (cluster of differentiation) receptor while the DTPA constituent binds to ^{99m}Tc. Lymphoseek® is licenced for intradermal, subcutaneous, subareolar and peritumoral injection routes for lymphatic mapping in the localization of sentinel lymph nodes draining a primary tumours in a variety of cancers. Theoretically, Lymphoseek® binding in high concentration will provide evidence of high numbers of macrophages (259, 261). The intravenous route of ^{99m}Tc-Tilmanocept injection into patients has been assessed in a single centre phase 1/2 clinical study to evaluate with Kaposi sarcoma as an open-label, non-randomized trial (262). Preclinical studies imply that subcutaneous radiolabelled Tilmanocept is excreted from plasma by means of glomerular filtration, passive secretion into the Bowman's capsule and also by binding to the CD206 receptors in the mesangial cell matrix (263).

7.3 Hypothesis

This study addressed the following hypotheses:

(1) Intravenously injected ^{99m}Tc labelled Lymphoseek® can accurately demonstrate high levels of activated macrophage cells in periprosthetic tissue.

(2) Intravenously injected ^{99m}Tc labelled Lymphoseek® SPECT-CT can accurately demonstrate the distribution of activated macrophages in periprosthetic tissue.

(3) Intravenously injected ^{99m}Tc labelled Lymphoseek® SPECT-CT can accurately diagnose aseptic loosening in periprosthetic tissue.

(4) Intravenously injected ^{99m}Tc labelled Lymphoseek® distribution in periprosthetic tissue does not accurately match the distribution of neutrophils and ^{99m}Tc labelled Lymphoseek will therefore distinguish aseptic loosening from periprosthetic joint infection.

7.4 Aim

The aim of this study is to validate the use of ^{99m}Tc-Tilmanocept (Lymphoseek®) as a viable in vivo agent to accurately demonstrate activated macrophage cell distribution in periprosthetic tissue sections. The aim is to validate high-levels of ^{99m}Tc-Tilmanocept Lymphoseek activity in aseptically loosened periprosthetic membrane in vivo following intravenously administered ^{99m}Tc-Tilmanocept (264, 265) and at the same time demonstrate low uptake in asymptomatic as well as septic periprosthetic membranes. In addition, ex vivo studies will be performed to reveal co-localization between ^{99m}Tc-Tilmanocept) and CD206 positive macrophages on periprosthetic membranes. Ex vivo experiments will be performed in 2 parts – (a) Immunohistochemistry with single antibody labelled

against CD206 and CD68 (b) Immunofluorescence with dual-labelled Tilmanocept with CD68 and CD206 antibodies detected using fluorescent markers such as Alexa 488 (266). These will quantify activated macrophages in periprosthetic membrane tissues and assess the concentration of periprosthetic membrane CD68 and CD206 positive macrophage infiltrates in tissue samples.

7.5 Methods

The studies will be performed following approval by local research ethics committee and the University Coventry and Warwickshire Research & Development department. Informed patient consent will be obtained. Two groups of experiments will be performed – in vivo intravenously injections in pre-surgery joint revision patients and ex vivo examination of surgically extracted periprosthetic membranes in patients with painful joint prostheses.

In vivo experiments will be performed on 10 patients with painful prosthetic joints prior to joint revision surgery. This imaging technique was developed to diagnose aseptic loosening using single photon emission computer tomography (SPECT) by analysing the presence of activated macrophages in symptomatic knee and hip periprosthetic membranes using mannose receptors (CD206) present in the macrophage cell membranes. This assumes that following the intravenous administration of ^{99m}Tc-Tilmanocept, periprosthetic membrane uptake would be proportional to the presence of activated macrophages present in the periprosthetic membrane (264) and that SPECT-CT-based quantification of ^{99m}Tc-Tilmanocept uptake would be feasible based on prior studies which measured ^{99m}Tc-Tilmanocept uptake in joints and the aorta (264, 266). Recent research studies refer to physiological accumulation of increased background activity in the kidneys and liver (266) and planar images of the abdomen will therefore be obtained for quality assurance and to confirm adequate injection and dosage.

Patients will receive intravenous injections 400µg Tilmanocept radiolabelled with 370 MBq of ^{99m}Tc. Planar images of the affected joints and the abdomen will be acquired at 60 minutes and 180 minutes post-injection. SPECT-CT images of the prosthetic joints will also be performed at 180 minutes post-injection (264, 266). Similar injection doses of 400µg Tilmanocept radiolabelled with 370 MBq of ^{99m}Tc will be administered to patients with bilateral lower limb prostheses followed by the acquisition of planar images of both joints and the abdomen at both 60 minutes and 180 minutes post-injection. Thereafter, SPECT-CT images of both prosthetic joints will be performed at 180 minutes post-injection (264, 266). Imaging will be performed with a Discovery NM/CT 670 gamma camera from GE™ Healthcare. Thereafter, SPECT-CT images of the symptomatic joint will be acquired with the dual head gamma camera and 16-slice CT scanner. Image projections will be acquired using the 140 KeV energy window and ordered subsets expectation maximization algorithm (OSEM) iterative reconstruction will be used to reconstruct the SPECT images. Corrections will be made for motion and misregistration. The acquired CT images will be used for attenuation correction. Target to background ratios will be calculated using fused SPECT-CT guided voxels (volumes of interest) in the reconstructed images by comparing pathological Tilmanocept uptake which will be normalized to a reference region in unaffected skeletal muscle because of the propensity of muscle to display consistent low levels of activity (266). The scan duration will be 15 to 30 minutes (depending on the metallic stem length). Three hours was chosen as the most ideal acquisition time point after intravenous administration because research and pharmacokinetics have shown this to be optimal (266). In patients with more than one knee or hip joint prosthesis, the ^{99m}Tc-Tilmanocept percentage uptake in the symptomatic joint prosthesis will be compared with the percentage uptake in non-symptomatic joints. Images will be analysed and reviewed on GE Xeleris^{TM} version 4 workstations. Identical in vivo imaging techniques can also be performed using a Discovery 710 PET-CT scanner with 64 slice CT capability instead of SPECT-CT to analyse subcellular localization of activated macrophages by substituting ^{99m}Tc-Tilmanocept with ^{68}Ga-Tilmanocept (128, 267).

Ex vivo experiments on fresh periprosthetic membranes from these same 10 patients will be performed subsequent to the surgical removal of periprosthetic membranes after joint revision surgery on painful failed knee and hip arthroplasties. The tissue specimens will be formalin-fixed, paraffin-embedded and then frozen immediately after removal (268) to prevent dehydration. 4 μm thick sections of the formalin-fixed, paraffin-embedded (FFPE) tissue blocks will be created from the resected surgical samples and then stored at ultralow temperatures (−80°C). The FFPE tissue sections will then be de-paraffinised and rehydrated in xylene and graded ethanol followed afterwards by antigen retrieval using high heat for 20 minutes as described by MV Zanni et al (266). The de-paraffinised sections will be incubated with peroxidase and washed in Tris Buffered Saline (TBS) followed by a 30 minute protein block (266).

Single label immunohistochemistry on tissue sections will be performed at 4°C by overnight incubation with mouse anti–CD68 antibody (1/50, DAKO Corporation, Trappes, France) to identify both M1 and M2 macrophage subtypes (269). Whilst the goat anti-mannose receptor (MR) antibody (1/50, Santa Cruz Biotechnology, Heidelberg, Germany) will be used to distinguish between the CD68 positive mannose receptor (M1) and CD68 positive mannose receptor positive (M2) subtypes (269). Immunostaining will be performed for visualization using biotinylated secondary antibodies (1/200, Vector laboratories, Burlingam, CA), streptavidin–horseradish peroxidase (Vectastain ABC kit, Vector laboratories), and the 3-amino-9-ethylcarbazole substrate–chromogen system (Sigma-Aldrich) (269). Alternately, single label immunohistochemistry will be performed with antibodies against CD206 (R&D Systems) (Serotec) (266) and then visualized using 3, 3’-diaminobenzidine tetrahydrochloride (DAB, Dako) (266). Afterwards, the relative numbers of CD68 positive mannose receptor (M1) and CD68 positive mannose receptor (M2) macrophages in the periprosthetic membrane tissue will be quantified to determine the M1/M2 ratio (269). Immunofluorescence will be performed with dual-labelled Tilmanocept with CD68 and CD206 antibodies and detected using fluorescent markers such as Alexa 488 (266). Alexa Fluor 488 is a fluorescent dye (266, 270) with emission/excitation spectra wavelength maximum of 488 nm (271). This will quantify activated macrophage levels in periprosthetic

membrane tissues samples. The average number of immune positive macrophages will be counted in 20 high power fields of view using a microscope (269).

The formalin-fixed, paraffin-embedded (FFPE) tissue blocks of periprosthetic membrane specimens will also be cut and stained with haematoxylin-eosin to rule-out infection based of the degree polymorphonuclear leukocytic infiltration (137) as stipulated in the proceedings from the 2013 International Consensus Meeting on Periprosthetic Joint Infection held in Philadelphia (272). Samples would have to demonstrate less than 5 neutrophils per high-power field with negative cultures on periprosthetic cultures extended to 2 weeks to exclude periprosthetic sepsis as a cause of symptoms (137, 272). Alternately, aseptic loosening consists of a dense mass like infiltrate of particle-laden macrophages with resultant central necrosis, increased osteoclastic activity and surrounding bone resorption and the histological samples would be examined for the presence of foreign body particles; macrophages and multinucleated giant cells (246).

7.6 Discussion

This is the first-in-human study to identify activated macrophages in aseptic loosening of periprosthetic membrane in joints using ^{99m}Tc-Tilmanocept SPECT-CT to detect the presence of CD206 positive macrophages in vivo. The ex vivo experiment will also confirm the presence of macrophages in the surgically excised periprosthetic membranes. Therefore, following the intravenous injection of ^{99m}Tc-Tilmanocept and the subsequent periprosthetic membrane ^{99m}Tc-Tilmanocept uptake quantified by SPECT-CT can be inferred to reflect CD206 positive macrophage concentration in periprosthetic membranes. From prior research studies, we expect that there will be an increased background activity in the kidneys as well as the liver and planar images of the abdomen will confirm adequate injection and absorption.

There is significant heterogeneity in the macrophage categories and an in vivo overlap exists between M1 and M2 subsets of macrophages due to in vivo plasticity that is not clearly witnessed in in vitro and ex vivo environments (266, 273). This is thought to result from phenotypical alteration in response to signals in the local environment (266, 273, 274). This study will reveal the important role of CD206 positive macrophages in aseptic loosening of periprosthetic membranes as well as demonstrate a connection between aseptic loosening in periprosthetic membranes and elevated levels of periprosthetic membrane ^{99m}Tc-Tilmanocept uptake. Additional research is required to determine optimal intravenous doses in human periprosthetic joint imaging and also to determine whether false positive cases occur in the asymptomatic early post joint replacement period. The likelihood of ^{99m}Tc-Tilmanocept becoming a mannose receptor imaging in CD206 positive macrophages in inflamed human joints has recently been proposed (128, 264, 275) but the potential role for Lymphoseek® in the imaging assessment of painful joint prostheses requires further research before it becomes an established imaging technique.

There are other MRC1 antibodies (Mannose Receptor, C Type 1) which are expressed by the Human MRC1 gene and also demonstrate cytoplasmic positivity in macrophages. Some of these exist as 3 clones of the MRC1 antibodies - HPA004114, HPA045134 and AMAb90746 which are all produced from rabbit host species. Alternately, the polyclonal antibodies - HPA004114 and HPA045134 or the monoclonal antibody - AMAb90746 may also be used (276). These antibodies are supplied by Sigma-Aldrich Company Ltd. The Old Brickyard, New Road, Gillingham, Dorset, SP8 4XT United Kingdom and Atlas Antibodies AB, Voltavägen 13A, SE-168 69 Bromma, Sweden (276).

PET scanners possess inherently better contrast and spatial resolutions than SPECT scanners (277).Therefore, significant improvement in imaging quality over ^{99m}Tc-Tilmanocept SPECT can potentially be achieved by imaging with ^{68}Gallium (^{68}Ga) labelled Tilmanocept (128, 267). ^{68}Ga-Tilmanocept is produced by chelating radioactive ^{68}Ga to the diethylenetriaminepentaacetic acid (DTPA) moiety of the Tilmanocept molecule. ^{68}Ga is produced by ^{68}Germanium (^{68}Ge)/^{68}Ga generators that serve as a stable source of ^{68}Ga for more than one

year (128) and has a half-life of 68 minutes and decays by emitting positrons (128, 267).

Critical analysis of the research methodology in this prospective uncontrolled in vivo and ex vivo trial to test whether a Lymphoseek® can detect wear particle induced loosening in hip and knee joint prostheses reveals advantages and disadvantages. The advantage of the in vivo study includes the relatively lower cost and also the fact that the prosthetic membranes would be studied in their 'native' environment. The downside of the in vivo study is that it would require an intravenous ^{99m}Tc-Tilmanocept which is a new radiopharmaceutical that binds to the mannose receptor on the cell surface of macrophages and is only licenced for subcutaneous use. The in vivo study assumes favourable pharmacokinetics of intravenous ^{99m}Tc-Tilmanocept and also that periprosthetic membrane uptake following the intravenous administration of ^{99m}Tc-Tilmanocept would be proportional to the activated macrophage numbers present in the periprosthetic membranes. The ex vivo material would also require technically challenging steps of tissue fixing and preservation as well as immunohistochemistry staining. Potential sources of error include the small number of in vivo and ex vivo experiments. Further limitations of the study include selection bias because only symptomatic joint prostheses would be included. The absence of control group potentially reduces the statistical power of the study. However, there will be 2 blinded readers to reduce intra-observer variability. New knowledge that will be identified includes the co-localisation between ^{99m}Tc-Tilmanocept and CD206+ macrophages in ex vivo aseptically loosened periprosthetic membranes and in vivo demonstration of high levels of ^{99m}Tc-Tilmanocept uptake in aseptically loosened periprosthetic membranes. There are limitations to this proof-of concept study. One of the most important limitations is the small non-blinded sample size. In addition, the ex vivo studies performed on periprosthetic membrane tissue specimens will have to be taken from all patients that undergo the in vivo ^{99m}Tc-Tilmanocept SPECT-CT scan. From past experience, this is not always achievable due to patients dropping out of trials and also because intended revision surgeries do not always proceed as planned in every single case. The study strengths include the first human application of a novel, simple macrophage mannose receptor imaging

technique which targets CD206 positive activated macrophages in prosthetic joint aseptic loosening. The experiment methodology may be extrapolated to larger multicentre studies to provide a clearer perspective into the non-invasive investigation and diagnosis of painful joint prostheses. It also is not clear if ^{99m}Tc-Tilmanocept SPECT-CT scan will result in false-positive studies in the early post-surgical period.

The products contain material of animal origin and human tissue and risk assessment for biohazards and safety will need to be performed. As with all human tissue samples, patient specimens will all be handled as potential biohazards. As with all biological material, direct handling will be reduced to a minimum and appropriate protective clothing will be worn. Chemical hazards will also be avoided when preservative products are added. Radiation hazards will also be avoided during the patient imaging process. For biosafety reasons, if samples need to be transported from the University Hospital across town to the chemistry laboratories at the University of Warwick then they may require screening for blood borne infections such as Human Immunodeficiency Virus (HIV) and hepatitis. Locked storage of biological samples and secure transportation between surgical theatres, laboratories and the imaging department.

We hope that the results will provide a new isotope for joint imaging by demonstrating co-localisation between ^{99m}Tc-Tilmanocept and CD206+ macrophages in ex vivo aseptically loosened periprosthetic membranes. The in vivo application of ^{99m}Tc-Tilmanocept single-photon emission computed tomography/computed tomography should demonstrate high levels of ^{99m}Tc-Tilmanocept uptake in aseptically loosened periprosthetic membranes assessed using regions of interest (246) and validated using immunohistochemistry by employing CD68 stains for confirmation.

7.7 Further Areas of Future Research

7.7.1 The Development of New Molecular Imaging Probes

Radiopharmaceuticals labelled with positron emitting isotopes provide more favourable physical characteristics in radionuclide imaging than single photon isotopes (278). On the other hand, radionuclides for single photon labelled compounds do provide a wider variety than PET agents and single photon labelled molecules also offer an important complimentary array of new possibilities in the development of new agents used in the process of drug development (278). Other advantages of PET agents over SPECT agents are the higher sensitivity and more accurate quantification features (278), but PET agents are disadvantaged by their shorter half-lives and they are also less abundant as well as more expensive (278). Single photon emission radionuclides on the other hand are foreign to the human physiology and biochemistry (279). Exploratory studies for investigational new drugs (IND) are also known as phase 0 studies (280) and improve or understanding of toxicity and efficacy thus reducing clinical trial time, costs as well as the high failure rate of new drugs that occur during the traditional phases I to IV clinical trial stage. Phase 0 studies follow on from preclinical pharmacology and toxicology tests and occur before the typical Phase I clinical trial. Phase 0 studies involve restricted human exposure to non-therapeutic quantities of the IND (280).

Radionuclide imaging with positron emission tomography (PET) and single-photon emission computed tomography (SPECT) enables speedier proof-of-concept testing and allows non-invasive visualization, characterization and quantification of biochemical processes that occur at cellular and subcellular levels in both humans and animals whilst only using nanomolar to picomolar concentrations of the IND (278).

Radionuclide imaging plays a big role in target identification and validation. The drug target can be a membrane, nuclear receptor, ion channel, enzyme, hormone, DNA or RNA molecule, or even unidentified biological entity (278).

Radionuclide imaging does not play a significant role in lead finding and optimization. This stage usually relies on in vitro drug target analysis with biochemical and cellular assays, e.g., for compound purity, integrity, solubility, lipophilicity, safety, dissociation constant, permeability and target affinity (278).

Radionuclide imaging is used in compound profiling in animal models at the preclinical stage. In this, the investigative drug itself is labelled with an imaging probe for in vivo imaging using animal models of disease to provide valuable information concerning drug absorption, distribution, metabolism, elimination and efficacy (ADME). The images provide pharmacodynamics and biodistribution properties of a candidate drug (278).

Safety evaluation can involve imaging with animal studies for toxicology and determining the proper dose to be tested in the clinical trials. Many pharmaceutical companies have established their own imaging laboratories to do carry out these processes (278).

Clinical evaluation with SPECT involves clinical studies in 4 sequential phases (I–IV) after authorization by regulatory agencies (278).

7.7.2 Regulatory Bodies

Worldwide, nuclear Medicine guidelines are developed by a number international, continental, national as well as local regulatory organisations (281) and the introduction of new isotopes or the institution of new usages of old isotopes would have to navigate these guidelines and regulations. In Europe, the European Association of Nuclear Medicine (EANM) coordinates the development of guidelines, but also recognises the need for national guidelines. Likewise, In the United Kingdom, there are national regulations on the administration of radioactive substances but differences in clinical practice and service delivery mean that guidelines do not readily apply across regional and national boundaries (282, 283).

Some examples of the various statutory nuclear medicine guidelines and regulatory bodies in England include: Medicines and Healthcare products Regulatory Agency (MHRA) which regulates the use of new and established medicines and devices; the Carriage of Dangerous Goods and Use of Transportable Pressure Equipment Regulations 2009 regulates the transportation of radioactive substances; the Administration of Radioactive Substances Advisory Committee (ARSAC); the Radioactive Substances Act 1993 (RSA93) in Scotland, or the Environmental Permitting Regulations 2010 (EPR2010) in England and Wales which oversees the management of radioactive wastes and is policed by the Environment Agency; the Medical and Dental Guidance Notes which covers Ionising Radiation Regulations (IRR99) and is policed by the Health and Safety Executive (HSE). Lastly, there is the Ionising Radiation (Medical Exposure) Regulations (IRMER) 2000 with inspections carried out by the Care Quality Commission (CQC).

^{99m}Tc-labelled Ciprofloxacin (Infecton®) was first postulated by Solanki (284). Its physiological distribution does not include the normal bone marrow and this allows for evaluation of the spine and proximal limbs unlike radiolabelled white cell and Gallium-67 scans which demonstrate background bone marrow uptake (285). Although initial reports for the use of ^{99m} Tc-labelled Ciprofloxacin in infection were promising (284). More recent accounts of the use of ^{99m}Tc-labelled Ciprofloxacin show a reduced specificity for detecting of bacterial infections. Also the radioisotope physically disappeared from sites of infection and inflammation with equal rapidity (286). Therefore, ^{99m}Tc-labelled Ciprofloxacin has no role of in diagnosing orthopaedic infections (286).

7.7.3 Future Research with Folate Imaging

The beta folate receptor (FR-β isoform) is overexpressed on activated macrophages which accumulate at sites of inflammation and infection. Folate receptor avid isotopes have been shown to accumulate at sites of inflammation and could act as markers for inflammatory processes such as rheumatoid arthritis (287). In addition, to the beta folate receptor (FR-β isoform), there are 3 other separate types of receptor polypeptides located in cell membranes (α, γ and δ) which also bind and endocytose folates and folate conjugates. The alpha folate receptor (FR-α isoform) demonstrates limited expression in normal tissue, mainly kidneys, choroid plexus, lungs, and placenta (288), but is upregulated in ovarian, uterine, brain, lung, kidney, breast as well as colorectal tumours (287). PET and SPECT folate imaging can be performed with ^{18}F-Fluorodeoxyglucose folate PET (288) and ^{99m}Tc-EC20 SPECT (288, 289) imaging respectively.

7.7.4 Future Research with 3-Phase ^{99m}Technetium Labelled Bone Scans with SPECT-CT

More data can be gleaned from current well established imaging methods of imaging PJI and loosening. A follow up retrospective research study into PJI and loosening with Time-Activity Curves and CT density maps obtained from 3-phase ^{99m}Technetium labelled bone scans with SPECT-CT is already in preparation in UHCW.

7.8 Summary and proposed imaging algorithms

Multiple different proposed imaging algorithms are being proposed to cover different imaging scenarios as well as the availability or unavailability of SPECT-CT and PET-CT scanners. The initial imaging of painful joint prostheses with 3-phase ^{99m}Tc bone scans SPECT-CT or ^{18}F-NaF PET-CT should be able to detect mechanical complications on the CT component as well as infection and aseptic loosening on the radionuclide images (Figures 47 and 48).

Infectious type (Type II) periprosthetic membranes which consist of granulation tissue with neutrophilic granulocytes, plasma cells and few, if any, wear particle are usually obvious on 3-phase ^{99m}Tc bone scans SPECT-CT and ^{18}F-NaF PET-CT (Figures 47 and 48), but these patients may be assessed further using labelled white cells (Figure 49) with SPECT-CT if required. In patients with no clear evidence of mechanical complications or infection on initial imaging with predominantly late-phase positive isotope planar or SPECT bone scans or late phase positive ^{18}F-NaF PET (41, 78), the periprosthetic membranes may be assessed for the presence of activated macrophages with Tilmanocept receptor imaging using either SPECT or PET imaging (Figures 50 and 51) depending on the availability of scanning equipment and local expertise. The presence of a high concentration of macrophages would suggest particulate-induced wear (Type-I) or the combined type (Type III).

The cost and availability of scans as well as the radiation dose to the patient should be factored in when considering the choice of imaging algorithms for prosthetic joint investigations (Table 22).

Table 20. *Prosthetic joint imaging with typical scan cost and radiation dose*

Diagnostic Procedure	Typical Effective Dose (mSv)	Equivalent Number of Chest X-Rays	Approximate Equivalent Period of Natural Background Radiation	Typical Cost
Radiography (Plain Film)				
Limbs and Joints (except hips)	<0.01	<1	<2 days	Tariff (bundled in Health Resource Groups (HRGs) (<£40)
Pelvis	0.3	20	1.5 months	Tariff (bundled in Health Resource Groups (HRGs) (<£40)
Ultrasound				
Ultrasound Joint	0	0	0	Tariff (including COR) (£39)
Computed Tomography (CT)				
CT Pelvis	6	370	2.5 years	Tariff (including COR) (£69)
Magnetic Resonance Imaging (MRI)				
MRI Limb	0	0	0	Tariff (including COR) (£108)
Radionuclide (Nuclear Medicine)				
Bone (^{99m}Tc-HDP)	3	200	1.3 years	Tariff (including COR) (£179)

Diagnostic Procedure	Typical Effective Dose (mSv)	Equivalent Number of Chest X-Rays	Approximate Equivalent Period of Natural Background Radiation	Typical Cost
^{18}F-NaF or ^{18}F-FDG PET-CT	18	1200	8.1 years	Tariff (not rebundled and no tariffs published- to be negotiated locally) (£700)

Note: including COR = including cost of reporting

Typical cost and radiation dose of commonly performed examinations. Source NHS National tariff payment system Annex A: The national tariff workbook (Unbundled service prices 2019/20) (290)

Some variances: 1 vial of Lymphoseek® costs circa £1,175 (because this is a new patented radiopharmaceutical agent).

A new PET-CT machine with service contract in place will cost approximately £1.6 million.

A modern SPECT-CT gamma camera machine with diagnostic CT capability and service contract in place will cost approximately £ 0.5 million.

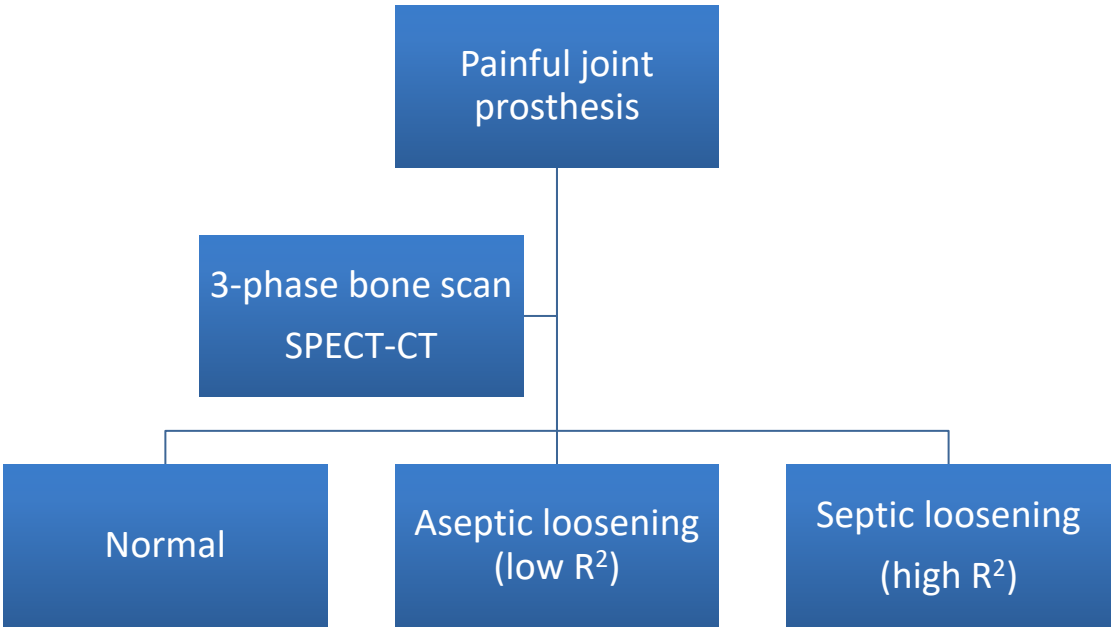

Figure 47. *Proposed radionuclide imaging algorithm using SPECT-CT*

Note: Imaging algorithm for dynamic SPECT-CT initial imaging of painful joint prostheses – yielding results compatible with normal, aseptic loosening or infection (if no PET-CT is available)

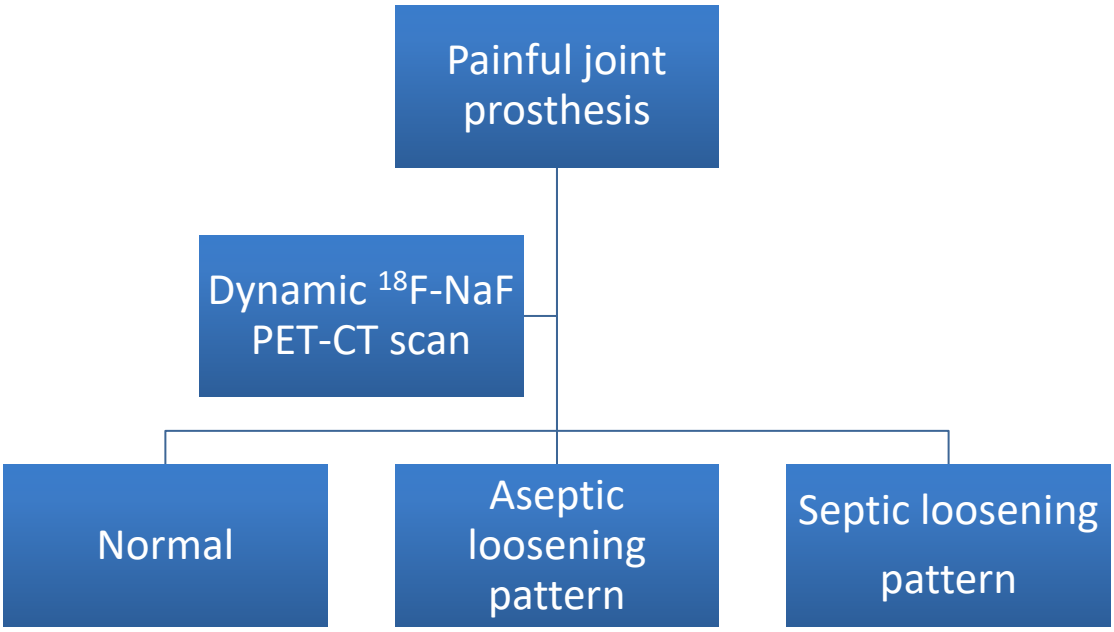

Figure 48. *Proposed radionuclide imaging algorithm using PET-CT*

Note: Imaging algorithm for dynamic PET-CT initial imaging of painful joint prostheses – yielding results compatible with normal, aseptic loosening or infection.

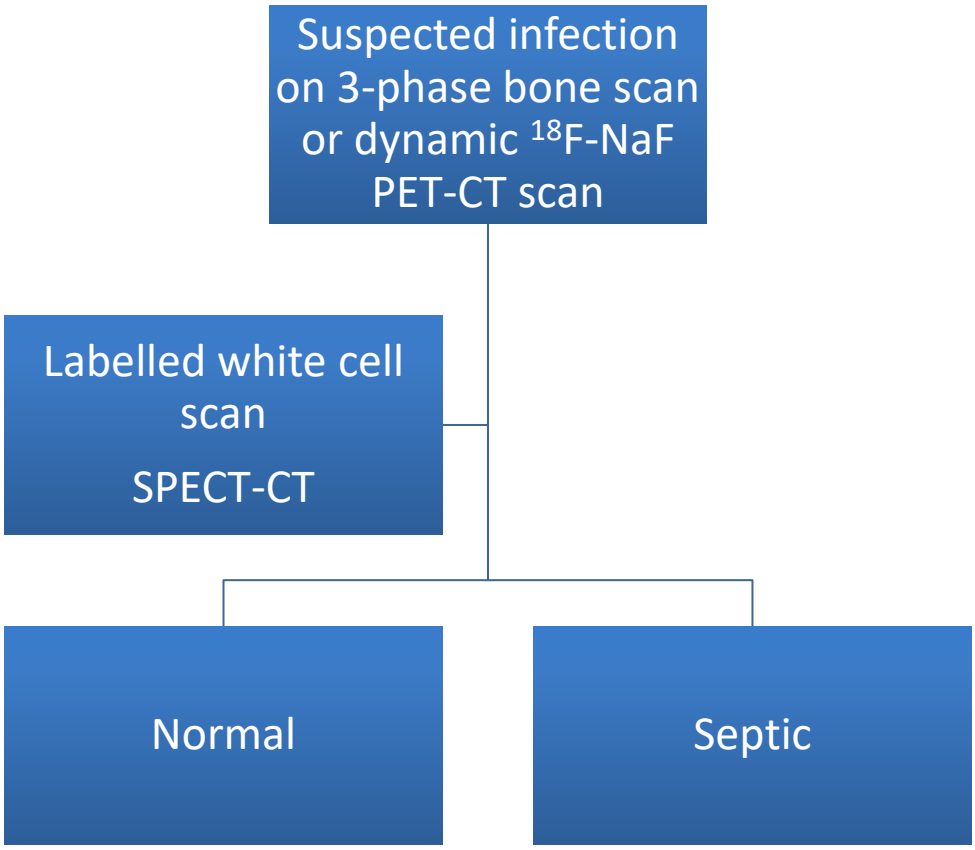

Figure 49. *Proposed radionuclide imaging algorithm for suspected infection with SPECT-CT*

Note: Imaging algorithm for SPECT-CT labelled white cell imaging of suspected infected joint prostheses – yielding results compatible with no infection or infection (if PET-CT scanner is not available).

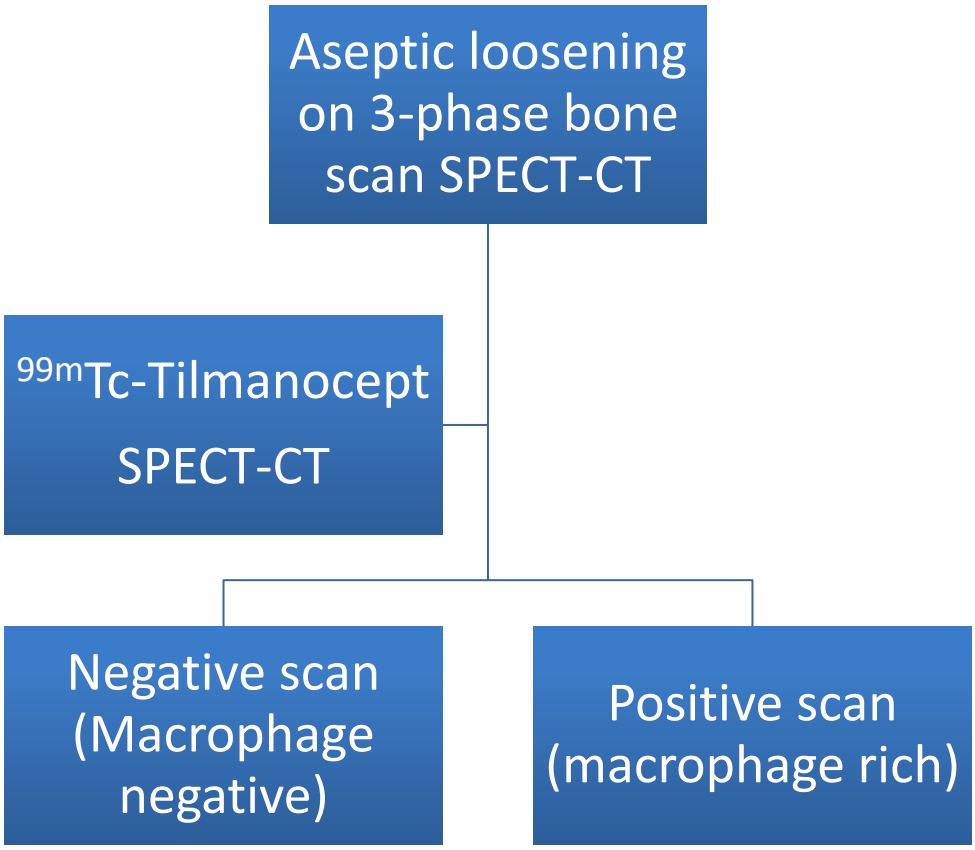

Figure 50. *Proposed Radionuclide imaging algorithm for suspected aseptic loosening with SPECT-CT*

Note: Imaging algorithm for SPECT-CT Tilmanocept imaging of suspected aseptic loosening in joint prostheses – yielding results compatible with a high macrophage burden or no macrophages (if PET-CT scanner is not available)

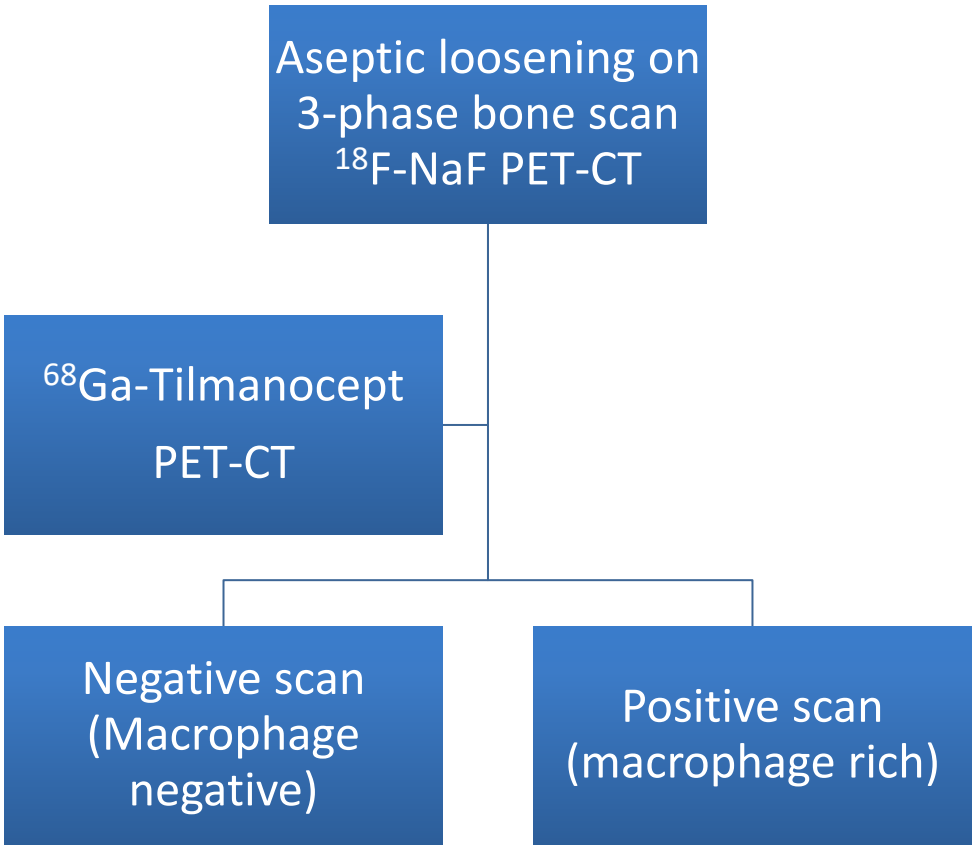

Figure 51. *Proposed radionuclide imaging algorithm for suspected aseptic loosening with PET-CT*

Note: Imaging algorithm for PET-CT Tilmanocept imaging of suspected aseptic loosening in joint prostheses – yielding results compatible with a high macrophage burden or no macrophages.

7.9 Conclusion

This is a novel technique and the first in-vivo use of a macrophage mannose receptor imaging in humans to demonstrate periprosthetic membrane aseptic loosening. Radionuclide scintigraphy with ^{99m}Tc-Tilmanocept SPECT-CT scan will be a useful imaging investigation in the assessment of the painful knee arthroplasty. A negative ^{99m}Tc-Tilmanocept scan should be reassuring and make a diagnosis of aseptic loosening unlikely. ^{68}Gallium (^{68}Ga) labelled Tilmanocept PET-CT imaging is an alternative to ^{99m}Tc-Tilmanocept SPECT imaging.

7.10 Summary

- Lymphoseek® is a relatively new radiopharmaceutical that binds to the mannose receptor on the cell surface of macrophages.
- Lymphoseek® imaging in the assessment of the painful arthroplasty can be performed with ^{99m}Tc-Tilmanocept SPECT-CT scan or ^{68}Gallium (^{68}Ga) labelled Tilmanocept PET-CT.
- A negative Tilmanocept scan should be reassuring and make a diagnosis of wear particle induced aseptic loosening unlikely.
- There are further radiopharmaceutical agents including beta folate receptor imaging.

Chapter 8 Conclusion

This dissertation aimed to show that dynamic ^{18}F-Fluoride PET-CT may have a role in the investigation of painful hip and knee prosthetic joint replacements as well as analyse the relationship between ^{18}F-Fluoride PET-CT and ^{99m}Tc-MDP dynamic bone scans.

There is a rising incidence of joint replacement surgery and a growing need for prosthetic joint imaging. Chapter 1 provided an overview of the background and history of joint prostheses with theoretical framework and context information. Because of the importance and expanding role of hybrid imaging the contribution of CT to prosthetic joint imaging was outlined along with a CT spectrum of pathological complications of prosthetic joints. The concept of prosthetic joint imaging with dynamic ^{18}F-NaF PET-CT as well as radionuclide imaging of activated macrophages in periprosthetic tissue were introduced as possible means of increasing diagnostic accuracy and efficiency.

Chapter 2 was a small retrospective investigation of the use of dynamic bone scans in painful hip and knee prosthetic joint replacements which demonstrated delays in diagnosing painful joint prostheses. The use of multiple tests was identified as possibly contributing to diagnostic delay and a streamlined reduced number of imaging tests may contribute to an improve the speed of diagnosing painful joint prostheses. Fused functional anatomical imaging may also reduce the number of imaging tests required.

Chapter 3 was a systematic review of ^{18}F-NaF PET in diagnosing and distinguishing between septic and aseptic loosening in hip and knee prostheses. Sodium fluoride positron emission tomography (^{18}F-NaF-PET) is an old isotope which is making a comeback as a promising tool with high sensitivity and specificity in bone imaging. The small series was a limiting factor of the series. ^{18}F-NaF PET is also of limited use before the ninth post-surgical month, but this can be overcome by routine baseline imaging ‘at risk’ prostheses at 3

month intervals for the detection of abnormal rates of decline in periprosthetic NaF uptake.

Chapter 4 introduced research on the promising role of dynamic ^{18}F NaF PET-CT in diagnosing symptomatic joint prostheses. The preliminary data validated early proof of principle that dynamic ^{18}F-NaF PET-CT can detect aseptic loosening of lower limb prostheses with anatomical correlation provided by the CT component. More research is required to establish a role for dynamic ^{18}F-NaF PET-CT for detecting aseptic loosening and septic loosening. Further comparative studies of dynamic ^{18}F-NaF PET-CT versus technetium-based 3-phase bone scans are needed with larger patient populations in the assessment of painful hip and knee prostheses before routine clinical use.

Beam hardening artefacts from prostheses have a significant deleterious effect on hybrid images. Hence, chapter 5 compared the use of pre-filtering with Aluminium; dual-energy CT and mathematical algorithms with MATLAB® filtered back projection to evaluate and correct beam hardening artefact from prostheses on Dynamic NaF PET-CT. Although pre-filtering with Aluminium; dual-energy CT and mathematical algorithms with MATLAB® filtered back projection can reduce beam hardening artefact, there was no significant difference and the use of these techniques introduced other artefacts with subsequent reduction in image quality.

Chapter 6 was a prospective study comparing dynamic ^{18}F-NaF PET-CT and 3-phase bone scans of hip and knee joint prostheses. The limitations and problems encountered in this clinical trial were recounted. Graphical and mathematical data was extracted from ^{99m}Tc-MDP dynamic bone scans to improve diagnostic accuracy but the trial population was small. Further research is required with a larger study to distinguish septic loosening or inflammation from aseptic loosening. Combining this method with CT periprosthetic lucency from SPECT-CT may improve the accuracy even further. Data from the ^{18}F-Sodium fluoride (^{18}F-NaF) study was partly corrupted and could not be retrieved resulting in inconsistent outcomes from the small numbers. Hence, no strong conclusion could be drawn especially in the infected category. ^{99m}Tc-MDP dynamic bone scans are significantly cheaper and more widely available than

^{18}F-NaF PET-CT. Therefore, the use of graphical and mathematical data from ^{99m}Tc-MDP dynamic bone scans may prove to be more cost effective than ^{18}F-Sodium fluoride (^{18}F- NaF) PET-CT. but more research is needed. While the corrupted ^{18}F-NaF data limits the accuracy of the ^{18}F-NaF results, this study provides new insight into how graphical and mathematical data extracted from ^{99m}Tc-MDP dynamic bone scans can improve diagnostic accuracy.

Chapter 7 provided new insights into future research and the use of Tilmanocept® and further future areas of research as well as the regulatory hurdles of radiopharmaceutical licencing. Tilmanocept® is a novel technique involves the first in-vivo use of an isotope-labelled macrophage mannose receptor imaging study in humans to demonstrate periprosthetic membrane aseptic loosening. This research will clearly illustrate that radionuclide scintigraphy with ^{99m}Tc-Tilmanocept SPECT-CT scan will be a useful imaging investigation in the assessment of the painful knee arthroplasty but it also raises the question of how early in the post-surgical period Tilmanocept® imaging can be used. It is likely that a negative ^{99m}Tc-Tilmanocept scan would be rule-out a diagnosis of aseptic loosening. Also, ^{68}Gallium (^{68}Ga) labelled Tilmanocept PET-CT imaging is an alternative to ^{99m}Tc-Tilmanocept SPECT imaging.

This study had several limitations. First, the study had selection bias because the dynamic ^{18}F-NaF PET-CT trial included only patients who were on the surgical waiting list for revision surgery. This may overestimate the sensitivity of the test because patients who did not undergo revision surgery could be more likely to have a negative or equivocal ^{18}F-NaF PET-CT results. The exclusion of patients not being considered for revision surgery could also affect the sensitivity because lesions in nonsurgical patient may be smaller and difficult to visualise on imaging. Secondly, the 3 month bone scan study was a retrospective study and images from the metal-artefact study were read by a single radiologist and a blinded review by more than one radiologist would have been more ideal. Lastly, the small population in the samples studied as well as the lack of dynamic NaF images for positive septic prostheses.

Future studies of dynamic ^{18}F-NaF PET-CT, 3-phase bone scans with graphical presentation as well as Tilmanocept® imaging these relative enhancement

patterns, combined with morphologic features of CT would be valuable in formulating a new imaging pathway.

This dissertation provides new knowledge into the optimising isotope bone SPECT-CT scans by extracting graphical and mathematical data whilst minimising prosthetic induced artefacts may be more cost effective.

The improved specificity provided by Tilmanocept® imaging is a novel approach to the assessment of prosthetic joint complications by directly demonstrating particle-laden macrophage infiltrates in the zone of bone resorption. Hence, combining mathematical data from ^{99m}Tc labelled bone scans and Tilmanocept® imaging into an algorithm (Figure 52) is likely to ultimately improve diagnostic accuracy but there is a need for future research with both ^{99m}Tc-Tilmanocept® SPECT-CT and ^{68}Gallium PET-CT.

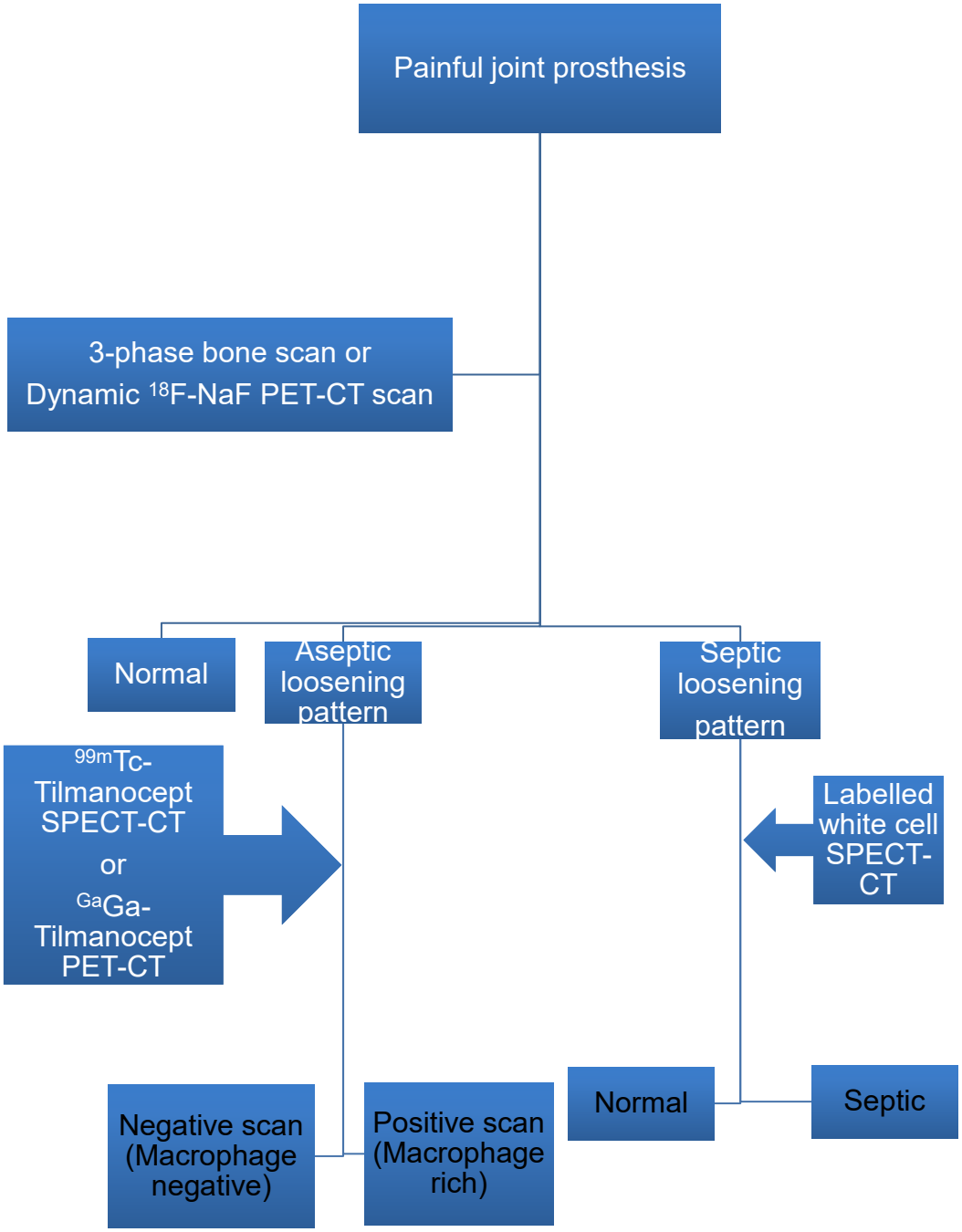

Figure 52. *Proposed combined radionuclide imaging algorithm for painful joint prostheses accounting for diverse equipment availability and local expertise*

Note: Proposed exhaustive radionuclide imaging algorithm for painful joint prostheses (including PET-CT and SPECT-CT options for ^{68}Ga)

Summary

- There is a rising incidence of joint replacement surgery and a growing need for prosthetic joint imaging
- Dynamic ^{18}F-Fluoride PET-CT may have a role in the investigation of painful hip and knee prosthetic joint replacements.
- There is an important contribution of CT to prosthetic joint hybrid imaging and may also reduce the number of imaging tests required.
- ^{18}F-NaF PET is also of limited use before the ninth post-surgical month
- Dynamic ^{18}F-NaF PET-CT can detect aseptic loosening of lower limb prostheses but beam hardening artefacts from prostheses have a significant deleterious effect on hybrid images. Pre-filtering with Aluminium; dual-energy CT and mathematical algorithms with MATLAB® filtered back projection can reduce beam hardening artefact to the same extent.
- Dynamic ^{18}F-NaF PET-CT was not proven to be more accurate than 3-phase bone scans in the diagnosis of aseptic loosening and infection of hip and knee joint prostheses partly due to limitations and problems encountered in the clinical trial.
- Graphical and mathematical data extracted from ^{99m}Tc-MDP dynamic bone scans may add further diagnostic information in distinguishing septic loosening or inflammation from aseptic loosening.
- Tilmanocept® is a novel technique with the potential for identifying macrophages in aseptic loosening in prosthetic joints.
- Algorithmic combinations of mathematical data from ^{99m}Tc labelled bone scans and Tilmanocept® hybrid imaging is likely improve diagnostic accuracy.

Appendix

Some trial documents and selected pages from the preclinical trial agreement with Norgine Limited.

University Hospitals Coventry and Warwickshire NHS Trust

University Hospital
Clifford Bridge Road
Walsgrave
Coventry
CV2 2DX

Tel: 024 7694000
Fax: 024 7696 6056
www.uhcw.nhs.uk

CONSENT FORM

A Direct Comparison of ^{18}F-Fluoride PET-CT and Conventional Radionuclide Bone Scans in the follow-up of patients with Prosthetic Joint Replacements in the Hips and Knees.

Trial Number:

Part 1 (please read carefully):

Please initial to agree

I confirm that I have read and understand the Patient Information Sheet dated ..... (version1.1) for the above study and have had the opportunity to ask questions.

I understand that my participation is voluntary and that I am free to withdraw at any time, without giving any reason, without my medical care or legal rights being affected.

I understand that sections of any of my medical notes may be looked at by responsible individuals involved in the running of the trial, or authorised personnel from the NHS Trust R & D for audit or other regulatory authorities where it is relevant to my taking part in research, and that I may followed up through usual NHS mechanisms (e.g. Office for National Statistics). All access to my data must be compliant with the Data Protection Act 1998.

I give permission for these individuals to have access to my records.

I understand that copies of my scans will be sent for radiological review for confirmation of diagnosis.

I understand that my General Practitioner will be informed of my treatment and may be contacted to supply details of my progress

I agree to take part in the above study.

Name of patient Date Signature

Name of person taking consent Date Signature

(if different from researcher)

Researcher Date Signature

3 copies: 1 for patient, 1 for researcher, 1 to be kept with hospital notes

University Hospitals Coventry and Warwickshire NHS Trust

University Hospital

Clifford Bridge Road Walsgrave Coventry CV2 2DX

Tel: 024 7694000 Fax: 024 7696 6056 www.uhcw.nhs.uk

PATIENT INFORMATION SHEET – PART 1

Version 1.5 Date 23.10.2012

Study title: A Direct Comparison of F-18-Fluoride PET-CT and Conventional Radionuclide Bone Scans in the follow-up of patients with Prosthetic Joint Replacements in the Hips and Knees.

Study acronym: F-18-Fluoride PET-CT in Prosthetic Joint Replacements (F18 Prosthetic Joint).

Introduction

This study has been reviewed by the Coventry and Warwickshire Research Ethics Committee and will count towards the attainment of a PhD by Dr Olu Adesanya at the University of Warwick. We have invited you to take part in a research study. Before you decide if you would like to take part, it is important that you understand why the research is being done and what it will involve. Please take time to read the following information carefully and discuss it with friends, relatives and your GP, if you wish. If you decide to enter the study your GP will be made aware of this. Please ask us if there is anything that is not clear or if you would like more information.

What is the purpose of the study?

This study is designed to test whether we can use a new type of scanning to tell why your joint replacement such as yours hurts. You have a painful joint

replacement and this occurs at some point in time for 4 in every 100 persons who have had this type of surgery. Treatment for the pain depends on its cause and but in some cases, for example when the replacement has become infected, the only effective treatment is further surgery. Currently, the only way of determining the presence or absence of infection involves inserting needles into the joint to draw off fluid and/or undergoing more than one imaging test. These tests include x-rays, bone scans and white cell imaging studies. With the introduction of PET-CT scanning in 2001– a type of scan which can tell the difference between active and inactive cells in the body –it has been made possible to detect small amounts of disease and infection in the body. We know that this type of scan is much more accurate than bone scans for all other common uses. It is our hope that we will be able to design an imaging study using this type of scan so that someone like you will receive a prompt and timely diagnosis involving only a single hospital visit.

What is PET scanning?

Unlike ordinary X-rays or computed tomography (CT) scans, PET scans are able to provide information regarding increased bone turnover around joint prostheses. We already know that PET scanning can be used to detect areas of infection and tumours, and we also know that if the scan is clear 12 months after surgery, it is very likely that there is no infection and that the prosthesis is normal or at worst simply loose. We also know that if the scan is not clear particularly in the early phase of the scan, there is a high chance of infection, so we think that people with a positive PET scan might benefit from targeted antibiotic treatment.

Why have I been chosen?

You have been diagnosed with a replaced joint which is causing discomfort pain or difficulty and will be re-treated surgically. Therefore you are suitable for this study and we are asking whether you would like to take part.

Initial Assessment

Prior to starting treatment a thorough assessment of your prosthesis will need to

be undertaken. This will involve blood tests, as well as weight/height measurement. Some of these tests may have already been carried out as they are routinely performed prior to starting treatment whether or not you take part in a study. As part of the study you will also be required to have a PET-CT scan. This type of scan is becoming part of the standard process for other diseases in the UK, although because it is quite new, not all centres are yet carrying it out routinely. It will therefore be necessary for you to travel to University Hospital Coventry to have your scan. The scan itself involves a simple intravenous injection of a mildly radioactive substance (^{18}F-NaF) followed immediately by a scanning procedure for about 30-45 minutes. You will not need to fast and may take all your usual medications. If travelling by car you should be free to go or drive yourself home afterwards.

What exactly would the study involve? This is a prospective uncontrolled longitudinal (case series) study. This means that all persons will undergo PET-CT imaging as well as a standard bone scan (if this has not already been performed recently). You will know what test you are undergoing at each point in time. The bone scan and PET-CT scan will occur over two separate days (possibly with a month), therefore, involve two injections given over a 1 month period. Imaging usually occurs between (9 am and 5pm between Monday and Friday as an outpatient (unless you need to stay in hospital for any other reason). After both the bone scan and the PET-CT scan have been performed, the treatment you receive will be the same regardless of the results of the PET-CT scan or bone scan. This treatment will have been decided by your doctor and will yield useful data for the trial. We hope that by demonstrating this novel use of PET-CT, this may improve the speed and accuracy of diagnosing people with prosthetic problems. For quality control purposes we plan to review the bone scans and PET-CT scans of everyone taking part in the trial and, if you agree, your images will be anonymized and also sent to a Radiology department in Birmingham. As part of the study, you will be required to provide blood samples as is the usual practice. **What will happen to any samples I give?**

Blood samples will be collected and processed in exactly the same way as

other blood samples taken from you or any other patient in your hospital. These will be destroyed after analysis.

All joint prostheses and tissue samples in this study will be collected and processed in exactly the same way as for a patient not in the study. All samples will be destroyed after analysis.

Assessment

You will be asked a few questions about how you have been since the last time you had surgery on your joint. People participating in this study would also be asked other questions as part of a questionnaire.

Follow up When you have completed your study treatment you will be seen as often as is deemed necessary by your clinical team. Finally, routine blood tests and x-rays may be taken during follow up.

Payment

You will not receive payment/reimbursement for participating in this study, but will have your travel expenses reimbursed up to a reasonable amount.

What are the possible risks of taking part?

The dose of the injected tracer for PET-CT is very low and there are no known side effects from it. If you do develop troublesome side effects, your doctor may need to adjust your treatment to try and avoid further problems. The more common side effects of HDP bone scans:

Allergic Reaction – this is very rare and if at all it occurs is limited to flushing or redness of skin.

Nausea and vomiting – this is also rare due to the very small amounts of injected tracer. It can usually be managed with anti-sickness (anti-emetic) drugs.

We have listed the most common side effects of these tracers, but it is unlikely that you would experience any of the side effects listed above. Tell your doctor

if you suffer from any of these side effects, or if you have experienced any new symptoms since your last visit. Your doctor can help you by giving you medication or advice, to reduce or stop these side effects from occurring in the future. PET-CT scans also involve exposure to radiation. However the doses are very small and we have kept the number of scans required to a minimum. In fact, you will only receive one more scan by taking part in the study than is currently received as part of normal clinical routine.

In total you will be receiving one bone scan and one PET-CT scan. Each CT scan is equivalent to about 4 years of natural background radiation exposure. Each PET-CT scan is equivalent to about 8 years of natural background radiation exposure. The radiation exposure you will be receiving will approximate from about 30 times that of natural background radiation over the same period of time, with an equivalent to a lifetime additional risk of approximately 1 in 280, of getting a fatal cancer from these examinations. These exposures are very unlikely to put you at significant health risk. A leaflet is available entitled “X-rays – How safe are they?” that provides further information on radiation exposure and which you may find useful.

What do I have to do?

It is important that you attend for all scheduled visits for blood tests, scans, clinic appointments and surgical treatment to ensure that the treatment can be delivered and you can be monitored for any complications.

What are the benefits of taking part? Although most people can expect to be cured with antibiotics and revision surgery, the standard treatment for infected prostheses, it is clear that separating aseptic loosening from infected prostheses will allow infected people receive the required more intensive treatment and also less intensive treatment in aseptic loosening. Before the advent of PET scanning the presence of infection around the prosthesis could be assessed with bone scans but these results are thought not to be very accurate. PET scanning is able to assess infection accurately, and by using this information we hope to tailor treatment more closely to your needs. Taking part in this study may help you directly, although this cannot be guaranteed. The

information gained from this study will help us to improve the future treatment of people like you with painful joint prostheses.

What are the potential disadvantages of taking part?

Having a bone and PET scan would involve the inconvenience of travelling to the hospital on 2 different days and in some cases 2 whole days off work may be required. Some people may find lying still for the scan unpleasant and the injection of ^{18}F-NaF or ^{99m}Tc-HDP into an arm vein will cause slight discomfort (like having a blood test) and sometimes minor bruising.

Do I have to take part?

No. It is up to you to decide whether or not to take part. If you decide to take part you will be given this information sheet to keep and be asked to sign a trial consent form. You may still decide to withdraw at any time without having to give a reason.

What if I decide not to enter the trial?

If you decide not to take part, or if you withdraw, this will not affect the standard of care you receive. Agreeing or refusing to take part will not affect your legal rights as an individual receiving treatment under the National Health Service. Your relationship with the doctors and nurses looking after you will not be affected. If you decide not to take part, your surgical treatment will proceed as planned.

What happens if the research study stops?

If the research study stops early your doctor will inform you and discuss the treatment options with you. If the research study is completed you will be followed up in clinic as is normal practice.

What if there is a problem?

If you wish to complain or have any concerns about any aspect of the way you have been approached or treated during the course of this trial, the normal National Health Service complaints mechanism will be available to you. If you

are harmed by taking part in this trial, there are no special compensation arrangements but if this is due to someone's negligence then you may have grounds for a legal action.

Contact for further information

If you have any concerns or questions about this study, please contact the Nuclear Medicine department on 02476 962812 who will be happy to give you further information. General information for joint prostheses is also available from the Prosthetic and Orthotic department on 0800 252060. If you have any further queries please contact our Patient Advice and Liaison Service (PALS) in the first instance in any of the following ways: By phone 0800 028 4203 (calls are free from a BT landline but mobile phone charges may vary); By email:feedback@uhcw.nhs.uk; In writing to: Patient Advice and Liaison Service (PALS), University Hospitals Coventry and Warwickshire NHS Trust, University Hospital, Clifford Bridge Road, Coventry, CV2 2DX**.** They will ensure that your query is directed promptly to the most appropriate person.

Contact details for concerns or complaints about the Research, Staff, Conduct etc: Please write to Ms Nicola Owen, Deputy Registrar, University of Warwick, Research Support Services, University House, Kirby Corner Road, Coventry CV4 8UW; or e-mail:

Nicola.Owen@warwick.ac.uk. Alternately, you may telephone: 024 7652 2785 or fax: 024 7652 4751

This completes Part 1 of the Information Sheet. If the information in Part 1 has interested you and you are considering participation, please continue to read the additional information in Part 2 before making any decision.

University Hospitals Coventry and Warwickshire NHS Trust

University Hospital
Clifford Bridge Road
Walsgrave
Coventry
CV2 2DX

Tel: 024 7694000
Fax: 024 7696 6056
www.uhcw.nhs.uk

GP LETTER

A Direct Comparison of F-18-Fluoride PET-CT and Conventional Radionuclide Bone Scans in the follow-up of patients with Prosthetic Joint Replacements in the Hips and Knees.

Trial Number:

Dear Dr _____

Version 1.0 Date 24.07.12

Your patient, _____ (date of birth dd/mm/yyyy), has a symptomatic joint prosthesis and has consented to participate in a study evaluating joint prostheses with F18 -NaF-PET-CT scans.

Please find enclosed a copy of the patient information sheet for this trial.

You will be kept up to date with your patient's progress but if you have any concerns or questions regarding this study please contact the responsible doctor:

Dr___Olu Adesanya_____at (University Hospitals Coventry & Warwickshire)

Tel: _____

Kind regards,

adesanya@doctors.org.uk Message 19/07/2012 21:59

Reply

From: Subject: RE: SCOPE: Protocol Review - F-18-Fluoride PET-CT in Prosthetic Joint Replacements (F18 Prosthetic Joint) **Date:** Fri, 29 Jun 2012 13:12:49 +0000 **To:** Oludolapo Adesanya <adesanya@doctors.org.uk>

Notification that a Clinical Trial Authorisation (CTA) is not required

Dear Ms O Adesanya,

Thank you for your email dated 17th June 2012.

I can confirm that your proposal is not a Clinical Trial of an Investigational Medicinal Product (IMP) as defined by the EU Directive 2001/20/EC and no submission to the Clinical Trials Unit at the MHRA is required.

Kind regards

Clinical Trial Helpline MHRA

-----Original Message-----From: Oludolapo Adesanya [mailto:adesanya@doctors.org.uk] Sent: 17 June 2012 00:53 To: clintrialhelpline@mhra.gsi.gov.uk. Subject: SCOPE: Protocol Review - F-18-Fluoride PET-CT in Prosthetic Joint Replacements (F18 Prosthetic Joint)

Would you please advise me as to whether comparison of ^{18}F-NaF PET-CT vs ^{99m}Tc-hydroxydi- phosphonate (HDP) isotope bone scans to diagnose infection of joint prostheses constitutes the clinical trial of an investigational medicinal product?

Regards

Olu Adesanya Radiologist UHCW

.

University Hospitals Coventry and Warwickshire NHS Trust

University Hospital
Clifford Bridge Road
Walsgrave
Coventry
CV2 2DX

Tel: 024 7694000
Fax: 024 7696 6056
www.uhcw.nhs.uk

Version 1.0

F18 Prosthetic Joint Study

Study patient questionnaire Modified GHAA-9

In terms of your satisfaction, how would you rate each of the following:				
1. How long you waited to get an appointment.				
Excellent	Very good	Good	Fair	Poor
2. Length of time spent waiting in the hospital for the procedure.				
Excellent	Very good	Good	Fair	Poor
3. Length of the procedure.				
Excellent	Very good	Good	Fair	Poor
4. How well did you tolerate the procedure				
Excellent	Very good	Good	Fair	Poor
5. The personal manner (courtesy, respect, sensitivity, friendliness) of the technologist who performed your procedure.				
Excellent	Very good	Good	Fair	Poor
6. The technical skills (thoroughness, carefulness, competence) of the staff that performed your tests.				
Excellent	Very good	Good	Fair	Poor
7. The personal manner (courtesy, respect, sensitivity, friendliness) of the staff.				
Excellent	Very good	Good	Fair	Poor
8. Adequacy of explanation of what was done for you—all your questions answered.				
Excellent	Very good	Good	Fair	Poor
9. Overall rating of the visit				
Excellent	Very good	Good	Fair	Poor

Research agreement between Norgine Limited and University Hospital Coventry (selected pages 1 and 11)

THIS RESEARCH AGREEMENT (the "**Agreement**") is made this _____ day of _____ (the "**Effective Date**")

BETWEEN

University Hospitals Coventry & Warwickshire NHS Trust whose registered office is at University Hospital, Clifford Bridge Road, Coventry, CV2 2DX("**UHCW**");

AND

NORGINE Limited, registered in the United Kingdom under registered number 00215668 whose registered office is at New Road, Tir-y-berth, Hengoed, Mid Glamorgan, South Wales, CF82 8SJ ("**NORGINE**"). Each of the foregoing may be referred to individually as a "**Party**" and collectively as the "**Parties**".

RECITALS:

A. NORGINE is a pharmaceutical company which, together with its Affiliates, carries on the business of manufacturing and selling pharmaceuticals including the Product (as defined in Clause 1).

B. UHCW wishes to conduct a research Study(as defined in Clause 1) utilising the Product and has approached NORGINE requesting Support (as defined in Clause 1) for the research study.

C. NORGINE is willing to provide UHCW with Support subject to the terms and conditions of this Agreement.

NOW, IT IS AGREED as follows:

1. DEFINITIONS AND INTERPRETATION

1.1. In this Agreement, unless the context otherwise requires, the following words and expressions shall have the following meanings:

"**Affiliate**" means, with respect to a Party, any corporation or other entity that controls, is controlled by, or is under common control with, a Party. A corporation or other entity shall be regarded as in control of another corporation or entity if it owns or directly or indirectly controls more than 50% of the voting securities or other ownership interest of the other corporation or entity, or if it possesses, directly or indirectly, the power to direct or cause the direction of the management and policies of the corporation or other entity;

Adverse Drug Reaction or "**ADR**": An adverse reaction is a response to a medicinal product which is noxious and unintended [DIR Art 1]. This includes adverse reactions which arise from:

- the use of a medicinal product within the terms of the marketing authorisation;
- the use outside the terms of the marketing authorisation, including overdose, off-label use, misuse, abuse and medication errors;
- occupational exposure

"**Business Day**" means any day other than a Saturday, Sunday or a Bank Holiday in the United Kingdon;

17.8. **Power & Authority**. Each Party hereby represents and warrants to the other that it has full power and authority to execute, deliver and perform its obligations under this Agreement, and that such Party is not bound by any other contractual obligation, express or implied, inconsistent with the terms hereof.

17.9. **Interpretation**. In the event that there is any inconsistency between the terms of the Protocol and the terms of the Agreement, the terms and conditions of the Protocol shall prevail with respect to allresearch matters , the conduct of the study , and the terms of the Agreement shall prevail with respect to all legal, business and/or commercial financial matters.

IN WITNESS WHEREOF, the duly authorised representatives of the Parties have signed this Agreement as of the Effective Date.

UHCW Limited

Signature: ..... Signature: .....

Name: Ceri Jones

Title: Head of Research, Development & Innovation

Name: Tom Halliwell

Title:Therapy Area Head, Norgine

Bibliography

1. Rabin DN, Smith C, Kubicka RA, Rabin S, Ali A, Charters J, et al. Problem prostheses: the radiologic evaluation of total joint replacement. Radiographics. 1987;7(6):1107-27.
2. Phillips J, Crane T, Noy M, Elliott T, Grimer R. The incidence of deep prosthetic infections in a specialist orthopaedic hospital: a 15-year prospective survey. Journal of Bone and Joint Surgery-British Volume. 2006;88-B(7):943-8.
3. Mumme T, Reinartz P, Alfer J, Muller-Rath R, Buell U, Wirtz DC. Diagnostic values of positron emission tomography versus triple-phase bone scan in hip arthroplasty loosening. Arch Orthop Trauma Surg. 2005;125(5):322-9.
4. Berquist TH. Musculoskeletal imaging companion: Lippincott Williams & Wilkins; 2006.
5. Trampuz A, Zimmerli W. Prosthetic joint infections: update in diagnosis and treatment. Swiss Med Wkly. 2005;135(17-18):243–251.
6. Lidwell O, Lowbury E, Whyte W, Blowers R, Stanley S, Lowe D. Effect of ultraclean air in operating rooms on deep sepsis in the joint after total hip or knee replacement: a randomised study. British medical journal (Clinical research ed). 1982;285(6334):10-4.
7. Berbari E, Mabry T, Tsaras G, Spangehl M, Erwin PJ, Murad MH, et al. Inflammatory blood laboratory levels as markers of prosthetic joint infection: a systematic review and meta-analysis. The Journal of Bone and Joint Surgery (American). 2010;92(11):2102-9.
8. Zimmerli W. Infection and musculoskeletal conditions: Prosthetic-joint-associated infections. Best practice & research Clinical rheumatology. 2006;20(6):1045-1063.
9. Gomez PF, Morcuende JA. Early attempts at hip arthroplasty: 1700s to 1950s. The Iowa Orthopaedic Journal. 2005;25:25-29.
10. Boston City Hospital. Medical And Surgical Report of the Boston City Hospital. Boston, [Mass.]: Little, Brown, and Co., 1870.
11. Pramanik S, Agarwal AK, Rai KN. Chronology of total hip joint replacement and materials development. Trends in Biomaterials & Artificial Organs. 2005;19(1):15-26.
12. Folz BJ, Silver CE, Rinaldo A, Ferlito A. Themistocles Gluck: biographic remarks emphasising his contributions to laryngectomy. Eur Arch Otorhinolaryngol. 2011;268(8):1175-9.
13. Alvarez KE. Total Hip Replacement. New Materials and Technologies for Healthcare. 2011:179-191.
14. Emery R. Surgery to the shoulder—shoulder replacement. Rheumatology. 1995;34(7):653-62.
15. Foruria AM, Antuña S, Rodríguez-Merchán EC. Shoulder hemiarthroplasty: review of basic concepts. Revista Española de Cirugía Ortopédica y Traumatología. 2008;52(6):392-406.
16. Brand RA, Bigliani LU. Biographical Sketch: Charles S. Neer, II, MD (1917–2011). Clinical Orthopaedics and Related Research®. 2011;469(9):2407-8.
17. Smith-Petersen MN. Arthroplasty of the hip: a new method. The Journal of Bone & Joint Surgery. 1939;21(2):269-88.
18. Emery R, Bankes M. Shoulder replacement: historical perspectives. Shoulder Arthroplasty Berlin: Springer-Verlag. 1999:3-9

doi.org/10.1007/978-3-642-58365-0_1.
19. Torrisi L, Visco AM, & Valenza A. Ion Implantation on Ultra High Molecular Weight Polyethylene (UHMWPE) for Medical Prosthesis, Radiation Effects and Defects in Solids. 2003; 158:(9): 621-633
20. Reingold N, Park J, Rice J. Materials research chronology, 1917-1957. Library of Congress Washington DC science and technology division. 1962
21. Venable CS, Stuck WG. Clinical uses of vitallium. Annals of Surgery. 1943;117(5):772-82.
22. Wang KK, Gustavson LJ, Dumbleton JH. Prosthesis formed from dispersion strengthened cobalt-chromium-molybdenum alloy produced by gas atomization. Google Patents; 1987.
23. Grigoris P, Roberts P, Panousis K, Jin Z. Hip resurfacing arthroplasty: the evolution of contemporary designs. Proceedings of the Institution of Mechanical Engineers, Part H: Journal of Engineering in Medicine. 2006;220(2):95-105.
24. MacAusland WR. The classic: Total replacement of the knee joint by a prosthesis. 1957. Clin Orthop Relat Res. 2011;469(1):5-9.
25. Fischer LP, Planchamp W, Fischer B, Chauvin F. [The first total hip prostheses in man (1890 - 1960)]. Hist Sci Med. 2000;34(1):57-70.
26. Wilson FC. Total Replacement of the Knee in Rheumatoid Arthritis A prospective study of the results of treatment with the Walldius prosthesis. The Journal of Bone and Joint Surgery (American). 1972;54(7):1429-43.
27. Jackson J. Father of the modern hip replacement: Professor Sir John Charnley (1911–82). Journal of Medical Biography. 2011;19(4):151-6.
28. Wroblewski BM. Professor Sir John Charnley (1911–1982). Rheumatology. 2002;41(7):824-5.
29. Burgers PT, van Gijn J. Sir John Charnley en de totale heupartroplastiek. Ned Tijdschr Geneeskd. 2011;155(A3564):1-2.
30. Gomez PF, Morcuende JA. A Historical and Economic Perspective on Sir John Charnley, Chas F. Thackray Limited, and the Early Arthroplasty Industry. The Iowa orthopaedic journal. 2005; 25:30-37
31. Jackson DW. The Century in Orthopedics. A Year by Year Review of the Advance, Events and Accomplishments of the Specialty. Orthopaedics Today. 2000 January issue:73-82.
32. Temmerman OPP, Raijmakers PGHM, Berkhof J, Hoekstra OS, Teule GJJ, Heyligers IC. Accuracy of diagnostic imaging techniques in the diagnosis of aseptic loosening of the femoral component of a hip prosthesis. Journal of Bone & Joint Surgery, British Volume. 2005;87(6):781-5.
33. Adams D, Quigley S. Hip resurfacing: past, present and future. Journal of Orthopaedic Nursing. 2005;9(2):87-94.
34. NCD Risk Factor Collaboration. Trends in adult body-mass index in 200 countries from 1975 to 2014: a pooled analysis of 1698 population-based measurement studies with 19·2 million participants. The Lancet. 2016;387(10026):1377-96.
35. Losina E, Thornhill TS, Rome BN, Wright J, Katz JN. The dramatic increase in total knee replacement utilization rates in the United States cannot be fully explained by growth in population size and the obesity epidemic. J Bone Joint Surg Am. 2012;94(3):201-7.
36. Lindahl H, Malchau H, Oden A, Garellick G. Risk factors for failure after treatment of a periprosthetic fracture of the femur. Bone & Joint Journal. 2006;88(1):26-30.

37. Peel T. Introduction to Prosthetic Joint Infection. Prosthetic Joint Infections: Springer; 2018. p. 1-4.
38. Kurtz SM, Ong KL, Schmier J, Mowat F, Saleh K, Dybvik E, et al. Future clinical and economic impact of revision total hip and knee arthroplasty. The Journal of Bone & Joint Surgery. 2007;89(suppl 3):144-51.
39. Manthey N, Reinhard P, Moog F, Knesewitsch P, Hahn K, Tatsch K. The use of [18F] fluorodeoxyglucose positron emission tomography to differentiate between synovitis, loosening and infection of hip and knee prostheses. Nuclear medicine communications. 2002;23(7):645-653.
40. Marmery H, Ostlere S. Imaging of prosthetic joints. Imaging. 2007;19(3):299-309.
41. Adesanya O, Sprowson A, Masters J, Hutchinson C. Review of the role of dynamic 18F-NaF PET in diagnosing and distinguishing between septic and aseptic loosening in hip prosthesis. J Orthop Surg Res. 2015;10(5):1-5.
42. Sterner T, Pink R, Freudenberg L, Jentzen T, Quitmann H, Bockisch A, et al. The role of [18F] Fluoride positron emission tomography in the early detection of aseptic loosening of total knee arthroplasty. International Journal of Surgery. 2007;5(2):99-104.
43. Palestro CJ. Nuclear medicine and the failed joint replacement: Past, present, and future. World J Radiol. 2014;6(7):446-58.
44. Swan JS, Braunstein EM, Wellman HN, Capello W. Contrast and nuclear arthrography in loosening of the uncemented hip prosthesis. Skeletal radiology. 1991;20(1):15-9.
45. Ostlere S, Soin S. Imaging of prosthetic joints. Imaging. 2003;15(4):270-85.
46. Gemmel F, Van den Wyngaert H, Love C, Welling MM, Gemmel P, Palestro CJ. Prosthetic joint infections: radionuclide state-of-the-art imaging. Eur J Nucl Med Mol Imaging. 2012;39(5):892-909.
47. Strobel K, Stumpe KDM. PET/CT in musculoskeletal infection. Semin Musculoskelet Radiol 2007; 11(4): 353-364.
48. Love C, Marwin SE, Tomas MB, Krauss ES, Tronco GG, Bhargava KK, et al. Diagnosing infection in the failed joint replacement: a comparison of coincidence detection 18F-FDG and 111In-labeled leukocyte/99mTc-sulfur colloid marrow imaging. J Nucl Med. 2004;45(11): 1864-71.
49. Kwee TC, Kwee RM, Alavi A. FDG-PET for diagnosing prosthetic joint infection: systematic review and metaanalysis. European journal of nuclear medicine and molecular imaging. 2008;35(11):2122-32.
50. Temmerman OP, Raijmakers PG, David EF, Pijpers R, Molenaar MA, Hoekstra OS, et al. A comparison of radiographic and scintigraphic techniques to assess aseptic loosening of the acetabular component in a total hip replacement. JBJS. 2004;86(11):2456-63.
51. Oyen WJ, Lemmens JA, Claessens RA, van Horn JR, Slooff TJ, Corstens FH. Nuclear arthrography: combined scintigraphic and radiographic procedure for diagnosis of total hip prosthesis loosening. Journal of nuclear medicine: official publication, Society of Nuclear Medicine. 1996;37(1):62-70.
52. Temmerman OPP, Raijmakers PGHM, Berkhof J, David EFL, Pijpers R, Molenaar MA, et al. Diagnostic accuracy and interobserver variability of plain radiography, subtraction arthrography, nuclear arthrography, and bone scintigraphy in the assessment of aseptic femoral component loosening. Archives of orthopaedic and trauma surgery. 2006;126(5):316-23.

53. Love C, Tomas MB, Marwin SE, Pugliese PV, Palestro CJ. Role of Nuclear Medicine in Diagnosis of the Infected Joint Replacement1. Radiographics. 2001;21(5):1229-38.
54. Sousa R, Massada M, Pereira A, Fontes F, Amorim I, Oliveira A. Diagnostic accuracy of combined 99mTc-sulesomab and 99mTc-nanocolloid bone marrow imaging in detecting prosthetic joint infection. Nucl Med Commun. 2011;32(9):834-9.
55. Love C, Palestro CJ. Radionuclide imaging of infection. Journal of nuclear medicine technology. 2004;32(2):47-57.
56. Pulled N, Market FU. Radiologists Weigh Challenges of Obesity. Radiol Technol 2006 77(3):238M-238M.
57. Pakos EE, Trikalinos TA, Fotopoulos AD, Ioannidis JPA. Prosthesis Infection: Diagnosis after Total Joint Arthroplasty with Antigranulocyte Scintigraphy with 99mTc-labeled Monoclonal Antibodies—A Meta-Analysis1. Radiology. 2007;242(1):101-8.
58. Palestro CJ, Love C, Miller TT. Diagnostic imaging tests and microbial infections. Cell Microbiol. 2007;9(10):2323-33.
59. Tsopelas C. Radiotracers used for the scintigraphic detection of infection and inflammation. The Scientific World Journal. 2015 Feb;1-33. doi:10.1155/2015/676719.
60. Wooley PH, Nasser S, Fitzgerald Jr RH. The immune response to implant materials in humans. Clinical orthopaedics and related research. 1996;326:63-70.
61. Palestro C. Radionuclide imaging of the painful joint replacement: past, present and future. Brazilian Archives of Biology and Technology. 2002;45(SPE):9-14.
62. Dollé F, Roeda D, Kuhnast B, Lasne MC, Tressaud A, Haufe G. Fluorine-18 chemistry for molecular imaging with Positron Emission Tomography: Elsevier, Amsterdam; 2008.
63. Coenen HH. Fluorine-18 labeling methods: Features and possibilities of basic reactions. PET Chemistry. 2007:15-50.
64. Anbar M, Guttmann S, Lewitus Z. Effect of monofluorosulphonate, difluorophosphate and fluoroborate ions on the iodine uptake of the thyroid gland. Nature. 1959;183(4674):1517-8.
65. Blau M, Nagler W, Bender MA. Fluorine-18: a new isotope for bone scanning. J Nucl Med. 1962 Jul;3:332-4.
66. Blau M, Ganatra R, Bender MA, F-fluoride for bone imaging. Semin Nucl Med. 1972 Jan;2(1):31-7.
67. Li J, Miller MA, Hutchins GD, Burr DB. Imaging bone microdamage in vivo with positron emission tomography. Bone. 2005;37(6):819-24.
68. Czernin J, Satyamurthy N, Schiepers C. Molecular mechanisms of bone 18F-NaF deposition. J Nucl Med. 2010;51(12):1826-9.
69. Schnockel U, Reuter S, Stegger L, Schlatter E, Schafers KP, Hermann S, et al. Dynamic 18F-fluoride small animal PET to noninvasively assess renal function in rats. Eur J Nucl Med Mol Imaging. 2008;35(12):2267-74.
70. Even-Sapir E. Imaging of malignant bone involvement by morphologic, scintigraphic, and hybrid modalities. J Nucl Med. 2005;46(8):1356-1367
71. Stumpe KDM, Nötzli HP, Zanetti M, Kamel EM, Hany TF, Görres GW, von Schulthess GK, Hodler J. FDG PET for Differentiation of Infection and Aseptic Loosening in Total Hip Replacements: Comparison with Conventional

Radiography and Three-Phase Bone Scintigraphy. Radiology. 2004;231(2):333-41.
72. Kumar R, Kumar R, Malhotra R, Sharma P, Bal C, Malhotra A. Role of F18-Fluoride PET-CT and F18-FDG PET-CT in differentiating septic from aseptic loosening in patients with painful hip prosthesis. Journal of Nuclear Medicine 2009, 50 (supplement 2): 89-89.
73. Mawlawi O, Townsend DW. Multimodality imaging: an update on PET/CT technology. European journal of nuclear medicine and molecular imaging. 2009;36(1):15-29.
74. Goerres GW, Ziegler SI, Burger C, Berthold T, von Schulthess GK, Buck A. Artifacts at PET and PET/CT Caused by Metallic Hip Prosthetic Material. Radiology. 2003;226(2):577-84.
75. Heiba SI, Luo JQ, Sadek S, Macalental E, Cacavio A, Rosen G, et al. Attenuation-correction induced artifact in F-18 FDG PET imaging following total knee replacement. Clinical Positron Imaging. 2000;3(6):237-9.
76. Li Y, Schiepers C, Lake R, Dadparvar S, Berenji GR. Clinical utility of (18)F-fluoride PET/CT in benign and malignant bone diseases. Bone. 2012;50(1):128-39.
77. Lim R, Fahey FH, Drubach LA, Connolly LP, Treves ST. Early experience with fluorine-18 sodium fluoride bone PET in young patients with back pain. J Pediatr Orthop. 2007;27(3):277-82
78. Adesanya O, Foguet P, Hutchinson C. The Promising Role of Dynamic 18F-NaF PET-CT in Diagnosing Symptomatic Joint Prosthesis. Integrative Biomedical Sciences. 2015;1(2):64-70.
79. Dixon T, Shaw M, Ebrahim S, Dieppe P. Trends in hip and knee joint replacement: socioeconomic inequalities and projections of need. Annals of the rheumatic diseases. 2004;63(7):825-30.
80. Mahomed NN, Barrett JA, Katz JN, Phillips CB, Losina E, Lew RA, et al. Rates and outcomes of primary and revision total hip replacement in the United States Medicare population. J Bone Joint Surg Am. 2003;85(1):27-32.
81. Brammen L, Palestro C, Sinzinger H. Radionuclide imaging: Past, present and future outlook in the diagnosis of infected prosthetic joints. Hellenic journal of nuclear medicine. 2015;18(3):95-102.
82. Sofka CM. Optimizing techniques for musculoskeletal imaging of the postoperative patient. Radiologic Clinics of North America. 2006;44(3):323.
83. Seynaeve PC, Broos JI. [The history of tomography]. J Belge Radiol. 1995;78(5):284-8.
84. Maizlin ZV, Vos PM. Do we really need to thank the Beatles for the financing of the development of the computed tomography scanner? J Comput Assist Tomogr. 2012;36(2):161-4.
85. Beckmann EC. CT scanning the early days. Br J Radiol. 2006;79(937):5-8.
86. Cahir J, Toms A, Marshall T, Wimhurst J, Nolan J. CT and MRI of hip arthroplasty. Clinical radiology. 2007;62(12):1163-71.
87. Hayter CL, Potter HG, Su EP. Imaging of metal-on-metal hip resurfacing. Orthopedic Clinics of North America. 2011;42(2):195-205.
88. Dai K-R, Yan M-N, Zhu Z-A, Sun Y-H. Computer-aided custom-made hemipelvic prosthesis used in extensive pelvic lesions. The Journal of arthroplasty. 2007;22(7):981-6.

89. Hafez M, Chelule K, Seedhom B, Sherman K. Computer-assisted total knee arthroplasty using patient-specific templating. Clinical orthopaedics and related research. 2006;444:184-92.
90. Zhang Z, Liao W, Hou C, Wu P, Kang Y, Zhao X. [Selectively upward placement of acetabular implants in patients with anatomically abnormal acetabulum during total hip arthroplasty]. Zhongguo Xiu Fu Chong Jian Wai Ke Za Zhi. 2014;28(5):566-70.
91. Renkawitz T, Haimerl M, Dohmen L, Gneiting S, Wegner M, Ehret N, et al. Minimally invasive computer-navigated total hip arthroplasty, following the concept of femur first and combined anteversion: design of a blinded randomized controlled trial. BMC Musculoskelet Disord. 2011;12:192-7.
92. Parratte S, Argenson JN, Flecher X, Aubaniac JM. [Computer-assisted surgery for acetabular cup positioning in total hip arthroplasty: comparative prospective randomized study]. Rev Chir Orthop Reparatrice Appar Mot. 2007;93(3):238-46.
93. Hsu AR, Davis WH, Cohen BE, Jones CP, Ellington JK, Anderson RB. Radiographic outcomes of preoperative CT scan–derived patient-specific total ankle arthroplasty. Foot & ankle international. 2015;36(10):1163-9.
94. Siebert W, Mai S, Kober R, Heeckt PF. Technique and first clinical results of robot-assisted total knee replacement. Knee. 2002;9(3):173-80.
95. Barrack RL, Ruh EL, Williams BM, Ford AD, Foreman K, Nunley RM. Patient specific cutting blocks are currently of no proven value. J Bone Joint Surg Br. 2012;94(11 Suppl A):95-9.
96. Ensini A, Timoncini A, Cenni F, Belvedere C, Fusai F, Leardini A, et al. Intra- and post-operative accuracy assessments of two different patient-specific instrumentation systems for total knee replacement. Knee Surg Sports Traumatol Arthrosc. 2014;22(3):621-9.
97. Wines AP, McNicol D. Computed Tomography Measurement of the Accuracy of Component Version in Total Hip Arthroplasty. The Journal of Arthroplasty. 2006;21(5):696-701.
98. National Joint Registry. www.njrcentre.org.uk. [Last updated 14 Jan 2021. Last accessed 16th January 2021]. Available from: http://www.njrcentre.org.uk/njrcentre/Healthcareproviders/Accessingthedata/StatsOnline/NJRStatsOnline
99. Day JS, Lau E, Ong KL, Williams GR, Ramsey ML, Kurtz SM. Prevalence and projections of total shoulder and elbow arthroplasty in the United States to 2015. Journal of shoulder and elbow surgery. 2010;19(8):1115-20.
100. Tomas X, Bori G, Garcia S, Garcia-Diez AI, Pomes J, Soriano A, et al. Accuracy of CT-guided joint aspiration in patients with suspected infection status post-total hip arthroplasty. Skeletal Radiol. 2011;40(1):57-64.
101. Mizu-uchi H, Matsuda S, Miura H, Okazaki K, Akasaki Y, Iwamoto Y. The evaluation of post-operative alignment in total knee replacement using a CT-based navigation system. J Bone Joint Surg Br. 2008;90(8):1025-31.
102. Parvizi J, Della Valle CJ. AAOS Clinical Practice Guideline: diagnosis and treatment of periprosthetic joint infections of the hip and knee. Journal of the American Academy of Orthopaedic Surgeons. 2010;18(12):771-2.
103. Lentino JR. Prosthetic joint infections: bane of orthopedists, challenge for infectious disease specialists. Clinical Infectious Diseases. 2003;36(9):1157-61.
104. Albanese CV, Faletti C. Imaging of prosthetic joints: Springer; 2016.

105. Beall DP, Martin HD, Ly JQ, Campbell SE, Anderson S, Tannast M. Postoperative imaging of the hip. The Radiologic clinics of North America. 2006;44(3): 343-365.
106. Roth TD, Maertz NA, Parr JA, Buckwalter KA, Choplin RH. CT of the hip prosthesis: appearance of components, fixation, and complications. Radiographics. 2012;32(4):1089-107.
107. DeSmet A, Kramer D, Martel W. The metal-cement interface in total hip prostheses. American Journal of Roentgenology. 1977;129(2):279-82.
108. McGee MA, Howie DW, Neale SD, Haynes DR, Pearcy MJ. The role of polyethylene wear in joint replacement failure. Proceedings of the Institution of Mechanical Engineers, Part H: Journal of Engineering in Medicine. 1997;211(1):65-72.
109. Hozack W, Parvizi J, Bender B. Surgical Treatment of Hip Arthritis: Reconstruction, Replacement, and Revision E-Book: Expert Consult-Online and Print: Elsevier Health Sciences; 2009.
110. Singh C, Kaplan A, Pambuccian SE. Necrotic granulomatous pseudotumor following metal-on-metal hip arthroplasty: a potential mimic of sarcoma on fine needle aspiration cytology. Diagn Cytopathol. 2012;40(Suppl 2):E104-8.
111. Frick MA, Collins MS, Adkins MC. Postoperative imaging of the knee. Radiologic Clinics of North America. 2006;44(3):367-89.
112. Miller TT. Imaging of knee arthroplasty. European journal of radiology. 2005;54(2):164-77.
113. Long M, Rack H. Titanium alloys in total joint replacement—a materials science perspective. Biomaterials. 1998;19(18):1621-39.
114. Pakos EE, Ntzani EE, Trikalinos TA. Patellar resurfacing in total knee arthroplasty; a meta-analysis. The Journal of Bone & Joint Surgery. 2005;87(7):1438-45.
115. Rodríguez-Merchán EC, Liddle AD. Microbiological concepts of the infected total knee arthroplasty. InThe Infected Total Knee Arthroplasty 2018 (pp. 11-17). Springer, Cham.
116. Bauer TW, Schils J. The pathology of total joint arthroplasty. Skeletal radiology. 1999;28(9):483-97.
117. Monti C, Molinari M, Bianco T, Sudanese A, Busanelli L, Toni A. Indications and limits of CT scan in prosthetic loosening. Chir Organi Mov. 1994;79(4):269-77.
118. Kiernan S, Hermann KL, Wagner P, Ryd L, Flivik G. The importance of adequate stem anteversion for rotational stability in cemented total hip replacement: a radiostereometric study with ten-year follow-up. Bone Joint J. 2013;95-b(1):23-30.
119. Adolphson P. Endosteal femoral bone loss after hip rearthroplasty. A controlled computed tomography study of 12 patients. Arch Orthop Trauma Surg. 1995;114(2):103-5.
120. Peterson JJ. Postoperative infection. Radiol Clin North Am. 2006;44(3):439-50.
121. Thornton-Bott P, Fung S, Walter W, Zicat B. Computerised tomography reports of osteolysis in ceramic-on-ceramic total hip arthroplasty; true lysis, stress-shield or cysts? Bone Joint J. 2016;98(Supp 10):124-124.
122. Bozic KJ, Kurtz SM, Lau E, Ong K, Chiu V, Vail TP, et al. The Epidemiology of Revision Total Knee Arthroplasty in the United States. Clinical Orthopaedics and Related Research®. 2010;468(1):45-51.

123. White LM, Buckwalter KA. Technical considerations: CT and MR imaging in the postoperative orthopedic patient. In Seminars in musculoskeletal radiology 2002;6(1):pp 5-18. Copyright© 2002 by Thieme Medical Publishers, Inc., 333 Seventh Avenue, New York, NY 10001, USA.
124. Xin CH, Chang-sheng ZH, Jun ZH, Hai-feng GU, SONG L, Ling ZH. Preliminary Experience of Joint Replacement-Knee by Spiral CT. Chinese Medical Equipment Journal. 2011(6):28-28.
125. Weber M-A, Egermann M, Thierjung H, Kloth J, editors. Modern radiological postoperative diagnostics of the hip joint in children and adults. Modern Radiological Postoperative Diagnostics. 2015; 187: 525–542.
126. Sudanese A, Toni A, Busanelli L, Furno A, Montina PP, Marraro MD, et al. Diagnostic protocol in prosthetic loosening. Chir Organi Mov. 1994;79(4):257-67.
127. Kaisidis A, Megas P, Apostolopoulos D, Spiridonidis T, Koumoundourou D, Zouboulis P, et al. [Diagnosis of septic loosening of hip prosthesis with LeukoScan. SPECT scan with 99mTc-labeled monoclonal antibodies]. Orthopade. 2005;34(5):462-9.
128. Adesanya O, Hutchinson C. Designing a New Molecular Probe: The Potential Role for Tilmanocept (Lymphoseek®) in the Assessment of Patients with Painful Hip and Knee Joint Prostheses. The open orthopaedics journal. 2017;11:212–224.
129. Choe H, Inaba Y, Kobayashi N, Ike H, Aoki C, Shizukuishi K, et al. Use of ^{18}F-fluoride PET to determine the appropriate tissue sampling region for improved sensitivity of tissue examinations in cases of suspected periprosthetic infection after total hip arthroplasty. Acta Orthop. 2011;82(4):427-32.
130. Siebelt M, Agricola R, Weinans H, Kim YJ. The role of imaging in early hip OA. Osteoarthritis and Cartilage. 2014;22(10):1470-80.
131. Kwon H, Kim KS, Chun YM, Wu HG, Carlson JN, Park JM, et al. Evaluation of a commercial orthopedic metal artifact reduction tool in radiation therapy of head and neck patients. Br J Radiol 2015;88(1052):20140536:
132. Huang JY, Kerns JR, Nute JL, Liu X, Balter PA, Stingo FC, et al. An evaluation of three commercially available metal artifact reduction methods for CT imaging. Phys Med Biol. 2015;60(3):1047-67.
133. Pessis E, Campagna R, Sverzut J-M, Bach F, Rodallec M, Guerini H, et al. Virtual monochromatic spectral imaging with fast kilovoltage switching: reduction of metal artifacts at CT. Radiographics. 2013;33(2):573-83.
134. Watzke O, Kalender WA. A pragmatic approach to metal artifact reduction in CT: merging of metal artifact reduced images. Eur Radiol. 2004;14(5):849-56
135. Cooper HJ, Della Valle CJ. Advances in the diagnosis of periprosthetic joint infection. Expert opinion on medical diagnostics. 2013;7(3):257-63.
136. Lavernia CJ, Drakeford MK, Tsao AK, Gittelsohn A, Krackow KA, Hungerford DS. Revision and Primary Hip and Knee Arthroplasty: A Cost Analysis. Clinical orthopaedics and related research. 1995;311:136-41.
137. Atkins BL, Athanasou N, Deeks JJ, Crook DW, Simpson H, Peto TE, et al. Prospective evaluation of criteria for microbiological diagnosis of prosthetic-joint infection at revision arthroplasty. Journal of clinical microbiology. 1998;36(10):2932-9.
138. Osmon DR, Berbari EF, Berendt AR, Lew D, Zimmerli W, Steckelberg JM, Rao N, Hanssen A, Wilson WR. Diagnosis and management of prosthetic joint

infection: clinical practice guidelines by the Infectious Diseases Society of America. Clinical Infectious Diseases, 2013;56(1):1–25.
139. Bancroft LW. Postoperative musculoskeletal imaging: Radiologic Cllinics of North America 2006; 44(3): page 323-472.
140. Barberán J, Aguilar L, Carroquino G, Giménez M-J, Sánchez B, Martínez D, et al. Conservative treatment of staphylococcal prosthetic joint infections in elderly patients. The American journal of medicine. 2006;119(11):993. e7-. e10.
141. Esposito S, Leone S. Prosthetic joint infections: microbiology, diagnosis, management and prevention. International journal of antimicrobial agents. 2008;32(4):287-93.
142. Lewis SS, Dicks KV, Chen LF, Bolognesi MP, Anderson DJ, Sexton DJ, et al. Delay in diagnosis of invasive surgical site infections following knee arthroplasty versus hip arthroplasty. Clinical Infectious Diseases. 2015;60(7):990-6.
143. Lonner JH, Siliski JM, Scott RD. Prodromes of failure in total knee arthroplasty. The Journal of arthroplasty. 1999;14(4):488-92.
144. Mikulin T, Hardcastle J. Gastric cancer—delay in diagnosis and its causes. European Journal of Cancer and Clinical Oncology. 1987;23(11):1683-90.
145. Geraghty O, Korompoki E, Filippidis FT, Rudd A, Veltkamp R. Cardiac diagnostic work-up for atrial fibrillation after transient ischaemic attacks in England and Wales: results from a cross-sectional survey. BMJ open. 2016;6(11):e012714.
146. Lidwell O, Lowbury E, Whyte W, Blowers R, Stanley S, Lowe D. Infection and sepsis after operations for total hip or knee-joint replacement: influence of ultraclean air, prophylactic antibiotics and other factors. Epidemiology & Infection. 1984;93(3):505-29.
147. Arndt V, Stürmer T, Stegmaier C, Ziegler H, Dhom G, Brenner H. Patient delay and stage of diagnosis among breast cancer patients in Germany–a population based study. British journal of cancer. 2002;86(7):1034–1040.
148. Santaguida PL, Hawker GA, Hudak PL, Glazier R, Mahomed NN, Kreder HJ, et al. Patient characteristics affecting the prognosis of total hip and knee joint arthroplasty: a systematic review. Canadian Journal of Surgery. 2008;51(6):428–436.
149. Werner Z. Prosthetic-joint-associated infections. Best Practice & Research Clinical Rheumatology. 2006;20(6):1045–63.
150. Moran E, Byren I, Atkins BL. The diagnosis and management of prosthetic joint infections. Journal of antimicrobial chemotherapy. 2010;65(suppl_3):iii45-54.
151. Hyman JL, Salvati EA, Laurencin CT, Rogers DE, Maynard M, Brause BD. The arthroscopic drainage, irrigation, and debridement of late, acute total hip arthroplasty infections: average 6-year follow-up. The Journal of arthroplasty. 1999;14(8):903-10.
152. Goodman LR, Lipchik RJ. Diagnosis of acute pulmonary embolism: time for a new approach. Radiology. 1996;199(1):25-7.
153. Attarian DE, Vail TP. Medicolegal aspects of hip and knee arthroplasty. Clinical orthopaedics and related research. 2005;433:72-6.
154. Thienpont E, Bellemans J, Delport H, Van Overschelde P, Stuyts B, Brabants K, et al. Patient-specific instruments: industry's innovation with a surgeon's interest. Knee Surgery, Sports Traumatology, Arthroscopy. 2013;21(10):2227-33.

155. Leung AN, Bull TM, Jaeschke R, Lockwood CJ, Boiselle PM, Hurwitz LM, et al. American Thoracic Society Documents: an official American Thoracic Society/Society of Thoracic Radiology clinical practice guideline—evaluation of suspected pulmonary embolism in pregnancy. Radiology. 2012;262(2):635-46.
156. Ruggeri J, Mariani L-L, Aix S, Bonnet A-M, Cormier F, Corvol J-C, et al. “De-novo” consultation: Evaluation of an outpatient's clinic dedicated to early diagnosis of parkinsonian syndromes. Revue Neurologique. 2017;173(1):55-61.
157. Fischer JE, Bachmann LM, Jaeschke R. A readers' guide to the interpretation of diagnostic test properties: clinical example of sepsis. Intensive Care Medicine. 2003;29(7):1043-51.
158. Purohit MR, Sharma M, Rosales-Klintz S, Lundborg CS. ‘Multiple-test’approach to the laboratory diagnosis of tuberculosis-perception of medical doctors from Ujjain, India. BMC infectious diseases. 2015;15(1):1-9.
159. Fleischer AE, Didyk AA, Woods JB, Burns SE, Wrobel JS, Armstrong DG. Combined clinical and laboratory testing improves diagnostic accuracy for osteomyelitis in the diabetic foot. The Journal of Foot and Ankle Surgery. 2009;48(1):39-46.
160. Mazurek A, Dziuk M, Witkowska-Patena E, Piszczek S, Gizewska A. The Utility of Hybrid SPECT/CT Lung Perfusion Scintigraphy in Pulmonary Embolism Diagnosis. Respiration. 2015;90(5):393-401
161. Ponzio DY, Lonner JH. Preoperative Mapping in Unicompartmental Knee Arthroplasty Using Computed Tomography Scans Is Associated with Radiation Exposure and Carries High Cost. J Arthroplasty. 2015;30(6):964-7.
162. Matthews PC, Berendt AR, McNally MA, Byren I. Diagnosis and management of prosthetic joint infection. BMJ (Clinical research ed.) 2009;338:b1773.
163. Zimmerli W. Bone and joint infections: from microbiology to diagnostics and treatment: Wiley Blackwell; 2014.p.113-46. ISBN 1118581709, 9781118581704
164. Vandenbroucke JP. Prospective or retrospective: what's in a name?. BMJ: British Medical Journal. 1991;302(6771):249.
165. Strobel K, Steurer-Dober I, Huellner MW, Veit-Haibach P, Allgayer B. [Importance of SPECT/CT for knee and hip joint prostheses]. Radiologe. 2012;52(7):629-35.
166. Cook GJR, Fogelman I.. PET Imaging of the Skeleton: Springer London; 2013. 317-35.
167. Kawaguchi M, Tateishi U, Shizukuishi K, Suzuki A, Inoue T. 18F-fluoride uptake in bone metastasis: morphologic and metabolic analysis on integrated PET/CT. Annals of Nuclear Medicine. 2010;24(4):241-7
168. Creutzig H. [A comparison of osteotropic radiopharmaceuticals. II. Plasma clearance of 18F and 99mTc-EHDP (author's transl)]. RoFo. 1975;123(4):313-8.
169. Kobayashi N, Inaba Y, Choe H, Ike H, Fujimaki H, Tezuka T, et al. Use of F-18 Fluoride PET to Differentiate Septic From Aseptic Loosening in Total Hip Arthroplasty Patients. Clinical Nuclear Medicine. 2011;36(11):E156-E61.
170. Sterner T, Pink R, Freudenberg L, Jentzen T, Quitmann H, Bockisch A, Löer F. The role of [18F]fluoride positron emission tomography in the early detection of aseptic loosening of total knee arthroplasty. Int J Surg. 2007 ;5(2):99-104.

171. Creutzig H. Bone imaging after total replacement arthroplasty of the hip joint. A follow-up with different radiopharmaceuticals. Eur J Nucl Med. 1976;1(3):177-80.
172. Levy PY, Fenollar F. The role of molecular diagnostics in implant-associated bone and joint infection. Clin Microbiol Infect. 2012;18(12):1168-75.
173. Bauer TW, Parvizi J, Kobayashi N, Krebs V. Diagnosis of periprosthetic infection. The Journal of Bone & Joint Surgery. 2006;88(4):869-82.
174. Zhuang H, Duarte PS, Pourdehnad M, Maes A, Acker FV, Shnier D, et al. The Promising Role of 18F-FDG PET in Detecting Infected Lower Limb Prosthesis Implants. J Nucl Med 2001;42(1):44–48
175. Park S-J, Ionascu D, Killoran J, Mamede M, Gerbaudo VH, Chin L, et al. Evaluation of the combined effects of target size, respiratory motion and background activity on 3D and 4D PET/CT images. Phys Med Biol. 2008 7;53(13):3661-79.
176. Wong KK, Piert M. Dynamic Bone Imaging with 99mTc-Labeled Diphosphonates and 18F-NaF: Mechanisms and Applications. Journal of Nuclear Medicine 2013, 54 (4) 590-599.
177. Tande AJ, Patel R. Prosthetic joint infection. Clinical microbiology reviews. 2014;27(2):302-45.
178. Love C, Marwin SE, Palestro CJ. Nuclear medicine and the infected joint replacement. Semin Nucl Med. 2009;39(1):66-78
179. Ryan P, Fogelman I, editors. Bone scintigraphy in metabolic bone disease. Seminars in nuclear medicine; 1997: Elsevier.
180. Segall, G., D. Delbeke, M. Stabin, E. Even-Sapir, J. Fair, R. Sajdak and G. Smith. SNM Practice Guideline for Sodium 18F-Fluoride PET/CT Bone Scans 1.0. The Journal of Nuclear Medicine 2010, 51(11):1813-1820.
181. Cyteval C, Bourdon A. Imaging orthopedic implant infections. Diagn Interv Imaging. 2012;93(6):547-57.
182. Palestro CJ, Love C, Schneider R. The evolution of nuclear medicine and the musculoskeletal system. Radiologic Clinics of North America. 2009;47(3):505-32.
183. Athwal KK, Hunt NC, Davies AJ, Deehan DJ, Amis AA. Clinical biomechanics of instability related to total knee arthroplasty. Clin Biomech (Bristol, Avon). 2014;29(2):119-28.
184. Love C, Tomas MB, Marwin SE, Pugliese PV, Palestro CJ. Role of Nuclear Medicine in Diagnosis of the Infected Joint Replacement. Radiographics 2001;21(5):1229-38.
185. Iyengar KP, Vinjamuri S. Role of 99mTc Sulesomab in the diagnosis of prosthetic joint infections. Nuclear medicine communications. 2005;26(6):489-96.
186. Smith BT. Introduction to Diagnostic and Therapeutic Monoclonal Antibodies Univ New Mex Heal Sci Cent 2012;17(0039):1–34.
187. European Medicines Agency. LeukoScan: Withdrawal of the marketing authorisation in the European Union 2018 . [Last accessed 15th February 2021] Available from:
https://www.ema.europa.eu/en/medicines/human/EPAR/leukoscan.
188. Glaudemans AW, Signore A. FDG-PET/CT in infections: the imaging method of choice? European journal of nuclear medicine and molecular imaging. 2010;37(10):1986-91.

189. Bauer P, Brannath W. The advantages and disadvantages of adaptive designs for clinical trials. Drug discovery today. 2004;9(8):351-7.
190. Yoon HJ, Jeong YJ, Son HJ, Kang D-Y, Hyun K-Y, Lee M-K. Optimization of the spatial resolution for the GE discovery PET/CT 710 by using NEMA NU 2-2007 standards. Journal of the Korean Physical Society. 2015;66(2):287-94.
191. Boas FE, Fleischmann D. CT artifacts: causes and reduction techniques. Imaging in Medicine. 2012;4(2):229-40.
192. Boas FE. Iterative reduction of artifacts in computed tomography images using forward projection and an edge-preserving blur filter. Google Patents; 2012.
193. Razifar P, Lubberink M, Schneider H, Långström B, Bengtsson E, Bergström M. Non-isotropic noise correlation in PET data reconstructed by FBP but not by OSEM demonstrated using auto-correlation function. BMC Medical Imaging. 2005;5(1):1-18.
194. Oliveira, E.F.; Dantas, C.C.; Vasconcelos, D.A.A.; Cadiz, F. Comparison Among Tomographic Reconstruction Algorithms With a Limited Data. In Proceedings of the International Nuclear Atlantic Conference-INAC 2011, Belo Horizonte, Brazil, 24–28 October 2011.
195. Gianni Schena. Mathworks®. Direct Fourier Reconstruction of a Tomographic Slice Experiments of reconstruction using Fourier Slice Theorem (rather than filtered back projection). Matlabcentral; 2018. [Last accessed 15th February 2021] . Available from: https://www.mathworks.com/matlabcentral/fileexchange/60257-direct-fourier-reconstruction-of-a-tomographic-slice.

196. Valeri G, Mazza FA, Maggi S, Aramini D, La Riccia L, Mazzoni G, et al. Open source software in a practical approach for post processing of radiologic images. La radiologia medica. 2015;120(3):309-23

197. Ratib O, Rosset A. Open-source software in medical imaging: development of OsiriX. International Journal of Computer Assisted Radiology and Surgery. 2006;1(4):187-96.
198. Yusoff S, Zakaria A. Determination of the optimum filter for qualitative and quantitative 99mTc myocardial SPECT imaging. Iranian Journal of Radiation Research. 2009;6(4):173-82.
199. Barrett JF, Keat N. Artifacts in CT: recognition and avoidance. Radiographics. 2004;24(6):1679-91.
200. Tohtz SW, Müller M, Morawietz L, Winkler T, Perka C. Validity of frozen sections for analysis of periprosthetic loosening membranes. Clinical Orthopaedics and Related Research®. 2010;468(3):762-8.
201. Pickhardt PJ, Shapiro B. Three-phase skeletal scintigraphy in gouty arthritis: an example of potential diagnostic pitfalls in radiopharmaceutical imaging of the extremities for infection. Clinical nuclear medicine. 1996;21(1):33-9.
202. Do TD, Sutter R, Skornitzke S, Weber MA. CT and MRI techniques for imaging around orthopedic hardware. InRöFo-Fortschritte auf dem Gebiet der Röntgenstrahlen und der bildgebenden Verfahren 2018;39(1);31-41 © Georg Thieme Verlag KG.
203. McDonald AM, Knight RC, Campbell MK, Entwistle VA, Grant AM, Cook JA, et al. What influences recruitment to randomised controlled trials? A review of trials funded by two UK funding agencies. Trials. 2006;7(1):9.

204. Hernán MA, Hernández-Díaz S, Robins JM. A structural approach to selection bias. Epidemiology. 2004:615-25.
205. Maida S, Dalla Costa G, Rodegher M, Falautano M, Comi G, Martinelli V. Overcoming recruitment challenges in patients with multiple sclerosis: Results from an Italian survey. Clin Trials. 2014;11(6):667-72..
206. Donovan JL, Peters TJ, Noble S, Powell P, Gillatt D, Oliver SE, et al. Who can best recruit to randomized trials?: Randomized trial comparing surgeons and nurses recruiting patients to a trial of treatments for localized prostate cancer (the ProtecT study). Journal of clinical epidemiology. 2003;56(7):605-9.
207. Featherstone K, Donovan JLJSs, medicine. “Why don’t they just tell me straight, why allocate it?” The struggle to make sense of participating in a randomised controlled trial. 2002;55(5):709-19.
208. Cohn E, Larson E. Improving participant comprehension in the informed consent process. Journal of nursing scholarship. 2007 Sep;39(3):273-80.
209. Seltzer SE, Sullivan DC, Hillman BJ, Staab EV. Factors Affecting Patient Enrollment in Radiology Clinical Trials: A Case Study of the American College of Radiology Imaging Network. Academic Radiology. 2002;9(7):862-9.
210. Vellinga A, Cormican M, Hanahoe B, Bennett K, Murphy AW. Opt-out as an acceptable method of obtaining consent in medical research: a short report. BMC medical research methodology. 2011;11(1):40.
211. Junghans C, Feder G, Hemingway H, Timmis A, Jones M. Recruiting patients to medical research: double blind randomised trial of “opt-in” versus “opt-out” strategies. BMJ. 2005;331(7522):940.
212. Hunt KJ, Shlomo N, Addington-Hall J. Participant recruitment in sensitive surveys: a comparative trial of ‘opt in’versus ‘opt out’approaches. BMC Medical Research Methodology. 2013;13(1):3.
213. Blanton S, Morris DM, Prettyman MG, McCulloch K, Redmond S, Light KE, et al. Lessons learned in participant recruitment and retention: the EXCITE trial. Physical therapy. 2006;86(11):1520-33.
214. Nyman SR, Victor CR. Older people's recruitment, sustained participation, and adherence to falls prevention interventions in institutional settings: a supplement to the Cochrane systematic review. Age and ageing. 2011;40(4):430-6.
215. Gotthardt M, Bleeker-Rovers CP, Boerman OC, Oyen WJ. Imaging of inflammation by PET, conventional scintigraphy, and other imaging techniques. Journal of nuclear medicine technology. 2013;41(3):157-69.
216. Munn Z, Jordan Z. The effectiveness of interventions to reduce anxiety, claustrophobia, sedation and non-completion rates of patients undergoing high technology medical imaging. JBI Libr Syst Rev. 2012;10(19):1122-85.
217. Vogel WV, Oyen WJ, Barentsz JO, Kaanders JH, Corstens FH. PET/CT: panacea, redundancy, or something in between? The Journal of Nuclear Medicine. 2004;45(1):15S-24S.
218. Steinert HC, von Schulthess GK. Initial clinical experience using a new integrated in-line PET/CT system. The British Journal of Radiology. 2002 Nov;75(suppl_9):S36-8.
219. Cohade C, Osman M, Marshall LT, Wahl RL. PET-CT: accuracy of PET and CT spatial registration of lung lesions. European journal of nuclear medicine and molecular imaging. 2003;30(5):721-6.

220. Even-Sapir E, Mishani E, Flusser G, Metser U. 18F-Fluoride positron emission tomography and positron emission tomography/computed tomography. Seminars in nuclear medicine 2007; 37(6):462-469..WB Saunders.
221. Silveira MB, Soares MA, Valente ES, Waquil SS, Ferreira AV, Santos RGd, et al. Synthesis, quality control and dosimetry of the radiopharmaceutical 18F-sodium fluoride produced at the Center for Development of Nuclear Technology-CDTN. Brazilian Journal of Pharmaceutical Sciences. 2010;46(3):563-9.
222. Competition and Markets Authority. A report on the completed acquisition by Alliance Medical Group Limited of the assets of IBA Molecular UK Limited used to manufacture 18F-Fluorodeoxyglucose 2014. Published 15 August 2014 [Last accessed 15th February 2021]. Available from https://www.google.co.uk/url?sa=t&rct=j&q=&esrc=s&source=web&cd=1&cad=rja&uact=8&ved=0ahUKEwik6dTc0_jaAhULKMAKHfOEAWgQFggpMAA&url=https%3A%2F%2Fassets.publishing.service.gov.uk%2Fmedia%2F53ee079140f0b62d98000001%2FFinal_report.pdf&usg=AOvVaw0DQ780uJKL1vddaZiBxKyZ.
223. UK PET Core Lab. Quality Control for PET Clinical Trials 2018. [Last accessed 15th February 2021] . Available from: http://www.ncri-pet.org.uk/radiotracer_supply.php.
224. Scarsbrook AF, Barrington SF. PET-CT in the UK: current status and future directions. Clinical radiology. 2016;71(7):673-90.
225. Oglevee C, Pianykh O. Losing images in digital radiology: more than you think. Journal of Digital Imaging. 2015;28(3):264-71.
226. Dickson JC, Tossici-Bolt L, Sera T, de Nijs R, Booij J, Bagnara MC, et al. Proposal for the standardisation of multi-centre trials in nuclear medicine imaging: prerequisites for a European 123 I-FP-CIT SPECT database. European journal of nuclear medicine and molecular imaging. 2012;39(1):188-97.
227. Boellaard R, Oyen WJ, Hoekstra CJ, Hoekstra OS, Visser EP, Willemsen AT, et al. The Netherlands protocol for standardisation and quantification of FDG whole body PET studies in multi-centre trials. European journal of nuclear medicine and molecular imaging. 2008;35(12):2320-33.
228. Mendelson DS, Erickson BJ, Choy G. Image sharing: evolving solutions in the age of interoperability. Journal of the American College of Radiology. 2014;11(12):1260-9.
229. Makris NE, Huisman MC, Kinahan PE, Lammertsma AA, Boellaard R. Evaluation of strategies towards harmonization of FDG PET/CT studies in multicentre trials: comparison of scanner validation phantoms and data analysis procedures. European journal of nuclear medicine and molecular imaging. 2013;40(10):1507-15.
230. Barrington SF, Qian W, Somer EJ, Franceschetto A, Bagni B, Brun E, et al. Concordance between four European centres of PET reporting criteria designed for use in multicentre trials in Hodgkin lymphoma. European journal of nuclear medicine and molecular imaging. 2010;37(10):1824-33.
231. Pocock SJ. Allocation of patients to treatment in clinical trials. Biometrics. 1979:183-97.
232. Peto R, Pike M, Armitage P, Breslow NE, Cox DR, Howard SV, Mantel N, McPherson K, Peto J, Smith PG. Design and analysis of randomized clinical trials requiring prolonged observation of each patient. II. analysis and examples. British journal of cancer. 1977;35(1):1-39.

233. Chalmers TC. Randomization of the first patient. Med Clin North Am. 1975;59(4):1035-8.
234. Senn S. Some controversies in planning and analysing multi-centre trials. Statistics in medicine. 1998;17(15-16):1753-65.
235. Hedman C, Andersen AR, Olesen J. Multi-centre versus single-centre trials in migraine. Neuroepidemiology. 1987;6(4):190-7.
236. Adams M, Caffrey L, McKevitt C. Barriers and opportunities for enhancing patient recruitment and retention in clinical research: findings from an interview study in an NHS academic health science centre. Health research policy and systems. 2015;13(1):1-9.
237. Chenok K, Teleki S, SooHoo NF, Huddleston III J, Bozic KJ. Collecting patient-reported outcomes: lessons from the California Joint Replacement Registry. eGEMs. 2015;3(1):1196
238. Wylde V, Marques E, Artz N, Blom A, Gooberman-Hill R. Effectiveness and cost-effectiveness of a group-based pain self-management intervention for patients undergoing total hip replacement: feasibility study for a randomized controlled trial. Trials. 2014;15(1):1-10.
239. European Association of Nuclear Medicine. Good practice for introducing radiopharmaceuticals for clinical use. International Atomic Energy Agency; 2016.
240. Neilly B, Allen S, Ballinger J, Buscombe J, Clarke R, Ellis B, Flux G, Fraser L, Hall A, Owen H, Paterson A. Future supply of medical radioisotopes for the UK report 2014. arXiv preprint arXiv:1501.03071. 2015 Jan 13.
241. Jenkins P, Clement N, Hamilton D, Gaston P, Patton J, Howie C. Predicting the cost-effectiveness of total hip and knee replacement: a health economic analysis. The bone & joint journal. 2013;95(1):115-21.
242. Meade RC, Bamrah VS, Horgan JD, Ruetz PP, Kronenwetter C, Yeh E-L. Quantitative methods in the evaluation of thallium-201 myocardial perfusion images. Journal of Nuclear Medicine. 1978;19(10):1175-8.
243. Matsuda H, Tsuji S, Shuke N, Sumiya H, Tonami N, Hisada K. A quantitative approach to technetium-99m hexamethylpropylene amine oxime. European journal of nuclear medicine. 1992;19(3):195-200.
244. Fiévet B, Della Vedova C. Dealing with non-detect values in time-series measurements of radionuclide concentration in the marine environment. Journal of environmental radioactivity. 2010;101(1):1-7.
245. Mick CG, James T, Hill JD, Williams P, Perry M. Molecular imaging in oncology: 18F-sodium fluoride PET imaging of osseous metastatic disease. American Journal of Roentgenology. 2014;203(2):263-71.
246. Morawietz L, Classen R, Schröder J, Dynybil C, Perka C, Skwara A, et al. Proposal for a histopathological consensus classification of the periprosthetic interface membrane. Journal of clinical pathology. 2006;59(6):591-7.
247. Ribera A, Morata L, Moranas J, Agulló J, Martínez J, López Y, et al. Clinical and microbiological findings in prosthetic joint replacement due to aseptic loosening. Journal of Infection. 2014;69(3):235-43.
248. Tigges S, Stiles RG, Roberson JR. Appearance of septic hip prostheses on plain radiographs. AJR American journal of roentgenology. 1994;163(2):377-80.
249. Kaya M, Nagoya S, Yamashita T, Niiro N, Fujita M. Peri-prosthetic tuberculous infection of the hip in a patient with no previous history of

tuberculosis. Journal of Bone & Joint Surgery, British Volume. 2006;88(3):394-5.
250. Chryssikos T, Parvizi J, Ghanem E, Newberg A, Zhuang H, Alavi A. FDG-PET imaging can diagnose periprosthetic infection of the hip. Clin Orthop Relat Res. 2008;466(6):1338-42.
251. Gollwitzer H, Diehl P, Gerdesmeyer L, Mittelmeier W. [Diagnostic strategies in cases of suspected periprosthetic infection of the knee. A review of the literature and current recommendations]. Der Orthopade. 2006;35(9):904, 906-8
252. Grant FD, Fahey FH, Packard AB, Davis RT, Alavi A, Treves ST. Skeletal PET with 18F-fluoride: applying new technology to an old tracer. J Nucl Med. 2008;49(1):68-78.
253. Adesanya O, Sprowson A, Masters J, Hutchinson C. Review of the role of dynamic 18F-NaF PET in diagnosing and distinguishing between septic and aseptic loosening in hip prosthesis. Journal of orthopaedic surgery and research. 2015;10(1):1-5.
254. van der Bruggen W, Bleeker-Rovers CP, Boerman OC, Gotthardt M, Oyen WJ. PET and SPECT in osteomyelitis and prosthetic bone and joint infections: a systematic review. Semin Nucl Med. 2010;40(1):3-15.
255. Delank KS, Schmidt M, Michael JP, Dietlein M, Schicha H, Eysel P. The implications of 18F-FDG PET for the diagnosis of endoprosthetic loosening and infection in hip and knee arthroplasty: results from a prospective, blinded study. BMC musculoskeletal disorders. 2006;7(1):20.
256. Palestro CJ. Nuclear medicine, the painful prosthetic joint, and orthopedic infection. Journal of Nuclear Medicine. 2003;44(6):927-9.
257. Bori G, Muñoz-Mahamud E, Garcia S, Mallofre C, Gallart X, Bosch J, et al. Interface membrane is the best sample for histological study to diagnose prosthetic joint infection. Modern Pathology. 2011;24(4):579-84.
258. Seifert S, Lapa C, Buck A, Kircher M. Tc-99 m-Tilmanocept lymphoscintigraphy after inconclusive Tc-99 m-Nanocolloid scan in breast cancer. Nuklearmedizin. 2019;58(02):TV7.
259. Pal D, De T, Baral A. Lymphatic Mappinh with A New Drug Lymphoseek (Technetium TC 99m Tilmanocept): A Receptor-Targeted Radiopharmaceutical.
260. Wallace AM, Hoh CK, Vera DR, Darrah DD, Schulteis G. Lymphoseek: a molecular radiopharmaceutical for sentinel node detection. Annals of surgical oncology. 2003;10(5):531-8.
261. Jarjour W, Rosol T, Schlesinger L, Blue M, Cope F. Fluorescent CD206-targeted Manocept-Cy3 (Mano-Cy3) specifically localizes on macrophages (MPs) derived from rheumatoid arthritis (RA) patients' synovial fluid & is quantitatively greater than that from non-RA patients. Journal of Nuclear Medicine. 2014;55(supplement 1):1229-1229.
262. Businesswire. Biopharmaceuticals N. Navidea Awarded $1.8M Fast Track NIH SBIR Grant for Evaluation of a Manocept™ Agent in Kaposi's Sarcoma Published September 03, 2015. [Last accessed 15th February 2021]. Available from: http://www.businesswire.com/news/home/20150903005639/en/
263. Qin Z, Hoh CK, Olson ES, Jahromi AH, Hall DJ, Barback CV, You YH, Yanagita M, Sharma K, Vera DR. Molecular imaging of the glomerulus via mesangial cell uptake of radiolabeled tilmanocept. Journal of Nuclear Medicine. 2019 Sep 1;60(9):1325-32.

264. Kardan A, Abbruzzese B, Kissling A, Haynam M, Ralph D, Hershey R, et al. Intravenous 99mTc-tilmanocept in Planar and Fused SPECT/CT Imaging of Activated Macrophage Infiltration in Subjects with Active Rheumatoid Arthritis. Journal of Nuclear Medicine. 2018;59(supplement 1):110-110.
265. Cope F, Bhambhvani P, McConathy J, Paluri R, Kissling A, Haynam M, Ralph D, Hershey R, Ismail A, Blue M, Hartings C. Intravenous 99mTc-tilmanocept in Planar and Fused SPECT/CT Imaging of Activated Macrophage Infiltration in Subjects with Metastatic Liver Colorectal Adenocarcinoma (ML-CRC). Journal of Nuclear Medicine. 2018;59(supplement 1):56-56.
266. Zanni MV, Toribio M, Wilks MQ, Lu MT, Burdo TH, Walker J, et al. Application of a novel CD206+ macrophage-specific arterial imaging strategy in HIV-infected individuals. The Journal of infectious diseases. 2017;215(8):1264-9.
267. Stroup SP, Kane CJ, Farchshchi-Heydari S, James CM, Davis CH, Wallace AM, et al. Preoperative sentinel lymph node mapping of the prostate using PET/CT fusion imaging and Ga-68-labeled tilmanocept in an animal model. Clinical & experimental metastasis. 2012;29(7):673-80.
268. Reubi J, Kvols L, Waser B, Nagorney D, Heitz P, Charboneau J, et al. Detection of somatostatin receptors in surgical and percutaneous needle biopsy samples of carcinoids and islet cell carcinomas. Cancer research. 1990;50(18):5969-77.
269. Boytard L, Spear R, Chinetti-Gbaguidi G, Acosta-Martin AE, Vanhoutte J, Lamblin N, et al. Role of proinflammatory CD68+ mannose receptor− macrophages in peroxiredoxin-1 expression and in abdominal aortic aneurysms in humans. Arteriosclerosis, thrombosis, and vascular biology. 2013;33(2):431-8.
270. Grinspoon S. Novel mechanisms and anti-inflammatory strategies to reduce cardiovascular risk in human immunodeficiency virus. Transactions of the American Clinical and Climatological Association. 2018;129:140-154.
271. Panchuk-Voloshina N, Haugland RP, Bishop-Stewart J, Bhalgat MK, Millard PJ, Mao F, et al. Alexa dyes, a series of new fluorescent dyes that yield exceptionally bright, photostable conjugates. Journal of Histochemistry & Cytochemistry. 1999;47(9):1179-88.
272. Zmistowski B, Craig Della Valle MD, US TW, Malizos KN. Workgroup 7: diagnosis of periprosthetic joint infection. In Consensus Meeting on Periprosthetic Joint Infection 2014; (p. 202).
273. Galli SJ, Borregaard N, Wynn TA. Phenotypic and functional plasticity of cells of innate immunity: macrophages, mast cells and neutrophils. Nature immunology. 2011;12(11):1035–1044.
274. Davis MJ, Tsang TM, Qiu Y, Dayrit JK, Freij JB, Huffnagle GB, et al. Macrophage M1/M2 polarization dynamically adapts to changes in cytokine microenvironments in Cryptococcus neoformans infection. MBio. 2013;4(3):e00264-13.
275. Young N, Rosol T, Schlesinger L, et al. OP0154 Manocept, A Derivative of FDA-Approved 99MTC-Tilmanocept, Exhibits Diagnostic Potential by Specifically Identifying Macrophages in Rheumatoid Arthritis: A Novel Application of an Existing Drug. Annals of the Rheumatic Diseases 2015;74:127-127.
276. The Human Protein Atlas: Sigma-Aldrich; [updated on 13-Mar-2020 Last Last accessed 15th February 2021]. Available from:

https://www.proteinatlas.org/ENSG00000260314-MRC1/antibody#antibody_summary.
277. Rahmim A, Zaidi H. PET versus SPECT: strengths, limitations and challenges. Nuclear medicine communications. 2008;29(3):193-207.
278. Cunha L, Szigeti K, Mathé D, Metello LF. The role of molecular imaging in modern drug development. Drug discovery today. 2014;19(7):936-48.
279. Wolf AP. Special characteristics and potential for radiopharmaceuticals for positron emission tomography. InSeminars in nuclear medicine 1981 Jan 1 (Vol. 11, No. 1, pp. 2-12). WB Saunders.
280. Gomes CM, Abrunhosa AJ, Ramos P, Pauwels EKJ. Molecular imaging with SPECT as a tool for drug development. Advanced Drug Delivery Reviews. 2011;63(7):547-54.
281. British Nuclear Medicine Society (BNMS). [Last updated 6th January 2021; Accessed 16th January 2021]. Available from: https://www.bnms.org.uk/page/guidelines.
282. Sampson CB. Textbk radiopharmacy. CRC Press; 1994 Mar 1.
283. Sharp PF. Practical Nuclear Medicine 3rd ed. Sharp PF, Gemmell HG, Murray AD, editors. London: Springer; 2005 Sep 30.
284. Britton KE. The Nuclear Medicine Point of View in Orthopaedic Infections: Imaging with Tc-99m-Ciprofloxacin, Infecton. In: Signore A, Liberatore M, Scopinaro F, editors. Nuclear Medicine in the Management of Inflammatory and Infectious Diseases. Berlin, Heidelberg: Springer Berlin Heidelberg; 2003. p. 70-8.
285. De Winter F, Van de Wiele C, Dumont F, Van Durme J, Solanki K, Britton K, et al. Biodistribution and dosimetry of 99mTc-ciprofloxacin, a promising agent for the diagnosis of bacterial infection. European Journal of Nuclear Medicine. 2001;28(5):570-4.
286. Welling M, Stokkel M, Balter J, Sarda-Mantel L, Meulemans A, Le Guludec D. The many roads to infection imaging. European journal of nuclear medicine and molecular imaging. 2008;35(4):848-9.
287. Müller C. Folate-based radiotracers for PET imaging—update and perspectives. Molecules. 2013;18(5):5005-31.
288. Fischer CR, Müller C, Reber J, Müller A, Krämer SD, Ametamey SM, et al. [18F]Fluoro-Deoxy-Glucose Folate: A Novel PET Radiotracer with Improved in Vivo Properties for Folate Receptor Targeting. Bioconjugate Chemistry. 2012;23(4):805-13.
289. Henne WA, Rothenbuhler R, Ayala-Lopez W, Xia W, Varghese B, Low PS. Imaging Sites of Infection Using a 99mTc-Labeled Folate Conjugate Targeted to Folate Receptor Positive Macrophages. Molecular Pharmaceutics. 2012;9(5):1435-40.
290. NHS Improvement. England National NHS Tariff 2020/21 2019 [Last updated: 26 November 2020; Accessed 16th January 2021]. Available from: https://improvement.nhs.uk/resources/national-tariff/